PHYSICO-CHEMICAL STUDIES ON THE INTERACTION OF SELECTED CATIONIC DYES WITH ALUMINOSILICATES

THESIS SUBMITTED FOR THE DEGREE OF
DOCTOR OF PHILOSOPHY (SCIENCE)
OF THE
UNIVERSITY OF NORTH BENGAL
1988

By

Pradip Kumar Sanyal, M. Sc.

NORTH BENGAL

DEPARTMENT OF CHEMISTRY
UNIVERSITY OF NORTH BENGAL
DARJEELING, WEST BENGAL
INDIA

ST - VERB

STOCKTAKING - 2011

Ref.
547.3412
S238p

103986

7 MAR 1900

Dedicated to the Sacred
Memory of My Beloved Father

A C K N O W L E D G E M E N T

I deem it a privilege to express my regards and profound sense of gratitude to my supervisor Dr. S.K. Chakravarti, Retired Professor of Chemistry, University of North Bengal for his valuable guidance, continued interest, watchful care and incessant encouragement during the progress of my work.

My thanks are also due to the University Grants Commission, New Delhi, for the award of a Teacher Fellowship and Siliguri College, Siliguri for granting leave.

I am also indebted to the Head of the Department of Chemistry and authorities of the University of North Bengal for extending laboratory facilities.

I am grateful to Dr. S.K. Saha, Lecturer in Chemistry, University of North Bengal for his keen interest and valuable discussion.

Dr. A.K. Majumder, Dr. S. Das, Dr. T.S. Basu Baul, Dr. R. Poddar, Sr J. Bhattacharjee, Sri B. Bagchi and Sri M. Chakraborty also merit due acknowledgement for their generous help.

Thanks are also due to Research fellows, Teacher fellows, Teaching and non-teaching staff of the Department for their kind co-operation.

I would like to express my thanks to my wife, brothers, sisters, son and other family members for their continued inspiration and encouragement during my work.

Finally I express my sincere regards to my mother whose kind blessing ceaselessly showered on me during my work.

P. K. Sanyal.

(P. K. SANYAL)

Department of Chemistry,
University of North Bengal
1988

PREFACE

The work embodied in the thesis deals with Physico Chemical Studies on the Interaction of Selected Cationic Dyes with Aluminosilicates. For this purpose two Xanthene dyes, viz., Rhodamine 6G and Rhodamine B having similar structure differing in shape and postion of alkyl substituents and one Oxazine dye viz., Brilliant Cresyl Blue obviously differing in size and structure from the other two have been chosen as adsorbates. Two natural exchangers viz. montmorillonite and kaolinite and one synthetic exchanger viz. laponite (hectorite) have been selected as adsorbents. Attempts have also been made to understand the sorption behaviour in the light of the structure of the adsorbate as well as adsorbent.

In order to understand physico chemical aspects of exchange equilibrium considerable attention has been devoted to studies on desorption of Rhodamine $6G^{+}$ and Rhodamine B^{+} ions from their respective exchangers. Monovalent and divalent inorganic Cations as well as alkyl quaternary ammonium ions and long chain surface active ions of varying size and shape have been used as desorbing ions.

A systematic attempt has been made to interpret the data of both sorption and desorption in the light of prevalent approach and model and also to express the data in qualitative and quantitative terms.

Attempts has been made to study the aggregation of the dyes on above mentioned exchangers. For this purpose above mentioned Cationic dyes belonging to different categories have been chosen.

The effect of temperature on the sorption of Xanthene dyes on the natural exchangers have also been investigated.

The present thesis embodies the results of research carried out by the candidate at the Department of Chemistry, University of North Bengal.

C O N T E N T S

CHAPTER - I

SECTION - A

Introduction and Review of previous work:

The process of ion exchange is the mechanism operative during uptake of ions by plant roots from clay minerals and other soil components. In this process the clay fraction of the soil plays a significant and vital role. The study of the exchange characteristics reflects generally, the exchange behaviour of the soil as a whole. The colloidal properties of clay minerals have been used for hundreds of years, especially in the manufacture of pottery and in foundry. The contribution of our knowledge of clay minerals is largely due to scientists, colloid Chemists, Ceramicists and physicists who have appreciated in their respective fields the importance of the clay minerals. A systematic attempt has however been made only in this century to understand the origin of their behaviour. Considerable success has been achieved in the past fifty years with regard to the search for high purity clays and for evidences of their crystallinity. The atomic structures of the common clay minerals have been to a great extent determined and applied to explain the properties of the individual members by numerous investigators.

In general clay means a natural fine-grained earthy material which develops plasticity when mixed with a limited quantity of water (1). Clay is basically the product of weathering of rocks or of hydrothermal action. It is also used in terms of particle size. In that case it is defined as a material having

particle size lower than 2.0 microns. The material below 2.0 micron is primarily the colloidal product of weathering and hence constitutes the active portion of the soil (2,3,4). The fraction is mainly composed of clay minerals but may sometimes be associated with non clay mineral substances.

The composition and crystalline structure of clay minerals are now well established with the help of such techniques as X-ray, electron diffraction, differential thermal analysis, electron microscopy and other optical studies (4) besides chemical, electrochemical, ion-exchange and viscous properties.

The clay minerals have been classified under separate headings, such as kaolinite, montmorillonite, illite, chlorite and vermiculites. Mixed layer lattice type minerals have also been identified in natural clays.

On the basis of crystal chemical approach, the correlation between the structures and the exchange properties of the clay minerals has been established from the important researches of Pauling (5), Bragg (6), Gruner (7), Brindley (8), Hoffmann (9), Marshall (10), Hendricks (11) and others (12-18). From these studies, clay minerals are recognised to consist essentially of two structural units. One is composed of two sheets of closely packed oxygens or hydroxyls in which aluminium or magnesium atoms are arranged in octahedral co-ordination so that they are equi-distant from six oxygens or hydroxyls. With aluminium in the Octahedral position, only two-thirds of the possible positions

are filled to balance the structure. It is the gibbsite structure having the formula $Al_2(OH)_6$; when magnesium is present, all the possible positions are filled up to balance the structure giving that of brucite which has the formula $Mg_3(OH)_6$. The second unit is the tetrahedrally co-ordinates silica. A silicon atom being placed at the centre of a regular tetrahedron is equidistant from four oxygens or hydroxyls. The silica tetrahedra are joined together in the a, b directions, through oxygen, to form a hexagonal network which is repeated indefinitely to form a sheet of composition $Si_4O_6(OH)_4$. The tips of all the tetrahedra are in the same direction. The structures for some of the alumino-silicates used in the present study are described briefly.

Kaolinite:

The kaolinite is composed of a single silica tetrahedral together with a single alumina octahedral sheet confined in a unit so that the tips of the silica tetrahedra and one of the layers of the octahedral sheet form a common layer. All the tips of the silica tetrahedra point in the same direction and toward the centre of the unit made of the silica and the octahedral sheets. These sheets which are continuous in the a, b directions are stacked one above the other in the c direction. During stacking the oxygens of the tetrahedral layer are placed very close to the hydroxyls of the octahedral layer, so that the sheets are held tightly by hydrogen bonding as a result of which very little expansion in the c-direction is possible.

Montmorillonite:

According to the currently accepted concept, montmorillonite is composed of units, made up of two silica tetrahedral sheets, with a central alumina octahedral sheet. All the tips of the tetrahedra are, pointed in the same direction and toward the centre of the unit. The tetrahedral and the octahedral sheets are combined in such a way that the tips of the tetrahedra of each silica sheet and one of the hydroxyl layers of the octahedral sheet form a common layer. The atoms common to the tetrahedral and octahedral layers become O instead of OH.

The minerals of the group are also developed by stacking of these unit sheets one above the other in the c-direction. During stacking, the O layers of one unit are close to the O layers of the other unit, so that there is an excellent cleavage between the sheets. Polar molecules can enter into the space between the sheets causing expansion of the axis in the c-direction.

Isomorphous substitution of other metal ions for silicon and aluminium by iron and magnesium is found in the minerals nontronite and saponite respectively. Substitution in the tetrahedral layer in montmorillonite does take place but to a limited extent.

Laponite:

Laponite is a synthetic clay of the hectorite variety. Hectorite is a natural mineral swelling clay and usually remains heavily contaminated with other minerals such as dolomite, quartz etc which are not easily removed. The deposits of hectorite are also limited. Laponite provides for the first time, a reliable consistent supply of high purity swelling clay. It has a number of other important properties not found in its natural equivalent. It is composed of magnesium silicates with a layer structure and is obtained as granular, free-flowing white powder. The powder forms thixotropic gels when dispersed in water. Laponite has a layer structure similar to that of the natural hectorite. Hectorite is the trioctahedral equivalent of montmorillonite and owes its charge to octahedral replacements of Mg by Li.

Its structural formula is

$$\angle Si_8 \rangle^{IV} \quad \angle Mg_{6-x} \underset{\downarrow}{\cdot} Li_x \rangle^{VI} \quad O_{20}(OH)_4$$
$$M_x$$

The charge x is of the order of 0.6 to 0.7 valencies per unit cell. The structural formula of Na-Laponite CP is

$$Na_{0.70}(Mg_{5.26}, Li_{0.59}) Si_{0.01} O_{24} H_{3.97}$$

In certain Laponite products, there are no fluorine atoms in the structure, these are being replaced by hydroxyl ions. The layers (platelets) are about 10A^{o} thick and are extended in two dimensions. If the cations present were only silicon and magnesium, a single layer would be electrically neutral. However, since some magnesium is substituted by lithium and some structural positions normally occupied by these cations may be unoccupied, these layers have a negative charge which is balanced by exchangeable cations, normally sodium ions, situated outside the structure, between the multiple layers.

Usually during crystal growth, the tetrahedra are not solely occupied by silicon or by aluminium or magnesium. Aluminium may substitute for some of the tetrahedral silicon atoms and Fe, Li, Mn, Cr and other metal ions of suitable size may occupy a part of the octahedral sites. This isomorphous replacement of ions unbalances the overall charge of the crystal lattice. An excess negative charge develops which is balanced by cations that are retained on the external layer silicate surfaces. These cations, e.g. Na^{+}, K^{+}, Ca^{2+} and others are more or less exchangeable, depending on the nature of the replacing cations, nature of the adsorbed cations and the magnitude and distribution of the structural charge. They are held between unit layers and bond the layers together. This brings the idea of cation exchange capacity (C.E.C.) of the clay.

The ion exchange sorption of inorganic as well as organic ions is known to occur in clay minerals (19,20). Hence the origins of the charge of the clay lattice are believed to be due to isomorphous substitution, lattice imperfections, broken bonds at the edges of the particles and exposed structural hydroxyls. The negative charge on the clay minerals is compensated by adsorption of cations. The counter ions are held on the external surfaces of the aggregates and between the unit layers in clays which swell in aqueous suspension, whereas the sorption of counter ions takes place onto the external surfaces only in non-swelling clays. In aqueous suspension, some of these cations remain in a closely held stern layer, others diffuse away from the surface and thus form a diffuse double layer. Provided that they are not fixed by engaging in strong, specific bonding with the clay or by being trapped between unit layers that have collapsed together irreversibly (lattice collapse), the counter ions can undergo ion exchange with other cations present in the system.

The magnitude of the C.E.C. of a clay depends largely on the type of clay and to a lesser extent on the source of a particular sample.

The experimentally measured specific surface area of a clay mineral depends on the type of clay and the method of measurement employed; among clays of the same type, the values differ from sample to sample, and the nature of the counter ions

present in the sample may also influence the measured surface area. The theoretical surface areas were calculated from the weights of the unit cells, and their dimensions as indicated by X-ray diffraction.

Systematic studies of cation exchange in pure clay minerals were carried out by Page and Baver (21), Bar and Tenderloo (22), Hendricks and Alexander (23), Schachtschabel (24), Mukherjee (25) and others. Most of these investigations were based upon exchange equilibria, selectivity etc. with simple inorganic ions (26,27). Exchange reactions involving clay minerals with organic compounds have also been established by different scientists (28-31).

Amongst earlier workers, Renold (32) was perhaps the first to study systematically the exchange behaviour of Cu, Pb, Ni, Ag, Zn, Hg and Cd permutites and observed an increase in the exchangibility of these cations in the order shown. Zn was found by him to be as effective as Ba in its exchanging power. Jenny and Elgabaly (33) showed, on the basis of exchange characteristics of Zn montmorillonite that Zn ion is partially rendered non-exchangeable by being coordinated to the clay mineral. Basu and Mukherjee (34-35) have studied in detail the interaction of montmorillonite clay and trace element cations. They observed the release of the metal ions in the order $Zn^{2+} > Mn^{2+} > Ni^{2+} = Co^{2+} > Cu^{2+}$ from the clay surface by H^{+}. Moreover,

quantitative measurements revealed that the amount released was much less than that adsorbed, so that a part of the adsorbed cations was considered to be "fixed". Martin and Glaeser (36) studied the adsorption of $Co(NH_3)_6Cl_3$ on montmorillonite under various pH conditions. They found that it also permits the estimation of internal and external exchange capacities. Chakravarti and Laitinen (37) studied the adsorption and desorption of $Coen_3Cl_3$ on pyrex glass. The exchange capacity determined from the exchange of $\left[Coen_3\right]^{3+}$ agreed well with those obtained from the sorption and desorption studies of Cr^{3+}_{51} and Cs^{+}_{137}. Das Kanungo, Chakravarti and Mukherjee (38, 39,40) studied adsorption and desorption of hexamine Cobalt (III) chloride and trisethylene diamine Cobalt (III) chloride on bentonite and vermiculite and observed that adsorption is according to Langmuir's equation and desorbing cations arrange themselves according to the lyotrope series. Recently, Sarkar and Das Kanungo (41) have shown that in the exchange of tri-strimethylene diamine Co (III) from the bentonite matrix by alkaline earth metal ions, both the hydrated ionic radius and the reciprocal of the Debye-Huckel ion-size parameter, a^{o}, may be used to correlate the relative affinities of the ions for the mineral while for the alkali metal ions only, $1/a^{o}$ may be utilised for the purpose. Thielmann and McAtee, Jr. (42) investigated the gas chromatographic behaviour of metal-tris

(ethylene diamine) complex cation-exchanged montmorillonites for the separation of oxides of nitrogen and light hydrocarbons and showed that N_2O is involved in an adsorption process on the oxygens of the basal surface of the clay, whereas the light hydrocarbons were most probably involved in a sieving separation. The cation exchange process between tris (ethylene diamine) Co(III) and Na^+ on montmorillonite was studied by Knudson, Jr. and McAtee, Jr. (43) and concluded that the exchange of $Co(en)_3^{3+}$ for Na^+ was extremely favourable, with a tendency towards segregation of the two kinds of cations in the mixed clays studied. The studies on exchange characteristics of Zeolite, either synthetic or natural by Barrer and his co-workers (44) and others have received a great deal of attention in recent years.

Interlayer complexes of clays with simple organic compounds are essentially of two types, those in which the adsorbed species exists (a) as a cation and (b) as a polar non-ionic compound. From a study of the reactions between organic compounds and different type of clays made by a large number of workers, the specific nature of the clay mineral organic ion reactions has now been fairly well established. Under suitable conditions, most organic cations are capable of replacing the interlayer inorganic cations occupying exchange sites in montmorillonite and vermiculite type minerals.

Hendricks (45) extended Gieseking's (46) study of organic bases, cations and proteins on montmorillonite to other aliphatic and aromatic amines, alkaloids, purines and nucleosides using H-montmorillonite as adsorbent. He was able to show that small organic bases neutralised the H^+ ions upto or close to the exchange capacity of montmorillonite as determined by the exchange with Ba^{2+}. On the other hand, large alkaloids, such as brucine and codeine, failed to neutralise all the H^+ ions present in the clay. This led Hendricks to postulate that the difference between the total amount of H^+ ions and that available for reacting with the alkaloid represents the quantity "covered" by the organic base. This cover-up-effect comes into operation when the size of the adsorbed organic molecules exceeds the area per exchange site. of the complexes formed in this way, those involving n-alkylammonium ions received the greatest amount of attention. The chemistry of clay-organic reactions has been well reviewed by Greenland (47), Mortland (48) and Theng (49). A number of general conclusions has emerged from these studies by Hendricks (45), Jordan (50), Cowan and White (51), Diamond and Kinter (52), Weiss (53), Theng et al (54), Walker (55), Vansant and Uytterheoven (56), Maes et al (57) and others and is summarized below:

(1) Adsorption reaches a maximum equal or close to the exchange capacity of the clay. For very long chain derivatives

($>C_8$), adsorption may exceed this capacity, the excess being present as the free amine.

(2) For montmorillonite, the affinity of the organic ion for the clay, increases regularly with molecular weight, that is, the larger the cation, the stronger its adsorption. This observation is ascribed to the increased contribution of van der Waals forces to the adsorption energy as the molecular weight increases and also to the changes of the hydration status of the ions in the clay interlayer.

(3) Basal spacing measurements suggest that the organic ion is adsorbed with its shortest axis perpendicular to the silicate layer, since such a flat conformation enables close van der Waals contact to be achieved between the adsorbate and substrate.

(4) Single-layer complexes [$d_{001} \simeq 12.5\text{-}13.5$ A°] are formed with montmorillonite provided that the area of the cation (upto C_{10}) is less than the area per exchange site since the organic ions adsorbed on one layer can fit into the gaps between those adsorbed on the opposing surface. If, however, the cation area ($>C_{10}$) exceeds the area per exchange position, this lock-and-key arrangement is no longer possible and double layer complexes [$d_{001} \sim 16.5 - 17.5$ A°] are obtained.

(5) At high surface concentrations, long-chain alkylammonium ions ($>C_{10}$) may assume an "end-on" orientation in which

the alkyl chain extends away from and makes a definite angle with the silicate surface. In this conformation greater van der Waals interactions between alkyl chains are possible. The interlayer space is also increased so that a larger amount of the organic ions can be accommodated.

(6) In vermiculites the tilted conformation is generally observed even for short-chain derivatives since the distance of separation of the negative charges in the silicate surface is less than for montmorillonite. The basal spacing of vermiculite complexes tends to show a continuous rather than a step-wise increase with the number of carbon atoms in the alkyl-chain. Double layer complexes of vermiculite have been observed at high solute concentrations.

(7) There is evidence to indicate that partially exchanged montmorillonite crystals are composed of "inorganic ion rich" and "alkyl ammonium rich" layers as shown by Barrer and Brummer (58), Theng et al (54) and others.

Sorption studies of dyes and large organic ions on different adsorbents, particularly on clays, have been made by innumerable workers over a period of many years. Most of the earlier studies have been confined to the measurement of the surface areas and c.e.c. of the adsorbents. Relevant literature is reviewed in the following paragraphs.

As early as 1910 Mare (59) observed that dyes could be adsorbed by crystals upto a saturation value. Ramachandran

et al (60) measured the surface area by low temperature nitrogen adsorption before and after adsorption of methylene blue, methyl violet and malachite green on the clay fraction of kaolinite, illite and montmorillonite. From the difference, the actual extent of the area of contact was evaluated. This was found to be relatively small showing that while the surface is available for nitrogen adsorption, it is not accessible to dye molecules. The cation exchange capacities, found from methylene blue and methyl violet sorption on kaolinite and montmorillonite, were in close agreement with those found by standard methods.

Brooks (61) adsorbed methylene blue on Na^+ forms (Na^{22} and Na^{23}) of kaolinite, montmorillonite and found the amount of dye adsorbed to be equivalent to the sodium displaced; he believed that the dyes were adsorbed, at the first stage, on the clay mineral surface through ion-exchange process. More dye is adsorbed after that, which was explained to be due to van der Waals forces. Plesch and Robertson (62) also proposed two distinct mechanisms to operate in the sorptions of dyes on surfaces of clay minerals viz. the partly irreversible ion-exchange and the fully reversible physical adsorption. Bergmann and O'Konski (63) reported that the adsorption of methylene blue on montmorillonite took place first through irreversible ion exchange mechanism and then by physical adsorption and verified the equation of Plesch and Robertson with their experimental results.

From the studies of adsorption of crystal violet on anatase and rutile and that of orange II on anatase, rutile and zinc oxide, Ewing and Liu (64) estimated the cross-sectional areas of crystal violet and orange II. They assumed that the dye molecules were adsorbed flat on the surface and accordingly they estimated the cross-sectional area of crystal violet to be 160 $\overset{o}{A}$ and 171 $\overset{o}{A}^2$ depending on whether the dye is adsorbed in the dehydrated or hydrated condition. The area occupied by one orange II molecule was calculated to be 140 $\overset{o}{A}^2$. The surface areas of the adsorbents, calculated on the basis of these cross-sections, were in excellent agreement with those found out by low temperature nitrogen gas adsorption and also by electron microscopic analysis. Clauss, Rohem and Hofmann (65) reported 78 $\overset{o}{A}^2$ as the cross-sectional areas of methylene blue from the adsorption data on graphitised and non-graphitised carbon. The value of 130 $\overset{o}{A}^2$, for a flat molecular orientation, agreed excellently with that observed by Loss and Tompkins (66) and Langville et al (67). Surface areas of calcined magnesia, alumina, silica and silica gel were calculated from methyl red adsorption (68). The results were reported to agree within 6%.

An agreement was also noticed in the values of surface areas calculated from the adsorption of monosulphonated acid wool dye (sodium salt of 1-amino, 4-anilino, anthraquinone, 2-sulfonic acid) from aqueous solution and that from nitrogen adsorption. An N-H...O bond between the dye and the adsorbate was suggested (69).

103986
27 MAR 1980

The surface areas measured through dye adsorption, however, did not agree with those obtained by nitrogen adsorption in all cases. Kipling and Wilson (70) found discrepancies in specific surface areas of porous and non-porous active charcoal measured by methylene blue and nitrogen adsorptions. Hofmann (71), on the basis of methylene blue and orange II adsorption on a wide variety of clays, showed that the surface area calculated was only 70% of the total surface area. Orr (72,73) found that the surface areas of two halloysite samples calculated by sorption of four dyes viz. malachite green oxalate, malachite green hydrochloride, amaranth and tetrazine, were apparently equal to one-fourth of the total surface. Similar discrepancies were also reported by Darau (74), van der Grinter (75) and Bancellin (76) in their respective adsorption studies, viz., ethyl violet on silica, crystal violet on glass and methylene blue on mercury. Bancroff et al (77) from adsorption of methylene blue on lead sulphate, Subrahmanya et al (78) from crystal violet adsorption on glass and Doss and Singh (79) from thymol blue sorption on active carbon, arrived at similar unsatisfactory results.

Giles et al (80) observed that the adsorption of basic dyes by silica from aqueous solution exceeded its monolayer coverage requirement. They opined that the dyes were adsorbed on the surface not as a single unit but as ionic micelles. This was confirmed by the adsorption of methylene blue and pseudocyanine chloride by spectroscopic examination of the solution before and

after adsorption. Association of the dye molecules in the adsorbed state has also been detected directly by electron micrography (81). That most of the dye molecules are associated in solution as micelles from 10 to 100 molecular units was reported by Lenhar and Smith (82,83), Vickerstaff and Lenin (84) and Bergmann and O'Konski (63). Mukherjee and Ghosh (85, 86,87) and Hertz et al (88) and Hertz (89) also observed that dye molecules, of which the monovalent organo cations are a sub-group, tend to aggregate into dimeric and polymeric species in aqueous solution. Kongonovoski (90) also viewed the adsorption of dyes to take place through monolayer sorption of associated micelles.

Brooks (61), however, advocated that the surface area and cation exchange capacity of the substrates, with methylene blue adsorption, could still be measured. To calculate the c.e.c. and surface areas, he suggested addition of dye solution to a mineral suspension in small increments till the equilibrium concentration was 1×10^{-6} (M), indicated by a slight blue colour of the supernatant.

Hang Pham Thi and Brindley (91) asserted that methylene blue can be used for the measurement of both surface areas and c.e.c. of clay minerals such as kaolinite, illite and montmorillonite. They attributed the cause of failures in measuring surface areas and exchange capacities by Faruki et al (92) and Bodenheimer and Heller (93) to the insufficient replacement of Ca^{2+} ions by

methylene blue from Ca-montmorillonite used in their studies. Using Na-clay instead of the Ca-clay these authors calculated surface areas from the amount of methylene blue adsorbed when optimum flouculation occurred. Fully exchanged values of methylene blue was used to calculate the c.e.c. of the montmorillonite. Methylene blue molecule was considered to possess approximately a rectangular volume of dimensions 17.0 x 7.6 x 3.25 $\overset{o}{A}^3$. They believed that coating of clay particles occurred first and visualised a flat face-on orientation of methylene blue molecules (i.e. lying on the 17.0 x 7.6 $\overset{o}{A}^2$ face for effective coverage of surfaces. Flat side-on orientation of the dye (i.e. 17.0 x 3.25 $\overset{o}{A}^2$ face)was assumed when full exchange took place. Brindley and Thompson (93a) later extended this work to montmorillonite saturated with different cations and obtained expected values of the surface areas and c.e.c.

West, Carrol and Whitcomb (94) investigated systematically the adsorption characteristics of more than thirty dyes on photographic bromo-iodides or chloro-bromides suspension in 70% aqueous gelatine solution in an attempt to correlate the sorption and optical sensitisation. It was noticed in some cases that the dye adsorbed was very little at first but the rate of increase of dye adsorption increased as more dye was adsorbed. They termed this as 'co-operative adsorption'. The intermolecular forces between the large dye molecules are so high that they polymerised

when the molecules came closer in the adsorbed state, giving rise to increased rate of adsorption.

De et al (95-104) made a series of exhaustive studies on sorption of dyes on to clay minerals and on their desorption from the clay-dye complexes by various inorganic and organic ions. They found Langmuir type of adsorption isotherms to operate in all cases. Surface area measurement, evaluation of c.e.c., determination selectivity coefficients and distribution coefficients are the highlights of their work. Narine and Guy (105) interacted thionine, methylene blue, New Methylene blue, paraquat and diquat with bentonite in dilute aqueous systems. They noted that the dye cations form aggregates on the clay surface and aggregation increases with ionic strength, raising the apparent adsorption capacity by 25%. The aggregates were, however, removable by washing with distilled water. They also observed that changes in adsorption due to changes in temperature were small and the dyes were irreversibly bound by the clay matrix.

Yamagashi (106) recently studied the effect of alkyl chain length ($-CH_3$ to $-C_{14}H_{29}$) for the adsorption of n-alkylated acridine orange cations on Na-montmorillonite. He observed that the length of the aliphatic tail had no appreciable effect on the binding constant of adsorption, the rate of adsorption and the angle of the transition moment due to a bound dye with respect to electric field but the 'mobility' of a bound dye to an empty

site of another colloidal particle was remarkably affected by the alkyl chain. Two factors, viz. steric hindrance and hydrophobic interactions among the alkyl chains of adjacent sorbed dye molecules, were supposed to influence the mobility of bound dye in opposite ways. This finding demonstrates the ability of a clay to recognise the shape of a molecule and strengthens the possibility of using clay as shape-sensitive catalyst (107). Mishra et al (108) studied the sorption behaviour of two basic dyes, brilliant cresyl blue and Safranine-T, on chemically pretreated hydrous tin (IV) oxide under varying surface phase pH, concentration, temperature and desorbents. Reed and Rogers (109) observed selective adsorption of methyl and ethyl orange on tailored silica gel.

So, it appears from the review above that the sorption of cationic dyes, although believed to be primarily an ion exchange process, is rather complicated by many other factors such as molecular size, molecular geometry, dye-dye interaction, besides, of course, the surface characteristics of the sorbents. Our knowledge of the physicochemical aspects of the desorption processes of the organic dye cations from the clay surfaces by organic ions is still meagre. It is in this context that an attempt has been made in the present investigation to study the sorption and desorption behaviours of Rhodamine B and Rhodamine 6G. On and from montmorillonite, kaolinite, laponite and monovalent, bivalent inorganic ions and organic ions of varying size and shape and also an approach has been made to study comparative adsorption behaviour between Rhodamine B and Rhodamine 6G with Brilliant cresyl blue on different aluminosilicates.

SECTION - B

Ion Exchange Formulations

A number of approaches, both qualitative and quantitative, have been made to understand the equilibria between an ion exchanger and the ions in solution (1). A review of cation exchange equations as they are being used in soils and in other exchnagers has been done by Bolt (2) and Helfferich (3) and their applicability to soils discussed by Babcock (4). Experiments were performed in which the ionic concentrations were varied and the result suggested an exponential relationship between the ions adsorbed (or desorbed) and the concentration of the exchanging ions. Limitations have been tacitly accepted in most mathematical treatments of exchange reactions.

Thus (A) the simultaneous occurrence of both cation and anion exchange reactions in a given system has been considered as a rare case, (B) the exchange capacity to be constant, though cases are known where the exchange capacity varies markedly with the change in pH and the nature of the exchanging ion; (C) simple stoichiometric equivalence between the ions taken up and released is generally assumed to be present, deviations are usually explained in terms of simultaneous adsorption and formation of complex ions, and (D) finally the perfect reversibility exists in an exchange process under consideration.

On this basis, various formulations similar to Fruendlich and Langmuir's adsorption equations (isotherms) were proposed. The Fruendlich equation is emperical and can be expressed as where 'X' is the amount of adsorbate taken up by 'm' gm of

$$\frac{X}{m} = k. C^{1/n}$$

adsorbent, 'k' and 'n' are constants and 'C' is the adsorbate concentration in solution at equilibrium.

Weigner (5) used this equation in 1912. But this equation has two limitations, (i) it does not flatten out at higher values of 'C' as a system of fixed exchange capacity should, and (ii) it shows that the exchange varies with variation of total volume, whereas Weigner (5) showed that the position of equilibrium was independent of volume. Weigner and Jenny (6), however, in 1927, overcome the second objection and modified the equation as

$$\frac{X}{m} = K \left(\frac{C}{a-c} \right)^{1/n}$$

[a = initial concentration of the adsorbate].

With the variable character of two constants incorporated in this equation, a good agreement is often obtained with experimental data over a limited range. However, Marshall and Gupta (7), has shown that it was superior as regards 'k' but $\frac{1}{n}$ varied erratically.

The Langmuir isotherm is based on sound kinetic and thermodynamic principles and was developed to describe the adsorption of gases onto solids. It assumes that only monomolecular adsorption takes place, that adsorption is on localised sites, that there are no interactions between adsorbate molecules and that the heat of adsorption is independent of surface coverage When V is the equilibrium volume of the gas adsorbed per unit mass of adsorbent at pressure P, then

$$V = \frac{V_m \cdot K.P}{1 + KP}$$

where K is a constant dependent on temperature, and V_m is the volume of the gas required to give monolayer coverage of unit mass of adsorbent. When applied to adsorption from solution, this equation takes the form (8)

$$\frac{X}{m} = \frac{(x/m)_{max} \cdot K.C}{1 + K.C}$$

where 'X' is the amount of the solute adsorbed by mass 'm' of adsorbent, 'C' is the equilibrium solution concentration, 'K' is a constant, and $\left(\frac{X}{m}_{max}\right)$ is the monolayer capacity.

By use of the reciprocal expression, the above equation becomes,

$$\frac{1}{(X/m)} = \frac{1}{K.\ (X/m)_{max}} \frac{1}{C} + \frac{1}{(X/m)_{max}}$$

So a plot of 1/x/m versus 1/C should give a straight line and a slope of $\frac{1}{K(X/m)_{max}}$ when the Langmuir relationship holds good.

A similar type of equation of the Langmuir's with two constants were proposed by Vageler (9,10) as

$$X = \frac{Sa}{a + C}$$

where X = amount exchange, a = electrolyte added

S and C = constants.

Application of the Langmuir's adsorption equation to cation exchange in soils was initiated by Vageler (9) in 1932. His equation appears to be an erroneous attempt to restate the Langmuir equation in terms of amounts of the cation added to the system rather than its concentration at equilibrium. It may be shown that only when the ratio of the forward and backward rate constants is close to unity such a restatement is acceptable and in all other cases it does not appear to be sound (11).

Aside from Vageler's equation, the original Langmuir equation is in its simplest form useless for cation exchange, as it does not take into consideration the competition between the cationic species. One may, however, introduce this competition effect into the Langmuir equation rather simply by using Kerr's (12) and Gapon's (13) equations as a starting point (2). However, should an ion-exchange mechanism predominate in the

adsorption process, the linear forms of the Langmuir and Fruendlich equations would not be obeyed because of coulombic effects in the adsorbent. Thus, in theory at least, it is possible to distinguish by means of different isotherm equations between ionic and other mechanisms of adsorption (14).

The ion exchange formulations are usually based on three theories i.e. (i) crystal lattice theory (ii) double layer theory and (iii) Donan membrance theory (15). The only differences in the various theories are the position and the origin of exchange sites. In all cases, this site is essentially a fixed, non-diffusible ionic grouping capable of forming an electrostatic bond with a small diffusible ion of opposite charge. The case with which this latter ion may be replaced depends on the strenth of the bond, which varies in a manner similar to the dissociation of weak and strong electrolytes. The laws governing the exchange of ions in these heterogeneous systems are analogous to the laws governing the solutions of electrolytes.

Jenny (16) envisaged a kinetic condition on the surface and derived from statistical approach the equation below,

$$W = \frac{+(S+N) \pm \sqrt{(S+N)^2 - 4SN\left(1-\frac{\nu_w}{\nu_b}\right)}}{2\left(1-\frac{\nu_w}{\nu_b}\right)}$$

where W = number of cations exchanged at equilibrium

N = number of cations added initially

S = saturation capacity

and W,b = constants for each ion.

For similar exchange properties of the two exchanging ions, the above equation reduces to

$$W = \frac{SN}{S + N}$$

which is quite similar to that of Vageler (9,10).

A more refined approach was introduced by Davis (17,18) and applied to exchange on soil clays by Krishnamoorty and Overstreet (19). Davis considered the probability of replacement of cations with different valency on a regular array of negative point charges as supposed to be present on the exchanger surface. Although, Davis, indicates that his treatment should apply to a monolayer in the widest sense of the word in each surface charge is being accompanied by one counter charge only in the adsorbed layer, it appears that other assumptions inherent in the treatment as, e.g., absence of anions, probability of replacement being based on a regular array of the position available for the ions, are warranted only if one considers a monolayer in a narrow sense, i.e. localized monolayer.

The first use of the law of mass action in formulating ion exchange as a completely reversible reaction was made by Gansen (20) and Kerr (12), investigating specific mass action equations for uni-univalent and uni-bivalent exchanges as

$$\bar{Y} + X^{+} \rightleftharpoons Y^{+} + \bar{X} \qquad 2\bar{Y} + X^{2+} \rightleftharpoons \bar{X} + 2Y^{+}$$

$$K_1 = \frac{[\bar{X}][Y^{+}]}{[\bar{Y}][X^{+}]} \qquad K_2 = \frac{[\bar{X}][Y^{+}]^2}{[\bar{Y}]^2[X^{2+}]}$$

The bar indicates the ion in the exchanger phase. The constants K_1 and K_2 are termed as selectivity coefficients. The ionic terms represent equilibrium concentration in solution. But owing to the lack of knowledge about the activities of the ionic species in the exchanger phase, the equilibrium constant could only be evaluated qualitatively or emperically. Bauman (21) and Gregor (22) pointed out the difficulties in terms of swelling and volume change particularly of the resins. The model introduced by Gregor (22) although thermodynamically less well-established, bring out clearly the physical action of the swelling pressure. A more rigorous application of the law of mass action has been made by Boyd and co-workers (23) in which the "solid solution" idea of Vanselow (24) has been the basis on the assumption that the ion exchange is a "solid solution" process. Vanselow visualizing the monolayer as an ideal two dimensional solid solution, assumes the activities of the two exchanger components to be proportional to their respective mole-fractions.

In the above formulations, all the exchange sites were assumed to be of equal value. Doubts regarding this, were first

clearly expressed by Weigner (25) and his co-workers. In order to explain some of their experimental data, they postulated the existence of loosely and firmly bound ions on the surface of the same exchanger. Without the necessary information regarding the surface characteristics of the silicates which Weigner used for this work, he had to invoke, the idea of the existence of micropores, edges and cleavages. A remark should be made here on the assumed reversibility of the exchange reaction. There is evidence that certain exchange reactions are incompletely reversible. The obvious example of such a system is the adsorption of potassium by certain clay minerals. There steric factors influence the relative affinity of the clay for different cations, which necessitates the recognition of a range of sites with different relative affinity (26,27). The fact that often the cationic composition in turn influences these steric factors (by a varying degree of collapse of the crystal lattice) suggests a considerable degree of hysteresis in exchange reaction involving inter-lattice sites.

Attempts to understand ion exchange reactions on the basis of electrical double layer, as postulated by Mukherjee (28) yields no doubt qualitative results but the concept in many respects, conforms better with observations. He assumed two categories of exchangeable ions, the osmotically active ions which constitute the mobile part of the double layer and osmotically inactive ones constituting the immobile part of the double layer. The

relationship of crystalline structure of clays with their electrochemical properties and ion exchange characteristics has been studied with fundamental details by Mukherjee and Mitra (29), Mitra and Bagchi (30), Ganguli and Mukherjee (31) and Chakravarti (32).

However, in a more detailed study of the exchange behaviour of soil materials, the monolayer model equations do not offer much perspective for interpretative usage. One should then rather use, the thermodynamic method of presentation as suggested by Gaines and Thomas (33,34). The most promising model for the description of adsorption on external surfaces appears, however, to be a Stern-Gouy double layer approach along with lines as used for the homovalent case by Heald et al (35) and further advanced by Shainberg and Kemper (36,37). Extension of this model to heterovalent exchange will increase its complexity considerably, as both the fraction of the multivalent ions in the Gouy layer and that in the Stern layer will depend on the valency. The contribution of Shainberg and Kemper (36,37) is of great interest as an effect to estimate the magnitude of the pair - formation constants on the basis of the physical properties of the ions and presents an important stepforward in the process of gaining understanding about the nature of the cation exchange equilibrium in clay systems.

Considerable progress has also been made by others (38, 39,40) in the formulation of ion exchange equilibria on a rigorous and quantitative basis. Further progress must await new advances in the fields of concentrated solutions of simple electrolytes and soluble, uncrosslinked polyelectrolyte solutions which has been stepped by Fuoss (41), Katchaesky (42) and others.

In the present thesis an attempt has been made to fit the adsorption data of two xanthene dyes viz. Rhodamine B and Rhodamine 6G and one oxyazine dye viz. Brilliant Cresyl blue on montmorillonite, kaolinite and laponite in the Langmuir equation and the desorption data of the two xanthene dye cations from their respective adsorbent complexes by monovalent and bivalent inorganic ions in the model of Pauley (43).

Pauley's Model:

Pauley has interpreted selectivities in ion exchange equilibrium in the language of a very simple model. Its essential feature is the electrostatic attraction between the counter ions and the fixed ionic groups. It is assumed that all the counter ions in the ion exchanger are found at their distance of closest approach to the fixed ionic groups. Writing AR and BR for the pairs of fixed ionic groups and counter ions at the distance of closest approach, one can split the exchange of A for B into two processes:

$$AR \longrightarrow A + R \qquad \ldots (1)$$

$$R + B \longrightarrow BR \qquad \ldots (2)$$

Coulomb's law (without any correction) leads to the following results for the above processes.

$$\Delta G_1^\circ = \int_{a_A^\circ}^{\infty} \frac{e^2}{r^2 \epsilon} dr = \frac{e^2}{a_A^\circ \epsilon} \qquad \ldots (3)$$

and $$\Delta G_2^\circ = \int_{\infty}^{a_B^\circ} \frac{e^2}{r^2 \epsilon} dr = -\frac{e^2}{a_B^\circ \epsilon} \qquad \ldots (4)$$

where ΔG_1° and ΔG_2° are the free energy charges for the processes (1) and (2), e = electronic charge, ϵ = dielectric constant, r = distance from the centre of the fixed charge, a_i° = distance of the closest approach between counter ion 'i' and fixed ionic group. Hence the overall free energy change for the whole process is

$$\Delta G^\circ = \Delta G_1^\circ + \Delta G_2^\circ = \frac{e^2}{\epsilon}\left(\frac{1}{a_A^\circ} - \frac{1}{a_B^\circ}\right) \qquad \ldots (5)$$

and the thermodynamic equilibrium constant K_A^B is

$$\ln K_A^B = -\frac{\Delta G^\circ}{kT} = \frac{e^2}{kT\epsilon}\left(\frac{1}{a_B^\circ} - \frac{1}{a_A^\circ}\right) \qquad \ldots (6)$$

In the exchange of various univalent counterions 'i' for an arbitrary univalent reference ion A, a linear relationship should exist between $\ln K_A^B$ and $\frac{1}{a_i^\circ}$.

For multivalent ions, the calculation is not quite as simple because assumptions must be made as to how the (univalent) fixed ionic groups and polyvalent counterions are paired. The model leads qualitatively to preference of the ion exchanger for counterion with smaller a° value and higher valency.

SECTION - C

Exchange studies and Selectivities of Clay minerals

A true ion-exchange equilibrium is completely reversible and may be approached from both sides of the reaction equilibrium provided that certain conditions are observed. These conditions are determined by the selectivity of the ion exchanger which in turn is influenced by Donnan effects, specific interactions, steric effects, ion association and other ion-sequestering effects (1). Where these effects are large the equilibrium will favour one side of the reaction. Specific interactions and Donnan effects largely determine ion selectivity in most situations. Specific interactions (e.g. hydrogen bonding, van der Waals forces, charge-transfer processes, etc.) can produce secondary adsorption interactions on the counterion bound by the exchanger. These increase the selectivity of the adsorbent for the adsorbed ion, and this ion is then held preferentially despite the presence of high concentrations of counterions in solution (2,3,4). Steric effects can also influence reversibility, as evidenced in ion trapping effects. In some systems ion-sequestering effects (including ion-pairing, complexing and precipitation) are important in determining selectivity. Generally, the adsorbent prefers the ion which associates least strongly in solution and most strongly with the adsorbent (4). A number of

workers have thoroughly investigated the exchange properties of the clay minerals, resins and molecular sieves and their characteristics have been well established. The following generalisations may be made regarding the tendency of a cation to exchange onto a negative surface. There is an increase in exchangeability (a) with decreasing hydrated ionic radius and increasing polarizability, (b) with decreasing case of cation hydration and (c) with increasing counterion charge.

The above criteria, however, do not hold good in cases where some specific interactions take place. In accordance with the above observations, the order of increasing preference of alkali metal ions for ion exchange onto montmorillonite (5-26), vermiculite (27) and kaolinite (28,29) is $Li^+ < Na^+ < K^+ < Rb^+ < Cs^+$. The exchange of NH_4^+ is complicated by physical adsorption of ammonia (30) and fixation of NH_4^+ ion (31). It was observed that NH_4^+ is held strongly than Na^+ (32) or even Rb^+ (33).

Similarly the exchange of H^+ is also complicated due to its attack onto clay lattice, displacing aluminium or magnesium ions which may be taken up by the exchange sites (34,35). It was reported that H^+ is apparently preferred over some divalent cations in ion exchange on montmorillonite and soil-clays (13,36) and over caesium on vermiculite (27). The reported relative orders of exchange on montmorillonite are $H^+ < Cs^+$ (16), $K^+ < H^+ < Ca^{2+}$ (7) and $K^+ < NH_4^+ < H^+ < Mg^{2+}$ (37). Under conditions which

minimise dissolution of clay by acid attack, the corresponding orders were $H^+ < Na^+ < K^+$ (10) and $Na^+ < H^+ < NH_4^+$ (32). The sequence of exchange of alkaline earth ions on clays has generally been reported as $Mg^{2+} < Mn^{2+} < Ca^{2+} < Sr^{2+} < Ba^{2+}$ (10,13,32,38-48), The reverse order is sometime found in vermiculite (45,49,50). For the exchange of divalent transition metal cations on clays, the reported orders of preference are $Mn^{2+} \simeq Ni^{2+} \simeq Fe^{2+} < Co^{2+} < Zn^{2+} < Cu^{2+}$ (51) $Ca^{2+} < Co(II)^{2+}$ (52) and $Ni^{2+} < Ba^{2+}$ (47). A generalisation may be made from studies comparing the exchange of mono, di and trivalent cations on clays that there is a preference for cations of higher charge (37,7,11,13,16,17,36,40,44-46,52-57) although there is exception to this trend. In the usual general purpose cation exchangers, the selectivity sequence of the most common cations is $Ba^{2+} > Pb^{2+} > Sr^{2+} > Ca^{2+} > Ni^{2+} > Cd^{2+} > Cu^{2+} > Co^{2+} > Zn^{2+} > Mg^{2+} > UO_2^{2+} > Tl^+ > Ag^+ > Cs^+ > Rb^+ > K^+ > NH_4^+ > Na^+ > Li^+$ (58-61).

Under suitable conditions, most organic cations are capable of replacing the interlayer inorganic cations, occupying exchange sites in bentonite, vermiculite and illite minerals.

The exchange reaction is stoicheiometric except for some bulky cations when a cover-up effect (62) may operate. Studies on the replacement of exchangeable sodium and calcium from montmorillonite by various alkyl ammonium cations were made by Theng et al (63). They found that the affinity of the clay for the organic cations was linearly related to molecular weight with the exception of the smaller methyl ammonium and larger quaternary

ammonium ions. Thus, the more the length of the alkyl ammonium chain increases, the greater is the contribution of physical, non-coulombic forces to adsorption. Within a group of primary, secondary and tertiary amines, the affinity of the alkyl ammonium ions for the clay decreased in the series $R_3NH^+ > R_2NH_2^+ > RNH_3^+$. These differences were explained in terms of size and shape of the ions. Theng et al also noted that Na^+ was much more easily exchanged by the alkyl ammonium ions than was Ca^{2+}. In studies in which the alkyl ammonium ion is replaced by metal cations, Mortland and Barake (64) showed that the order of effectiveness in replacing ethylammonium ion was $Al^{3+} > Ca^{2+} > Li^{2+}$. Furthermore, X-ray diffraction studies on partially exchanged systems revealed that the organic and inorganic cations were not distributed uniformly throughout all the surfaces of montmorillonite, but that a segregation of the two kinds of ions took place in various layers. This suggests that when the displacement of ethylammonium ion by the metal ion from one interlamellar position begings, it is completed before ethylammonium ions from other layers are exchanged. Similar observations have been reported by Barrer and Brummer (65), McBride and Mortland (66) and Theng et al (63). The exchange of various alkylammonium cations from aqueous solution by Na-Laponite has been carried out by Vansant and Peeters (67). They observed that the affinity of these organic cations was linearly related to molecular weight, molecular size or chain length of the alkylammonium ions. The affinity sequence has been

attributed to the increasing contribution of van der Waals force to adsorption energy as the size of the ions increases (68) and also to the change in hydration state of the ions in the clay interlayer (69,70).

Charge density of the clay mineral may also affect the orientation of adsorbed organic cations through steric effects. Thus, Serratosa (71) showed by infra red absorption technique that in pyridinium montmorillonite, the organic cation assumed an orientation where the plane of the pyridine ring was parallel with the platelets of the clay mineral and a resulting d_{001} spacing of 12.5 A^{o}. On the other hand, pyridinium-vermiculite has the pyridinium cations vertically positioned with respect to the clay platelets and a d_{001} spacing of 13.8 A^{o}. Apparently, the close proximity of the cation exchange sites one to another prevents the pyridinium ring from assuming the parallel position because of the restricted area permitted for each pyridinium unit. When neutral but polar organic molecules are bound to the clay surface by other mechanisms, such as ion-dipole interaction, charge density would also be expected to affect their orientation within the interlamellar regions of swelling clay minerals. It is apparent from the review above that the exchange properties of clay minerals have been thoroughly studied by a number of workers and their characteristics have been well established. The more important characteristics are :

(i) The observations of the lyotropic series though exceptions are often observed.

(ii) Obedience to the Langmuir equation of the data on exchange sorption of large organic molecules (specially the dye molecules). A simple equivalent fraction exchange equation has been proposed to fit in the exchange data of Na^+, K^+, Ca^{2+} on bentonite (72) at 0.5(M) and 1.0(M) external salt concentration.

(iii) Formulation of selectivity coefficient:

Exchange measurements can be written in a general way as follows:

$$\frac{1}{Z_1}\bar{A} + \frac{1}{Z_2}B \rightleftharpoons \frac{1}{Z_1}A + \frac{1}{Z_2}\bar{B}$$

Where the bar denotes the species in in the adsorbed phase and Z_1, Z_2 and the valencies of A and B respectively.

From the above equation, the selectivity coefficient is expressed as follows:

$$K_A^B = \frac{[A]^{1/Z_1}\,[\bar{B}]^{1/Z_2}}{[\bar{A}]^{1/Z_1}\,[B]^{1/Z_2}}$$

The measurement of selectivity coefficient and the obedience of Langmuir's equation are not, however, exclusive of one another.

All these studies are confined to the replacement of one inorganic cation for another. There is very little work on exchange reactions involving two organic cations. The exchange of a large organic cation for another organic cation on montmorillonite had been reported by McAtee (73). Since the organomontmorillonite is organophilic and hydrophobic, the exchange was carried out in an isooctane isopropyl alcohol mixture. It was found that under the condition of the experiment upto 16 per cent of dimethylbenzyllauryl ammonium cation can be replaced from montmorillonite with dimethyldioctadecyl ammonium cation. De, Das Kanungo and Chakravarti (74-77) have shown that cationic dyes e.g. methylene blue, crystal violet, and malachite green adsorbed onto bentonite, vermiculite, kaolinite and asbestos can be exchanged by long-chain surface active ions like cetyltrimethyl ammonium and cetyl pyridinium ions. In the present work, desorption of two xanthene dyes viz. Rhodamine B and Rhodamine 6G has also been studied with tetraalkyl ammonium and long-chain surface active ions of varying size and shape.

CHAPTER - II

Scope and Object of Work

In spite of the wide occurrence and practical applications, adsorption at the interface between the suspended particles of aluminosilicates and an aqueous solution of Cationic dyes still presents one of the complicated problems in surface Chemistry. It is in this context that an attempt has been made to study the Physico-Chemical aspects on the interaction of different cationic dyes with clay minerals and allied aluminosilicates. The term interaction has been applied to mean mainly the sorption and desorption phenomena along with other effects as may accrue from or be related to them. In studies of clay-dye interaction adsorption data will be meaningful only when both adsorbates and adsorbents are well characterized. Small organic cations are seen to be taken up by aluminosilicates upto the extent corresponding to cation exchange capacity while large ions may be adsorbed in excess being held up by van der Waal's and/or hydrophobic forces. It has been observed that the sorption of organic molecules takes place on the surface of aluminosilicates of the fixed lattice group viz. kaolinite when they penetrate between the unit layer of montmorillonite or the clays of the expanding lattice group. This complicated process of interaction of organic ions with clays is accompanied by significant variation of properties of the solid which needs thorough investigation in

any attempt to interpret the data on equilibrium and also to explain different types of adsorptive forces involved such as (1) Chemisorption (2) Ion-exchange (3) Hydrogen bond (4) Hydrophobic bonding (5) van der Waal's forces, etc. Several approaches both qualitative and quantitative have been made to understand the equilibria between ion-exchangers and solution.

Dye desorption measurements were used by earlier workers mainly to estimate the surface areas and c.e.c. of the adsorbents. Not always could satisfactory results be obtained. A proper knowledge of the interaction of the adsorbate with adsorbent was lacking in most of the studies, unless this is known in reasonable details, an appreciation of the adsorption measurements may be difficult. It is therefore appropriate to carry out systematic study of sorption phenomenon for which adsorpbates of known structures and adsorbents with well defined surface characteristics would be most convenient. The clay minerals montmorillonite, kaolinite and laponite (a synthetic trioctahedral hectorite) used in the present study provide more or less known features.

Rhodamine B and Rhodamine 6G (Xanthene series), Brilliant cresyl blue (oxazine series) are dye compounds of known structures used in the present investigation as adsorbates. Some basic data regarding these dyes are known. Being structurally similar with like charge delocalisation the two Xanthene dyes differ from each other only in the position of alkyl substituents, whereas

oxazine dye differs in structure and molecular weight from the xanthane dyes. As such, it is an excellent opportunity to study the effect of shape and size of the adsorbate on sorption and desorption phenomena as well as to compare the sorption behaviour of xanthane dyes with that of an oxazine.

The main object of the present investigation is to study in fundamental detail the physico-chemical aspects of ion exchange equilibrium of the above dye cations onto the exchangers mentioned in the preceding paragraph with a view to derive some in sight into the factors that govern and influence the exchange processes. For this purpose, the study of interaction has been approached from three different angles : sorption-desorption forming the main bulk of the thesis, heat of adsorption and the metachromatic behaviour of the dye spectra due to adsorption. The adsorption isotherms have been studied and analysed in the light of Langmuir equation for Rhodamine B, Rhodamine 6G and Brilliant cresyl Blue on the adsorbents mentioned above. Further, in order to investigate the influence of the type of clay mineral on ion exchange behaviour, natural and synthetic clays having widely different structural characteristics, charge densities and swelling properties have been chosen. Although large amount of work is recorded in the literature on the adsorption of dyes on clay minerals, the desorption characteristics of the dyes have not been studied thoroughly with different inorganic and organic ions by previous workers. So the desorption

of Rhodamine B and Rhodamine 6G from their respective clay complexes have been studied with monovalent, divalent inorganic ions as well as with tetraalkyl ammonium and long chain surface active ions of varying sizes in order to acquire a better knowledge of the nature of adsorbate-adsorbent interaction relative strength of binding of the adsorbents, cation specificity etc. Such studies also reveal the extent of extractibility of the dye cation from the adsorbent surfaces from which we can have an idea of the affinity of the ions for the minerals vis-a-vis the relative desorbing efficiency of the ions with size, shape and charge of the ions. An attempt has also been made to analyse the desorption data obtained with the inorganic ions in the electrostatic model of Pauley. There exists sufficient scope for a further use of these experimental data to test and develop different existing theoretical models and equations, describing ion-exchange equilibria.

The heats of adsorption of selected xanthane dyes onto montmorillonite and kaolinite have been calculated from measurement of adsorption at three different temperatures. This parameter provides useful information for the interpretation of the adsorption process and on the strength of bonding of the adsorbed species with the adsorbent surface.

In view of the conflicting theories reported in literature about the causes of metachromasy when cationic dyes are sorbed

onto clay minerals, the present study has been carried out to throw further light in this area by investigating the spectral behaviour of selected dyes exchanged onto montmorillonite, kaolinite and laponite. X-ray diffraction data have been used to supplement the observations. This study may lead to an important insight into the mechanism of the interaction between the adsorbate and the adsorbent. The correlation of the spectral shifts with the surface concentration may be an interesting study. A direct determination of surface concentration may also be possible, from which the surface area of the substrate can be easily derived.

CHAPTER III

EXPERIMENTAL

SECTION - A

Three cationic dyes viz. Rhodamine B and Rhodamine 6G of Xanthene series and Brilliant cresyl blue (oxazine series) were chosen for the present work.

The description of the above mentioned dyes are being summarised in the following table (1).

Table 1

Sample	Symbol used	Description	Source
1. Rhodamine B	RB	Brown crystals hygroscopic	Merck
2. Rhodamine 6G	RG	Reddish brown crystal hygroscopic	Merck
3. Brilliant Cresyl Blue	BB	Dark blue crystal hygroscopic	The British Drug House, England

Preparation of Pure Dye

(a) Recrystallisation of Rhodamine B.

Rhodamine B chloride was purified by adding slowly with stirring about ten volumes of anhydrous ether to a saturated solution of the dye in absolute ethanol. It precipitated in

the form of golden green flakes. The process was repeated and the filtered solution was washed with ether and air dried. The structure of Rhodamine B is

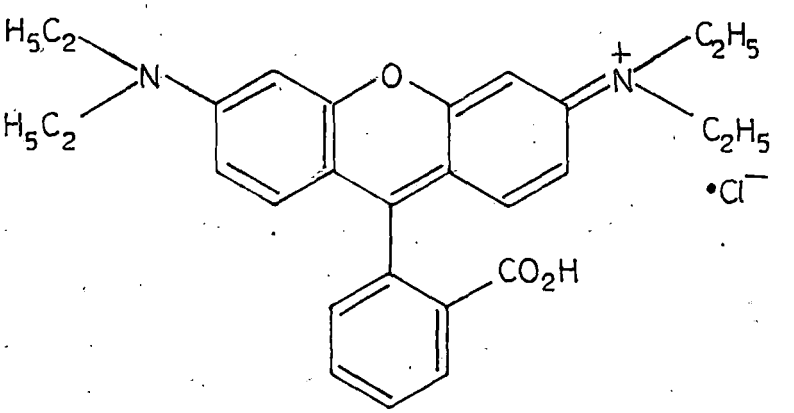

(b) Recrystallisation Rhodamine 6G

The Rhodamine 6G was obtained from Merck. It was twice recrystallised from ethanol and dried in a vacuum oven. The structure of Rhodamine 6G is

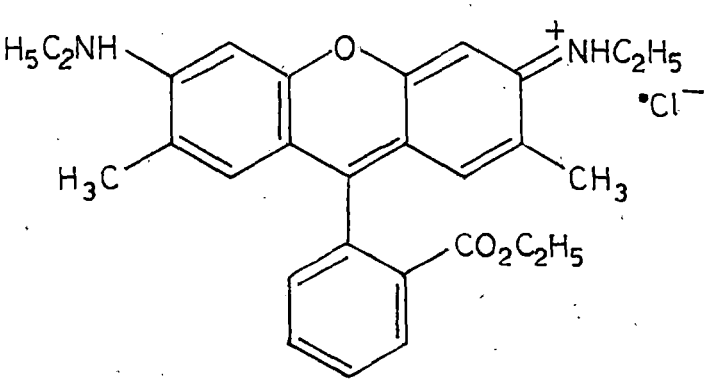

(c) Recrystallisation of Brilliant Cresyl Blue

The dye Brilliant Cresyl Blue was purified by repeated crystallisation from ethanol : water (1:1 v/v) mixture and dried at 80^{o} for 24 hrs. The homogeneity of the samples was tested chromatographically.

The structure of Brilliant Cresyl Blue is :

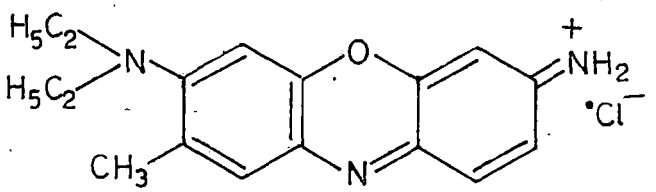

Preparation of Stock Solution of the Dyes:

Stock solutions of RB, RG and BB were prepared by accurately weighing vacuum dried samples of the dyes and dissolving them in distilled water upto a definite volume. The concentration of these stock solutions, stored in polypropylene bottles, was of the order of 10^{-3}(M) and counter-checked through estimation by Ascorbometric Titration (1).

Ascorbometric Titration of Dyes:

2 ml of dye solution was mixed with 2 ml of 4(M) HCl in a glass vessel and kept in water bath at $70^{o}C$, CO_2 was passed into the solution to prevent aerial oxidation. The dye

solution was treated with standard ascorbic acid solution of the order of 10^{-2} (M) and the course of titration followed potentiometrically with Pt. indicator electrode. At the equivalent point the dye lost its colour and the potential attained a constant value.

SECTION - B

The alumino-silicates used for the interaction with the Cationic dyes discussed above, are described below in Table (2).

Table 2

Sample	Description	*Cation exchange capacity meq/100g	Source
1. Montmorillonite	Light grey powder	86*	Evans Medical Ltd., Liverpool, England
2. Kaolinite	White powder	5.4*	BDH, England
3. Laponite, XLG	White powder	88**	Supplied by Laponite Industries Ltd., England, as gift.

* Determined by $BaCl_2$ - $Ba(OH)_2$ method

** Reported from source.

The clay fractions of minerals 1 and 2 having particle size < 2.00 mμ were isolated by the usual method of dispersion and fraction by sedimentation. The fractions so collected were then treated several times with dilute HCl and after removal of acid, warmed with 6% H_2O to remove trace of any

organic matter present. Excess H_2O_2 was decomposed by heating the samples over water bath. The iron present in the clay minerals was then removed by treating the clay sample with sodium metabisulphide and sodium dithionite in acetate buffer solution (pH≃5) at 60°C followed by centrifugation, washing etc. as recommended by Bromfield (2). Finally the clay residues were washed to dispersion and dialysed. The clay suspension was then converted into Na-form by stirring an approximately 2 per cent suspension of the clay with ion-exchange resin (Dowex 50W x 8) in the Na-form for about four hours. The process was repeated once again to ensure complete conversion of the clay mineral to Na-form. Na-clays (pH 7) so formed were used for adsorption and desorption studies.

Preparation of Na-laponite:

The synthetic hectorite clay used in this investigation was Na-laponite XLG. To ensure complete saturation with sodium, the Na-laponite was brought into dialysis bags and washed several times with 1(N) NaCl solutions, before dialysing against distilled water until free of chloride.

Adsorption Studies:

10 ml portions of the suspensions of known clay content, were pipetted into separate stoppered polypropylene bottles (3) and dye solution of known concentration, was added in increasing amount. The total volume was brought to 20 ml by quantitatively adding the necessary amount of distilled water. The bottles, with their contents, were shaken for three hours

and allowed to stand for at least 24 hours to attain exchange equilibrium. Experiments with several days equilibriation produced the same results indicating that 24 hours were sufficient for attaining equilibrium. The resulting exchanged clays were then centrifuged (10,000 r.p.m.) for 10 minutes or so, and the supernatant liquids were analysed spectrophotometrically using spekol of Carl Zeiss. From the difference between the initial concentration and the equilibrium concentration, the amount adsorbed was determined. All operations were carried out at constant room temperature.

The clay content of the suspension was measured by evaporating a known volume of the clay suspension to dryness at $100^{o}C$ to $105^{o}C$ in an air oven. The contents expressed in g/100 ml are given in Table 3.

Table 3

Sample	Clay content in g/100 ml
1. Na-montmorillonite	1.0
2. Na-Kaolinite	0.70
3. Na-Laponite	0.722

Desorption Studies:

For studying desorption, the clay mineral suspensions were mixed with dye solution of such a concentration that the equilibrium concentration was maintained at 1×10^{-5} (M) or so to ensure monomer sorption (4) as far as possible. The mixtures were shaken for four hours and allowed to equilibrate overnight at constant temperatures. The excess dye was washed off with distilled water by repeated centrifugation of the clay-dye complex till the leachate gave zero optical density. The resulting clay dye complex was then resuspended in distilled water and used for desorption studies. The percentages of colloid contents of the suspensions were determined by drying a known amount of each at $100^{o}C$ to constant weights, and are given in Table 4.

For the purpose of desorption studies, 10 ml portions of the suspension were taken in a number of stoppered polypropylene bottles and varying amounts of different electrolytes were added. The total volumes were adjusted to 30 ml by quantitatively adding requisite amounts of distilled water. The bottles, with their contents, were shaken for four hours and kept overnight to equilibrate. Preliminary studies showed that this period was sufficient for the purpose. The mixtures were then centrifuged (100,000 r.p.m.) for 15 minutes or so and the dye content of the clear centrifugate was estimated spectrophotometrically as described earlier.

Table 4

Sample	Content
1. Na-montmorillonite-RG	0.112
2. Na-montmorillonite-RB	0.108
3. Na-Kaolinite-RG	0.132
4. Na-Kaolinite-RB	0.1281
5. Na-Laponite RG	0.08
6. Na-Laponite RB	0.114

The clay content is different from each sample. It is known however, that the difference does not affect the exchange reactions to a great extent (5)

Of the various electrolytes used in the desorption studies, LiCl, NaCl, KCl, NH_4Cl, RbCl and CsCl were of E. Merck quality : cetyl pyridium Bromide (CPBr), Cetyltrimethyl ammonium bromide (CTMABr), dodecylpyridinium bromide (DDPBr), dodecyltrimethylammonium bromide (DDTMABr) were of BDH-AR quality. Standard solution of these electrolytes were prepared by direct weighing of vacuum dried salts. Tetramethyl ammonium Bromide (TMABr), tetraethyl ammonium Bromide (TEABr), tetrapropyl ammonium Bromide (TPABr), and tetrabutyl ammonium

Bromide (TBABr) were all of "Fluka" (Switzerland products). These were standardized by titration with $AgNO_3$ of E. Merck quality using potassium chromate as indicator.

$MgCl_2$ and $CaCl_2$ solutions were prepared with BDH. AR quality samples were standardized by EDTA titration, using Eriochrome Black T as indicator and the concentration of $SrCl_2$ and $BaCl_2$ prepared with A.R. quality samples were determined by precipitating as sulphates.

Spectrophotometric Study of Dye aggregation

On clay surface:

Varying amounts of increasing percentage of clays were added to a definite volume of a fixed concentration of dye. These were shaken and the spectra of the mixtures were recorded in Graphicord Model No. UV-240, double beam uv-vis Spectrophotometer (Shimadzu, Japan), using cell of 1 cm and 1 mm path in the visible region. The spectra were taken within 15-20 minutes after the preparation of the clay-dye suspensions to eliminate theeffects of flucculations due to aging on the intensities of adsorption bands (6).

X-ray measurements:

For preparing clay-dye complex at different percentage of saturation, appropriate amounts of selected dyes were added to Na-montmorillonite suspension, equilibrated and centrifuged

several times to wash off the excess dye. The samples were then allowed for drying in an air oven at 120°C, then gently grounded with a mortar and pestle and stored in a vacuum dessicator over silica gel. The X-ray diffraction study of the finely powdered samples containing different clay-dye complexes and Na-montmorillonite clay alone (dried as per above method) was carried out at the Department of Physics, College of Engineering, Anna University, Madras, using Philips, PW-1010, X-ray Diffractometer with CuK_α radiation at 25 KV and 20 mA.

Infrared Analysis

The infrared analysis of different clays was carried out in our own laboratory with Beckman IR-20 Spectrophotometer using KBr pellete. Spectra of dyes and clay-dye complexes were recorded with KBr pellete at North Hill University, Shillong, Meghalay using instrument of Perkin Elmer, Model No. 297.

Effect of temperature on Adsorption

Adsorption experiments as described earlier were made in thermostatic shaker, at three different temperatures. The results are discussed in Chapter VII.

Measurement of concentration of the dyes

Quantity of adsorbed or exchanged dyes onto a clay from an aqueous solution was measured by determining with Graphicord, Model No. UV-240, double beam UV-VIS Spectrophotometer (Shimadzu, Japan) using cell of 1 cm path in the visible region, the amounts remaining in solution. In case of dimerisation of the dyes (Bergman and O'Konski, 1963) at higher concentration and salting out effect of the electrolytes at higher concentration, this measurement will be complicated. Beer's law was found through trial run to be applicable within 5% error at concentration below 8×10^{-6} (M) for RB, 9×10^{-6} (M) for RG and 6×10^{-6} (M) for BB. The measurements were made at wave lengths which showed maximum absorptions (λ-peaks) which were 525 nm for RG, 552 nm for RB, 640 nm for BB. Salt effects were noticed for electrolyte concentrations above 0.5(M). The absorption of these dyes by glass was another possible source of error. Hence the following measures were considered in carrying out adsorption and desorption studies of dyes.

(1) Polypropylene containers were used all along in carrying out the various experiments (3).

(2) The readings in Spectrophotometer were taken always after adequate dilution of the experimental solutions.

CHAPTER IV

Sorption and desorption and Rhodamine B and Rhodamine 6G on and from Na-montmorillonite System

Most of the work concerning sorption and desorption on clay minerals have been performed with montmorillonite because of its high exchange capacity and other interesting surface properties it exhibits. The uptake of a large amount of gases by montmorillonite-organic derivatives, due to the opening of their interlamellar spacings, has been shown by Barrer and his co-workers (1). The sedimentation volume and zeta potential measurements by Chakravarti (2) have shown that the maximum sedimentation volumes of Aquagel (montmorillonite) recorded by addition of quaternary ammonium salts, is obtained when the salt added is 75 to 80% of the base exchange capacity of the clay. Organic derivatives of montmorillonite exhibit organophilic characteristics and also water proofness, as observed by uptake of tolnene/water (3). In the context of the interaction with the organic substances the sorption and desorption characteristics of large dye molecules on and from the surface of montmorillonite are likely to be of interest.

A montmorillonite clay has been found advantageous for the investigation on the sorption and desorption of RG and RB due to its high exchange capacity and other interesting

surface properties. The sorption and desorption characteristics of RG and RB on and from Na-montmorillonite are discussed below.

The characteristics of sorption are presented in Section A and those of desorption in Section B. The experimental procedures for the studies of sorption and desorption have been described earlier (page 50-54, Chapter III). The clay used for this study was essentially pure montmorillonite as confirmed by X-ray diffraction analysis. Also in Section A, X-ray diffraction and Infrared studies of cationic dyes exchanged Na-montmorillonite has been discussed.

SECTION - A

Studies on Sorption

Sorption of Rhodamine 6G on Na-montmorillonite at pH 7:

The adsorption isotherm of RG on Na-montmorillonite at pH 7, and the corresponding reciprocal Langmuir plot is shown in Fig. 1a. The isotherm is of the H-type or high affinity class of Giles et al (4) and is indicative of species adsorbed flat on the surface. An H-type curve is a special case of the L-type, caused by a very high solute/substrate interaction. The adsorption data are seen to fit into the linear form of the Langmuir adsorption equation. Accordingly the plot of C/X vs C where C is the equilibrium concentration of RG and x is the amount adsorbed in meq per 100 gm of Na-clay, yields a good straight line (Fig. 1b). From the slope of the line, the value of V_m (the amount required to form a complete monolayer) is found to be 107 meq/100g, as against the c.e.c. of montmorillonite 86 meq/100g. The maximum amount of the dye adsorbed corresponding to the flat portion of the isotherm is 105 meq/100g. The excess uptake may be explained by assuming multilayer formation of the adsorbed dye molecules due to dye-dye interaction and sorption of aggregated cations(5) onto the montmorillonite surfaces. Since the dye molecules are not staggered and can approach each other close enough, the adsorption of the dyes on montmorillonite probably imparts greater mobility to bring them in optimum proximity and proper

orientation for micellisation. Besides, intercalation of the unionised dye molecules may also take place to account for the sorption beyond c.e.c. A similar observation was made by De et al (6) in their work on methylene blue, Crystal violet and malachite green. It is believed that the adsorption is mostly due to ionic and van der Waals forces upto the cation exchange capacity of the mineral and due solely to van der Waals forces beyond it.

The calculated Langmuir bonding constants of RG obtained from the slope and intercept of the linear plot is equal to $2.33 \times 10^{5} M^{-1}$. It should be pointed out that when adsorption is in excess of c.e.c. due to sorption of aggregated dye species, the original meaning of the calculated V_m and the Langmuir bonding constant is somewhat altered. Nevertheless, the latter parameter still gives some idea about the relative bonding strengths of adsorbents sorbed onto a particular substrate.

The sorption of dye molecules at low concentrations is almost complete, a strong adsorption of RG cations by Na-montmorillonite being thus indicated.

Sorption of Rhodamine B on Na-montmorillonite at pH 7

The adsorption isotherm of RG is like that of RG adsorption and is initially sharp due to strong affinity of

the dye for the montmorillonite surface (Fig. 8). The value of V_m calculated from the slope of the linear graph of C/x against C is 96 meq/100g. This is equal to the maximum of the adsorption isotherm and is also higher than the c.e.c. of Na-montmorillonite (86 meq/100g). The excess uptake may be on account of the sorption of the aggregated dye cations, micellisation of the dye cation on the surface of the mineral and the intercalation of the unionised dye molecules in the interlamellar spaces. The value of the Langmuir bonding constant computed from the linear plot is equal to $3.45 \times 10^{5} M^{-1}$.

It has been noted earlier that the c.e.c. of Na-montmorillonite is 86 meq/100g while the maximum adsorption of RG and RB onto the clay at 1.5×10^{-4} M equilibrium concentration of the dyes are 105 and 92 meq/100g respectively, which may be attributed to the shape and size of organic dye molecules resulting from the positional difference of alkyl substituents in two dyes. In general however, the adsorption of organic compounds increases with size of the ionsin smectite due to increased contribution of van der Waals forces to adsorption energy (7,8). This behaviour may also be attributed to the fact that the dimerisation or the aggregation tendency of RG is higher than that of RB at any specific value of concentration in solution and also in the adsorbed clay phase. As a consequnce

when adsorption takes place from their solutions RG is adsorbed with larger fraction of the aggregates than that of RB at any particular concentration, thus accounting for higher adsorption of RG. In fact the monomerdimer dissociation constant of RG and RB in aqueous medium determined by observed absorbance are 5.9×10^{-4} and 6.8×10^{-4} (9) respectively, which is in agreement with the above explanation.

X-ray diffraction studies on RG^+ and RB^+ exchanged Na-montmorillonite.

X-ray diffraction data has been obtained following the method given in Chapter - III, page 54 for different percentage of clay-dye saturated complex and clay itself. It indicates that the dye cation is intercalated by Na-montmorillonite. From the experimental results (Table 5) it is found that the d_{001} basal spacings of Na-montmorillonite (Fig. 15) and 25%, 50%, 75% and 100% RG - exchanged Na-montmorillonite (Fig. 16, 17) after heating at 120^{o}, show progressive interlayer penetration of the dye with sorption. Similarly gradual intercalation of RB dye with sorption is found for 25%, 50%, 75%, 100% RB - exchanged Na-montmorillonite (Fig. 18, 19) after heating at 120^{o}. Upto certain degree of saturation viz. 50%, a monolayer of RG and RB is formed in the interlayer space with the aromatic ring parallel to the aluminosilicate layer (10). At this stage there is no possibility for any kind of aggregation of the dye cations in the interlayer space. With large amounts of RG and RB, basal spacings data indicates the presence of multilayer or tilting of the cationic dyes relative to the aluminosilicate layer (10). Under such conditions it may be possible that the interlayer space is populated by aggregates of the cationic dyes.

Infrared Spectral studies on RG^+ and RB^+ exchanged Na-montmorillonite.

The infrared spectra of Na-montmorillonite, RG, RB, 100% RG - exchanged and 100% RB - exchanged Na-montmorillonite are represented in Fig. 20-24) respectively. The infrared spectra have been recorded following the method given in Chapter - III, page 55. The infrared spectrum of RG (Fig. 21) shows the characteristic ring vibration band at 1580 cm^{-1} which has been shifted to 1610 cm^{-1} in case of 100% RG - exchanged Na-montmorillonite (Fig. 23). This type of shifting of the band may be attributed to the aggregation of the cationic dye in the interlayer space (11). In case of RB (Fig. 22) however, this band appears at 1602 cm^{-1} which has been shifted to 1590 cm^{-1} (Fig. 24).

SECTION - B

Desorption Studies

The desorption of the dyes from the clay complexes shows the extent to which the dyes are replaceable from the clay matrics and also the selectivities of different ions in the process. For the study of desorption process the experimental procedures have been described earlier (page 52, Chapter -III).

Desorption of Rhodamine 6G:

The results of desorption of RG from Na-montmorillonite RG complex by inorganic and organic ions are given in Figs. 2-6.

Adsorption of RG on montmorillonite is known to proceed through ion exchange process (12). So it is possible that desorption should also be an ion exchange process. Accordingly an exchange equilibrium,

$$\bar{D}^+ + \frac{1}{Z} i^{Z+} \rightleftharpoons \frac{1}{Z} \bar{i}^{Z+} + D^+$$

may be assumed where D stands for the dye, the bar denotes the species in the clay phase and Z is the valency of the desorbing ion i. The selectivity coefficient is given by

$$K_D^i = \frac{[i^{z+}]^{1/z}[D^+]}{[D^+][i^{z+}]^{1/z}}$$

where the bracket means the concentration of the enclosed substances.

The concentration used to calculate K_D^i are expressed in moles/dm^{-3} for the liquid phase. Since the values of the activity coefficient of Rhodamine ions are not available in literature, the concentrations of the ions have been employed in the present work to calculate the selectivity coefficients and so, the values are somewhat approximate.

The distribution coefficients have been calculated according to the equation

$$\lambda_i = \frac{\bar{m}_i}{m_i}$$

where $\bar{m}_i$ and m_i are the molal concentrations of the species i in the solid and liquid phases respectively.

The values of distribution coefficients and selectivity coefficients as obtained by using the above relations for RG are given in Table 6.

The selectivity coefficient is a measure of the preference of the desorbing species i with respect to the dye for the mineral surface. If the value is less than 1.0, the

species i has smaller affinity for the clay surface than the dye. If it is greater than 1.0, which is very rarely observed, both the species will have equal affinities for the exchanger. It is, however, not a constant quantity and varies with the concentration of the species.

The values of the selectivity coefficient of the desorbing inorganic ions are less than 1.0 suggesting that RG ions are much preferred by montmorillonite to the monovalent and divalent ions. By reasons of their comparatively small sizes, these ions are unable to dislodge the sorbed dye ions from the clay matrix effectively. The selectivity coefficients of the inorganic ions may be placed in the order : $Na^+ \angle Li^+ \lesssim K^+ \angle NH_4^+ \angle Rb^+ \angle Cs^+$ for the monovalent cations and $Mg^{2+} \angle Ca^{2+} \angle Sr^{2+} \angle Ba^{2+}$ for the bivalent cations. The selectivity reversal of Li^+ and Na^+; a deviation from the general Lyotrope series, is to be noted. However, this similarity has also been noticed by Gieseking and Jenny (13) on putnam clay (beidellite) and Das Kanungo and Chakravarti (14) in the desorption of Mg^{2+} ions from Mg-bentonite.

The distribution and selectivity coefficients of the monovalent organic ionsare in the sequence: Tetrabutyl ammonium (TBA^+) $\rangle$ tetrapropyl ammonium (TPA^+) $\rangle$ tetraethyl ammonium (TEA^+) $\rangle$ tetramethyl ammonium (TMA^+) for the tetraalkyl ammonium halides and cetyepyridinium (CP^+) $\rangle$ Cetyltrimethyl ammonium ($CTMA^+$) $\rangle$ dodecyl pyridinium (DDP^+) $\rangle$ dodecyl trimethyl ammonium ($DDTMA^+$)

for the long-chain surface active agents. It has been found that large organic cations are of greater efficiency than that of the inorganic ions in desorbing RG from its Na-montmorillonite complex. The selectivity coefficient with most of the desorbing organic ions are greater than unity, the preference of these ions to the dye cation by the clay surface being thus indicated.

The exchange isotherms of RG from its Na-montmorillonite complex by various organic ions are shown in Figs. 4,5,6. It is found that in each case the extent of desorption increases with chain length of the organic ions, this may be due to the increased contribution of van der Waals forces to the adsorption energy (7,8) as well as to the change in the hydration status of the ions in the clay interlayer. Such exchange behaviour would, however, be expected for a flat orientation of the ions at the clay surface as van der Waals type of interactions are additive and therefore would increase with the size of the interacting species. It is interesting that the extent of the dye released from the clay matrix is higher with comparatively smaller $(C_4H_9)_4N^+$ ions than with the larger CP^+ or CTA^+. This can be explained from the covering up effect of some of the exchange sites by the larger surface active ions lying flat on the surface (15) and consequently a fraction of RG^+ initially adsorbed by the clay remaining unavailable for exchange. Further, among the surfactants the relative exchanging efficiency $DDTMA^+ \angle$ $DDP^+ \angle$ $CTMA^+ \angle$ CP^+ may be related to their decreasing critical

micelle concentration (cmc) values (16) which are 1.5×10^{-2}, 1.5×10^{-2}, 9.2×10^{-4}, 9.0×10^{-4} (M) respectively at 25^{o}C.

Although all the exchange isotherms are of the L type the desorption isotherm obtained with $DDTMA^{+}$ is of the 'C' type and those with TEA^{+}, TPA^{+}, $CTMA^{+}$ and CP^{+} belong to the 'S' type in the classifications of isotherms of Giles et al (4). The C-type of curve was also observed by Greenland et al (17) in the adsorption studies of amino acids and peptides from water on Ca-montmorillonite and Sarkar and Das Kanungo (18) in the desorption of tris-trimethylene diamine Co(III) i.e. $Co(tn)_3^{3+}$, from its Na-bentonite complex by 1,3, propanediammonium chloride. This type of curve represents constant partition between the solution and surface suggesting that new sites become available as solute is taken up by the microporous substrate and adsorption is always proportional to the solute concentration. De et al (6,19) earlier observed S-type of isotherms in the desorption of cationic dyes by CTA^{+} and CP^{+} from clay-dye complexes. Usually the S-curve indicates 'Co-operative' adsorption with solute molecules tending to be adsorbed or paced in rows or clusters. The converse however does not necessarily apply. In the S-curve the slope at first increases with concentration because sites capable of retaining a solute molecule increase in co-operative adsorption but eventually, the slope falls and becomes nil at the saturation

point when no vacant sites remain. This may explain the S-group of curves as obtained in the desorption of RG with TEA^+, TPA^+, $CTMA^+$ and CP^+. Recent study by Giles et al (20) shows that S-curve occurs when the activation energy for the desorption of the solute is concentration dependent, and/or is markedly reduced by large negative contributions of the solvent or a second solute. The higher value of selectivity coefficient of monovalent long-chain surface active ions indicates their preference by the clay matrix. This can be explained in terms of the shape and size of these ions and degree of van der Waals contact between organic ions and the montmorillonite surface. Greenland et al (21) have illustrated the importance of the shape and size of the organic cations in determining the extent of van der Waals contact with the clay surface. The contribution of van der Waals force to adsorption energy would be greater of these ions which are in closest contact with the surface, or enable close contact to be maintained with the adjacent adsorbed ions. For the straight chain larger organic ions like CP^+ or $CTMA^+$, the size is more important than charge in determining their preference for the aluminosilicate surface because the dispersion forces increase significantly with the length of the carbon chain. Moreover, the solubility of the organic cations in water decreases with the size of the ions, and, so large ions once adsorbed, have a lower tendency to return to

the solution phase (22).

An attempt has been made to correlate the selectivity coefficient of the inorganic ions, which gives a relative measure of the affinities of the ions for the clay surface, with some other properties of the ions, viz. hydrated ionic radius (23) and the parameter, a^{o}, (24) of the Debye Huckel equation,

$$-\log \gamma_{\pm} = \frac{AZ_{+}Z_{-}\sqrt{\mu}}{1+Ba^{o}\sqrt{\mu}}$$

where the symbols have their usual significance. In Fig. 7 the plot of selectivity coefficients with hydrated ionic radii and the reciprocal of a^{o} i.e. the distance of closest approach of the two ions have been shown. The latter plot has been done on the basis of the simple electrostatic ion-exchange model of Pauley (25), which assumes that coulombic forces play the main role in the interaction between the counter ions and the charged clay surface and that the counter ions in the ion exchange are found at their distance of closest approach to the fixed ionic groups.

It may be noticed from the plot of log (selectivity coefficient) vs hydrated ionic radius (23) of the monovalent

ions (Fig. 7) that K^+, NH_4^+, Rb^+ and Cs^+ are more strongly attached to the clay surface that what should normally be expected of them from the values of their hydrated ionic radii. In comparison with Li^+ and Na^+, a distinct fixation tendency of these ions for the montmorillonite surface is indicated. It had been thought earlier that for such a selective sorption/fixation of these ions are due to their close fit within the hexagonal cavities of basal oxygen planes (26,27,28) but the recent works of Shainberg and Kemper (29) and Kittrick (30) show that low hydration energy of the ionsis the major factor in cation selectivity and fixation. Smaller the hydration energy, greater is the fixation tendency of the ion. Having the least hydration energy, Cs^+ is adsorbed the most. Further K^+, NH_4^+, Rb^+, Cs^+ having low hydration energy produce interlayer dehydration and layer collapse and are, therefore, fixed in interlayer position, while cations with high hydration energy such as Li^+, Na^+, Ca^{2+}, Mg^{2+}, Sr^{2+} and Ba^{2+} produce expanded interlayers and are not fixed (38). If $1/a^o$ of the alkali metal chlorides (24) is plotted against log (selectivity coefficient) a linear relationship is obtained as shown in Fig. 7 with alkaline earth metal chlorides both the hydrated ionic radius and $1/a^o$ yield straight lines with the selectivity coefficients (Fig. 7) . From the Fig. 7 the displacement of RG

from clay-complex by alkali metal chlorides $1/a^{o}$ may be used to correlate and predict the relative affinities of the ions for the mineral while for the alkaline earth metal chlorides both hydrated ionic radii and $1/a^{o}$ value may be used for the purpose. The non linearity of the plot of log (selectivity coefficient) against hydrated ionic radius of the alkali cations may be attributed to the unequal fixation tendencies of these ions in the clay structure.

Plot of log (selectivity coefficient) with hydrated ionic radius may be utilised to detect ion fixation within the same valency type vis-a-vis layer collapse in ion exchangers especially in expanding type clay minerals. Further more the obedience of the desorption data in accordance with the Pauley's model suggests that coulombic forces play the major role in the interaction between the counter ions and the charged exchanger surface.

Desorption of RB

The results of desorption isotherms of RB from RB - Na montmorillonite complex is shown in Figs. 9-13 and calculated distribution and selectivity coefficients of the various electrolytes are recorded in Table 7. Desorption curves for inorganic and organic ions are similar in nature to those obtained in the case of Na-montmorillonite-RG complex of RG desorption from the clay complex but the extent of desorption

with monovalent and bivalent inorganic ions is smaller. The order of preference of the ions according to their performance as desorbing agent:

(a) $Li^+ \leqslant Na^+ < K^+ < NH_4^+ < Rb^+ < Cs^+$

(b) $Mg^{2+} < Ca^{2+} < Sr^{2+} < Ba^{2+}$

(c) $TMA^+ < TEA^+ < TPA^+ < TBA^+$

(d) $DDTMA^+ < DDP^+ < CTMA^+ < CP^+$

Compared to the inorganic ions, the percentage of exchange of the adsorbed dye with the organic ions are much higher and increases with size of ions. This is also reflected in the higher values of the selectivity and distribution coefficients (Table 7) of the latter ions. Here also the desorption curves with TEA^+, TPA^+, TBA^+, $CTMA^+$ and CP^+ are S-shaped and may be explained in similar manner (as in page 69-70).

The plot of log (selectivity coefficient) against $1/a^o$ of the alkali metal chlorides gives linear relationship while similar plot against hydrated ionic radius of the ions is not linear. For the alkaline earth metal chlorides however both the parameters yield straight lines. Same result also has been found in Na-montmorillonite RG systems and so similar conclusion may be drawn from the plots as in pages 72-73.

It can be observed from the desorption isotherms that the percentage of RG desorbed as well as the calculated distribution and selectivity coefficients are higher than those of RB. The order of bonding strength of the dyes is, therefore, RB $>$ RG, whihh is in the reverse order of their desorption. This is also reflected in the computed Langmuir bonding constants for the two adsorption isotherms which are $2.33 \times 10^{5} M^{-1}$ for RG and $3.45 \times 10^{5} M^{-1}$ for RB. The higher value of the constant is suggestive of a stronger binding of RB in Na-montmorillonite as the Langmuir bonding constant is directly proportional to the heat of adsorption (31).

TABLE -5

Basal Spacings (in A^{o}) of Na-montmorillonite treated with RG and RB as computed from the X-ray Diffraction Spectra (Fig. 15-19)

Name of the Dye	% Sorbed	d_{001}
	0	11.024
RG	25	13.929
	50	13.810
	75	14.255
	100	15.781
	0	11.024
RB	25	14.489
	50	14.372
	75	16.994
	100	17.327

TABLE 6

Desorption characteristics of RG from Na-montmorillonite-RG with respect to different ions.

Electrolytes used	Concentration of Electrolyte	Distribution Coefficient	Selectivity Coefficient
1:1 Electrolyte			
	0.1 (M)	0.046	1.31×10^{-7}
LiCl	0.2 (M)	0.033	1.36×10^{-7}
	0.3 (M)	0.026	1.30×10^{-7}
	0.5 (M	0.019	1.19×10^{-7}
	0.75 (M)	0.014	9.50×10^{-8}
	0.1 (M)	0.033	6.79×10^{-8}
NaCl	0.2 (M)	0.026	8.24×10^{-8}
	0.3 (M)	0.020	7.64×10^{-8}
	0.5 (M)	0.014	6.41×10^{-8}
	0.75 (M)	0.0099	4.50×10^{-8}
	0.1 (M)	0.049	1.45×10^{-7}
KCl	0.2 (M)	0.037	1.68×10^{-7}
	0.3 (M)	0.027	1.42×10^{-7}
	0.5 (M)	0.019	1.19×10^{-7}
	0.75 (M)	0.014	9.84×10^{-8}

Contd..

TABLE - 6 (Contd..)

Electrolyte used	Concentration of Electrolyte	Distribution Coefficient	Selectivity Coefficient
NH_4Cl	0.1 (M)	0.060	2.15×10^{-7}
	0.2 (M)	0.042	2.23×10^{-7}
	0.3 (M)	0.033	2.20×10^{-7}
	0.5 (M)	0.023	1.68×10^{-7}
	0.75 (M)	0.017	1.43×10^{-7}
RbCl	0.1 (M)	0.109	7.38×10^{-7}
	0.2 (M)	0.074	6.83×10^{-7}
	0.3 (M)	0.062	7.16×10^{-7}
	0.5 (M)	0.047	6.98×10^{-7}
	0.75 (M)	0.036	6.19×10^{-7}
CsCl	0.1 (M)	0.147	1.33×10^{-6}
	0.2 (M)	0.102	1.30×10^{-6}
	0.3 (M)	0.080	1.22×10^{-6}
	0.5 (M)	0.060	1.12×10^{-6}
	0.75 (M)	0.044	9.62×10^{-7}

Contd..

TABLE - 6 (Contd..)

Electrolyte used	Concentration of Electrolyte	Distribution Coefficient	Selectivity Coefficient
2:1 Electrolyte			
$MgCl_2$	0.05 (M)	0.410	2.11×10^{-6}
	0.1 (M)	0.354	2.72×10^{-6}
	0.2 (M)	0.280	2.73×10^{-6}
	0.3 (M)	0.238	2.50×10^{-6}
	0.4 (M)	0.210	2.26×10^{-6}
$CaCl_2$	0.05 (M)	0.440	2.60×10^{-6}
	0.1 (M)	0.360	2.84×10^{-6}
	0.2 (M)	0.287	2.93×10^{-6}
	0.3 (M)	0.238	2.50×10^{-6}
	0.4 (M)	0.211	2.34×10^{-6}
$SrCl_2$	0.05 (M)	0.487	3.56×10^{-6}
	0.1 (M)	0.381	3.40×10^{-6}
	0.2 (M)	0.302	3.44×10^{-6}
	0.3 (M)	0.250	2.93×10^{-6}
	0.4 (M)	0.222	2.72×10^{-6}

Contd..

TABLE - 6 (Contd..)

Electrolytes used	Concentration of Electrolyte	Distribution Coefficient	Selectivity Coefficient
$BaCl_2$	0.05 (M)	0.498	3.80×10^{-6}
	0.1 (M)	0.385	3.54×10^{-6}
	0.2 (M)	0.302	3.45×10^{-6}
	0.3 (M)	0.258	3.23×10^{-6}
	0.4 (M)	0.228	2.96×10^{-6}
Quaternary Ammonium Salt			
TMABr	0.05 (M)	0.149	6.73×10^{-7}
	0.1 (M)	0.136	6.95×10^{-7}
	0.2 (M)	0.121	1.83×10^{-6}
	0.3 (M)	0.105	2.11×10^{-6}
	0.4 (M)	0.093	2.21×10^{-6}
TEABr	0.05 (M)	0.248	1.88×10^{-6}
	0.1 (M)	0.186	2.14×10^{-6}
	0.2 (M)	0.179	4.13×10^{-6}
	0.3 (M)	0.170	5.65×10^{-6}
	0.4 (M)	0.170	8.17×10^{-6}

TABLE - 6 (Contd..)

Electrolyte used	Concentration of Electrolyte	Distribution Coefficient	Selectivity Coefficient
TPABr	0.05 (M)	0.347	3.73×10^{-6}
	0.1 (M)	0.304	5.85×10^{-6}
	0.2 (M)	0.260	8.92×10^{-6}
	0.3 (M)	0.235	1.13×10^{-5}
	0.4 (M)	0.217	1.32×10^{-5}
TBABr	0.05 (M)	1.736	1.05×10^{-4}
	0.1 (M)	1.241	1.15×10^{-4}
	0.2 (M)	0.880	1.30×10^{-4}
	0.3 (M)	0.694	1.31×10^{-4}
	0.4 (M)	0.558	1.17×10^{-4}
DDTMABr	2×10^{-4} (M)	63.468	4.83×10^{-4}
	4×10^{-4} (M)	64.225	1.00×10^{-3}
	6×10^{-4} (M)	66.296	1.69×10^{-3}
	8×10^{-4} (M)	62.143	2.01×10^{-3}
	1×10^{-3} (M)	62.186	2.58×10^{-3}

TABLE - 6 (Contd..)

Electrolyte used	Concentration of Electrolyte	Distribution Coefficient	Selectivity Coefficient
CTMABr	2×10^{-4} (M)	379.79	1.94×10^{-2}
	4×10^{-4} (M)	413.33	5.42×10^{-2}
	6×10^{-4} (M)	390.91	8.64×10^{-2}
	8×10^{-4} (M)	357.87	1.12×10^{-1}
	1×10^{-3} (M)	318.14	1.22×10^{-1}
DDPBr	1×10^{-4} (M)	130.32	9.94×10^{-4}
	2×10^{-4} (M)	96.37	1.11×10^{-3}
	3×10^{-4} (M)	104.02	2.04×10^{-3}
	4×10^{-4} (M)	93.46	2.22×10^{-3}
	5×10^{-4} (M)	99.60	3.23×10^{-3}
CPBr	1×10^{-4} (M)	1484.04	1.60×10^{-1}
	2×10^{-4} (M)	1142.10	2.29×10^{-1}
	3×10^{-4} (M)	936.24	2.88×10^{-1}
	4×10^{-4} (M)	833.41	3.57×10^{-1}
	5×10^{-4} (M)	734.53	3.94×10^{-1}

TABLE - 7

Desorption characteristics of RB from Na-montmorillonite-RB with respect to different ions.

Electrolyte used	Concentration of Electrolyte	Distribution Coefficient	Selectivity Coefficient
1:1 Electrolyte			
LiCl	0.1 (M)	0.030	5.52×10^{-8}
	0.2 (M)	0.022	6.06×10^{-8}
	0.3 (M)	0.017	5.72×10^{-8}
	0.5 (M)	0.012	4.61×10^{-8}
	0.75 (M)	0.0084	3.20×10^{-8}
NaCl	0.1 (M)	0.036	7.96×10^{-8}
	0.2 (M)	0.023	6.39×10^{-8}
	0.3 (M)	0.017	5.72×10^{-8}
	0.5 (M)	0.012	4.26×10^{-8}
	0.75 (M)	0.0081	2.95×10^{-8}
KCl	0.1 (M)	0.042	1.08×10^{-7}
	0.2 (M)	0.026	8.58×10^{-8}
	0.3 (M)	0.020	7.68×10^{-8}
	0.5 (M)	0.015	7.52×10^{-8}
	0.75 (M)	0.011	5.82×10^{-8}

TABLE -7 (Contd..)

Electrolyte used	Concentration of Electrolyte	Distribution Coefficient	Selectivity Coefficient
NH_4Cl	0.1 (M)	0.053	1.71×10^{-7}
	0.2 (M)	0.034	1.44×10^{-7}
	0.3 (M)	0.025	1.14×10^{-7}
	0.5 (M)	0.015	7.29×10^{-8}
	0.75 (M)	0.011	5.82×10^{-8}
RbCl	0.1 (M)	0.091	5.02×10^{-7}
	0.2 (M)	0.054	3.53×10^{-7}
	0.3 (M)	0.037	2.58×10^{-7}
	0.5 (M)	0.024	1.75×10^{-7}
	0.75 (M)	0.016	1.19×10^{-7}
CsCl	0.1 (M)	0.101	6.15×10^{-7}
	0.2 (M)	0.057	3.95×10^{-7}
	0.3 (M)	0.040	2.98×10^{-7}
	0.5 (M)	0.025	1.94×10^{-7}
	0.75 (M)	0.017	1.31×10^{-7}

TABLE - 7 (Contd..)

Electrolyte used	Concentration of Electrolyte	Distribution Coefficient	Selectivity Coefficient
2:1 Electrolyte			
$MgCl_2$	0.05 (M)	0.340	1.18×10^{-6}
	0.1 (M)	0.277	1.27×10^{-6}
	0.2 (M)	0.201	9.77×10^{-7}
	0.3 (M)	0.166	8.25×10^{-7}
	0.4 (M)	0.146	7.46×10^{-7}
$CaCl_2$	0.05 (M)	0.382	1.67×10^{-6}
	0.1 (M)	0.282	1.35×10^{-6}
	0.2 (M)	0.208	1.09×10^{-6}
	0.3 (M)	0.173	9.27×10^{-7}
	0.4 (M)	0.150	8.20×10^{-7}
$SrCl_2$	0.05 (M)	0.398	1.88×10^{-6}
	0.1 (M)	0.294	1.52×10^{-6}
	0.2 (M)	0.216	1.22×10^{-6}
	0.3 (M)	0.180	1.06×10^{-6}
	0.4 (M)	0.157	9.31×10^{-7}

TABLE - 7 (Contd..)

Electrolyte used	Concentration of Electrolyte	Distribution Coefficient	Selectivity Coefficient
	0.05 (M)	0.413	2.11×10^{-6}
$BaCl_2$	0.1 (M)	0.303	1.67×10^{-6}
	0.2 (M)	0.221	1.30×10^{-6}
	0.3 (M)	0.183	1.11×10^{-6}
	0.4 (M)	0.160	9.84×10^{-7}
Quaternary Ammonium Salt			
	0.05 (M)	0.103	3.20×10^{-7}
TMABr	0.1 (M)	0.061	2.26×10^{-7}
	0.2 (M)	0.045	2.50×10^{-7}
	0.3 (M)	0.036	2.41×10^{-7}
	0.4 (M)	0.028	2.02×10^{-7}
	0.05 (M)	0.170	8.73×10^{-7}
TEABr	0.1 (M)	0.134	1.08×10^{-6}
	0.2 (M)	0.097	1.16×10^{-6}
	0.3 (M)	0.085	1.34×10^{-6}
	0.4 (M)	0.077	1.50×10^{-6}

TABLE - 7 (Contd..)

Electrolyte used	Concentration of Electrolyte	Distribution Coefficient	Selectivity Coefficient
	0.05 (M)	0.183	1.00×10^{-6}
TPABr	0.1 (M)	0.170	1.77×10^{-6}
	0.2 (M)	0.167	2.02×10^{-6}
	0.3 (M)	0.157	4.76×10^{-6}
	0.4 (M)	0.152	6.10×10^{-6}
	0.05 (M)	0.640	1.27×10^{-5}
TBABr	0.1 (M)	0.457	1.33×10^{-5}
	0.2 (M)	0.343	1.56×10^{-5}
	0.3 (M)	0.264	1.42×10^{-5}
	0.4 (M)	0.259	1.91×10^{-5}
	2×10^{-4} (M)	37.15	1.62×10^{-4}
DDTMABr	4×10^{-4} (M)	34.35	2.78×10^{-4}
	6×10^{-4} (M)	35.15	4.44×10^{-4}
	8×10^{-4} (M)	32.43	5.11×10^{-4}
	1×10^{-3} (M)	37.95	8.10×10^{-4}

TABLE - 7 (Contd..)

Electrolyte used	Concentration of Electrolyte	Distribution Coefficient	Selectivity Coefficient
CTMABr	2×10^{-4} (M)	353.15	1.57×10^{-2}
	4×10^{-4} (M)	325.33	3.07×10^{-2}
	6×10^{-4} (M)	254.33	2.98×10^{-2}
	8×10^{-4} (M)	206.93	2.72×10^{-2}
	1×10^{-3} (M)	196.55	2.89×10^{-2}
DDPBr	1×10^{-4} (M)	81.33	3.50×10^{-4}
	2×10^{-4} (M)	70.63	5.71×10^{-4}
	3×10^{-4} (M)	67.31	8.01×10^{-4}
	4×10^{-4} (M)	65.69	1.03×10^{-3}
	5×10^{-4} (M)	62.24	1.17×10^{-3}
CPBr	1×10^{-4} (M)	501.55	1.44×10^{-2}
	2×10^{-4} (M)	385.26	1.89×10^{-2}
	3×10^{-4} (M)	319.72	2.06×10^{-2}
	4×10^{-4} (M)	281.53	2.22×10^{-2}
	5×10^{-4} (M)	248.97	2.24×10^{-2}

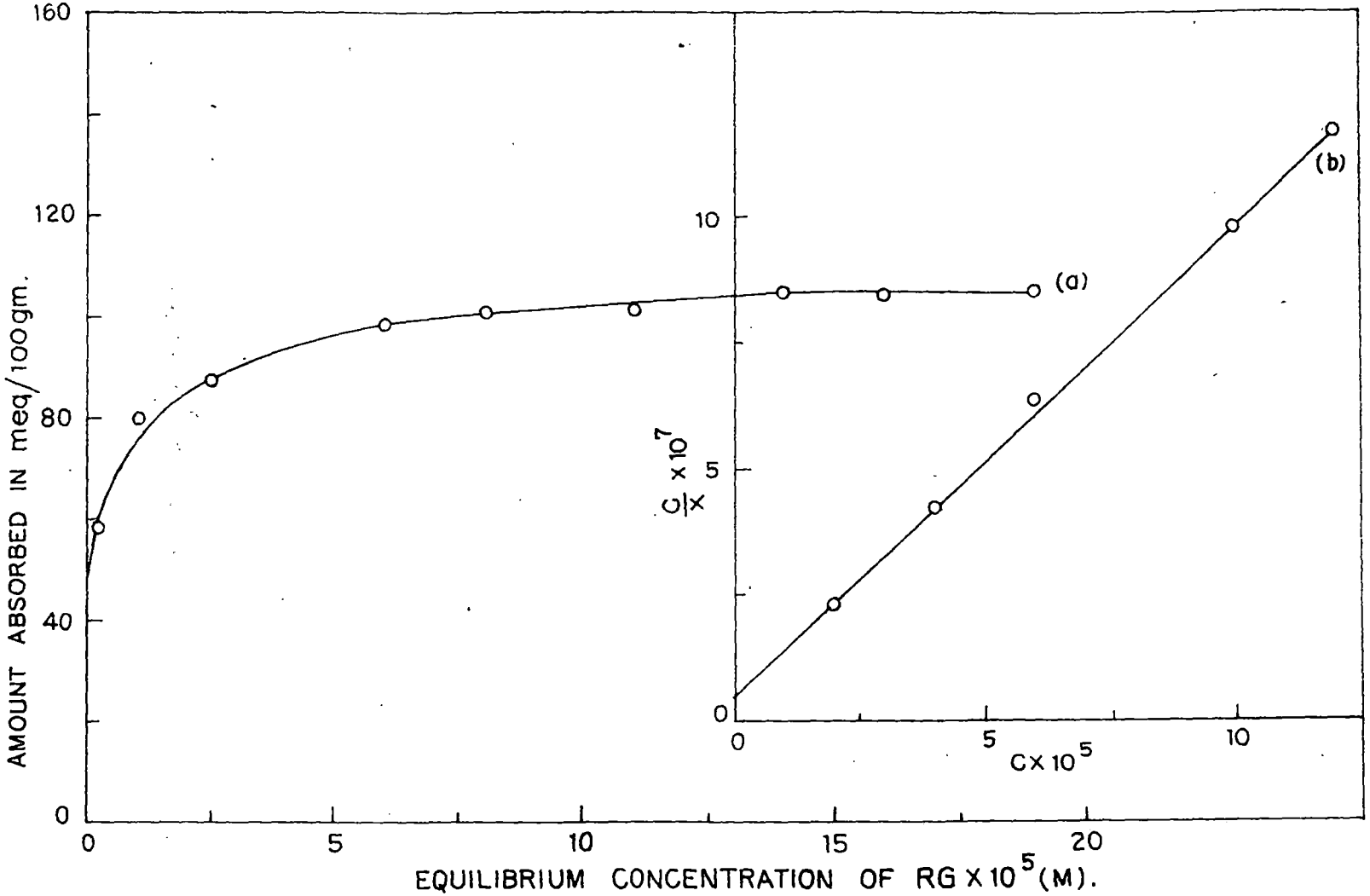

FIG. 1. ADSORPTION ISOTHERM AT 28°C (a) AND LANGMUIR PLOT (b) OF RG ON Na-MONTMORILLONITE

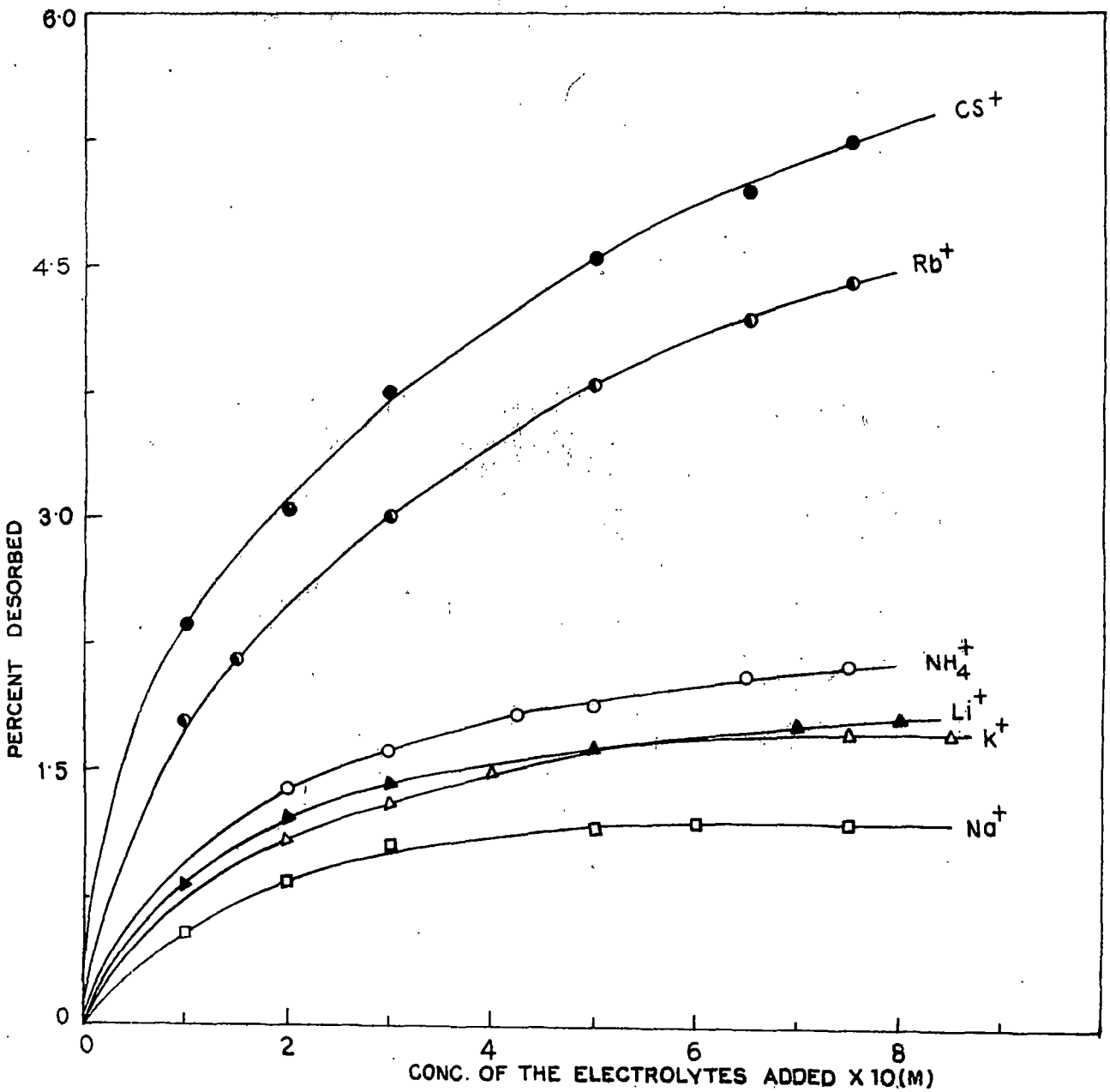

FIG. 2. DESORPTION OF RG FROM Na-MONTMORILLONITE-RG BY VARIOUS MONOVALENT IONS.

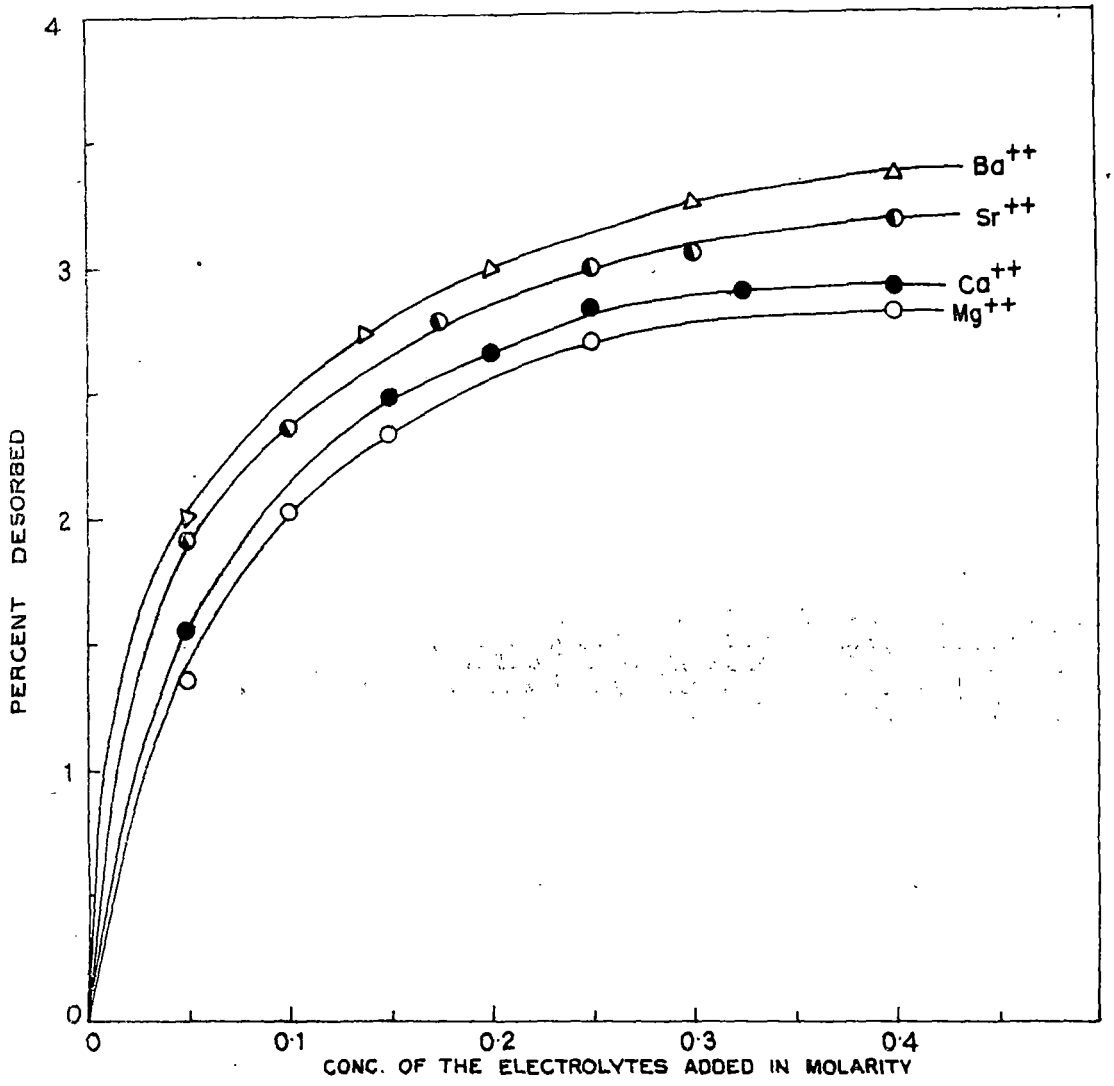

FIG. 3. DESORPTION OF RG FROM Na-MONTMORILLONITE-RG BY VARIOUS BIVALENT IONS.

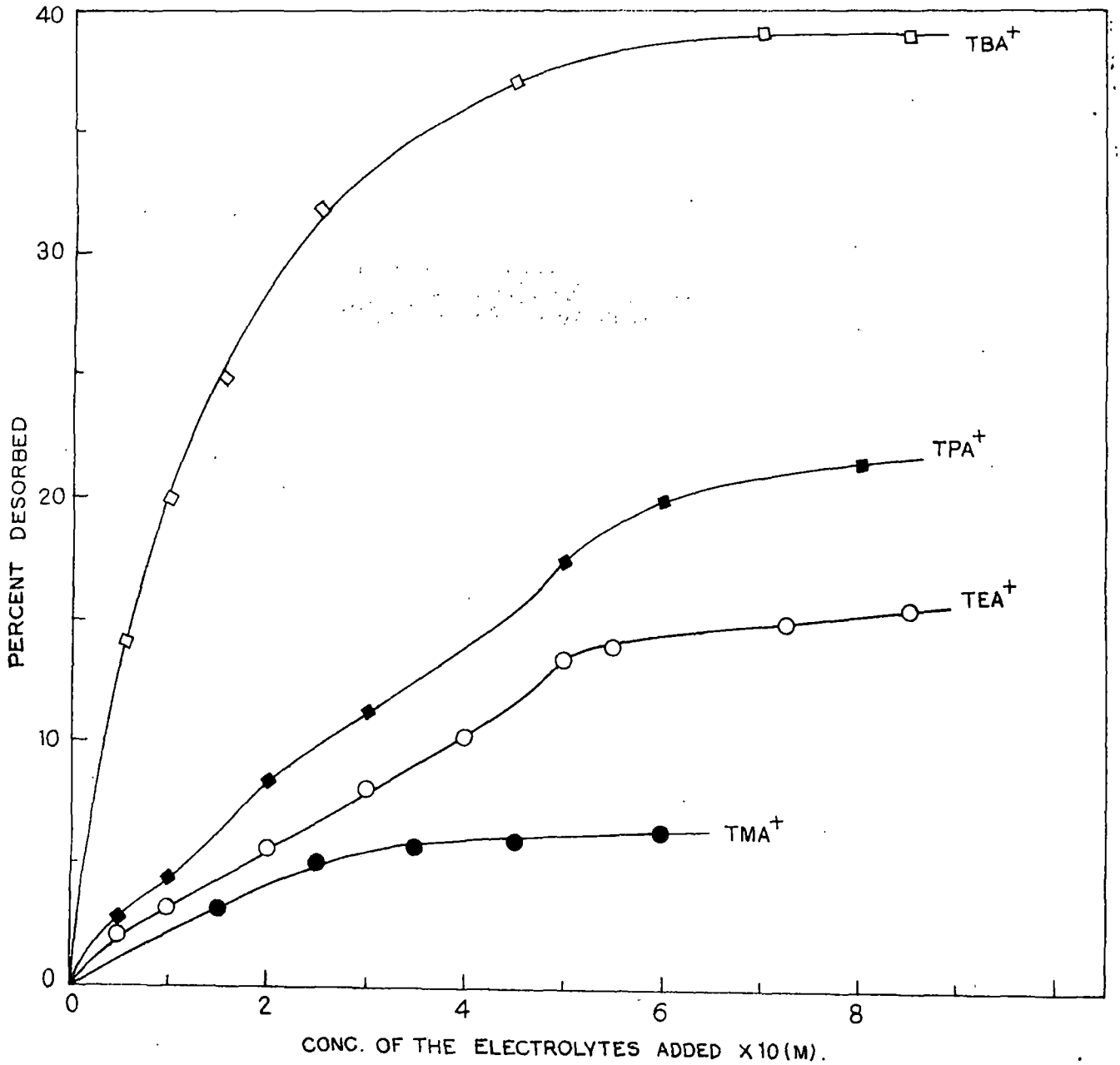

FIG. 4. DESORPTION OF RG FROM Na-MONTMORILLONITE-RG BY VARIOUS TETRA ALKYLAMMONIUM HALIDES.

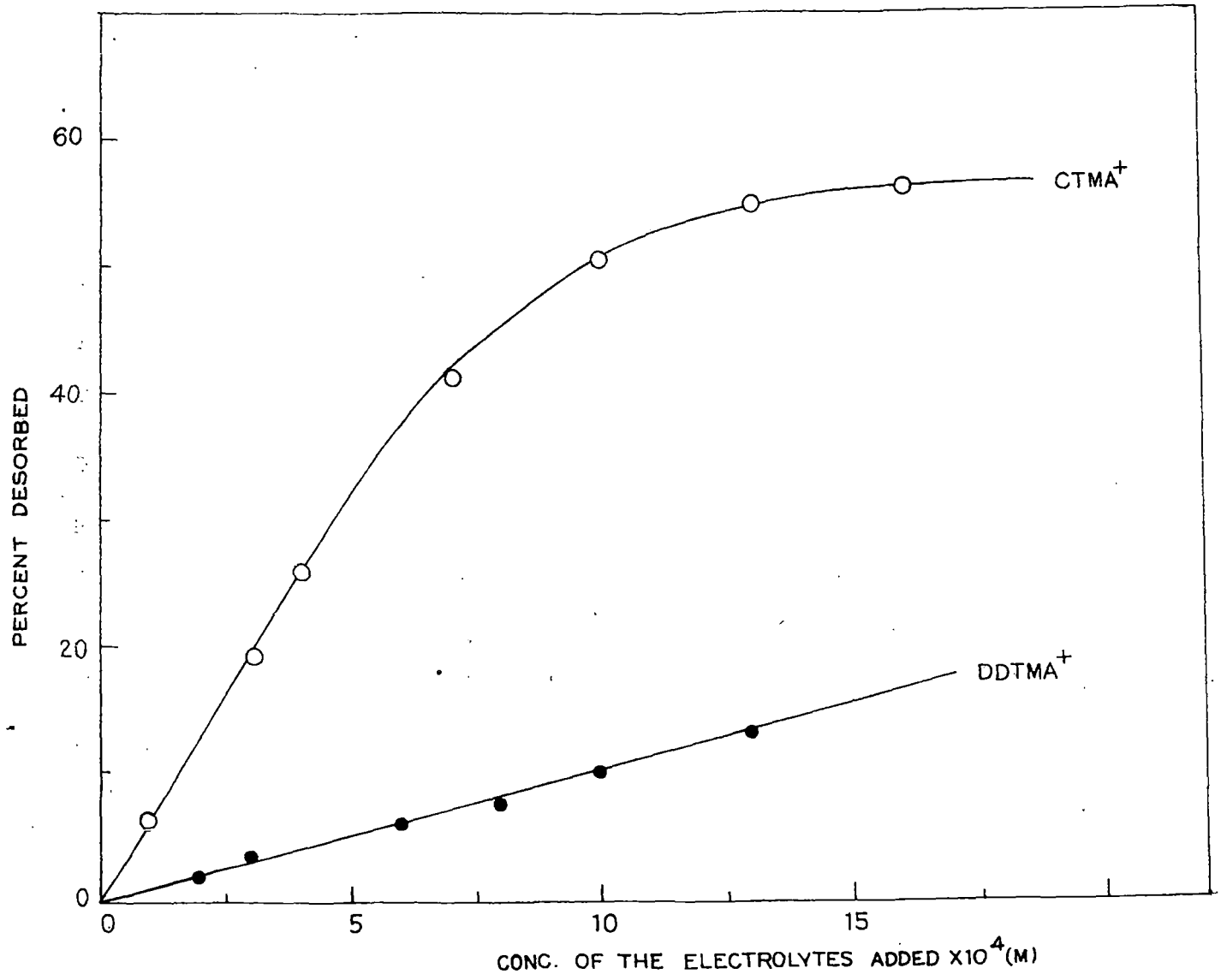

FIG. 5. DESORPTION OF RG FROM Na-MONTMORILLONITE-RG BY VARIOUS LONG-CHAIN SURFACE ACTIVE ALKYLTRIMETHYL AMMONIUM HALIDES.

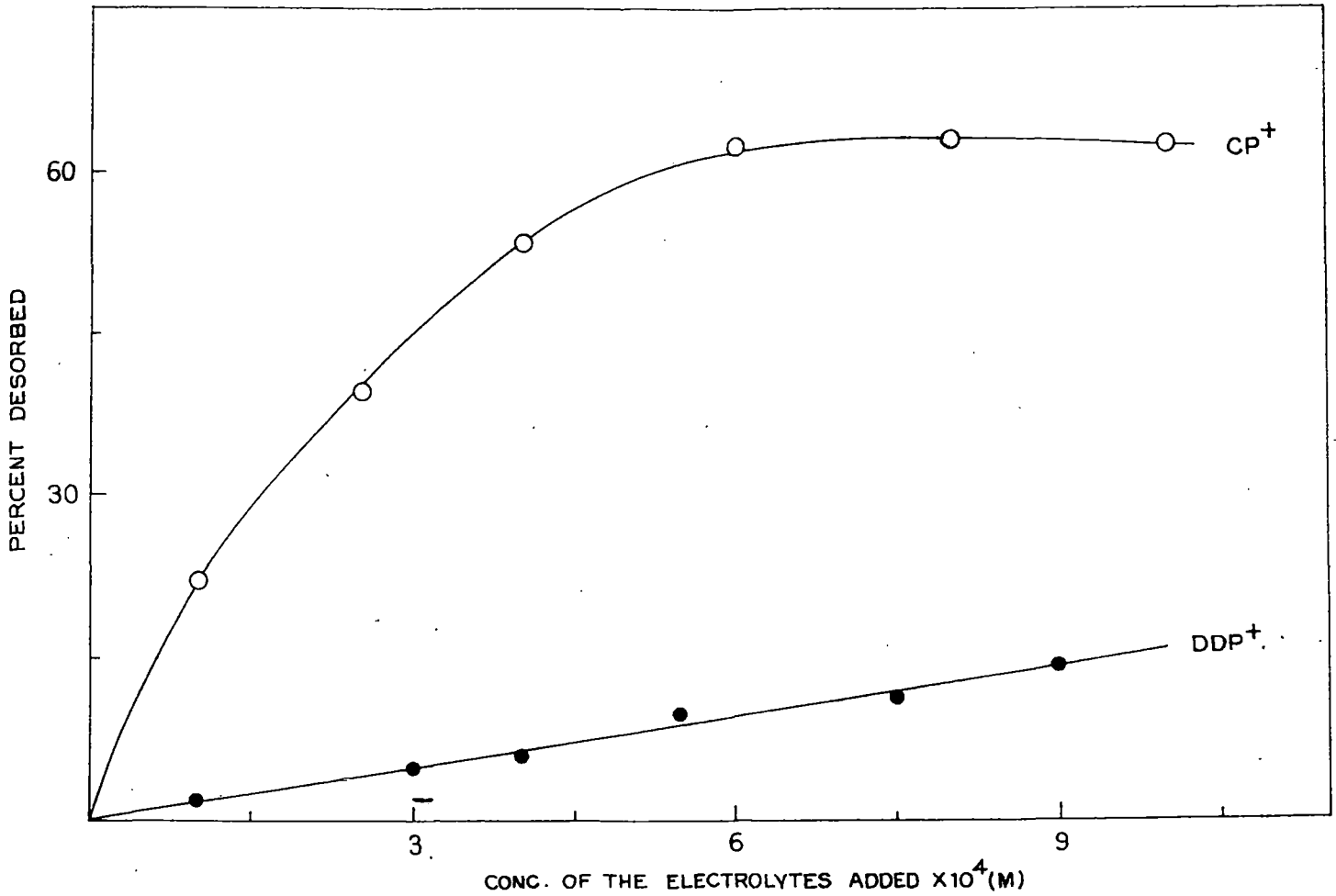

FIG. 6. DESORPTION OF RG FROM Na-MONTMORILLONITE-RG BY VARIOUS LONG-CHAIN SURFACE ACTIVE ALKYLPYRIDINIUM HALIDES.

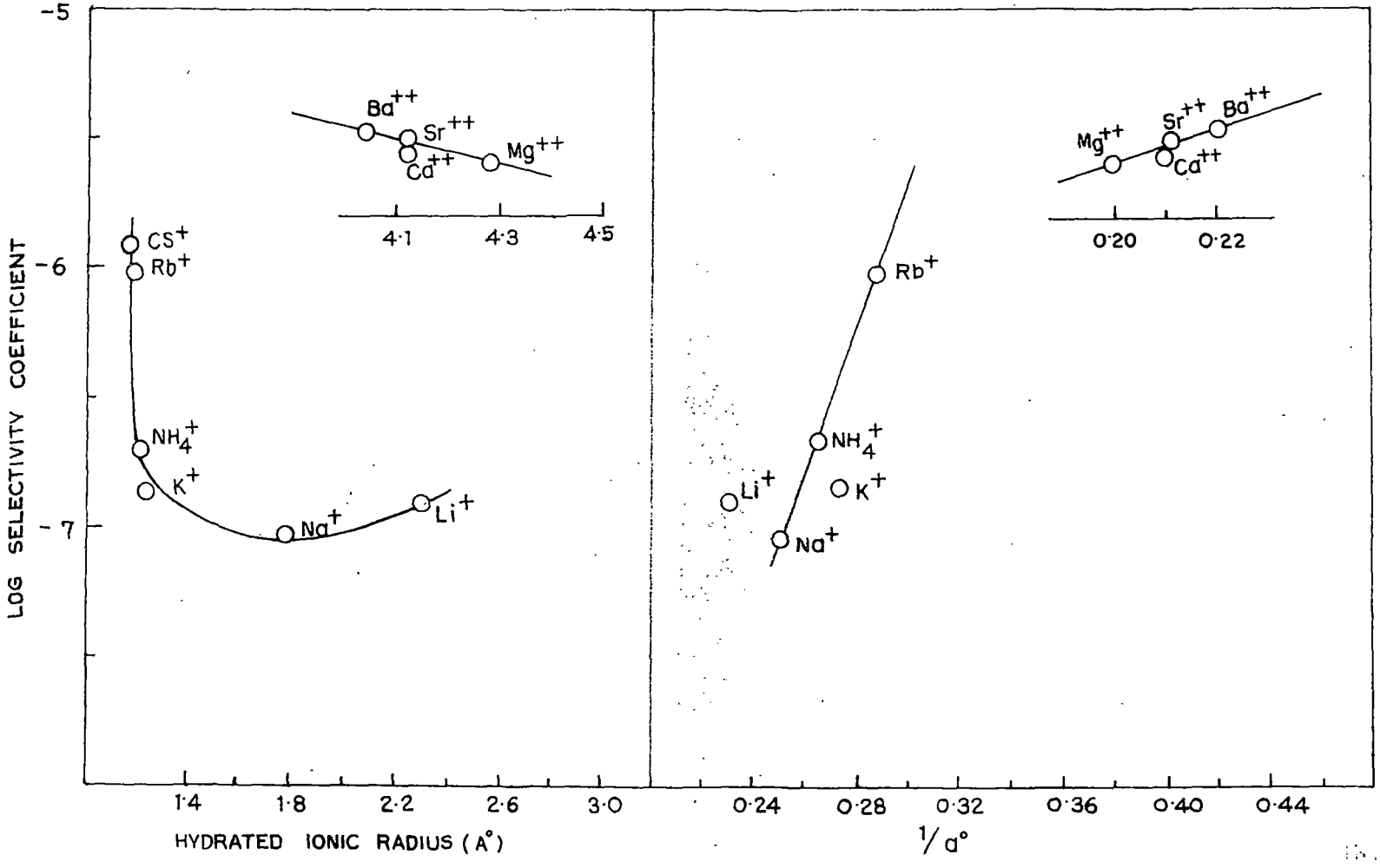

FIG. 7. CORRELATION OF SELECTIVITY COEFFICIENT WITH HYDRATED IONIC RADIUS AND DEBYE-HUCKEL PARAMETER, a°, IN THE DESORPTION OF RG FROM Na-MONTMORILLONITE - RG .

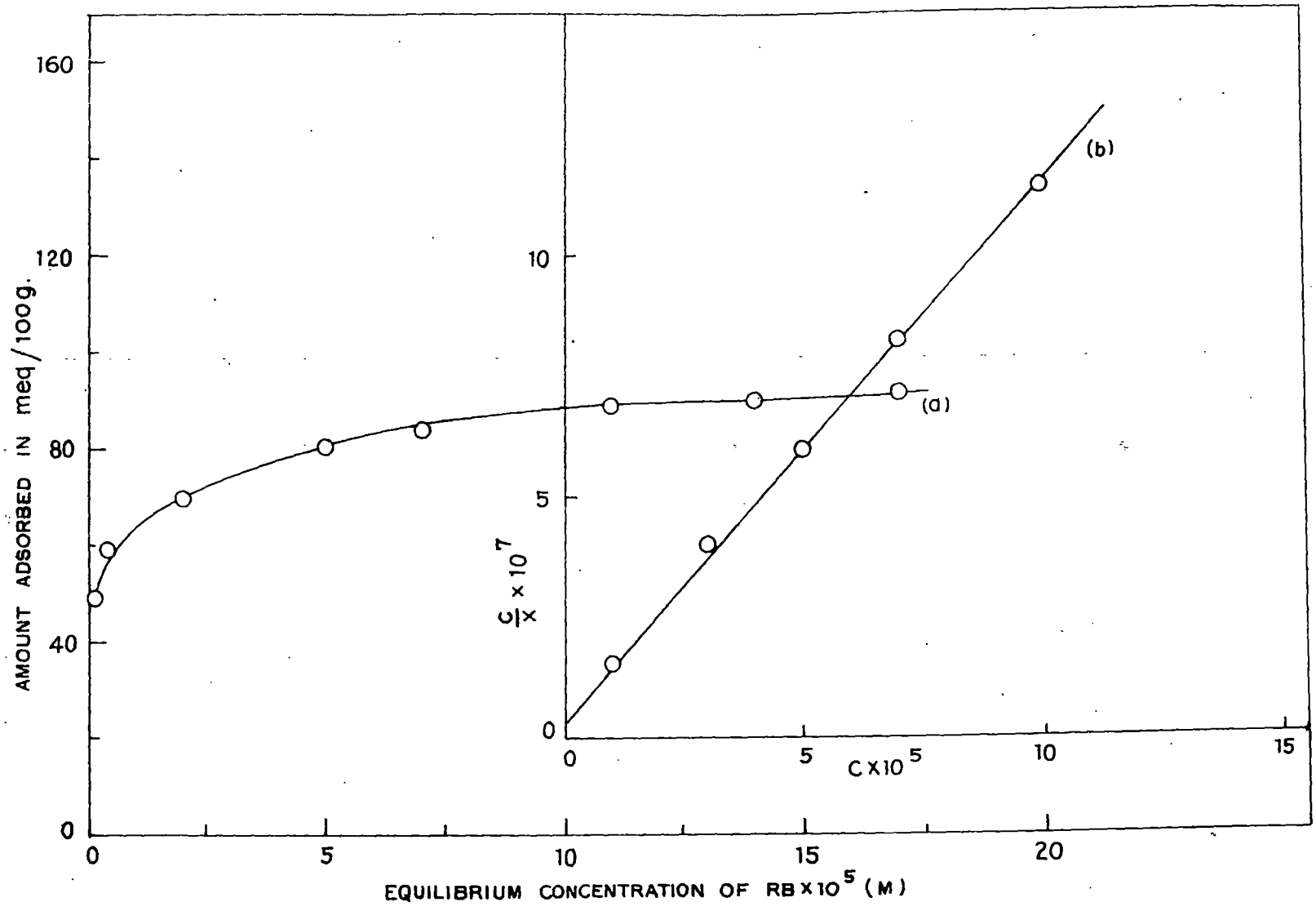

FIG. 8. ADSORPTION ISOTHERM AT 28°C (a) AND LANGMUIR PLOT (b) OF RB ON Na-MONTMORILLONITE.

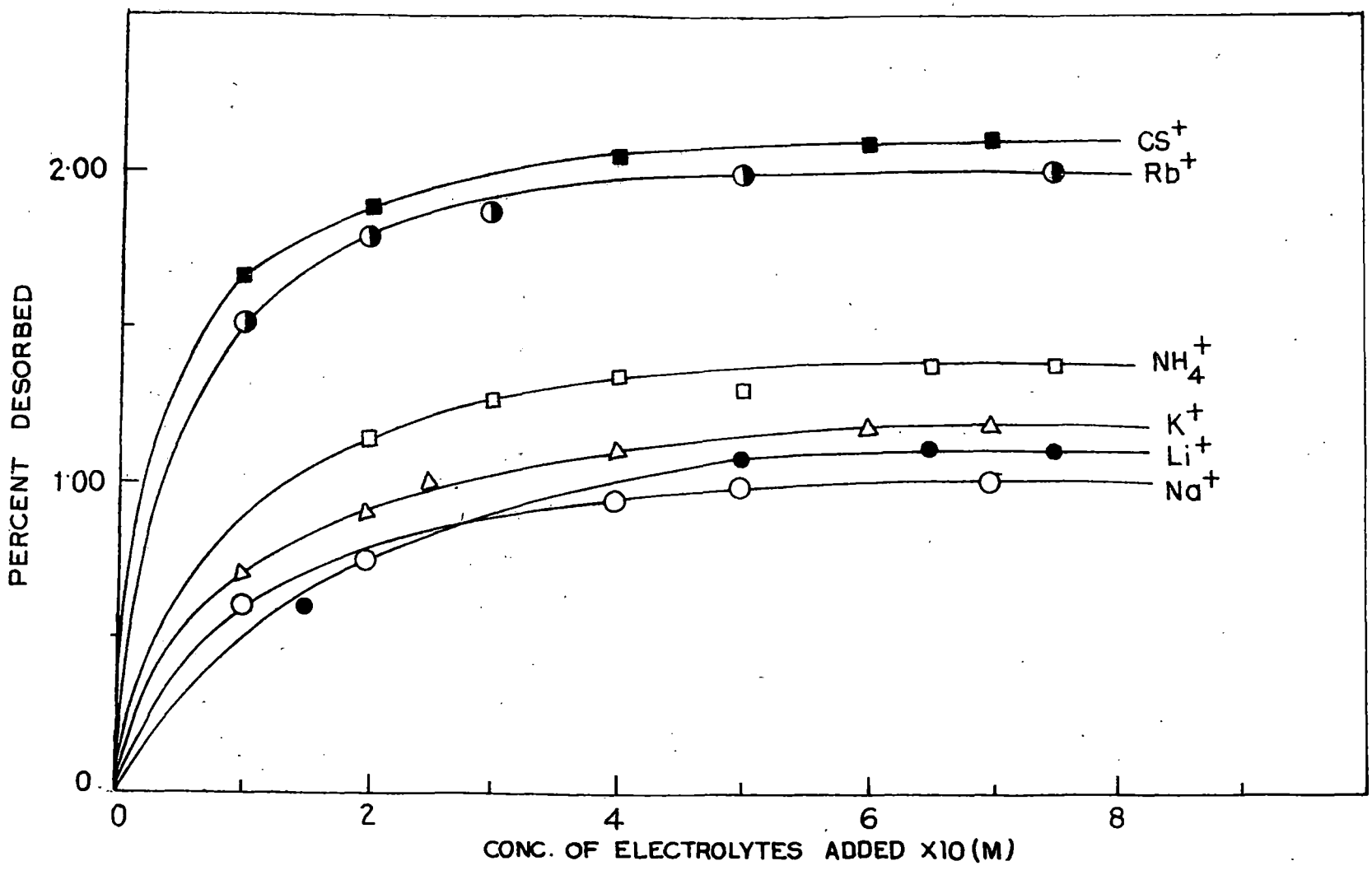

FIG. 9. DESORPTION OF RB FROM Na-MONTMORILLONITE-RB BY VARIOUS MONOVALENT IONS.

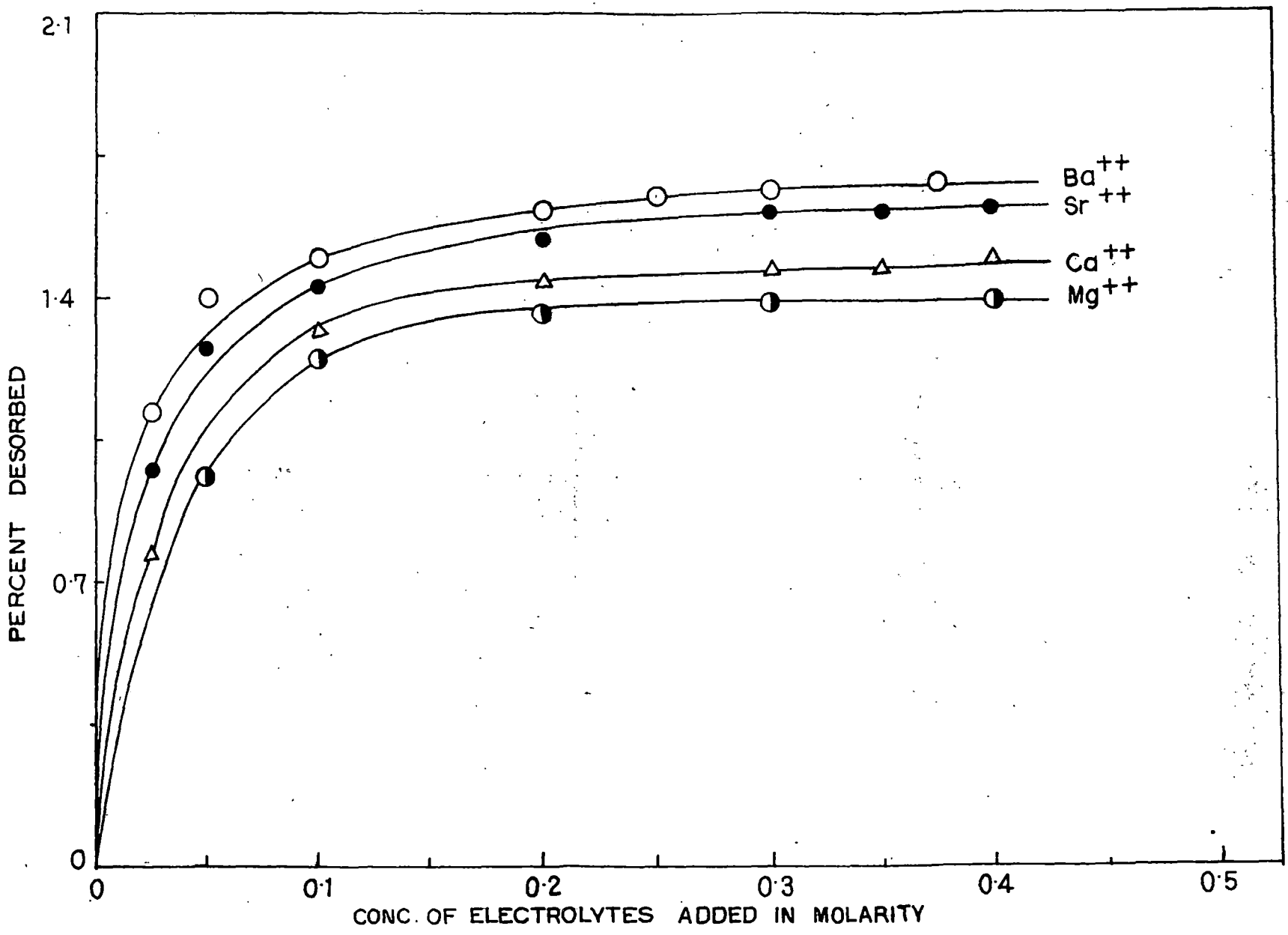

FIG. 10. DESORPTION OF RB FROM Na- MONTMORILLONITE-RB BY VARIOUS BIVALENT IONS.

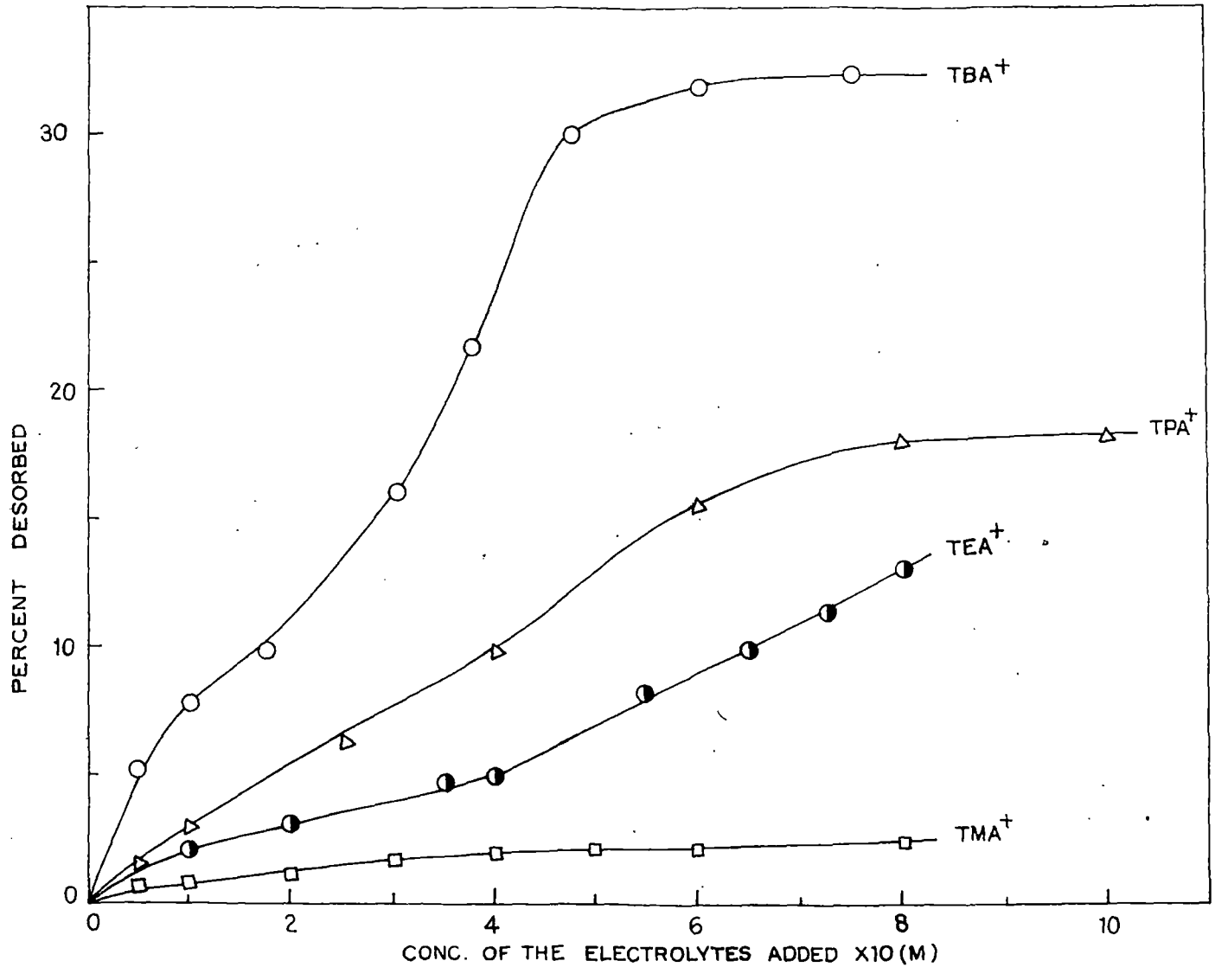

FIG. 11. DESORPTION OF RB FROM Na-MONTMORILLONITE-RB BY VARIOUS TETRAALKYL AMMONIUM HALIDES.

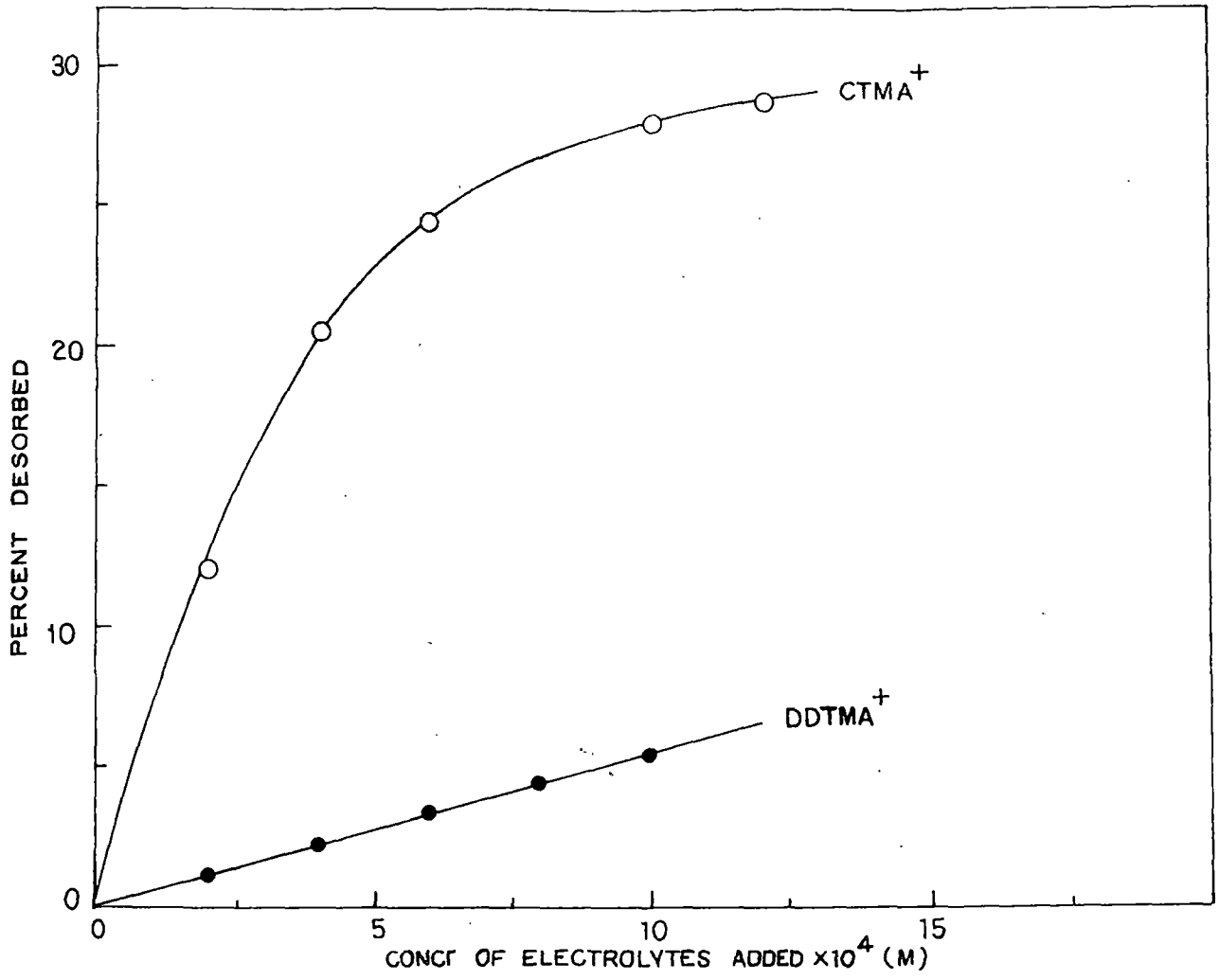

FIG. 12. DESORPTION OF RB FROM Na-MONTMORILLONITE-RB BY VARIOUS LONG-CHAIN SURFACE ACTIVE ALKYLTRIMETHYLAMMONIUM HALIDES.

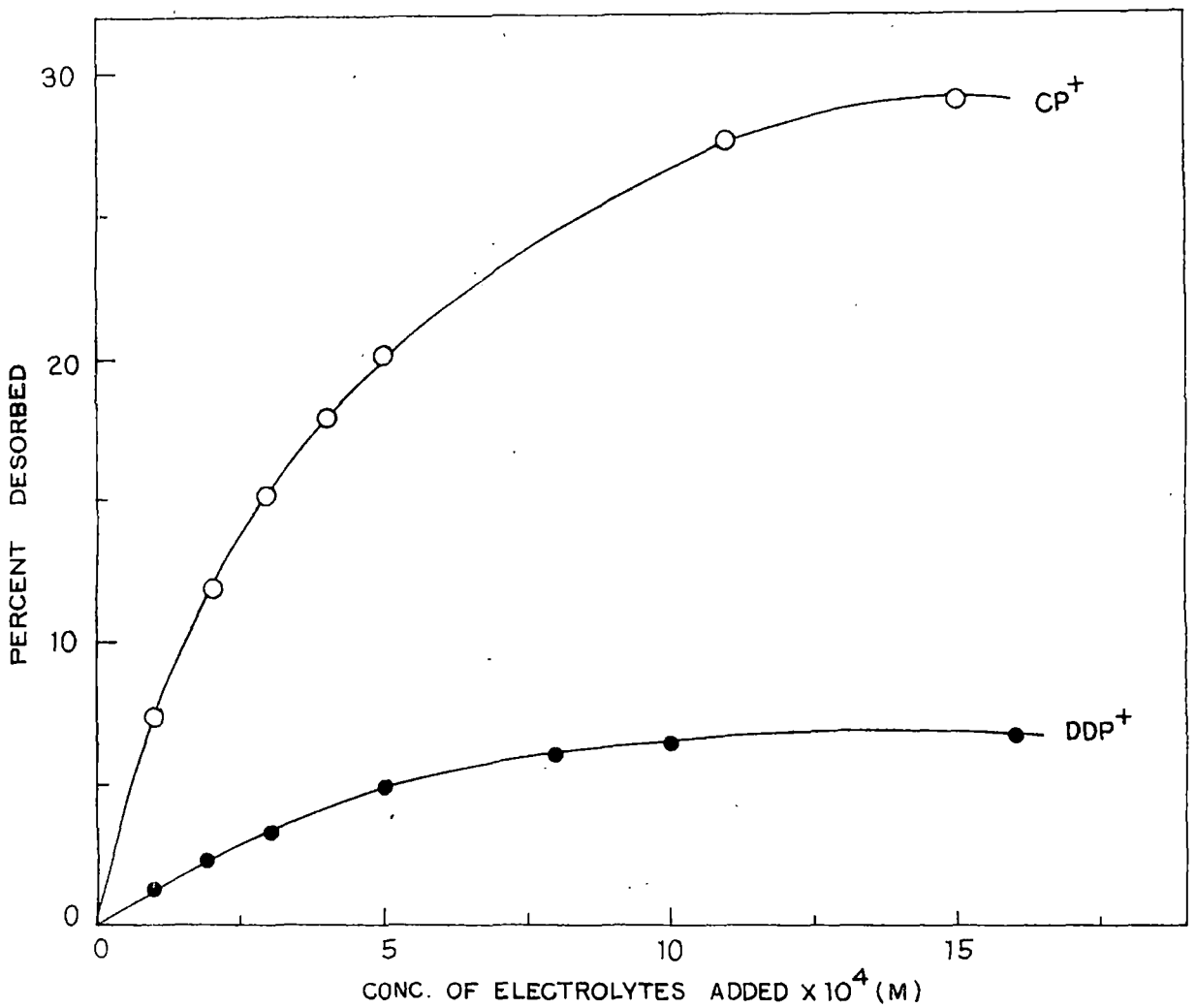

FIG. 13. DESORPTION OF RB FROM Na-MONTMORILLONITE-RB BY VARIOUS LONG-CHAIN SURFACE ACTIVE ALKYLPYRIDINIUM HALIDES.

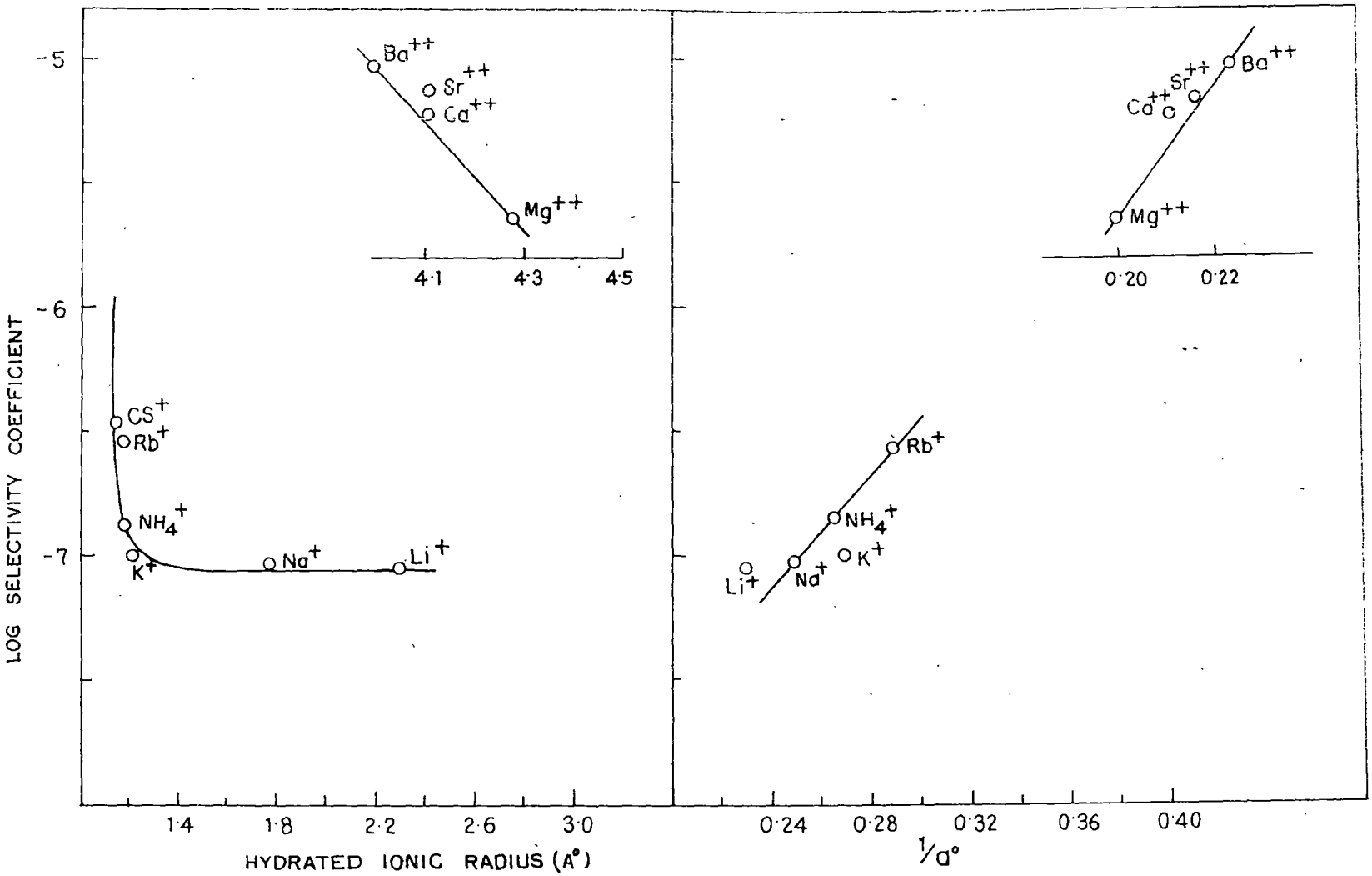

FIG. 14. CORRELATION OF SELECTIVITY COEFFICIENT WITH HYDRATED IONIC RADIUS AND DEBYE-HUCKEL PARAMETER, a°, IN THE DESORPTION OF RB FROM Na- MONTMORILLONITE.

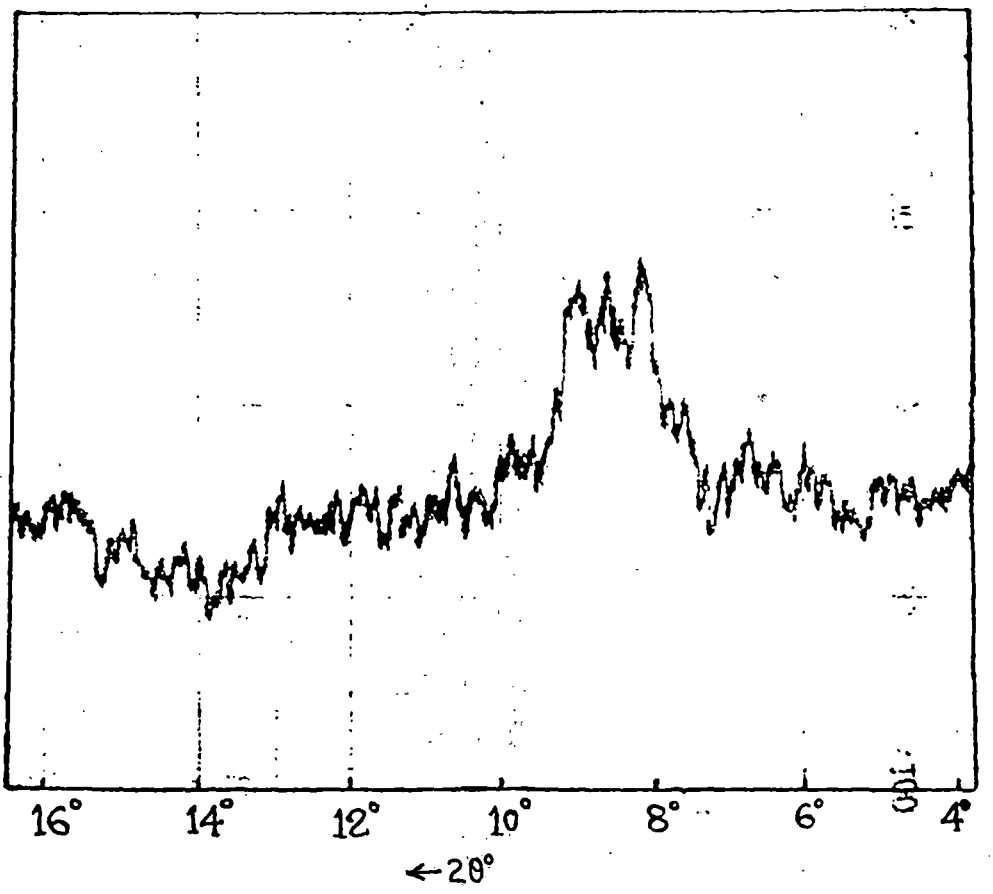

Fig. 15. X-ray diffraction spectra of Na-Montmorillonite .

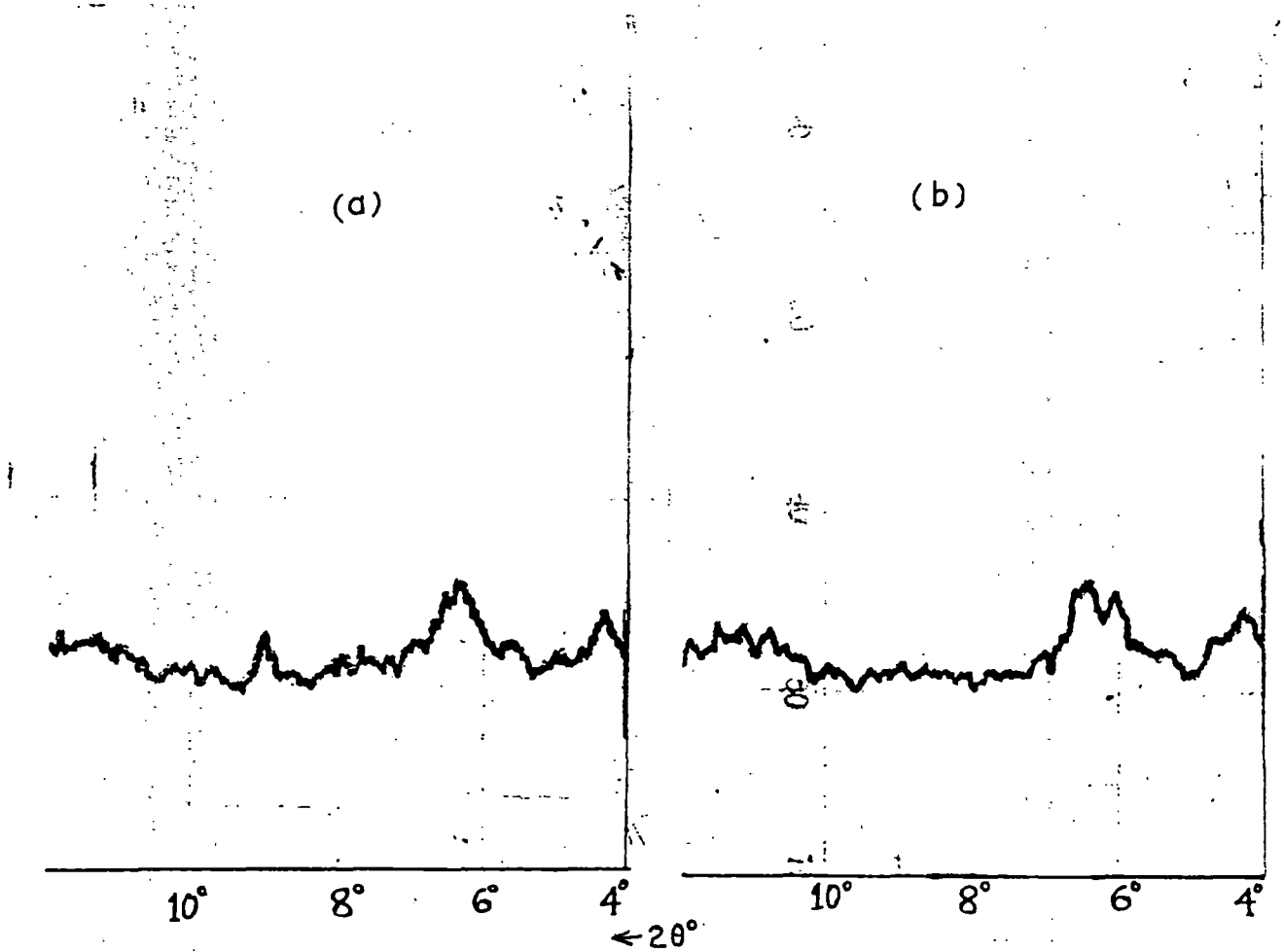

Fig. 16. X-ray diffraction spectra of Na-Montmorillonite with (a) 25% RG sorbed and with (b) 50% RG sorbed.

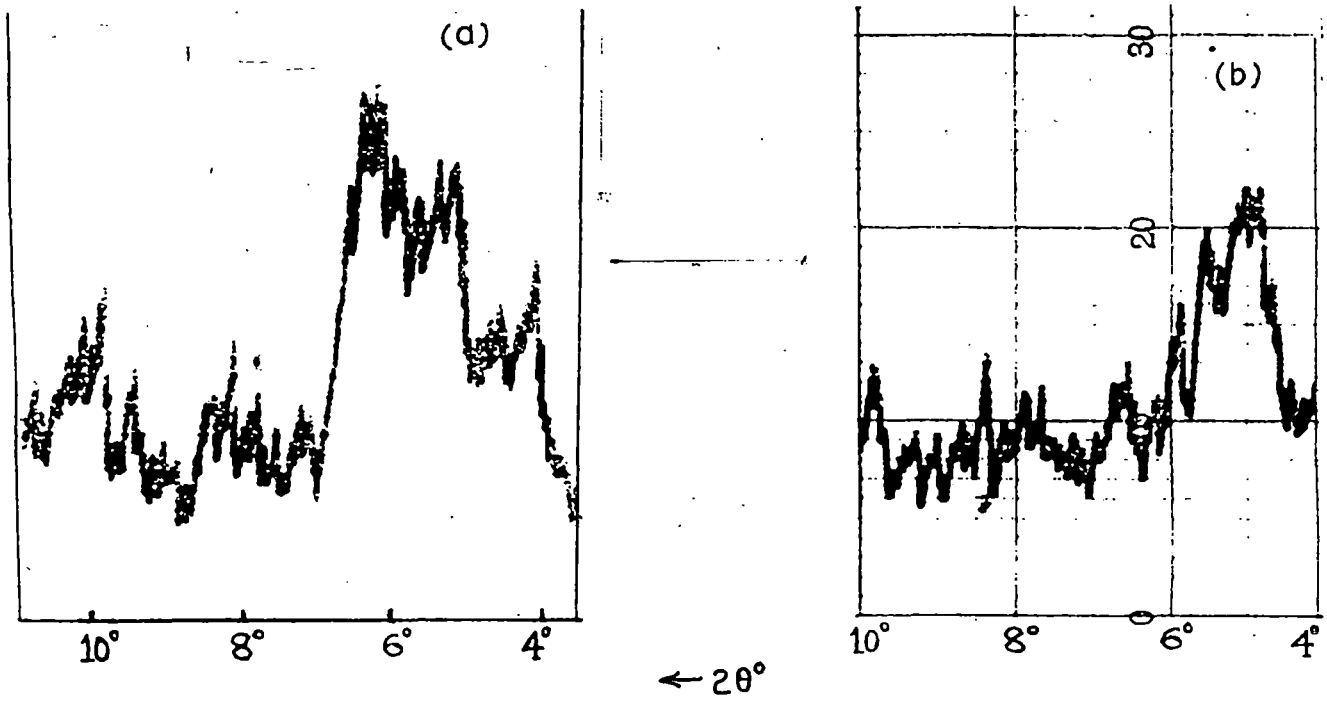

Fig. 17. X-ray diffraction spectra of Na-Montmorillonite with (a) 75% RG sorbed and (b) 100% RG sorbed.

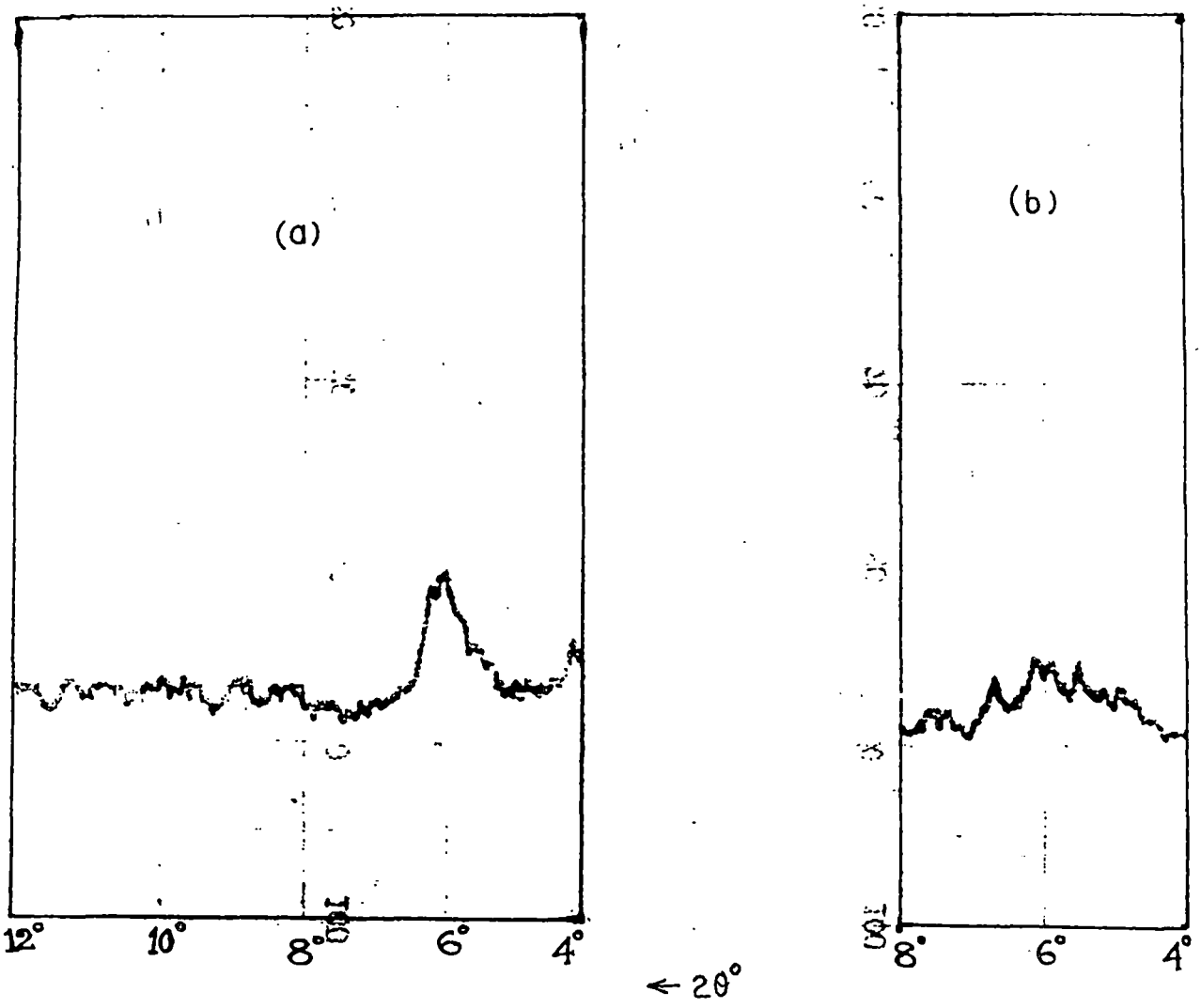

Fig. 18. X-ray diffraction spectra of Na-Montmorillonite with (a) 25% RB sorbed and (b) 50% RB sorbed.

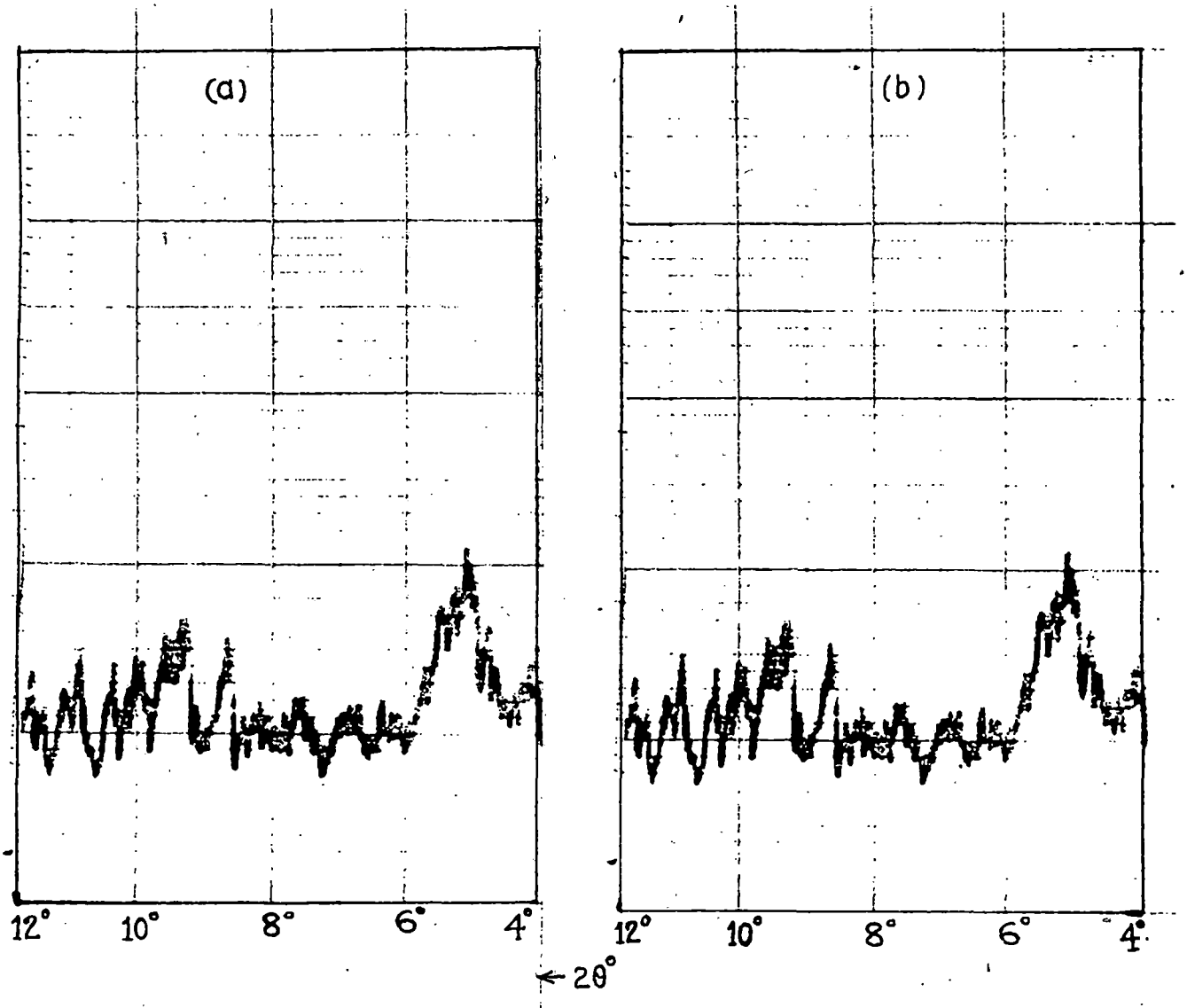

Fig. 19. X-ray diffraction spectra of Na-Montmorillonite with (a) 75% RB sorbed and (b) 100% RB sorbed.

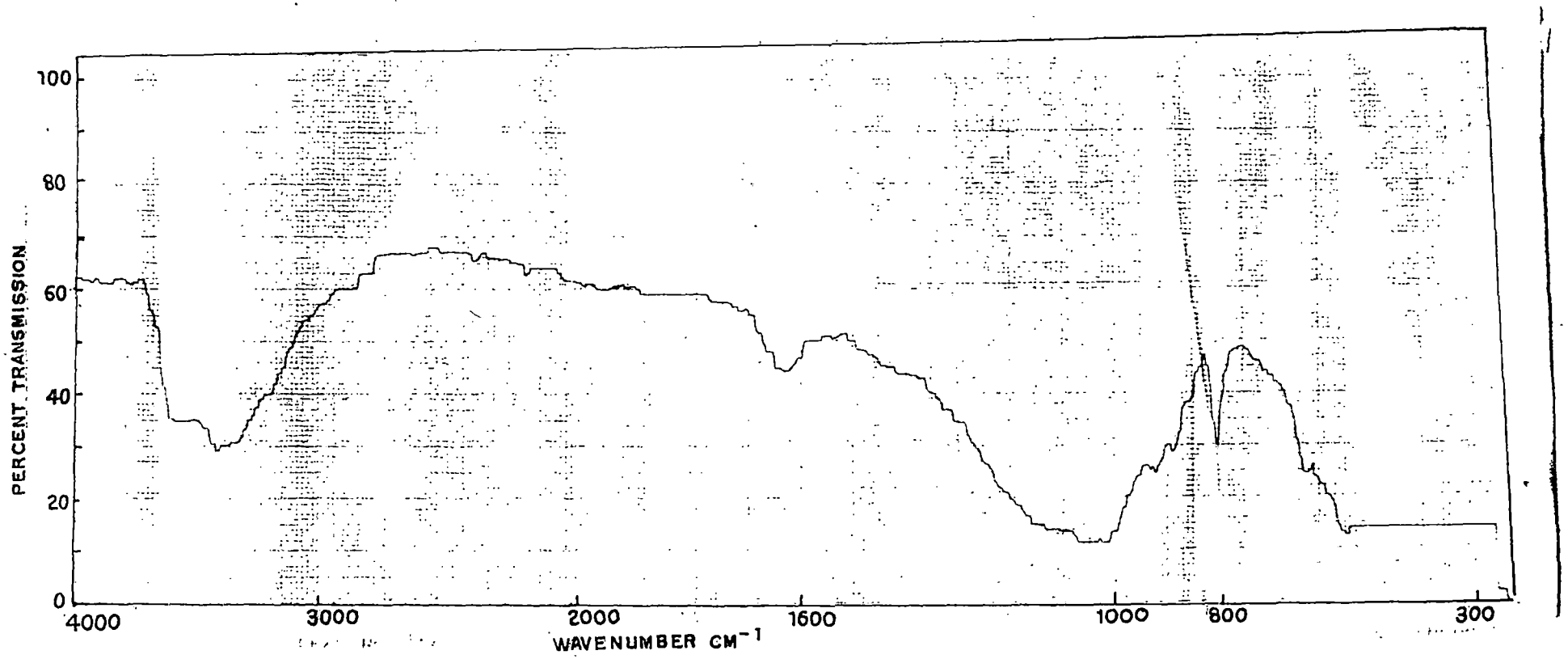

Fig. 20. Infrared Spectrum of Na-Montmorillonite

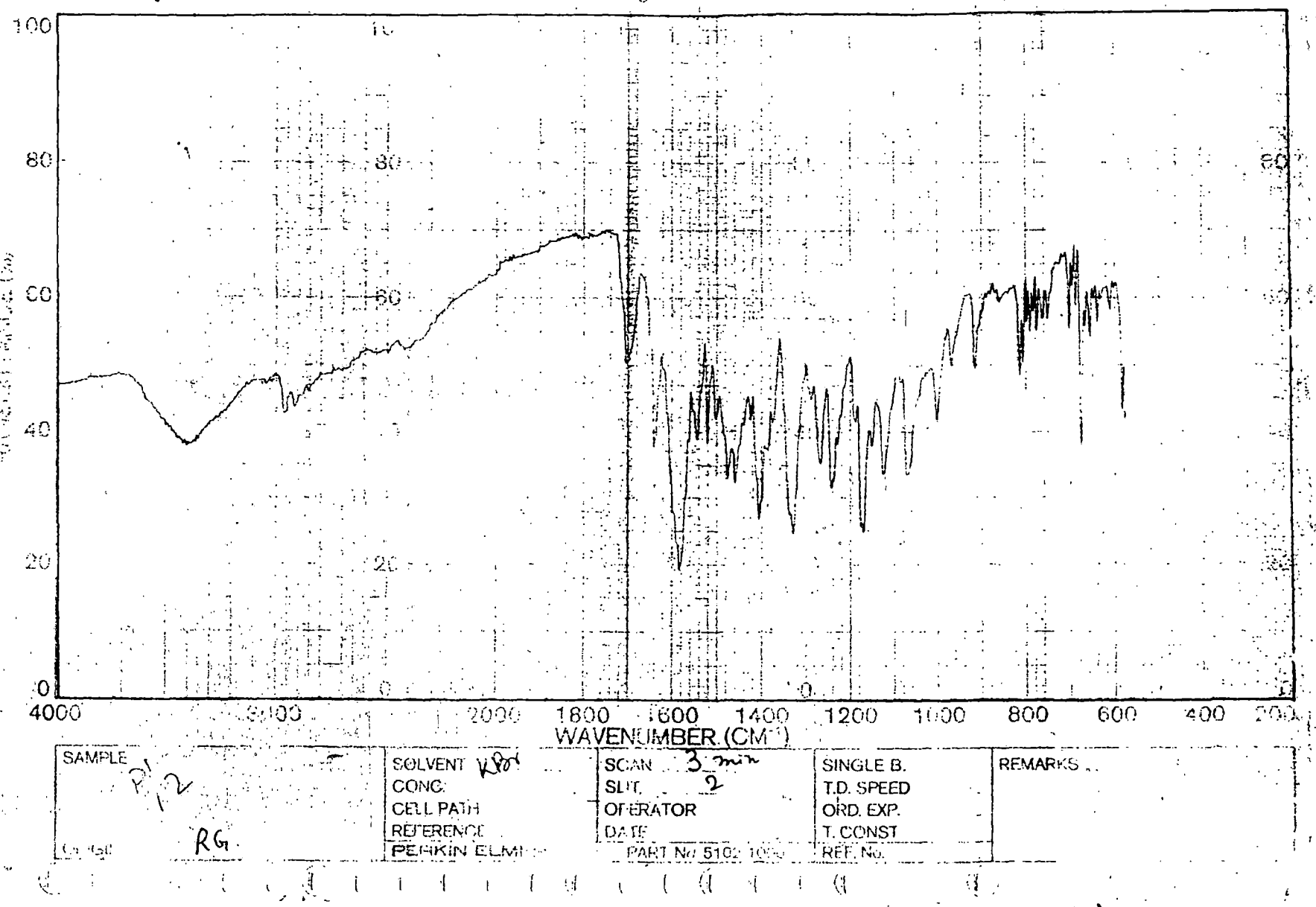

Fig. 21. Infrared spectrum of RG (In K Br pellet).

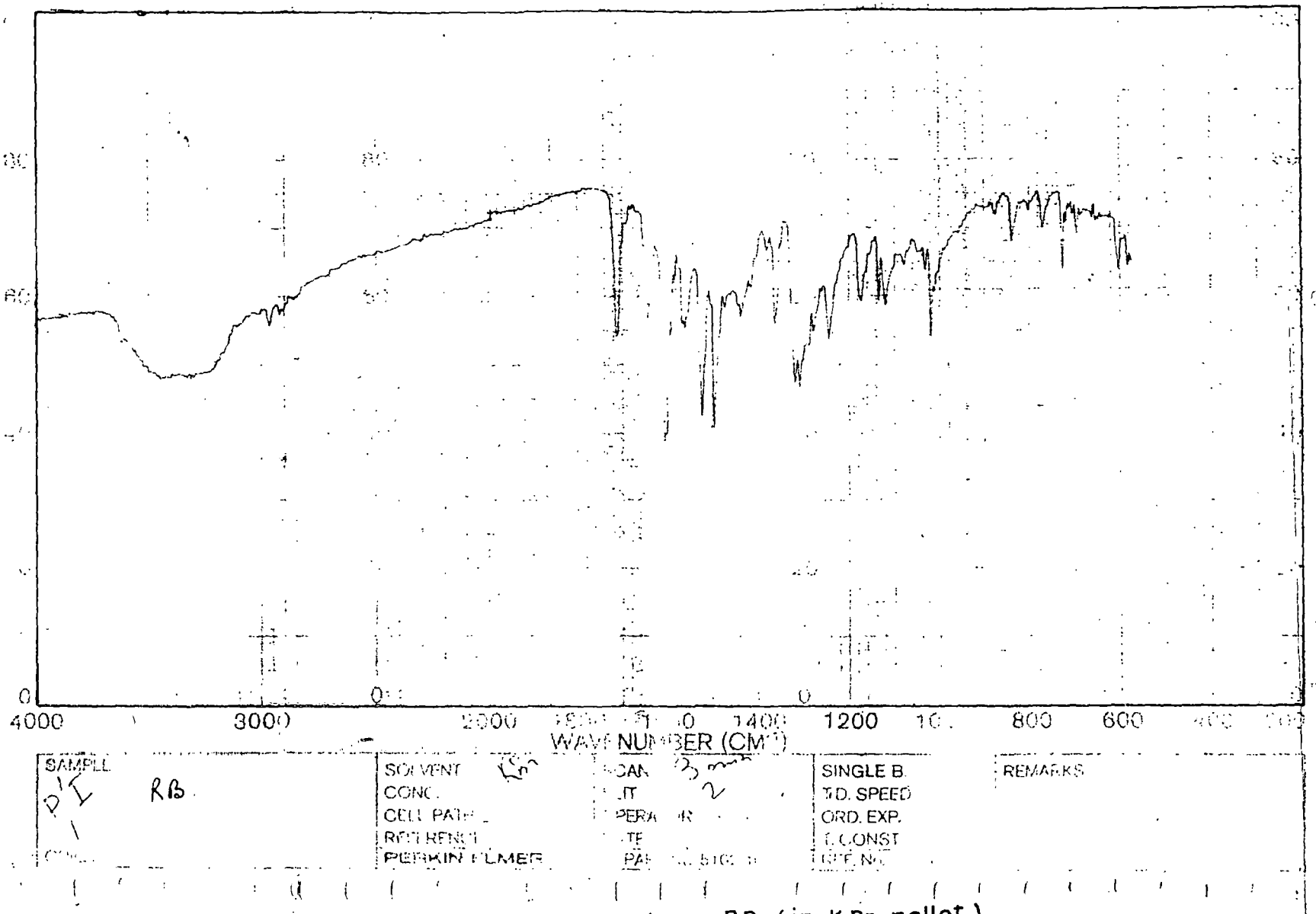

Fig. 22. Infrared spectrum RB (in KBr pellet).

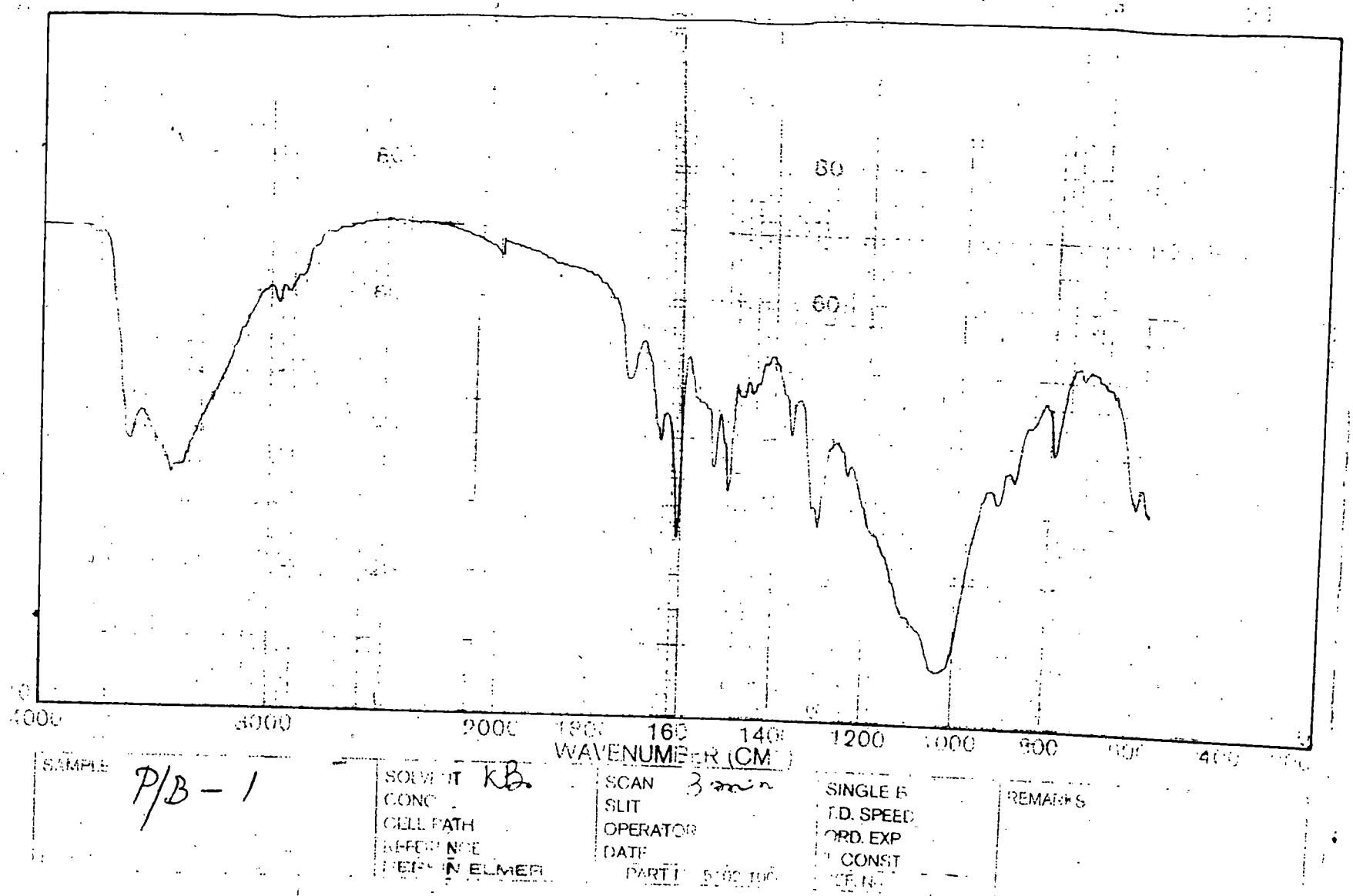

Fig. 23. Infrared spectrum of 100% exchanged Na- Montmorillonite-RG (in KBr pellet)

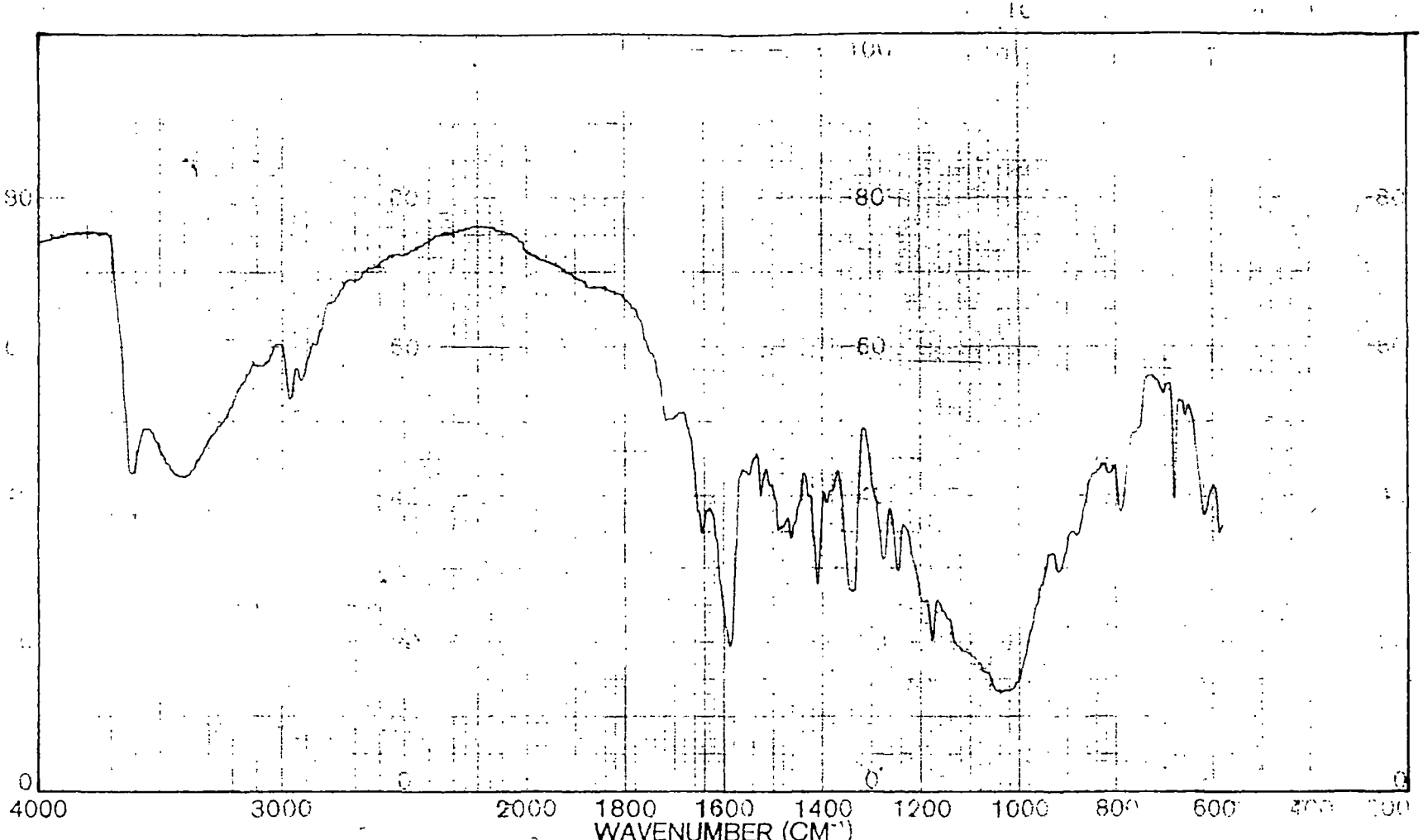

Fig. 24. Infrared spectrum of 100% exchanged Na-Montmorillonite-RB (in KBr pellet)

CHAPTER - V

Sorption and Desorption of RG and RB on Kaolinite System

The structure of kaolinite was first suggested in general outlines by Pauling (1) and it was worked out in some detail by Gruner (2) and later revised by Brindley and his colleagues (3,4). Kaolinite belongs to the "kaolin" group of minerals and its composite sheet consists of a gibbisite layer and a silica layer. These composite sheets are lightly bound in the C-directions by H-bonding between oxygens of the tetrahedral layer of one composite sheet and the hydroxyls of the octahedral layer of the next one. Very little expansion is, thus, possible in C-direction. The basal spacing value of kaolinite is 7.37 A^{o} (5). Grim, Allaway and Cuthbert (6) observed that kaolinites enter into exchange reactions with organic ions upto their exchange capacity and showed that large organic ions added in excess of the exchange capacity tend to be adsorbed by van der Waals forces. Mortenson (7) showed that unsatisfied valence bonds of the exposed lattice aluminium are involved in the bond formation in exchange reactions.

The sorption and desorption behaviour of methylene blue, malachite green and crystal violet on and from kaolinite were studied by De, Das Kanungo and Chakravarti (8). The present study

of the sorption and desorption characteristics of RG and RB on and from kaolinite aims at gaining some more knowledge in this fascinating area.

The sorption and desorption characteristics of RG and RB on and from Na-kaolinite are discussed below. The characteristics of sorption are presented in Section A and those of desorption in Section B.

In Section A, short discussion on infrared study of both RG and RB exchanged Na-kaolinite has been included.

SECTION - A

Sorption Studies

Sorption of RG^+ on Na-kaolinite:

The adsorption isotherm of RG^+ on Na-kaolinite together with the reciprocal linear plots are given in Fig. 25(a) and 25(b) respectively. It is a typical Langmuir H-type of isotherm indicative of strong adsorbate-adsorbent interaction and adsorbed species lying flat on the surface. The dye molecules are adsorbed so strongly on the mineral surface at low concentration that the equilibrium concentration becomes negligible upto about 4 meq/100g of dye sorption. Both the value of V_m (7.1 meq/100g), calculated from the linear Langmuir plot, and the maximum sorption of the dye from the isotherm (6.9 meq/100g) are greater than the c.e.c. of the mineral (5.4 meq/100g). As observed in montmorillonite here also RG is adsorbed in excess of c.e.c. The higher uptake of RG as exaplained earlier (page 61) as a consequence of the greater association tendency of the dye in solution and the resulting sorption of aggregation and/or unionised dye molecules onto the mineral.

The adsorption is mostly due to ionic and van der Waals forces upto the c.e.c. beyond which it is solely due to van der Waals forces. The value of the Langmuir bonding constant calculated from the linear plot, is $1.75 \times 10^5 M^{-1}$.

Sorption of RB^+ on Na-kaolinite:

The sorption isotherm of RB^+ on kaolinite (Fig. 32a) is also of the Langmuir type indicating flat orientation of the adsorbed dye onto the mineral. Accordingly the plot of C/X vs C is linear [Fig. 32(b)]. From the slope of the line, the value of V_m is found to be 6.25 meq/100g which is almost equal to the value of the maximum adsorption of the dye 6.4 meq/100g obtained from the isotherm. These values though slightly lower than those of RG^+, are still higher than the c.e.c. value of Na-kaolinite. This is probably due to sorption of aggregated ions from the solution of dimerisation or stacking of dye ions over the one already present in the adsorbed state.

As mentioned before the amount of RB^+ adsorbed by Na-kaolinite is less than the amount of RG^+ adsorbed. This is perhaps due to lower aggregation tendency of RB^+ compared to RG^+ in aqueous medium (page 61) and consequently there is less amount of aggregated RB molecules adsorbed.

The computed Langmuir, constant for RB^+ on to Na-kaolinite is equal to $2.66 \times 10^5 M^{-1}$, which is higher than that of RG-Na-kaolinite system signifying that the former dye is more firmly anchored to the mineral. A similar behaviour of these dyes has been observed earlier in Na-montmorillonite.

Infrared Spectral Studies on RG^+ and RB^+ exchanged Na-kaolinite:

The infrared spectra of RG, RB, Na-kaolinite, 100% RG exchanged, 100% RB-exchanged are shown in Fig. 21, 22, 39, 40, 41 respectively. From such observations it shows that the significant ring vibration at 1580 cm^{-1} has been shifted to 1603 cm^{-1} indicating aggregation tendency of the dye in the interlayer space. Similar behaviour has been found in Na-montmorillonite (page 64).

But for RB (Fig. 22) this band which appears at 1602 cm^{-1} can not be distinguishable in 100% RB-exchange-kaolinite suggesting very little sorption of dye on the clay surface.

SECTION - B

Desorption Studies

Desorption of Rhodamine RG^+ from Na-Kaolinite -RG :

The procedure for desorption studies has already been described (page 52). Figs. 26-30 show the isotherms of desorption by various inorganic and organic ions whose selectivity coefficients and distribution coefficients are given in table 8. The exchange curve are very similar in nature to those obtained in the case of Na-montmorillonite-RG complex. The extent of release of RG^+ from the clay-matrix is directly related to the size of the desorbing ions. According to there exchange efficiency the desorbing ions may be arranged as follows: $Li^+ < Na^+ < K^+ \geq NH_4^+ < Rb^+ < Cs^+$ for monovalent, $Mg^{2+} < Ca^{2+} < Sr^{2+} < Ba^{2+}$ for bivalent ion. Interestingly the percentage of desorption of RG^+ from its Na-kaolinite complex by the monovalent and divalent inorganic ions is much higher compared to montmorillonite while it has got lower value by the larger organic ions, although the extent of desorption increases with the size of the ions in both the cases. This can be, however, understood on the basis of the structural characteristics of this mineral. In kaolinite the exchange capacity is very low and its surface area is ($\simeq 7.0\ m^2/g$) (9). The area per exchange site in kaolinite is smallest as compared to other minerals structures here.

Judging from the structural behaviour of this mineral, the exchange sites are located only on the exterior surfaces of the crystal due to its non-expansible character and the distance between two exchange sites is the smallest in this mineral. So the strength of binding of this dye with kaolinite is expected to be weak as compared to that with other minerals and owing to the close proximity of the exchange sites it may so happen that the small-sized inorganic ions can match the exchange positions more appropriately to displace the adsorbed dye. Probably small sized ions have also got less "Cover-up" effect. Conversely, the larger organic ions blanket some of the closely spaced exchange sites though higher dispersion force owing to their bigger size, tends to enhance the extent of exchange. Due to this resultant effect, the extent of desorption in kaolinite is lower than in other mineral systems studied here.

As in the desorption of RG^+ from its montmorillonite complexes, have also both $1/a^o$ and the hydrated ionic radius of the alkaline earth metal ions plotted against log (selectivity coefficient) behave linearly (Fig. 31). But for monovalent inorganic ions the plot of hydrated ionic radii vs log (selectivity coefficient) is non-linear whereas it behaves linearly (Fig. 31) when $1/a^o$ values are plotted against log (selectivity coefficient). A similar behaviour was noted earlier in the other minerals studied.

Desorption of RB^+ from Na-Kaolinite-RB :

The desorption of RB^+ from its kaolinite complex by inorganic and organic ion (Figs. 33-37) are similar to those for RG-kaolinite. The only difference is that the percentage of RG^+ desorbed as well as the calculated distribution and selectivity coefficients are higher than those of RB^+ indicating a stronger binding of latter to this clay.

According to the values of the distribution and selectivity coefficients, the inorganic ions (Table 9) may be placed in the order : $Li^+ < Na^+ < K^+ \leqslant NH_4^+ < Rb^+ < Cs^+$ for the monovalent ions, $Mg^{2+} < Ca^{2+} < Sr^{2+} < Ba^{2+}$ for the bivalent ions. The extent of RB^+ desorption is directly proportional to the size of the inorganic ions and agrees with other cases of dye desorption. The selectivity coefficients, as will be seen from the data given in Table 9 are much lower than 1.0, which indicates a much smaller affinity of the desorbing ions than RB^+ for the kaolinite surfaces. As noted earlier in the desorption of RG^+ from the Na-kaolinite-RG, here also the extent of exchange of RB^+ by monovalent and bivalent inorganic ions is much higher than in montmorillonite complex and may be explained on the basis of the difference in interchange separation of the minerals vis-a-vis the smaller size of these ions.

The percentates of release of the adsorbed dye from clay-RB complex by the large organic ions are lower in Na-Kaolinite-RB complex than in the complexes of montmorillonite. This may be interpreted in a similar manner on the basis of the proximity of the exchange sites and contribution of van der Waals forces vis-a-vis size of the ions and cover up effect as done for RG^+ desorption from its Na-Kaolinite Complex (page 95).

The plot of log selectivity coefficient against hydrated ionic radii yields straight lines for bivalent inorganic ions whereas for the monovalent inorganic ions it is non-linear (Fig. 38). However $1/a^o$ vs log selectivity coefficient plot for both monovalent and bivalent inorganic ions is linear (Fig. 38). This type of behaviour had also been found in other exchanges and its usefulness had already been discussed in page 73.

The extent of desorption of RG^+ from its kaolinite complex is higher than that of RB^+ from Na-Kaolinite-RB complex, indicating thereby a weaker binding of RG^+ to this exchanger. The higher value of Langmuir bonding constant for RB^+ is also compatible with this observation.

Such an order in the values of the bonding strengths of the two dyes in question has also been noticed in previous mineral system studied here. The explanation for this is similar which has already been discussed in the earlier case (page 75).

TABLE - 8

Desorption characteristics of RG from Na-kaolinite-RG with respect to different ions.

Electrolyte used	Concentration of electrolyte	Distribution Coefficient	Selectivity Coefficient
1:1 Electrolyte			
LiCl	0.1 (M)	1.31×10^{-2}	1.48×10^{-8}
	0.2 (M)	1.03×10^{-2}	1.74×10^{-8}
	0.3 (M)	8.08×10^{-3}	1.71×10^{-8}
	0.5 (M)	5.79×10^{-3}	1.48×10^{-8}
	0.75 (M)	4.21×10^{-3}	1.18×10^{-8}
NaCl	0.1 (M)	1.63×10^{-2}	2.30×10^{-8}
	0.2 (M)	1.13×10^{-2}	2.24×10^{-8}
	0.3 (M)	8.96×10^{-3}	2.12×10^{-8}
	0.5 (M)	6.43×10^{-3}	1.83×10^{-8}
	0.75 (M)	4.77×10^{-3}	1.53×10^{-8}
KCl	0.1 (M)	0.022	4.27×10^{-8}
	0.2 (M)	0.015	4.14×10^{-8}
	0.3 (M)	0.012	4.07×10^{-8}
	0.5 (M)	0.009	3.75×10^{-8}
	0.75 (M)	0.006	3.01×10^{-8}

TABLE -8 (Contd..)

Electrolyte used	Concentration of electrolyte	Distribution Coefficient	Selectivity Coefficient
	0.1 (M)	0.0179	2.77×10^{-8}
NH_4Cl	0.2 (M)	0.013	3.30×10^{-8}
	0.3 (M)	0.010	3.06×10^{-8}
	0.5 (M)	0.008	3.22×10^{-8}
	0.75 (M)	0.006	2.94×10^{-8}
	0.1 (M)	0.029	7.43×10^{-8}
RbCl	0.2 (M)	0.021	8.28×10^{-8}
	0.3 (M)	0.016	7.54×10^{-8}
	0.5 (M)	0.011	6.42×10^{-8}
	0.75 (M)	0.008	4.88×10^{-8}
	0.1 (M)	0.036	1.22×10^{-7}
CsCl	0.2 (M)	0.023	1.05×10^{-7}
	0.3 (M)	0.018	9.52×10^{-8}
	0.5 (M)	0.012	9.86×10^{-8}
	0.75 (M)	0.009	6.41×10^{-8}

TABLE - 8 (Contd..)

Electrolyte used	Concentration of electrolyte	Distribution Coefficient	Selectivity Coefficient
2:1 Electrolyte			
	0.05 (M)	0.180	2.47×10^{-7}
$MgCl_2$	0.10 (M)	0.155	3.30×10^{-7}
	0.20 (M)	0.123	3.30×10^{-7}
	0.30 (M)	0.103	2.95×10^{-7}
	0.40 (M)	0.090	2.66×10^{-7}
	0.05 (M)	0.210	4.06×10^{-7}
$CaCl_2$	0.10 (M)	0.162	3.76×10^{-7}
	0.20 (M)	0.123	3.30×10^{-7}
	0.30 (M)	0.104	3.07×10^{-7}
	0.40 (M)	0.092	2.83×10^{-7}
	0.05 (M)	0.220	4.47×10^{-7}
$SrCl_2$	0.10 (M)	0.167	4.11×10^{-7}
	0.20 (M)	0.130	4.00×10^{-7}
	0.30 (M)	0.107	3.34×10^{-7}
	0.40 (M)	0.097	3.36×10^{-7}

TABLE - 8 (Contd..)

Electrolyte used	Concentration of electrolyte	Distribution Coefficient	Selectivity Coefficient
	0.05 (M)	0.224	4.99×10^{-7}
$BaCl_2$	0.10 (M)	0.171	4.48×10^{-7}
	0.20 (M)	0.129	3.86×10^{-7}
	0.30 (M)	0.109	3.50×10^{-7}
	0.40 (M)	0.009	3.33×10^{-7}
Quaternary Ammonium Salts			
	0.05 (M)	0.028	3.47×10^{-8}
TMBABr	0.10 (M)	0.026	5.98×10^{-8}
	0.20 (M)	0.019	6.76×10^{-8}
	0.30 (M)	0.015	6.88×10^{-8}
	0.40 (M)	0.013	6.30×10^{-8}
	0.05 (M)	0.034	5.22×10^{-8}
TEABr	0.10 (M)	0.031	8.88×10^{-8}
	0.20 (M)	0.023	1.03×10^{-7}
	0.30 (M)	0.018	1.01×10^{-7}
	0.40 (M)	0.015	9.48×10^{-8}

TABLE - 8 (Contd..)

Electrolyte used	Concentration of electrolyte	Distribution Coefficient	Selectivity Coefficient
	0.05 (M)	0.047	9.83×10^{-8}
TPABr	0.10 (M)	0.039	1.41×10^{-7}
	0.20 (M)	0.028	1.51×10^{-7}
	0.30 (M)	0.022	1.47×10^{-7}
	0.40 (M)	0.018	1.34×10^{-7}
	0.05 (M)	0.094	4.12×10^{-7}
TBABr	0.10 (M)	0.063	3.79×10^{-7}
	0.20 (M)	0.039	3.13×10^{-7}
	0.30 (M)	0.029	2.62×10^{-7}
	0.40 (M)	0.023	2.20×10^{-7}
	2×10^{-4} (M)	9.754	1.65×10^{-5}
DDTMABr	4×10^{-4} (M)	6.852	1.65×10^{-5}
	6×10^{-4} (M)	5.542	1.63×10^{-5}
	8×10^{-4} (M)	4.743	1.61×10^{-5}
	1×10^{-3} (M)	3.956	1.41×10^{-5}

TABLE - 8 (Contd..)

Electrolyte used	Concentration of electrolyte	Distribution Coefficient	Selectivity Coefficient
	2×10^{-4} (M)	23.990	1.05×10^{-4}
CTMABr	4×10^{-4} (M)	14.496	7.88×10^{-5}
	6×10^{-4} (M)	11.420	7.50×10^{-5}
	8×10^{-4} (M)	8.828	6.01×10^{-5}
	1×10^{-3} (M)	7.174	4.96×10^{-5}
	1×10^{-4} (M)	11.336	2.24×10^{-5}
DDPBr	2×10^{-4} (M)	7.906	2.22×10^{-5}
	3×10^{-4} (M)	6.061	1.97×10^{-5}
	4×10^{-4} (M)	4.941	1.76×10^{-5}
	5×10^{-4} (M)	4.162	1.57×10^{-5}
	1×10^{-4} (M)	31.635	1.89×10^{-4}
CPBr	2×10^{-4} (M)	18.581	1.34×10^{-4}
	3×10^{-4} (M)	13.265	1.03×10^{-4}
	4×10^{-4} (M)	10.343	8.47×10^{-5}
	5×10^{-4} (M)	8.440	7.07×10^{-5}

TABLE - 9

Desorption characteristics of RB from Na-kaolinite-RB with respect to different ions.

Electrolytes used	Concentration of electrolyte	Distribution Coefficient	Selectivity Coefficient
1:1 Electrolyte			
LiCl	0.1 (M)	6.84×10^{-3}	3.80×10^{-9}
	0.2 (M)	4.73×10^{-3}	3.70×10^{-9}
	0.3 (M)	3.68×10^{-3}	3.37×10^{-9}
	0.5 (M)	2.73×10^{-3}	3.11×10^{-9}
	0.75 (M)	2.03×10^{-3}	2.59×10^{-9}
NaCl	0.1 (M)	1.05×10^{-2}	9.17×10^{-9}
	0.2 (M)	7.10×10^{-3}	8.41×10^{-9}
	0.3 (M)	5.61×10^{-3}	7.92×10^{-9}
	0.5 (M)	3.89×10^{-3}	6.38×10^{-9}
	0.75 (M)	2.94×10^{-3}	5.51×10^{-9}
KCl	0.1 (M)	1.73×10^{-2}	2.53×10^{-8}
	0.2 (M)	1.07×10^{-2}	1.96×10^{-8}
	0.3 (M)	8.06×10^{-3}	1.66×10^{-8}
	0.5 (M)	5.26×10^{-3}	1.18×10^{-8}
	0.75 (M)	3.64×10^{-3}	7.96×10^{-9}

TABLE - 9 (Contd..)

Electrolyte used	Concentration of Electrolyte	Distribution Coefficient	Selectivity Coefficient
	0.1 (M)	1.31×10^{-2}	1.44×10^{-8}
NH_4Cl	0.2 (M)	9.73×10^{-3}	1.59×10^{-8}
	0.3 (M)	8.06×10^{-3}	1.66×10^{-8}
	0.5 (M)	5.99×10^{-3}	1.54×10^{-8}
	0.75 (M)	4.27×10^{-3}	1.11×10^{-8}
	0.1 (M)	2.63×10^{-2}	5.91×10^{-8}
RbCl	0.2 (M)	1.76×10^{-2}	5.40×10^{-8}
	0.3 (M)	1.36×10^{-2}	4.94×10^{-8}
	0.5 (M)	9.78×10^{-3}	4.28×10^{-8}
	0.75 (M)	7.22×10^{-3}	3.54×10^{-8}
	0.1 (M)	3.15×10^{-2}	8.61×10^{-8}
CsCl	0.2 (M)	2.05×10^{-2}	7.41×10^{-8}
	0.3 (M)	1.59×10^{-2}	6.82×10^{-8}
	0.5 (M)	1.14×10^{-2}	5.99×10^{-8}
	0.75 (M)	8.55×10^{-3}	5.07×10^{-8}

TABLE - 9 (Contd..)

Electrolyte used	Concentration o electrolyte	Distribution Coefficient	Selectivity Coefficient
2:1 Electrolyte			
	0.05 (M)	0.121	7.35×10^{-8}
$MgCl_2$	0.10 (M)	0.107	1.03×10^{-7}
	0.20 (M)	0.097	1.55×10^{-7}
	0.30 (M)	0.087	1.72×10^{-7}
	0.40 (M)	0.077	1.60×10^{-7}
	0.05 (M)	0.125	8.16×10^{-8}
$CaCl_2$	0.10 (M)	0.114	1.25×10^{-7}
	0.20 (M)	0.103	1.89×10^{-7}
	0.30 (M)	0.091	1.97×10^{-7}
	0.40 (M)	0.082	1.93×10^{-7}
	0.05 (M)	0.145	1.18×10^{-7}
$SrCl_2$	0.10 (M)	0.129	3.87×10^{-7}
	0.20 (M)	0.111	2.48×10^{-7}
	0.30 (M)	0.093	2.07×10^{-7}
	0.40 (M)	0.087	2.29×10^{-7}

TABLE -9 (Contd..)

Electrolyte used	Concentration of electrolyte	Distribution Coefficient	Selectivity Coefficient
	0.05 (M)	0.171	2.11×10^{-7}
$BaCl_2$	0.10 (M)	0.148	2.78×10^{-7}
	0.20 (M)	0.121	3.07×10^{-7}
	0.30 (M)	0.104	2.94×10^{-7}
	0.40 (M)	0.093	2.81×10^{-7}
Quaternary Ammonium Salt			
	0.05 (M)	2.52×10^{-2}	2.65×10^{-8}
TMABr	0.10 (M)	1.73×10^{-2}	2.53×10^{-8}
	0.20 (M)	1.18×10^{-2}	2.38×10^{-8}
	0.30 (M)	9.47×10^{-3}	2.30×10^{-8}
	0.40 (M)	7.89×10^{-3}	2.15×10^{-8}
	0.05 (M)	4.73×10^{-2}	9.52×10^{-8}
TEABr	0.10 (M)	2.92×10^{-2}	7.33×10^{-8}
	0.20 (M)	1.77×10^{-2}	5.48×10^{-8}
	0.30 (M)	1.31×10^{-2}	4.55×10^{-8}
	0.40 (M)	1.08×10^{-2}	4.16×10^{-8}

TABLE - 9 (Contd..)

Electrolyte used	Concentration of electrolyte	Distribution Coefficient	Selectivity Coefficient
	0.05 (M)	6.15×10^{-2}	1.63×10^{-7}
TPABr	0.10 (M)	3.79×10^{-2}	1.25×10^{-7}
	0.20 (M)	2.40×10^{-2}	1.03×10^{-7}
	0.30 (M)	1.81×10^{-2}	8.94×10^{-8}
	0.40 (M)	1.54×10^{-2}	8.78×10^{-8}
	0.05 (M)	8.83×10^{-2}	3.46×10^{-7}
TBABr	0.10 (M)	5.21×10^{-2}	2.44×10^{-7}
	0.20 (M)	3.15×10^{-2}	1.83×10^{-7}
	0.30 (M)	2.36×10^{-2}	1.56×10^{-7}
	0.40 (M)	1.89×10^{-2}	1.36×10^{-7}
	2×10^{-4}	3.964	2.57×10^{-6}
DDTMABr	4×10^{-4}	3.025	3.04×10^{-6}
	6×10^{-4}	2.367	2.80×10^{-6}
	8×10^{-4}	1.974	2.60×10^{-6}
	1×10^{-3}	1.737	2.53×10^{-6}

TABLE - 9 (Contd..)

Electrolyte used	Concentration of electrolyte	Distribution Coefficient	Selectivity Coefficient
	2×10^{-4} (M)	18.419	5.91×10^{-5}
CTMABr	4×10^{-4} (M)	12.391	5.48×10^{-5}
	6×10^{-4} (M)	9.571	4.99×10^{-5}
	8×10^{-4} (M)	7.702	4.35×10^{-5}
	1×10^{-3} (M)	6.423	3.81×10^{-5}
	1×10^{-4} (M)	7.929	1.04×10^{-5}
DDPBr	2×10^{-4} (M)	5.405	9.86×10^{-6}
	3×10^{-4} (M)	4.039	8.31×10^{-6}
	4×10^{-4} (M)	3.291	7.39×10^{-6}
	5×10^{-4} (M)	2.843	6.93×10^{-6}
	1×10^{-4} (M)	27.225	1.33×10^{-4}
CPBr	2×10^{-4} (M)	16.478	1.11×10^{-4}
	3×10^{-4} (M)	11.854	8.07×10^{-5}
	4×10^{-4} (M)	9.348	6.60×10^{-5}
	5×10^{-4} (M)	7.634	5.52×10^{-5}

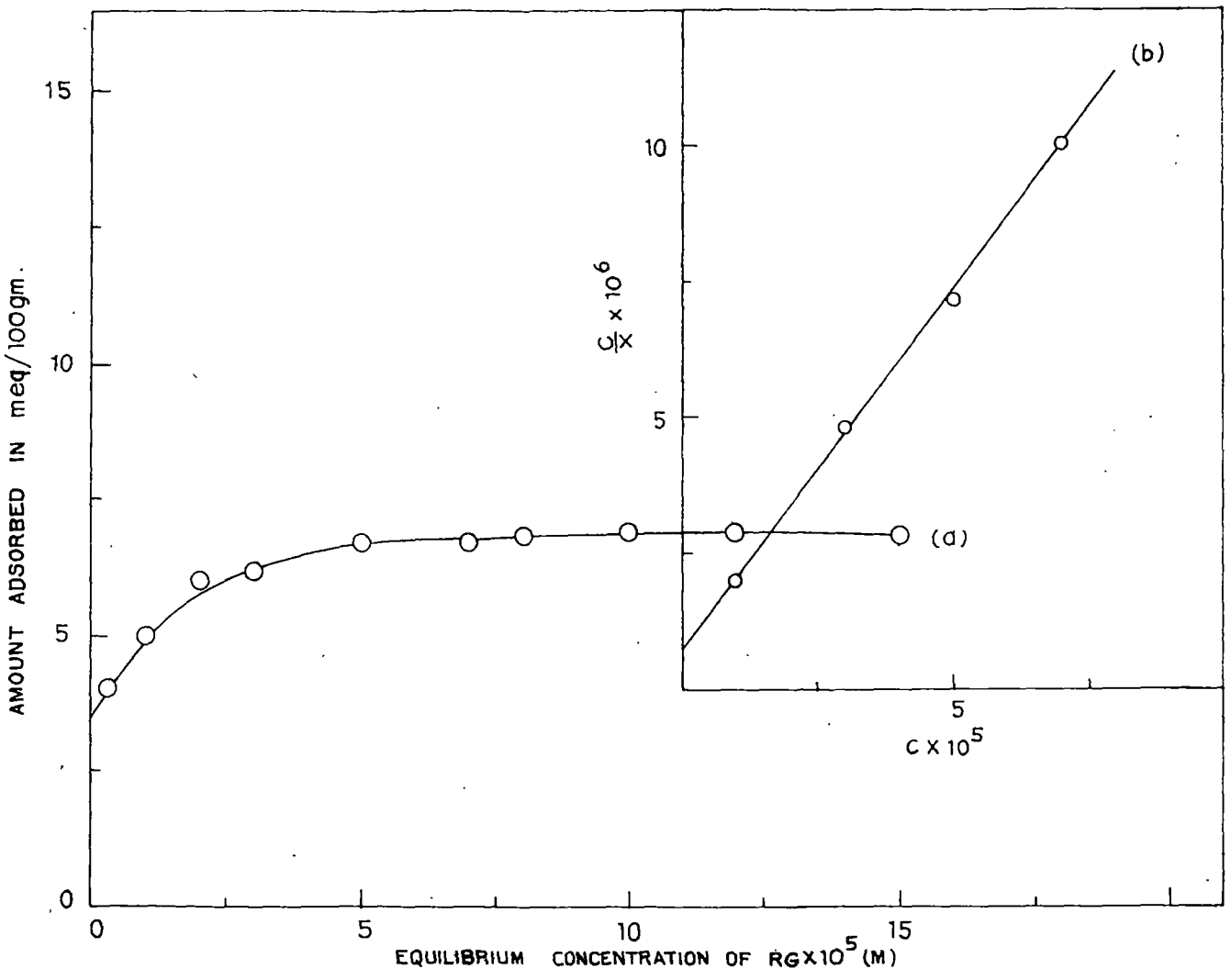

FIG. 25. ADSORPTION ISOTHERM AT 28°C (a) LANGMUIR PLOT (b) OF RG ON Na-KAOLINITE .

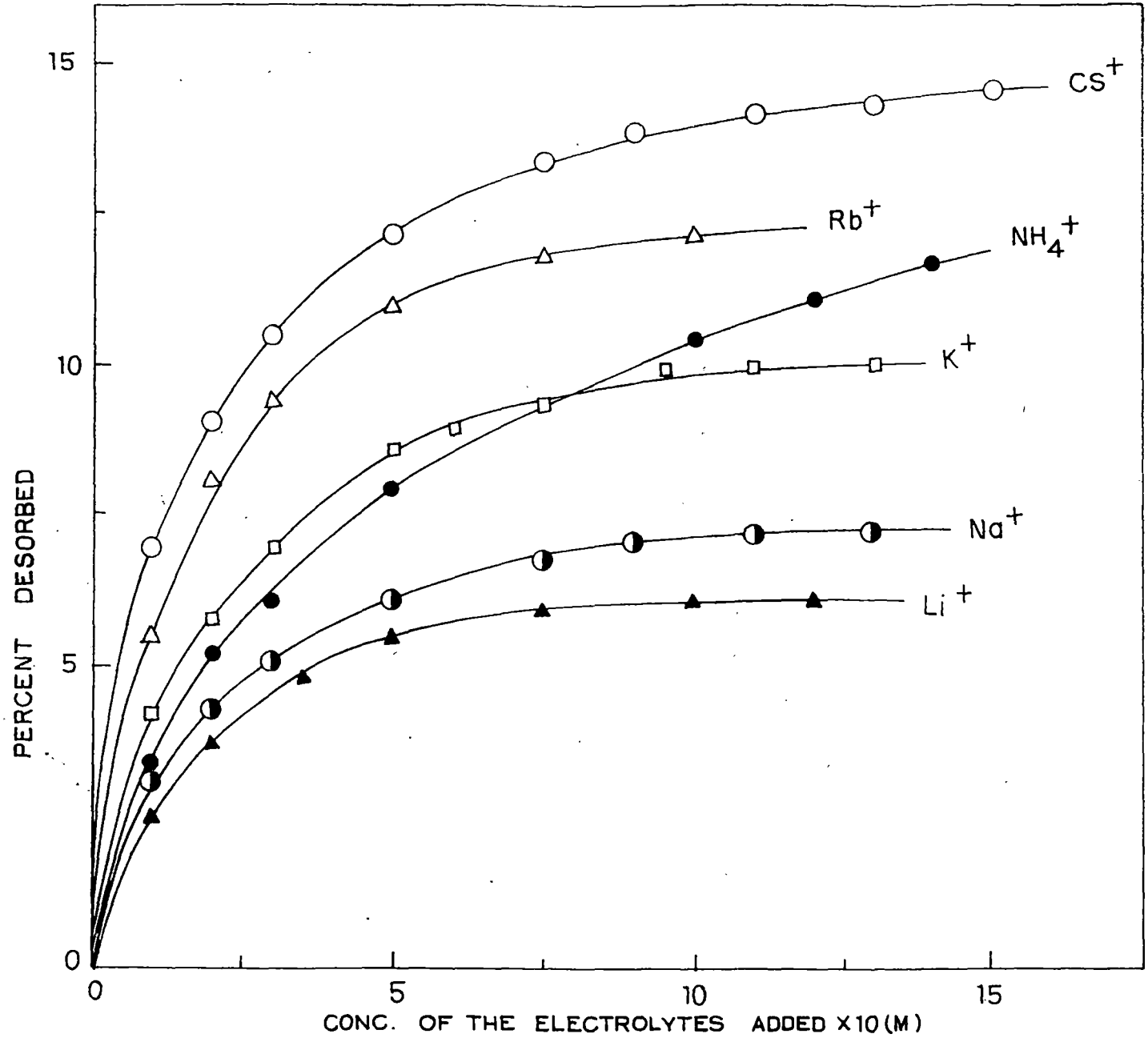

FIG. 26. DESORPTION OF RG FROM Na-KAOLINITE-RG BY VARIOUS MONOVALENT IONS.

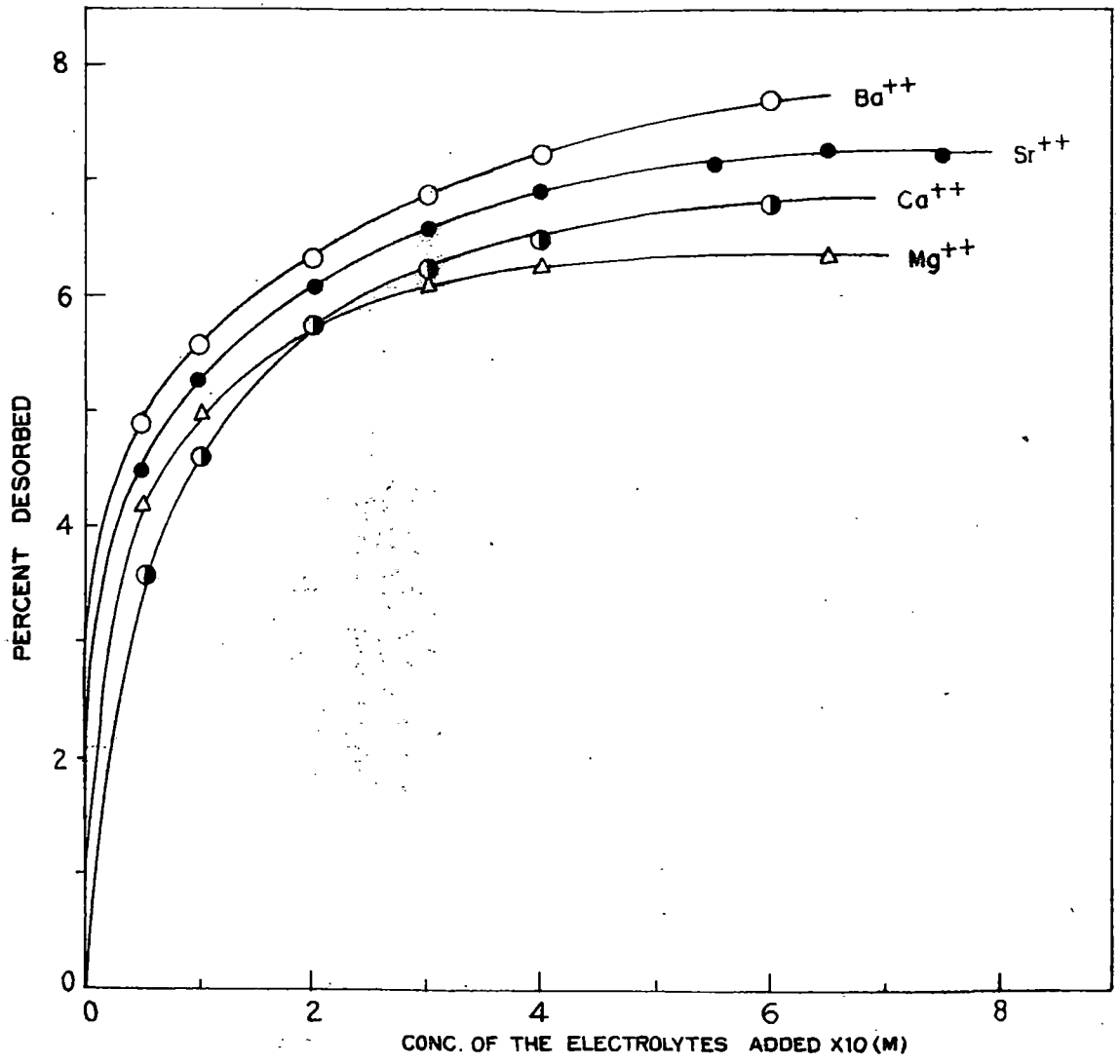

FIG. 27. DESORPTION OF RG FROM Na- KAOLINITE-RG BY VARIOUS BIVALENT IONS.

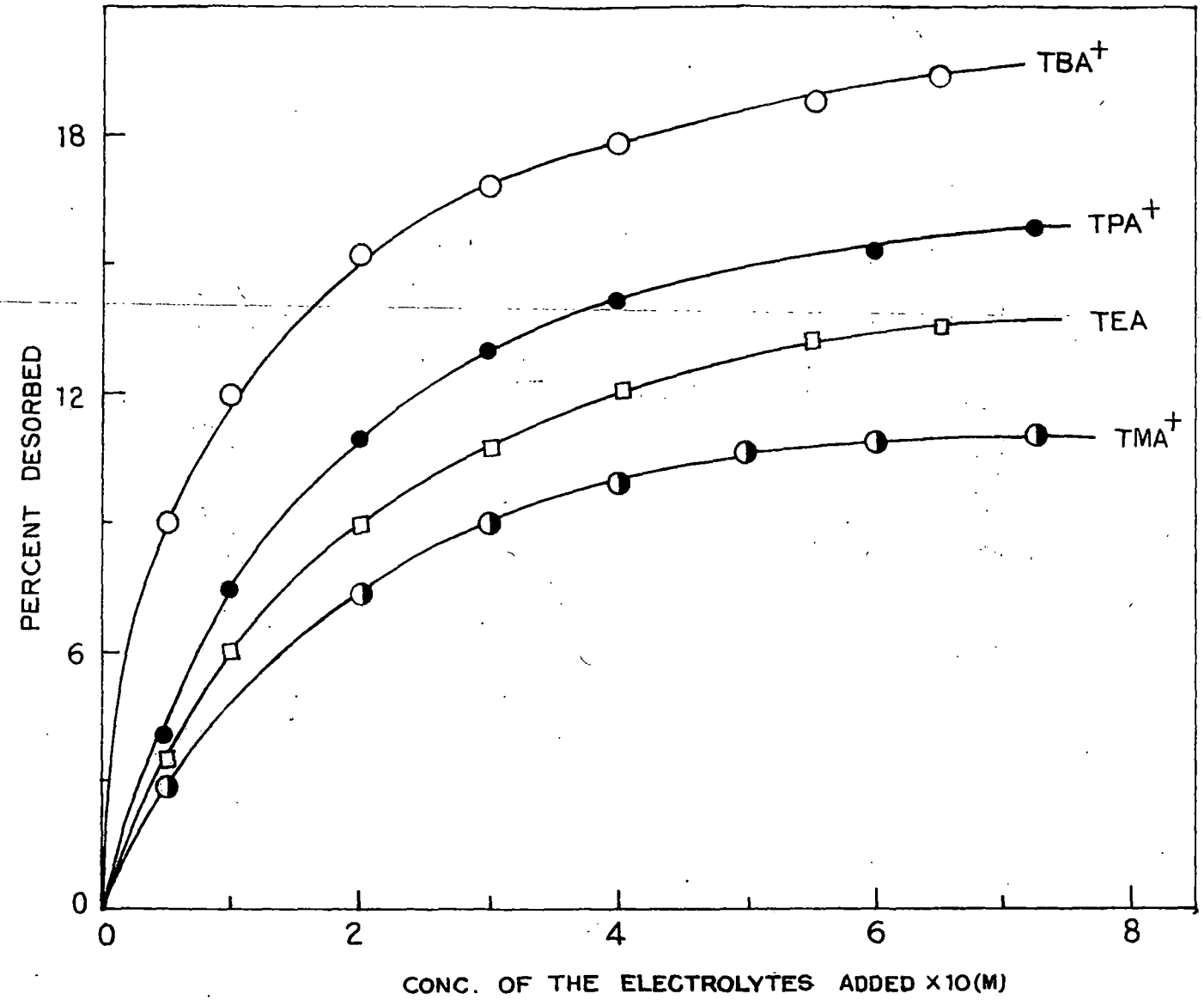

FIG. 28. DESORPTION OF RG FROM Na-KAOLINITE-RG BY VARIOUS TETRA-ALKYL AMMONIUM HALIDES.

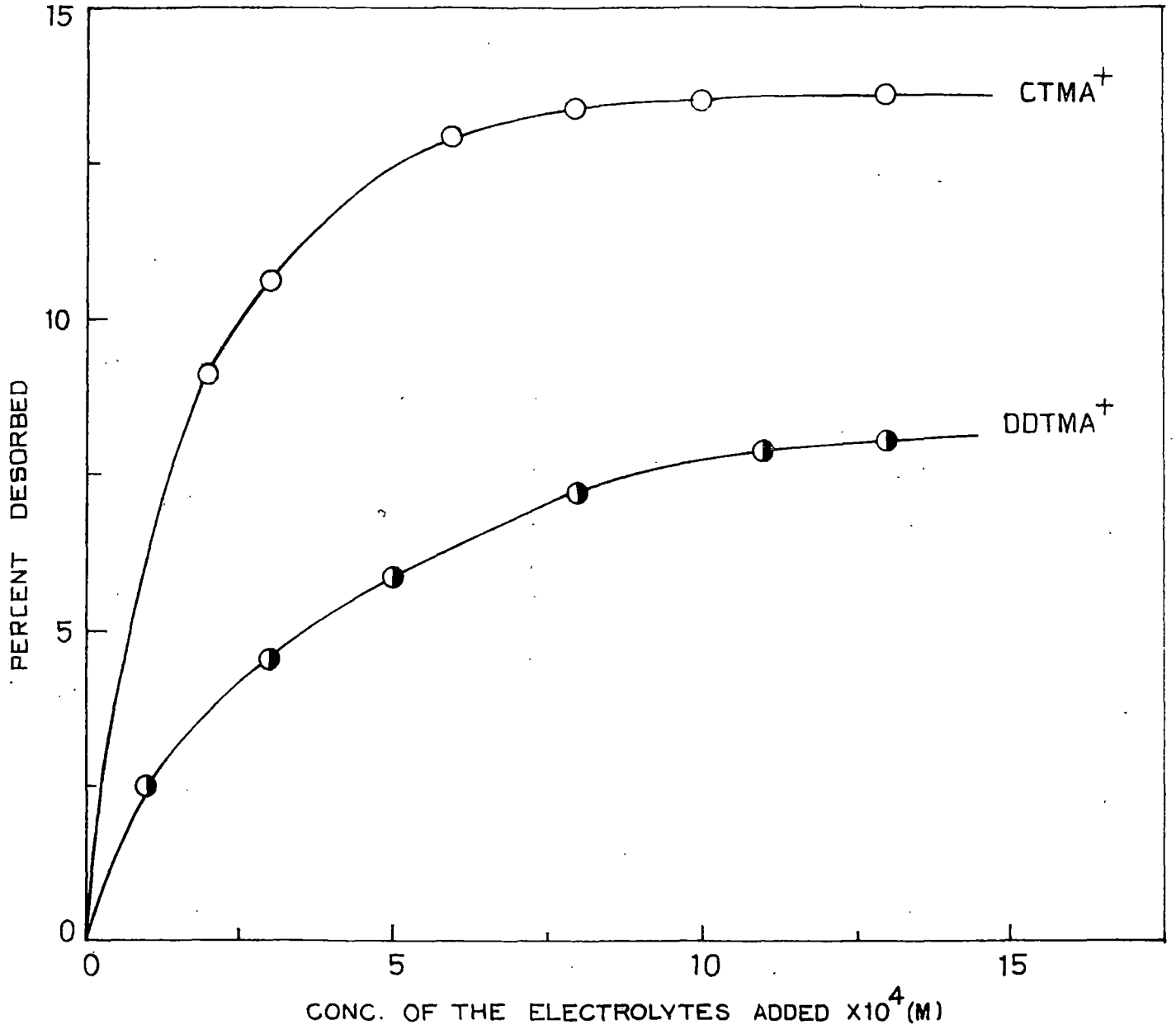

FIG. 29. DESORPTION OF RG FROM Na-KAOLINITE - RG BY VARIOUS LONG-CHAIN SURFACE ACTIVE ALKYLTRIMETHYLAMMONIUM HALIDES.

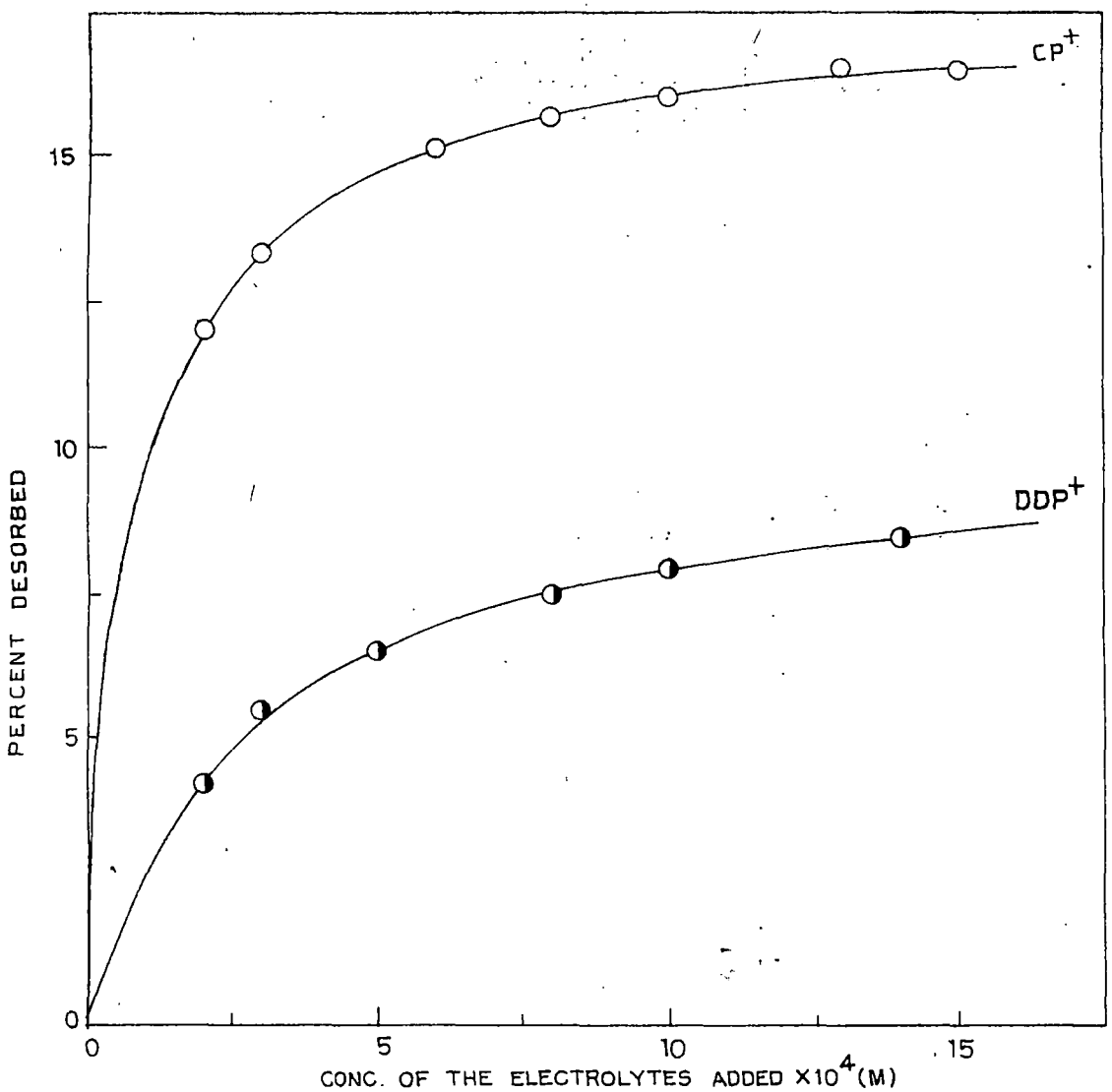

FIG. 30. DESORPTION OF RG FROM Na-KAOLINITE-RG BY VARIOUS LONG-CHAIN SURFACE ACTIVE ALKYLPYRIDINIUM HALIDES.

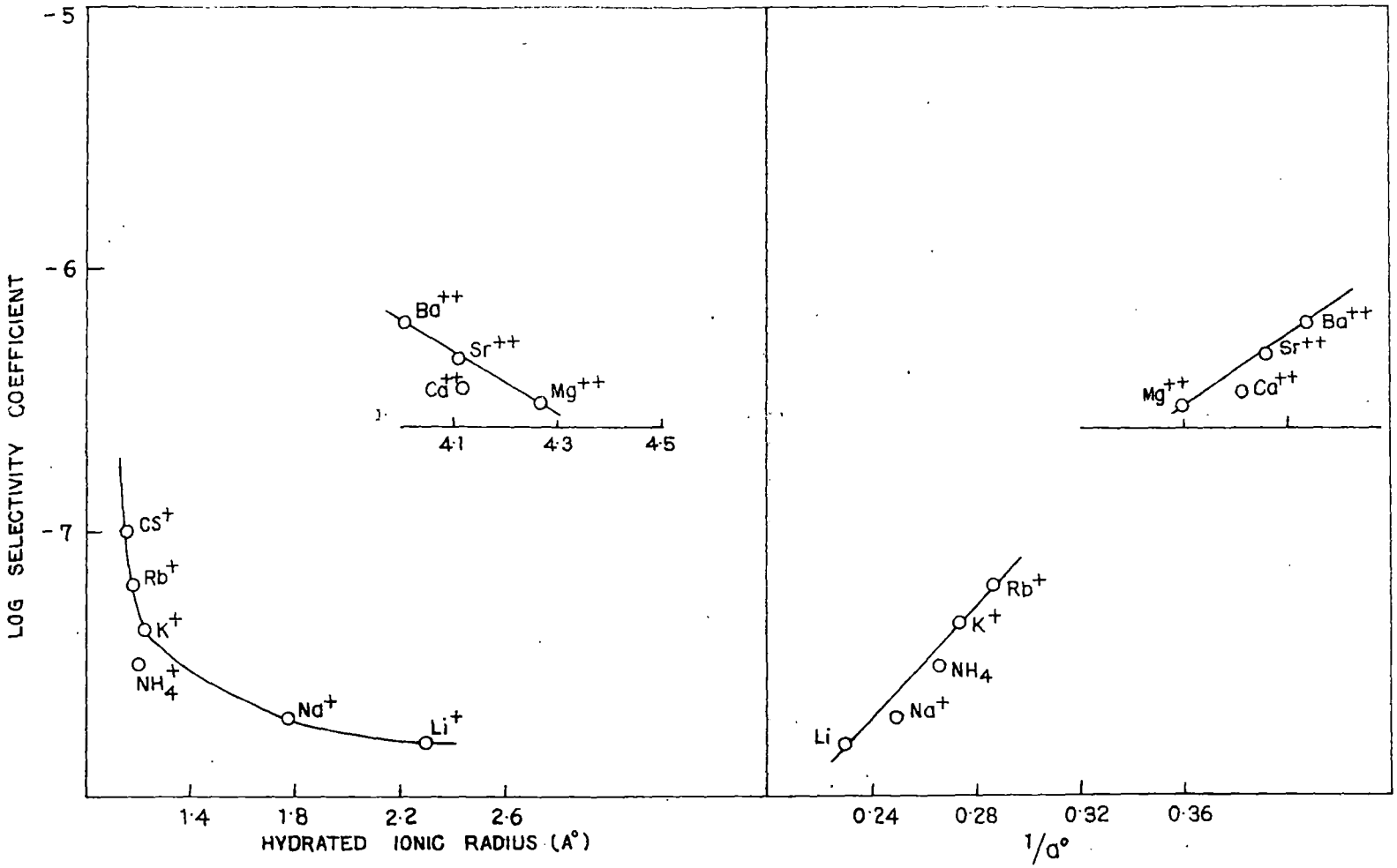

FIG. 31. CORRELATION OF SELECTIVITY COEFFICIENT WITH HYDRATED IONIC RADIUS AND DEBYE-HUCKEL PARAMETER, a°, IN THE DESORPTION OF RG FROM Na-KAOLINITE-RG.

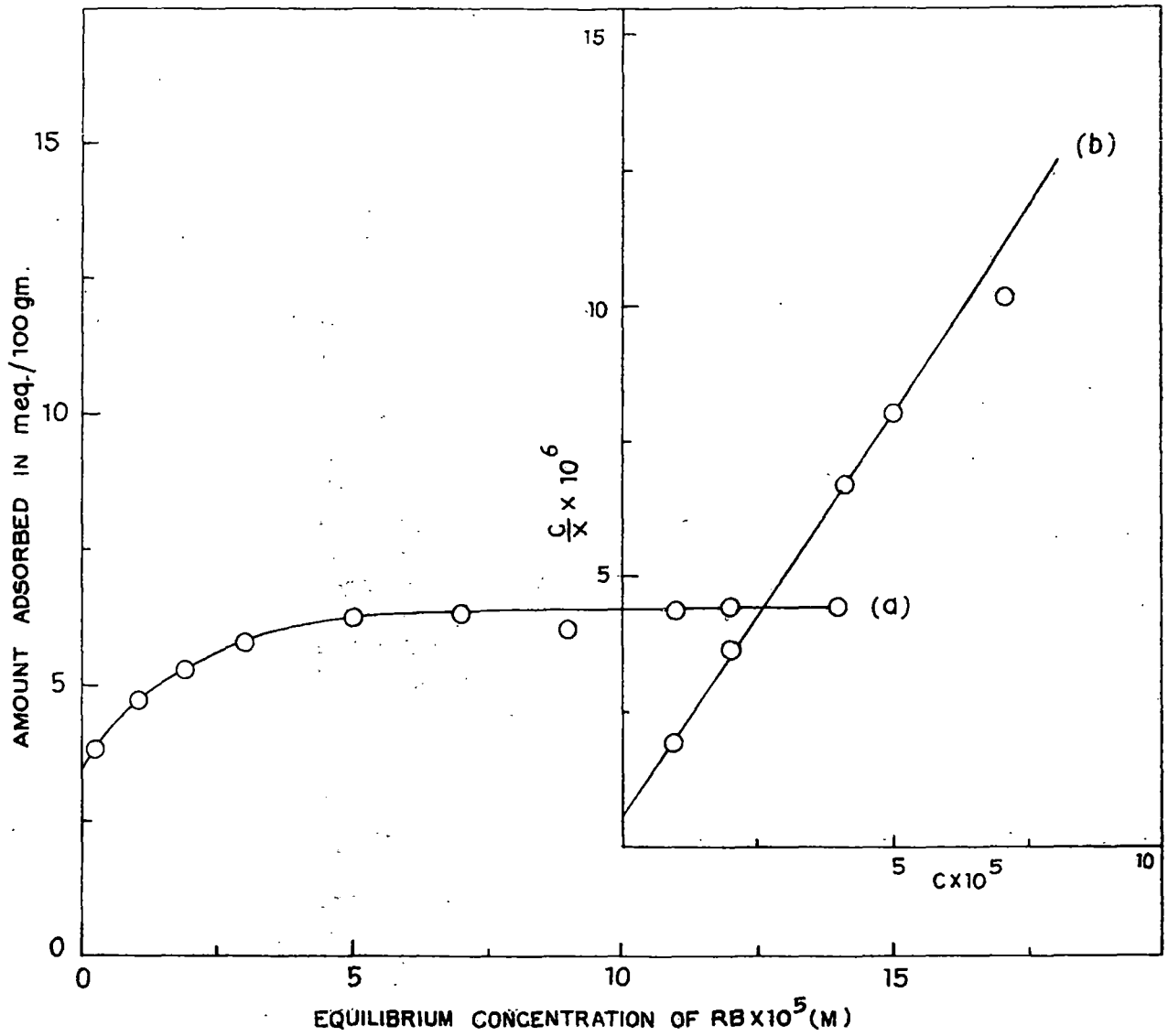

FIG. 32. ADSORPTION ISOTHERM AT 28°C (a) AND LANGMUIR PLOT (b) OF RB ON Na-KAOLINITE.

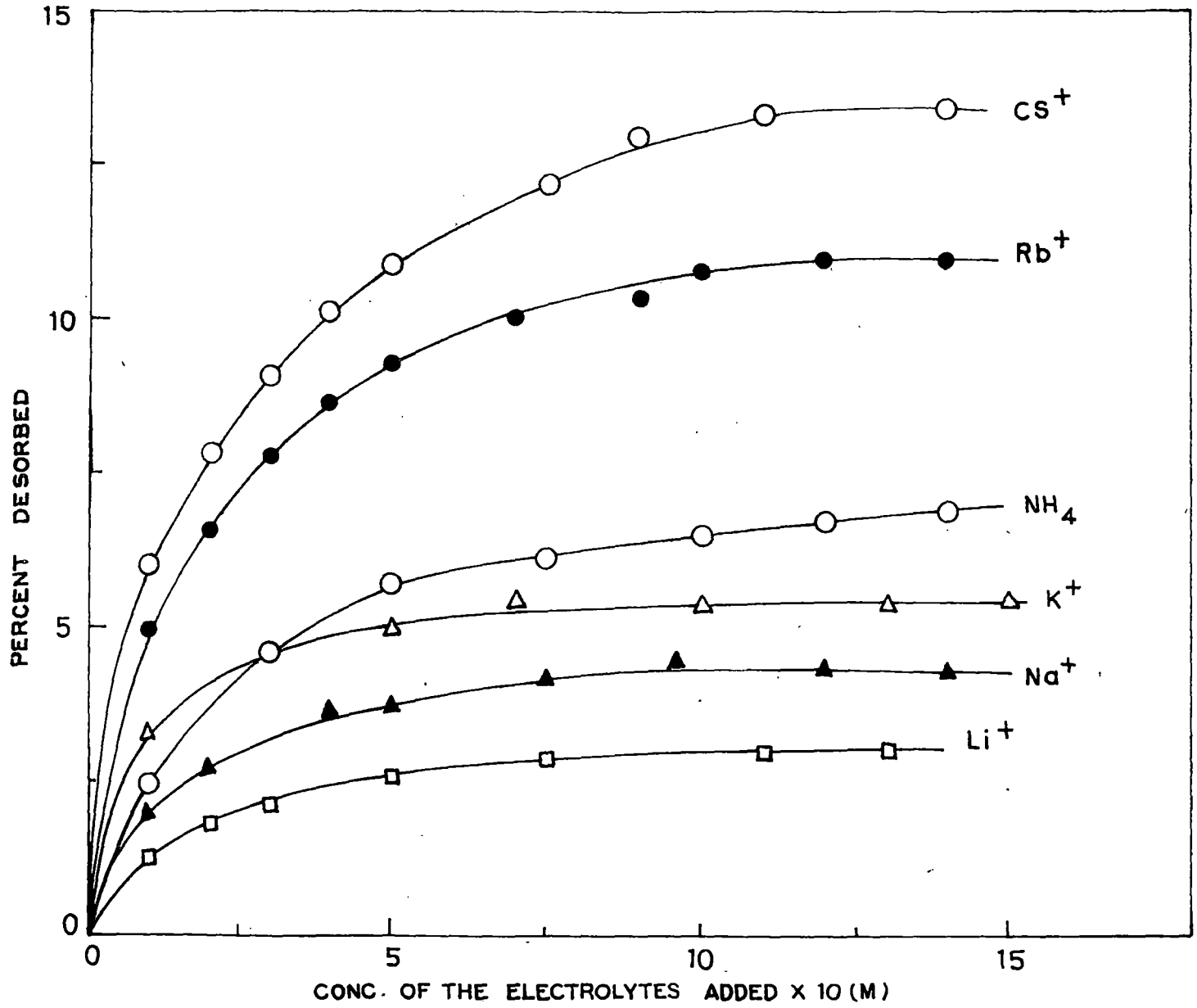

FIG. 33. DESORPTION OF RB FROM Na-KAOLINITE-RB BY VARIOUS MONOVALENT IONS.

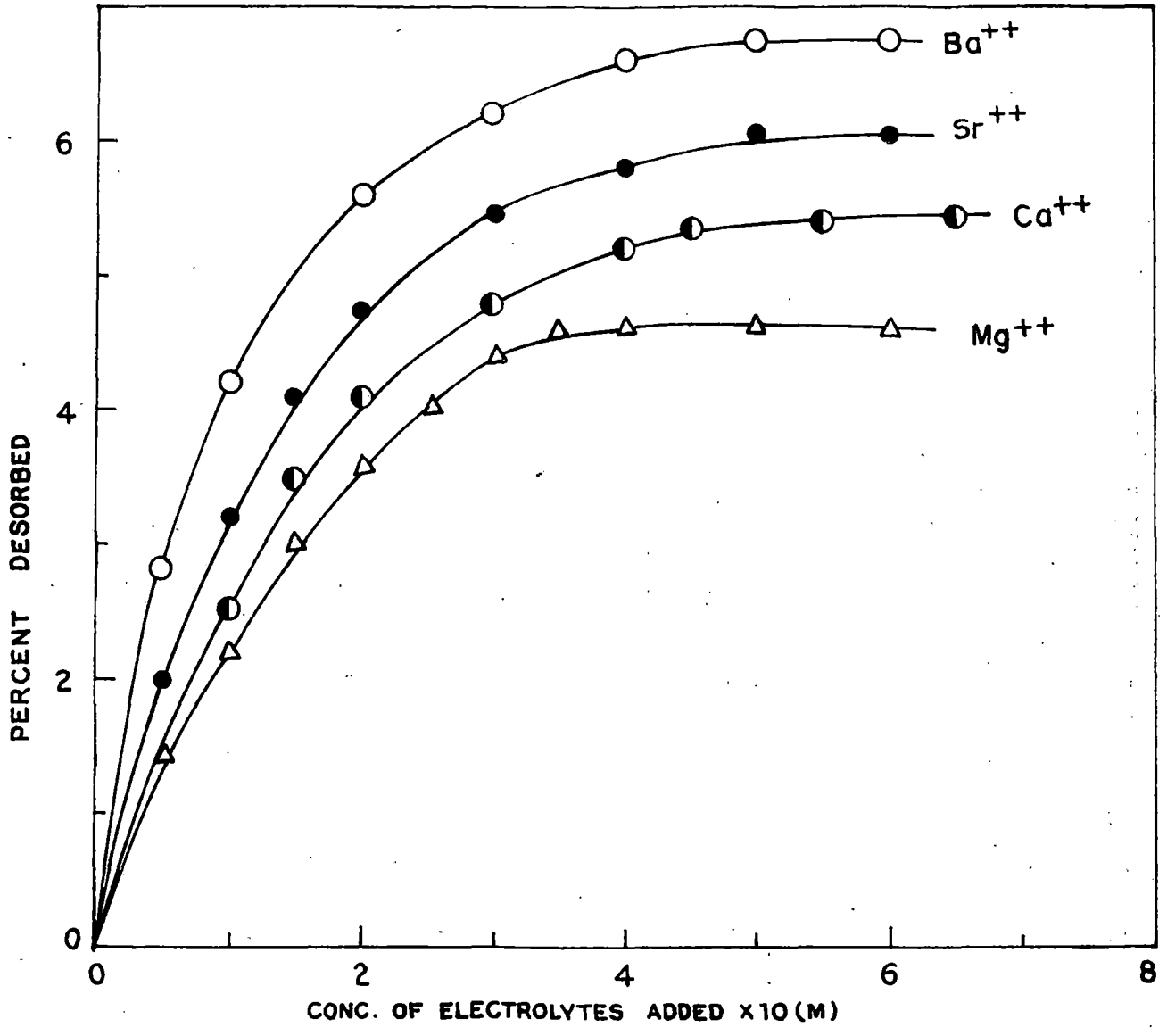

FIG. 34. DESORPTION OF RB FROM Na- KAOLINITE - RB BY VARIOUS BIVALENT IONS.

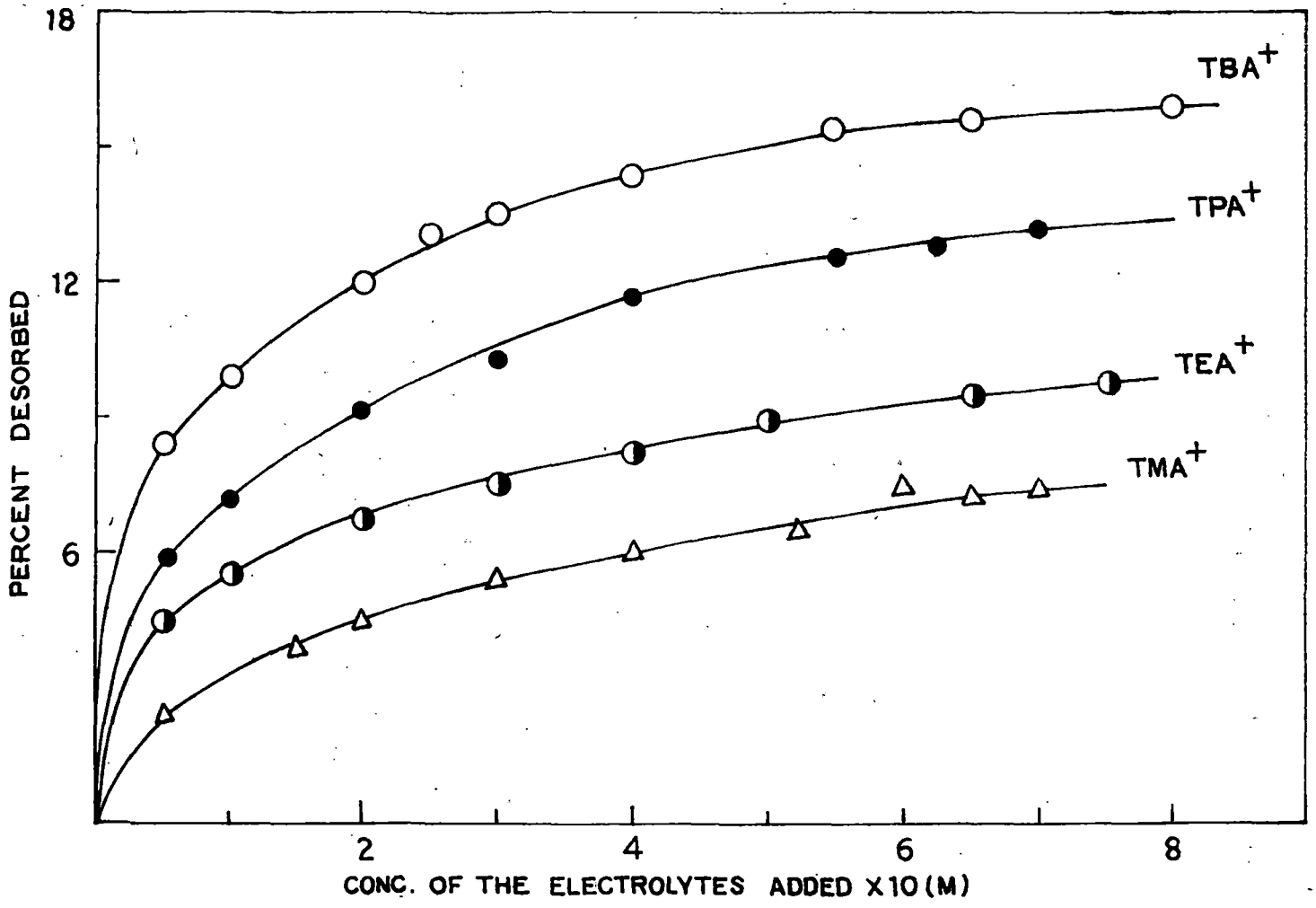

FIG. 35. DESORPTION OF RB FROM Na-KAOLINITE RB BY VARIOUS TETRA ALKYL-AMMONIUM HALIDES.

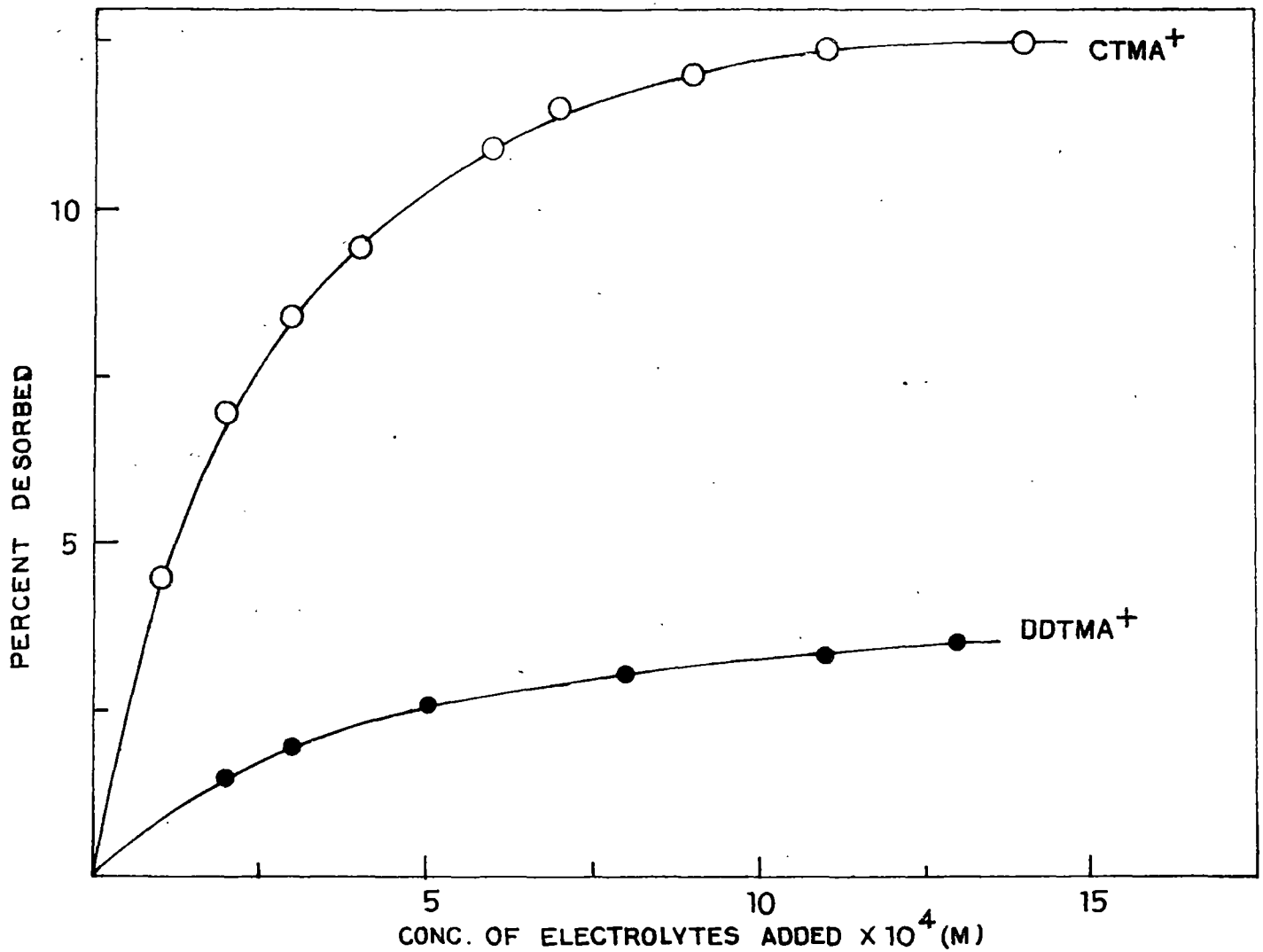

FIG. 36. DESORPTION OF RB FROM Na-KAOLINITE BY VARIOUS LONG-CHAIN SURFACE ACTIVE ALKYLTRIMETHYL AMMONIUM HALIDES.

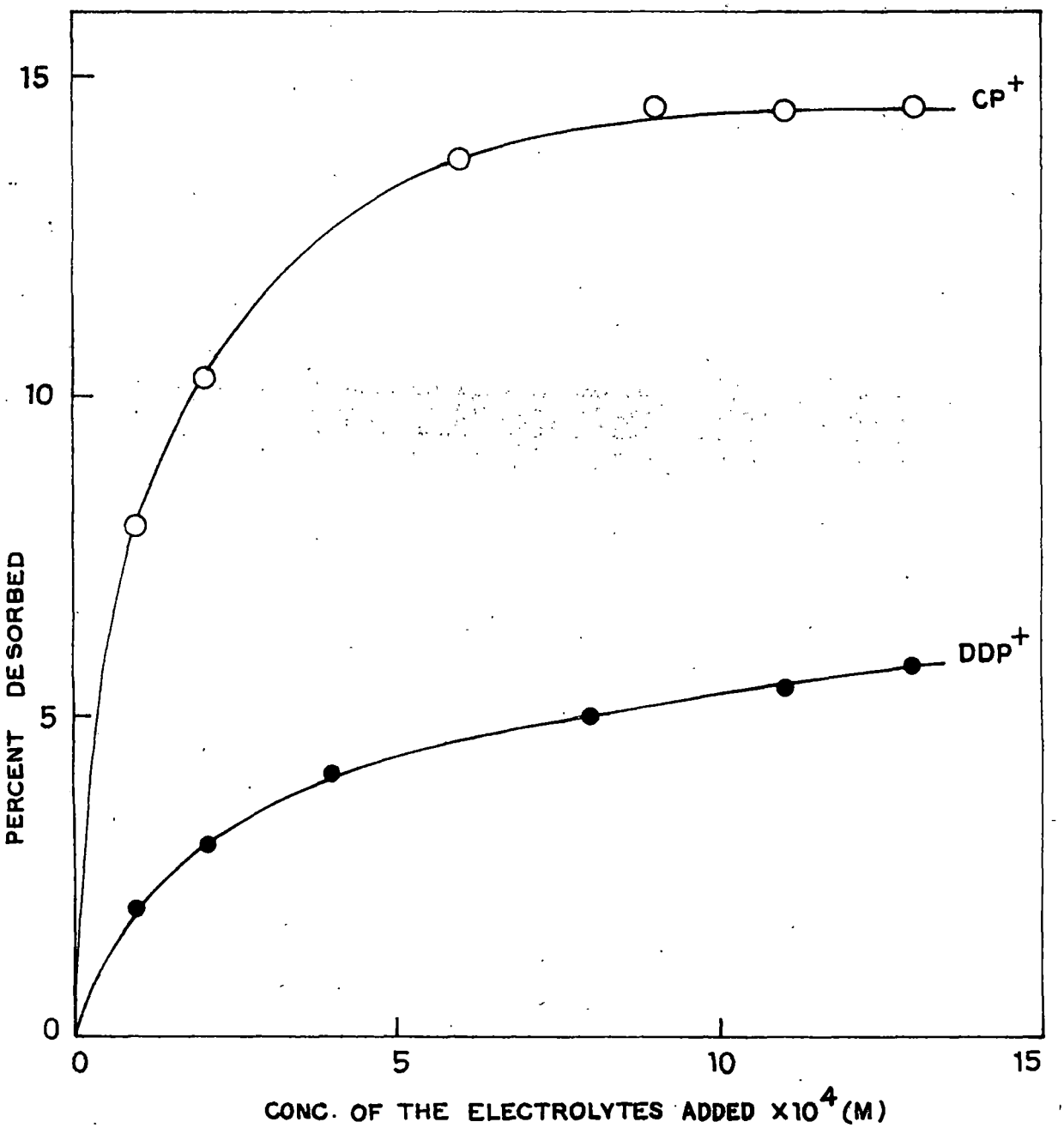

FIG. 37. DESORPTION OF RB FROM Na-KAOLINITE-RB BY VARIOUS LONG-CHAIN SURFACE ACTIVE ALKYLPYRIDINIUM HALIDES.

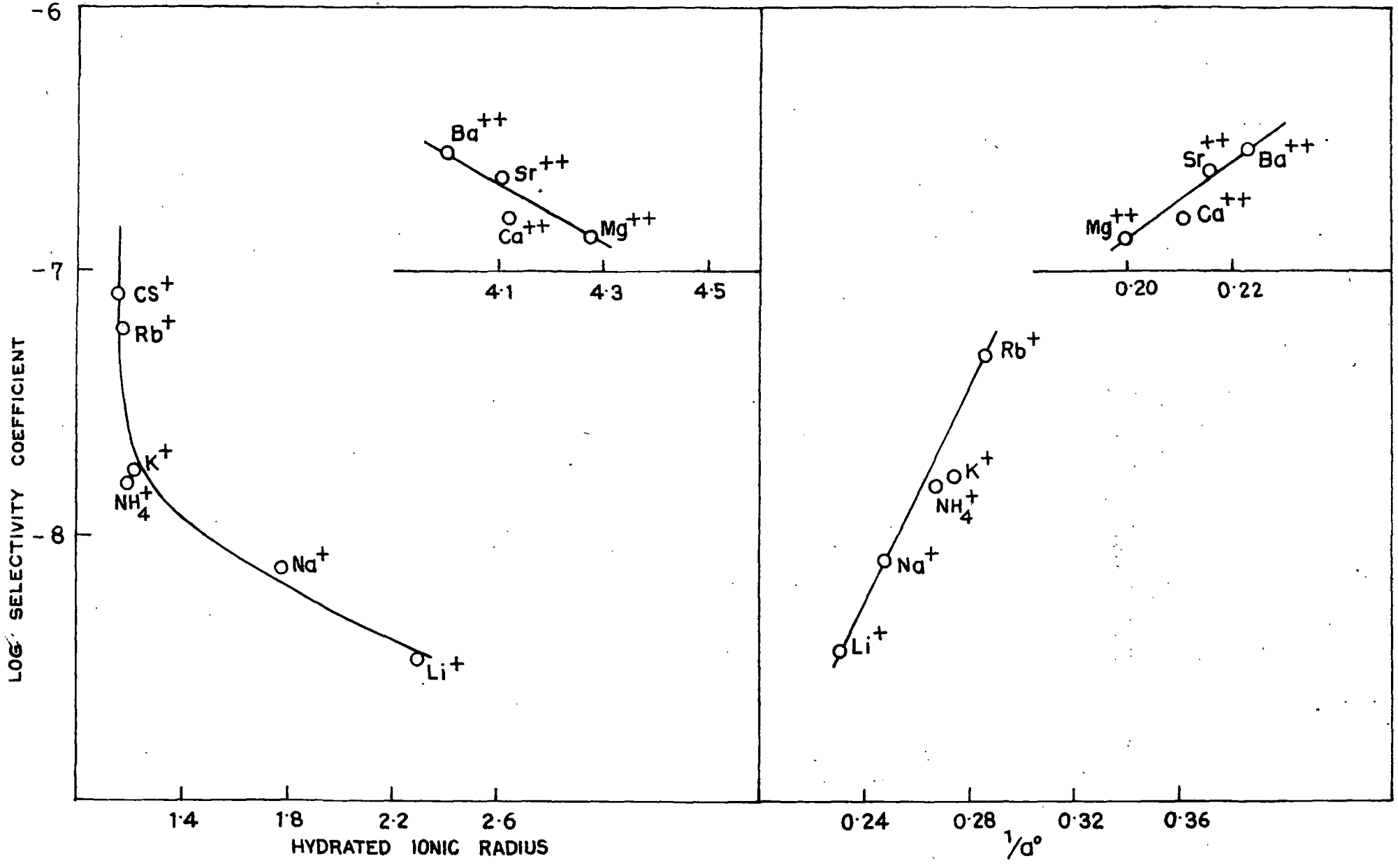

FIG. 38. CORRELATION OF SELECTIVITY COEFFICIENT WITH HYDRATED IONIC RADIUS AND DEBYE-HUCKEL PARAMETER, a°, IN THE DESORPTION OF RB FROM Na- KAOLINITE - RB.

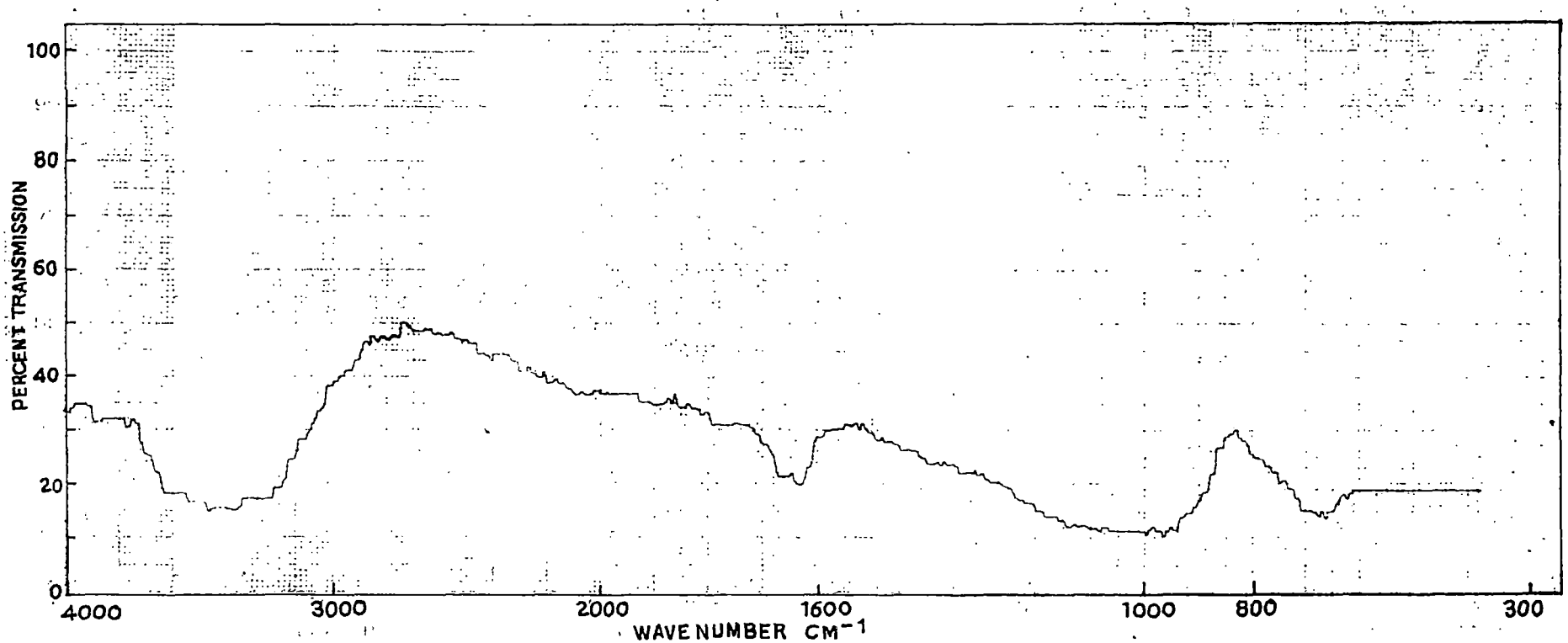

Fig. 39. Infrared Spectrum of Na-Kaolonite

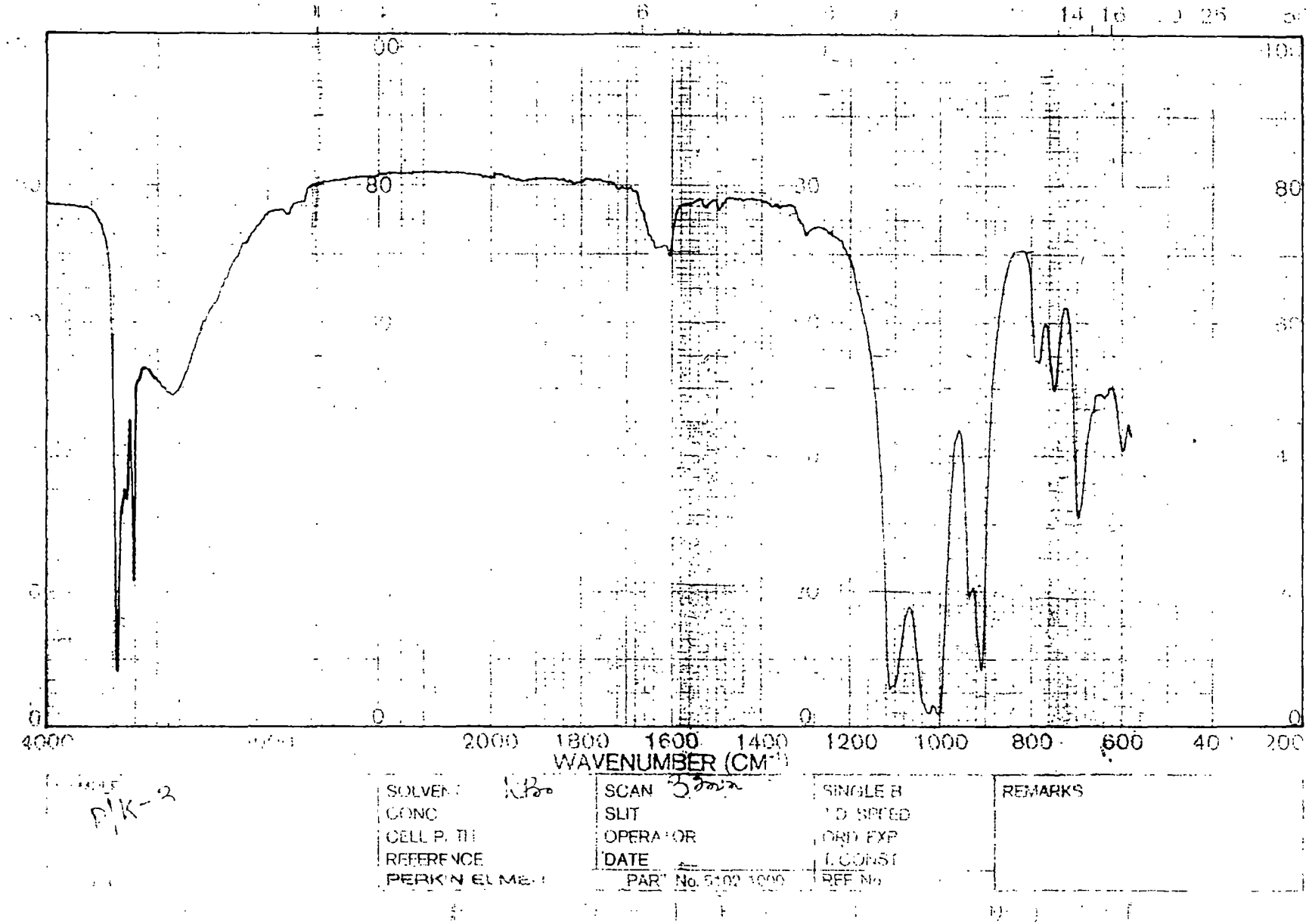

Fig. 40. Infrared spectrum of 100% exchanged Na-Kaolinite-RG (in KBr pellet).

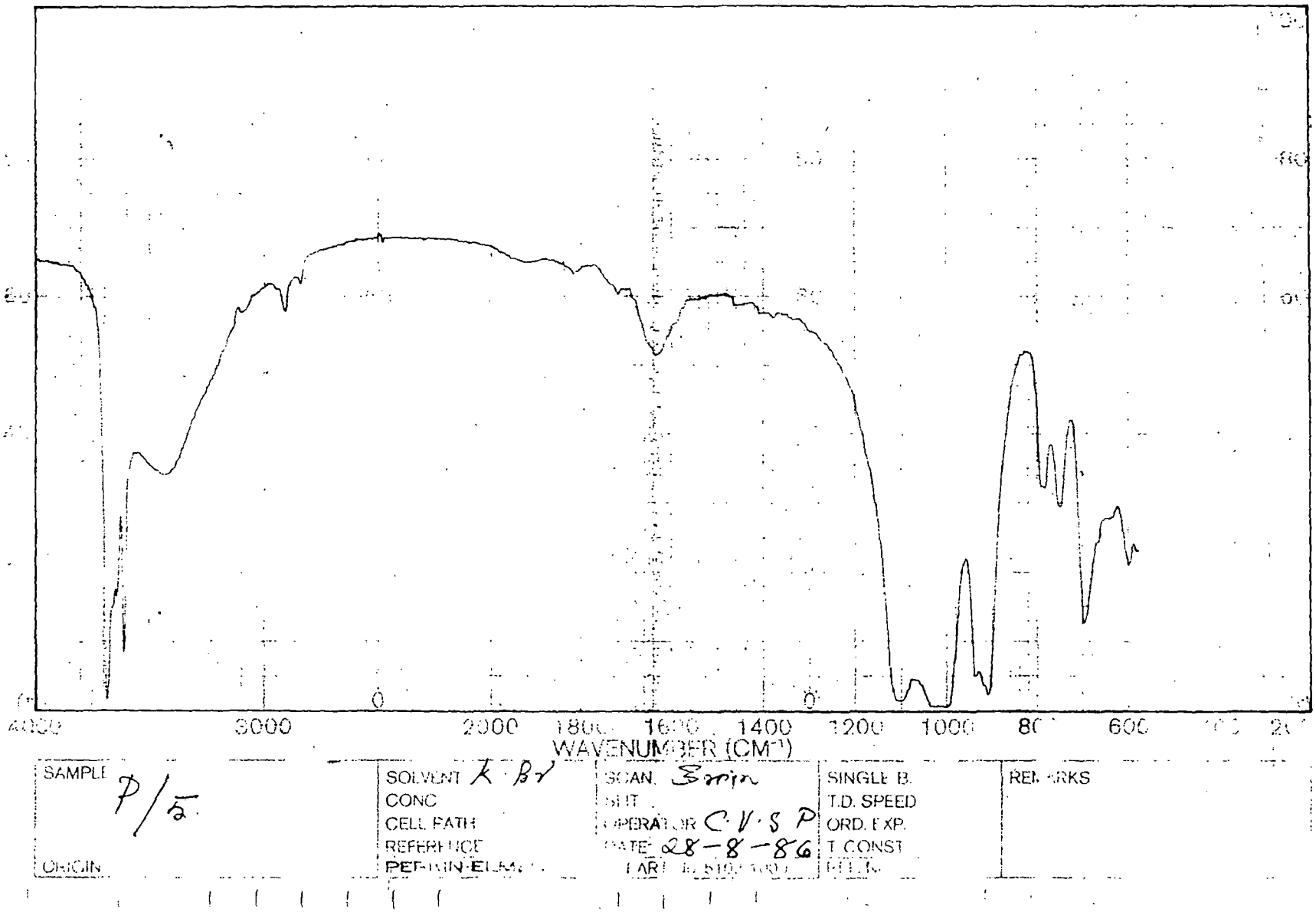

Fig. 41. Infrared spectrum of 100% exchanged Na- Kaolinite - RB (in KBr pellet) .

CHAPTER - VI

Sorption and Desorption of Rhodamine 6G and Rhodamine B on Na-Laponite System.

In order to investigate further, the influence of the type of clay mineral on ion-exchange behaviour of Na-Laponite XLG, a synthetic hectorite, has been used for the sorption and desorption of RG^+ and RB^+. Although laponite, montmorillonite are members of the expanding three layer clays, the difference among these members is in the type and degree of the isomorphic substitution. Laponite owes its charge to octahedral replacement of Mg^{2+} by Li^+ while in montmorillonite it is primarily Mg^{2+} for Al^{3+} in the octahedral layer (1,2). Consequently the electrical attraction between montmorillonite plate differs greatly from that of laponite as a result of which laponite possesses lower charge density than montmorillonite (3) and can well more freely in aqueous medium.

The properties of this synthetic clay mineral has been described by Fripiat (4) and Neuman et al (5,6). The stability of a laponite CP Sol in presence of Chlorides of lithium, sodium, potassium, ammonium, magnesium calcium, barium, lanthanum and hexadecyltrimethylammonium bromide has been studied over a wide range of pH by Perkins et al (7). They observed that the sols

are stable over the pH range $\approx$ 7-12 and laponite CP particle - charge becomes more negative as the pH increases. At pH $<$ 7, sols are destabilised. Thus laponite CP clay suspension behaves quite differently with regard to the stability towards electrolytes as a function of pH than montmorillonite. Laponite CP is also chosen because it forms stable colloid solutions suitable for spectrophotometric studies. So the present investigation has been carried out with the synthetic laponite XLG, supplied by Laponite Industries Ltd., England.

The sorption and desorption characteristics of RG^+ and RB^+ on Na-laponite are discussed below on the basis of experimental results. The characteristics of sorption are presented in Section A and those of desorption in Section B. In Section A also infrared studies on RG^+ and RB^+ exchanged Na-Laponite are briefly discussed.

SECTION - A

Studies on Sorption

Sorption RG^+ at pH 8.5

The adsorption isotherm of RG^+ on Na-laponite is shown in Fig. 42(a) and the Fig. 42(b) represents linear Langmuir reciprocal graph from which the value of V_m is found to be 96 meq/100 gm as against the amount of dye exchanged at 1.2×10^{-4} (M) which is 92 meq/100g. Both these values are higher than cation exchange capacity of the clay mineral. The top portion of the isotherm has not attained a plateau upto the concentration used in this study. But this nature was not shown in case of montmorillonite (page 59). Since laponite can swell to an unlimited extent, the dye molecules get sufficient space for an easy entry into the interlamellar region and stack themselves upto formation of a bilayer or multilayer. Also the higher aggregation tendency of RG^+ in aqueous medium favours this process (page 61). The Langmuir bonding constant of the dye calculated from the slope and intercept of the linear plot is $2.14 \times 10^5\ M^{-1}$.

Sorption of RB^+ at pH 8.5

The adsorption of RB^+ on Na-laponite is drawn in Fig. 49(a). The plot of C/XVX C, where C is the equilibrium concentration of RB^+ and X is the amount adsorbed per 100 gm of the adsorbent, yields a good straight line Fig. 49(b). This indicates that the sorption data conform to the Langmuir equation suggesting a monolayer adsorption. From the slope of the straight line, the value of V_m (the amount required to form a complete monolayer) is found to be 89 meq/100 gm. The maximum exchange from the adsorption isotherm is 92 meq/100 gm while the c.e.c. of the mineral is 88 meq/100 gm. These values are lower than those for RG^+ but still slightly higher than the c.e.c. value of Na-laponite. This is probably due to sorption of aggregated ions from the solution or dimerisation or stacking of dye ions over those already present in the adsorbed state. Here the value of V_m is less than that of RG^+ adsorbed. This may be due to lower aggregation tendency of RB^+ compared to RG^+ in aqueous medium. The calculated Langmuir constant for RB^+ on to laponite is equal to $2.26 \times 10^5 M^{-1}$. which is higher than that of RG-Na-laponite system, signifying that the former dye is more firmly anchored to the mineral. Similar characteristics of these dyes have been found earlier on montmorillonite and kaolinite.

Infrared Spectral Studies on RG^+ and RB^+ exchanged Na-Laponite.

Following the method given in Chapter - III page 55 infrared spectra are obtained for RG, RB, Na-laponite, 100% RG - exchanged and 100% RB-exchanged laponite shown in Figs. 21, 22, 56, 57, 58 respectively. It appears that the ring vibration band of RG^+ at 1580 cm^{-1} (Fig. 21) has been shifted to 1605 cm^{-1} (Fig. 57) for 100% RG-exchanged Na-laponite. This band of RB at 1602 cm^{-1} (Fig. 22) has been shifted to 1590 cm^{-1} (Fig. 58) for 100% RB-exchanged Na-laponite. Experimental result reflects their behaviour towards aggregation in the interlayer space (8).

SECTION - B

Desorption Studies

Desorption of RG^+ from Na-Laponite - RG:

The results of desorption of RG^+ from Na-laponite-RG complex by inorganic and organic ions are shown in Figs. 43-47. The desorption curves for inorganic and organic ions are similar to those obtained in the case of Na-montmorillonite. From table 10 it can be seen that selectivity coefficients increase in the order $Li^+ < Na^+ < K^+ \leqslant NH_4^+ < Rb^+ < Cs^+$ for the monovalent and $Mg^{++} < Ca^{++} < Sr^{++} < Ba^{++}$ for the bivalent cations. Similarly for the monovalent organic ions used the selectivity coefficients are in the following sequence: $(CH_3)_4N < (C_2H_5)_4N < (C_3H_7)_4N < (C_4H_9)_4N$ and for the organic monovalent long chain surface active ions $DDTMA^+ < DDP^+ < CTMA^+ < CP^+$. The higher exchange ability of NH_4^+ than K^+ is to be noted which has also been observed by Bhattacharyya (9) in the desorption of $diquat^{2+}$ from Na-laponite-diquat complex and by Sunwar (10) in the desorption of $thionine^+$ from Na-laponite-thionine complex. It is interesting to note that the extent of desorption of RG^+ by inorganic monovalent, and bivalent cations (Figs. 43-44) is lower than that observed in montmorillonite. The charge density of the minerals is in the order : Laponite < montmorillonite and so the strength of binding would be the greater with montmorillonite than laponite.

This would lead probably to the expectation that the extent of desorption of the dye will be more in laponite system and lesser in montmorillonite system.

However, nitrogen sorption study shows that the surface area of laponite is larger than that of montmorillonite (11) and so the exchange sites in the former are more widely spaced than in the latter as a result of which the smaller inorganic ions are unable to approach the exchange spots effectively to displace the adsorbed dye from the laponite matrix.

It is also observed that the amount of RG^+ desorbed from Na-laponite-RG complex by $CTMA^+$ or CP^+ is greater than the smaller ions $(CH_3)_4N^+$ or $(C_2H_5)_4N^+$. Since Na-laponite shows considerable interlamellar swelling in an aqueous medium, steric and space factors do not influence the extent of exchange. As such from the observed isotherms (Fig. 45) it reveals that there is a regular increase in the affinity of alkyl ammonium ions for laponite with increasing molecular weight and molecular size. Similar behaviour is found in chain lengths of the long chain surface active ions (Figs. 46, 47). This applies, to the adsorption of organic compounds by expanding clay minerals in general and is ascribed to the increased contribution of van der Waals forces to the adsorption energy (12) and changes in the hydration states of the ions in the clay interlayer (13,14).

As in the desorption of RG^+ from its montmorillonite complexes, both $1/a^o$ and hydrated ionic radius of the alkaline earth metal ions when polotted against log (selectivity coefficient)

behave linearly (Fig. 48). While only $1/a^{o}$ in the case of alkali metal ions yield a straight line when plotted against log (selectivity coefficient) but show non linear when log (selectivity coefficient) plotted against hydrated ionic radii (Fig. 48). Thus the linear relationship of these parameters with log (selectivity coefficient) may be used to correlate and predict the relative affinities of the respective ions for the aluminosilicate surface. As mentioned earlier (page 73) the obedience of the exchange data to the Pauley's model demonstrates that the coulombic interaction between the counter ions and the fixed ionic groups is the predominant factor in this type of exchange reactions.

SECTION - B

Desorption Studies

Desorption of RB^+ from Na-Laponite - RB :

The extent of RB^+ desorbed from Na-laponite-RB complex by various inorganic ions is much smaller than in Na-laponite-RB systems (Figs. 50,51). This is probably due to combined effect of the stronger binding of RB^+ ions onto the mineral reflected from Langmuir bonding constant value and the weak desorbing power of the above ions owing to their relative shape and size vis-a-vis the widely placed exchange sites in laponite interlayer.

In the desorption study with organic ions the percentage of the dye released from Na-laponite-RB complex is lesser than from Na-laponite-RG complex (Figs. 52-54). However, the desorption of the dye increases with the size of the organic ions as in other cases. According to their order of the exchange power, as well as distribution and selectivity coefficients shown in Table 11 the ions may be arranged as $Li^+ < Na^+ < K^+ < NH_4^+ < Rb^+ < Cs^+$ for the monovalent ions, $Mg^{+2} < Ca^{+2} < Sr^{+2} < Ba^{+2}$ for the bivalent ions, in inorganic electrolytes.

According to their exchanging power, the organic ions may be arranged as $TMA^+ < TEA^+ < TPA^+ < TBA^+$ for the tetraalkylammonium ions and $DDTMA^+ < DDP^+ < CTMA^+ < CP^+$ for the monovalent

long chain surface active ions. The exchange isotherm with DDP^+, $DDTMA^+$, $CTMA^+$ and CP^+ are S-shaped and may be explained as done earlier (page 69). Here also CP^+ desorbs a greater amount of dye from $CTMA^+$ due to its lower cmc value. The desorption by $CTMA^+$ and CP^+ at the initial stages is the result of the competition between these electrolytes as single ions and the adsorbed dye ions. But as the concentration of the quarternary salts increases beyond the cmc, the probability of micelle formation increases in the bulk solution and in the adsorbed states. Consequently, the dye ions face a stronger competition and more readily displaced by the quaternary ammonium ions.

As noted in the case of other mineral systems, the extent of desorption of RG^+ from its laponite complex, is higher than that of RB^+ from Na-laponite-RB complex, suggesting thereby a weaker binding to RG^+ to this exchanger. Such order in the binding strengths of RB and RG has also been observed in montmorillonite and kaolinite systems. The higher bonding constant of RB^+ sorption isotherm (page 113) compared to that of RG^+ (page 112) also leads support to this conclusion.

The plot of hydrated ionic radii vs log (slectivity coefficient) though non linear in the case of monovalent inorganic ions, gives a straight line for bivalent inorganic

ions. However, a linear plot is obtained for monovalent and bivalent inorganic ions when their values $1/a^{o}$ are plotted against log (selectivity coefficient) (Fig. 55). A similar behaviour was noted earlier in the other minerals studied.

TABLE - 10

Desorption characteristics of RG from Na-Laponite-RG with respect to different ions

Electrolytes used	Concentration of Electrolyte	Distribution Coefficient	Selectivity Coefficient
1:1 Electrolyte			
LiCl	0.1 (M)	0.029	3.57×10^{-8}
	0.2 (M)	0.022	4.14×10^{-8}
	0.3 (M)	0.018	4.37×10^{-8}
	0.5 (M)	0.014	4.11×10^{-8}
	0.75 (M)	0.010	3.26×10^{-8}
NaCl	0.1 (M)	0.040	6.93×10^{-8}
	0.2 (M)	0.027	6.56×10^{-8}
	0.3 (M)	0.022	6.12×10^{-8}
	0.5 (M)	0.015	5.23×10^{-8}
	0.75 (M)	0.017	4.44×10^{-8}
KCl	0.1 (M)	0.078	2.61×10^{-7}
	0.2 (M)	0.048	2.02×10^{-7}
	0.3 (M)	0.036	1.72×10^{-7}
	0.5 (M)	0.025	1.39×10^{-7}
	0.75 (M)	0.018	1.10×10^{-7}

TABLE - 10 (Contd..)

Electrolytes used	Concentration of Electrolyte	Distribution Coefficient	Selectivity Coefficient
	0.1 (M)	0.063	1.69×10^{-7}
NH_4Cl	0.2 (M)	0.041	1.48×10^{-7}
	0.3 (M)	0.033	1.45×10^{-7}
	0.5 (M)	0.025	1.40×10^{-7}
	0.75 (M)	0.019	1.23×10^{-7}
	0.1 (M)	0.094	3.84×10^{-7}
RbCl	0.2 (M)	0.056	2.77×10^{-7}
	0.3 (M)	0.042	2.28×10^{-7}
	0.5 (M)	0.028	1.75×10^{-7}
	0.75 (M)	0.021	1.50×10^{-7}
	0.1 (M)	0.138	8.32×10^{-7}
CsCl	0.2 (M)	0.082	5.92×10^{-7}
	0.3 (M)	0.061	4.92×10^{-7}
	0.5 (M)	0.041	3.83×10^{-7}
	0.75 (M)	0.029	2.94×10^{-7}

TABLE -10 (Contd..)

Electrolytes used	Concentration of Electrolyte	Distribution Coefficient	Selectivity Coefficient
2:1 Electrolyte			
$MgCl_2$	0.05 (M)	0.449	1.94×10^{-6}
	0.10 (M)	0.327	1.50×10^{-6}
	0.20 (M)	0.236	1.14×10^{-6}
	0.30 (M)	0.196	9.82×10^{-7}
	0.40 (M)	0.172	8.79×10^{-7}
$CaCl_2$	0.05 (M)	0.468	2.21×10^{-6}
	0.10 (M)	0.342	1.73×10^{-6}
	0.20 (M)	0.247	1.30×10^{-6}
	0.30 (M)	0.205	1.13×10^{-6}
	0.40 (M)	0.181	1.02×10^{-6}
$SrCl_2$	0.05 (M)	0.476	2.32×10^{-6}
	0.10 (M)	0.344	1.75×10^{-6}
	0.20 (M)	0.252	1.38×10^{-6}
	0.30 (M)	0.210	1.20×10^{-6}
	0.40 (M)	0.183	1.07×10^{-6}

TABLE - 10 (Contd..)

Electrolytes used	Concentration of Electrolyte	Distribution Coefficient	Selectivity Coefficient
	0.05 (M)	0.526	3.15×10^{-6}
$BaCl_2$	0.10 (M)	0.385	2.48×10^{-6}
	0.20 (M)	0.280	1.91×10^{-6}
	0.30 (M)	0.231	1.62×10^{-6}
	0.40 (M)	0.202	1.44×10^{-6}
Quaternary Ammonium Salt			
	0.05 (M)	0.189	7.67×10^{-7}
TMABr	0.10 (M)	0.151	9.87×10^{-7}
	0.20 (M)	0.104	9.46×10^{-7}
	0.30 (M)	0.075	7.53×10^{-7}
	0.40 (M)	0.066	7.73×10^{-7}
	0.05 (M)	0.415	3.78×10^{-6}
TEABr	0.10 (M)	0.302	4.06×10^{-6}
	0.20 (M)	0.204	3.79×10^{-6}
	0.30 (M)	0.157	3.40×10^{-6}
	0.40 (M)	0.132	3.23×10^{-6}

TABLE - 10 (Contd..)

Electrolytes used	Concentration of Electrolyte	Distribution Coefficient	Selectivity Coefficient
	0.05 (M)	1.739	7.42×10^{-5}
TPABr	0.10 (M)	1.072	5.85×10^{-5}
	0.20 (M)	0.730	5.88×10^{-5}
	0.30 (M)	0.596	6.31×10^{-5}
	0.40 (M)	0.510	6.52×10^{-5}
	0.05 (M)	4.032	5.06×10^{-4}
TBABr	0.10 (M)	2.270	3.40×10^{-4}
	0.20 (M)	1.285	2.36×10^{-4}
	0.30 (M)	0.941	2.03×10^{-4}
	0.40 (M)	0.756	1.86×10^{-4}
	2×10^{-4} (M)	189.94	3.23×10^{-3}
DDTMABr	4×10^{-4} (M)	197.36	7.51×10^{-3}
	6×10^{-4} (M)	151.76	7.42×10^{-3}
	8×10^{-4} (M)	134.04	7.32×10^{-3}
	1×10^{-3} (M)	119.82	7.49×10^{-3}

TABLE -10 (Contd..)

Electrolytes used	Concentration of Electrolyte	Distribution Coefficient	Selectivity Coefficient
	2×10^{-4} (M)	709.10	5.49×10^{-2}
CTMABr	4×10^{-4} (M)	481.57	5.63×10^{-2}
	6×10^{-4} (M)	373.37	5.48×10^{-2}
	8×10^{-4} (M)	295.68	4.73×10^{-2}
	1×10^{-3} (M)	245.94	4.19×10^{-2}
	1×10^{-4} (M)	472.97	1.02×10^{-2}
DDPBr	2×10^{-4} (M)	378.18	1.37×10^{-2}
	3×10^{-4} (M)	294.09	1.27×10^{-2}
	4×10^{-4} (M)	252.63	1.28×10^{-2}
	5×10^{-4} (M)	220.54	1.24×10^{-2}
	1×10^{-4} (M)	1009.00	5.12×10^{-2}
CPBr	2×10^{-4} (M)	866.68	8.76×10^{-2}
	3×10^{-4} (M)	705.85	9.48×10^{-2}
	4×10^{-4} (M)	576.31	8.83×10^{-2}
	5×10^{-4} (M)	492.38	8.39×10^{-2}

TABLE - 11

Desorption characteristics of RB from Na-Laponite-RB with respect to different ions.

Electrolyte used	Concentration of Electrolyte	Distribution Coefficient	Selectivity Coefficient
1:1 Electrolyte			
	0.1 (M)	0.012	9.45×10^{-9}
LiCl	0.2 (M)	0.010	9.92×10^{-9}
	0.3 (M)	0.008	1.56×10^{-8}
	0.5 (M)	0.006	1.33×10^{-8}
	0.75 (M)	0.005	1.21×10^{-8}
	0.1 (M)	0.017	1.85×10^{-8}
NaCl	0.2 (M)	0.013	2.08×10^{-8}
	0.3 (M)	0.010	1.98×10^{-8}
	0.5 (M)	0.007	1.82×10^{-8}
	0.75 (M)	0.005	1.64×10^{-8}
	0.1 (M)	0.037	8.82×10^{-8}
KCl	0.2 (M)	0.023	6.50×10^{-8}
	0.3 (M)	0.017	5.59×10^{-8}
	0.5 (M)	0.012	3.68×10^{-8}
	0.75 (M)	0.008	3.30×10^{-8}

TABLE - 11 (Contd..)

Electrolytes used	Concentration of electrolyte	Distribution Coefficient	Selectivity Coefficient
	0.1 (M)	0.042	1.33×10^{-7}
NH_4Cl	0.2 (M)	0.026	8.79×10^{-8}
	0.3 (M)	0.020	7.31×10^{-8}
	0.5 (M)	0.013	5.66×10^{-8}
	0.75 (M)	0.009	1.87×10^{-8}
	0.1 (M)	0.049	1.48×10^{-7}
RbCl	0.2 (M)	0.029	1.07×10^{-7}
	0.3 (M)	0.021	8.75×10^{-8}
	0.5 (M)	0.014	6.64×10^{-8}
	0.75 (M)	0.010	5.37×10^{-8}
	0.1 (M)	0.055	1.92×10^{-7}
CsCl	0.2 (M)	0.033	1.36×10^{-7}
	0.3 (M)	0.025	1.18×10^{-7}
	0.5 (M)	0.017	9.50×10^{-8}
	0.75 (M)	0.013	7.86×10^{-8}

TABLE - 11 (Contd..)

Electrolytes used	Concentration of electrolyte	Distribution Coefficient	Selectivity Coefficient
2:1 Electrolyte			
$MgCl_2$	0.05 (M)	0.294	7.89×10^{-7}
	0.10 (M)	0.228	7.34×10^{-7}
	0.20 (M)	0.172	6.35×10^{-7}
	0.30 (M)	0.144	5.60×10^{-7}
	0.40 (M)	0.127	5.07×10^{-7}
$CaCl_2$	0.05 (M)	0.316	9.83×10^{-7}
	0.10 (M)	0.241	8.70×10^{-7}
	0.20 (M)	0.179	7.17×10^{-7}
	0.30 (M)	0.150	6.37×10^{-7}
	0.40 (M)	0.132	5.82×10^{-7}
$SrCl_2$	0.05 (M)	0.328	1.09×10^{-6}
	0.10 (M)	0.249	9.56×10^{-7}
	0.20 (M)	0.185	7.91×10^{-7}
	0.30 (M)	0.155	6.99×10^{-7}
	0.40 (M)	0.136	6.37×10^{-7}

TABLE -11 (Contd..)

Electrolytes used	Concentration of electrolyte	Distribution Coefficient	Selectivity Coefficient
	0.05 (M)	0.340	1.21×10^{-6}
$BaCl_2$	0.10 (M)	0.255	1.03×10^{-6}
	0.20 (M)	0.192	8.90×10^{-7}
	0.30 (M)	0.163	8.10×10^{-7}
	0.40 (M)	0.145	7.60×10^{-7}
Quaternary Ammonium Salt			
	0.05 (M)	0.031	2.95×10^{-8}
TMABr	0.10 (M)	0.031	5.92×10^{-8}
	0.20 (M)	0.018	4.26×10^{-8}
	0.30 (M)	0.021	8.75×10^{-8}
	0.40 (M)	0.018	8.58×10^{-8}
	0.05 (M)	0.093	2.67×10^{-7}
TEABr	0.10 (M)	0.062	2.38×10^{-7}
	0.20 (M)	0.054	3.67×10^{-7}
	0.30 (M)	0.049	4.63×10^{-7}
	0.40 (M)	0.054	7.47×10^{-7}

TABLE - 11 (Contd..)

Electrolytes used	Concentration of Electrolyte	Distribution Coefficient	Selectivity Coefficient
	0.05 (M)	0.124	4.76×10^{-7}
TPABr	0.10 (M)	0.124	9.62×10^{-7}
	0.20 (M)	0.107	1.45×10^{-6}
	0.30 (M)	0.117	2.64×10^{-6}
	0.40 (M)	0.123	4.04×10^{-6}
	0.05 (M)	0.077	1.96×10^{-5}
TBABr	0.10 (M)	0.670	3.08×10^{-5}
	0.20 (M)	0.488	3.47×10^{-5}
	0.30 (M)	0.382	3.29×10^{-5}
	0.40 (M)	0.321	3.20×10^{-5}
	2×10^{-4} (M)	93.46	1.09×10^{-3}
DDTMABr	4×10^{-4} (M)	93.23	2.26×10^{-3}
	6×10^{-4} (M)	84.87	2.88×10^{-3}
	8×10^{-4} (M)	85.26	4.00×10^{-3}
	1×10^{-3} (M)	77.57	4.14×10^{-3}

TABLE - 11 (Contd..)

Electrolytes used	Concentration of electrolyte	Distribution Coefficient	Selectivity Coefficient
	2×10^{-4} (M)	341.27	1.60×10^{-2}
CTMABr	4×10^{-4} (M)	310.77	2.95×10^{-2}
	6×10^{-4} (M)	242.87	2.83×10^{-2}
	8×10^{-4} (M)	193.77	2.45×10^{-2}
	1×10^{-3} (M)	158.25	2.05×10^{-2}
	1×10^{-4} (M)	186.18	2.18×10^{-3}
DDPBr	2×10^{-4} (M)	155.07	3.10×10^{-3}
	3×10^{-4} (M)	144.77	4.13×10^{-3}
	4×10^{-4} (M)	108.52	3.68×10^{-3}
	5×10^{-4} (M)	124.29	3.16×10^{-3}
	1×10^{-4} (M)	775.77	4.21×10^{-2}
CPBr	2×10^{-4} (M)	697.84	7.69×10^{-2}
	3×10^{-4} (M)	568.52	8.19×10^{-2}
	4×10^{-4} (M)	488.37	8.53×10^{-2}
	5×10^{-4} (M)	427.88	8.56×10^{-2}

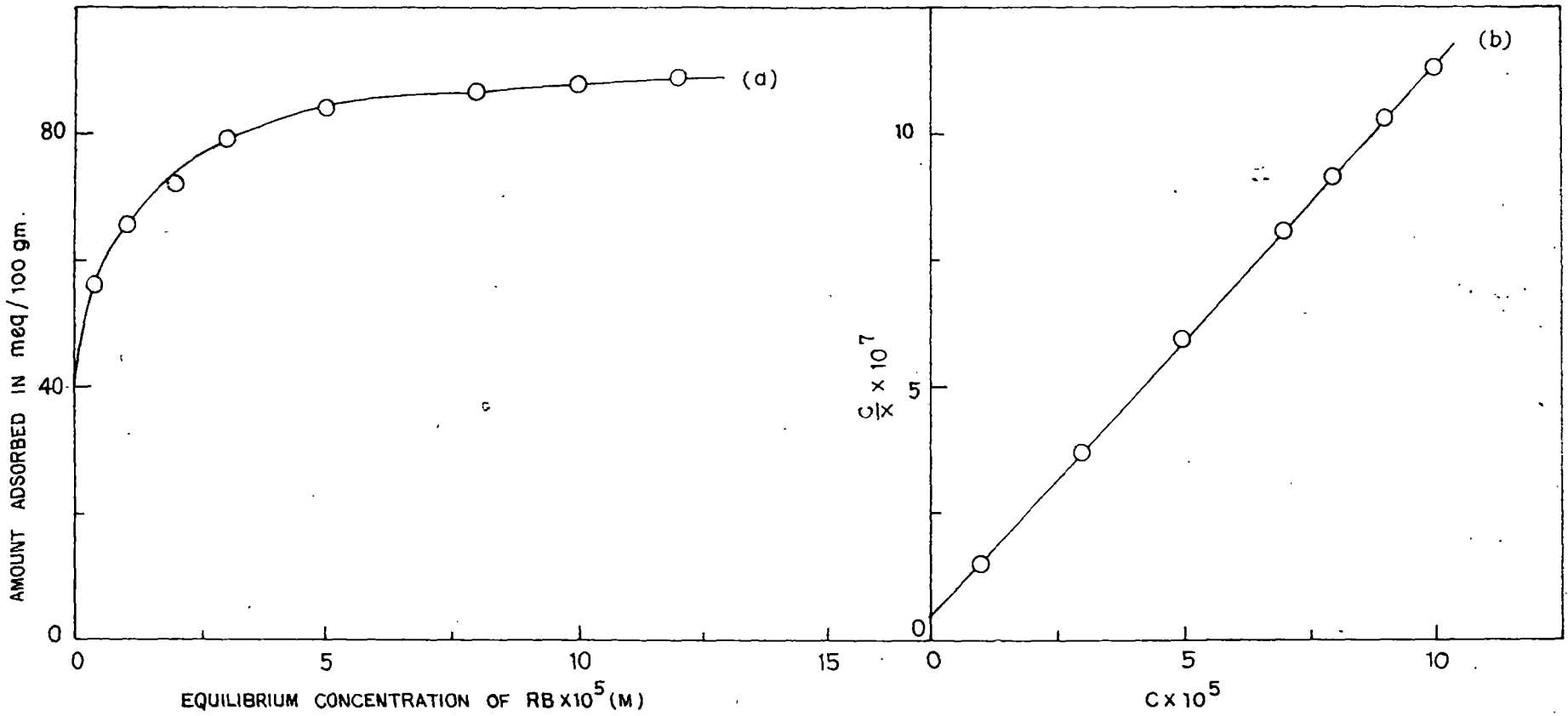

FIG. 42. ADSORPTION ISOTHERM AT 28°C (a) AND LONGMUIR PLOT (b) OF RG ON Na- LAPONITE.

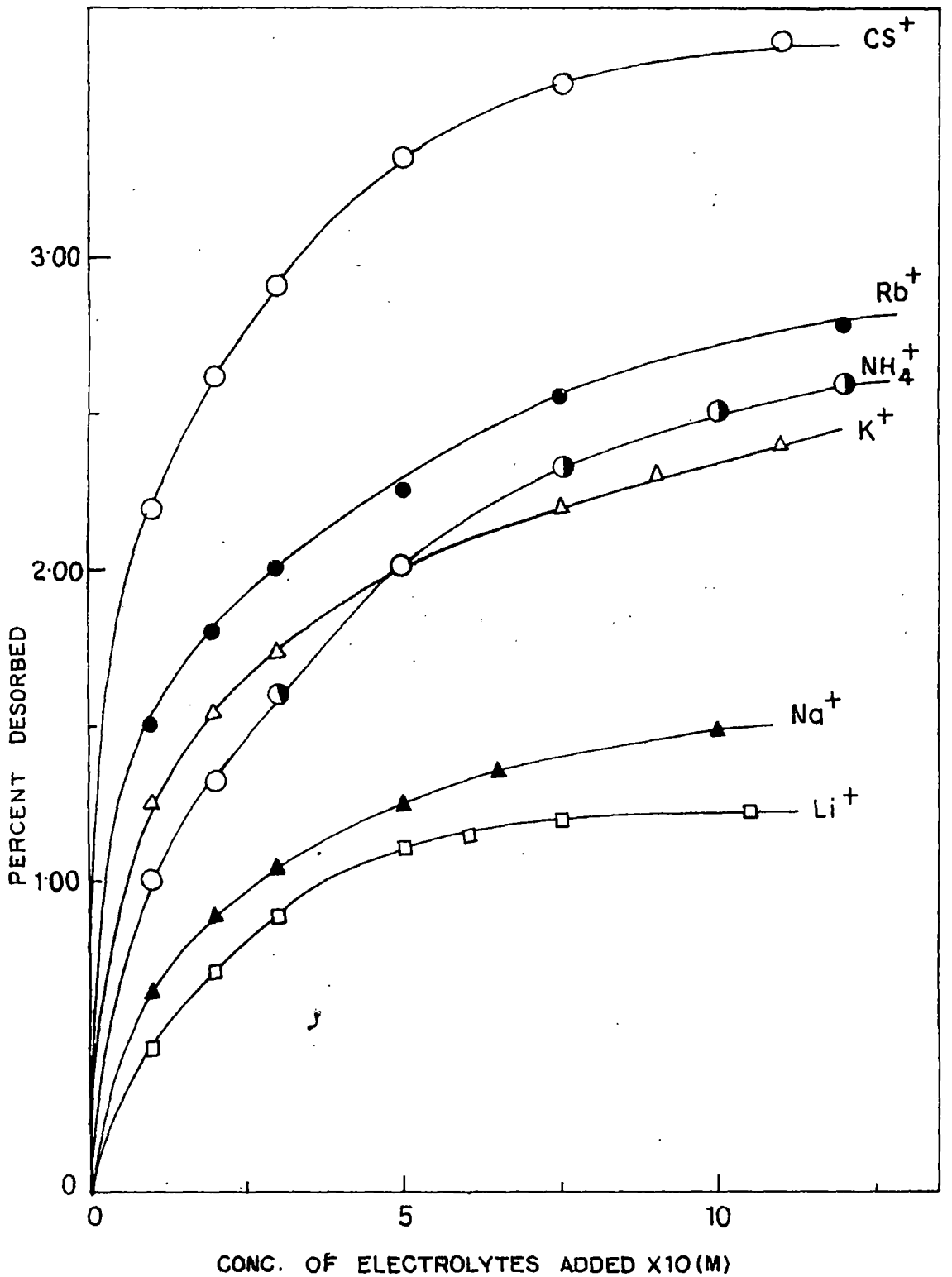

FIG. 43. DESORPTION OF RG FROM Na-LAPONITE-RG BY VARIOUS MONOVALENT IONS.

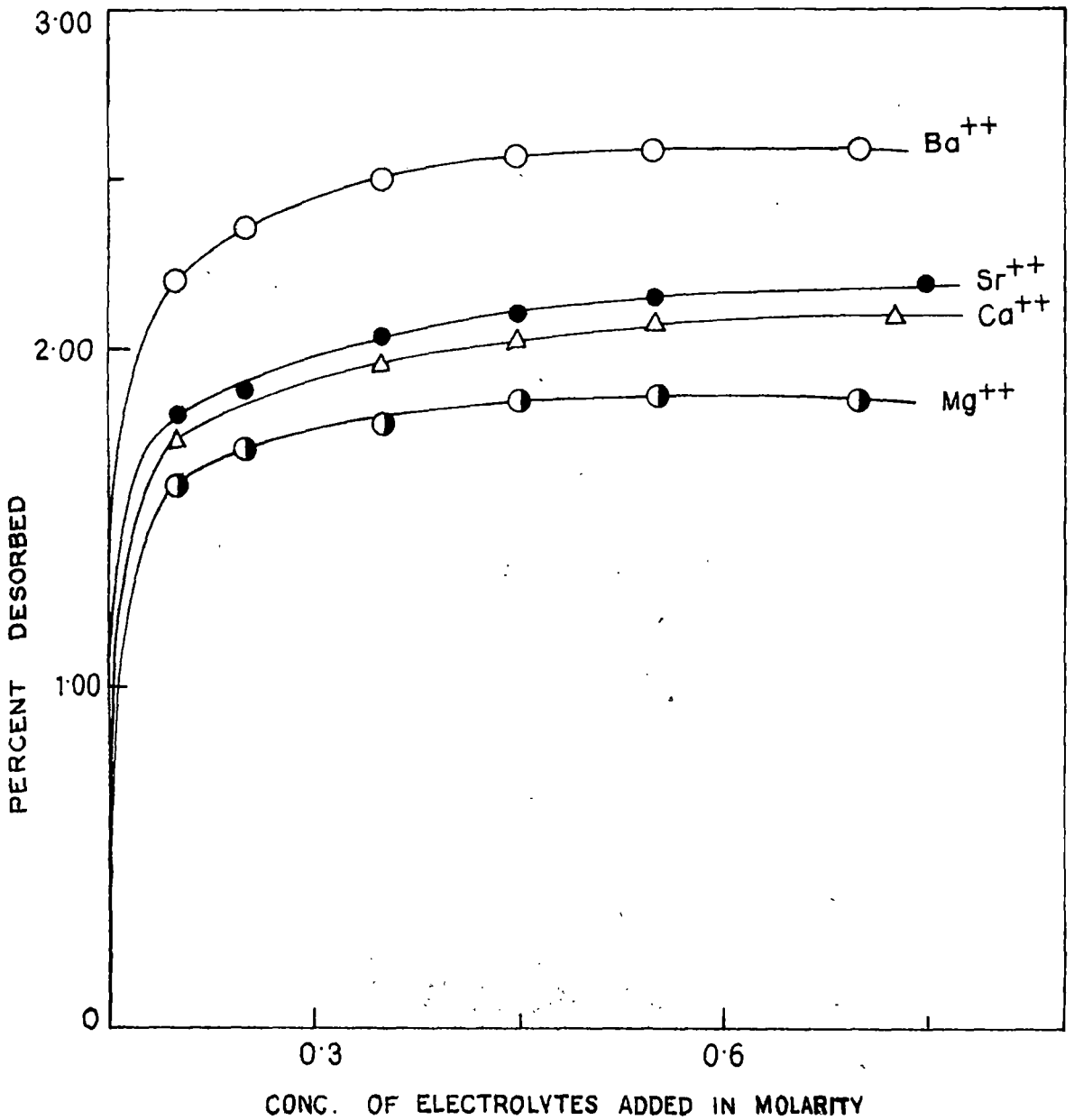

FIG. 44. DESORPTION OF RG FROM Na- LAPONITE - RG BY VARIOUS BIVALENT IONS.

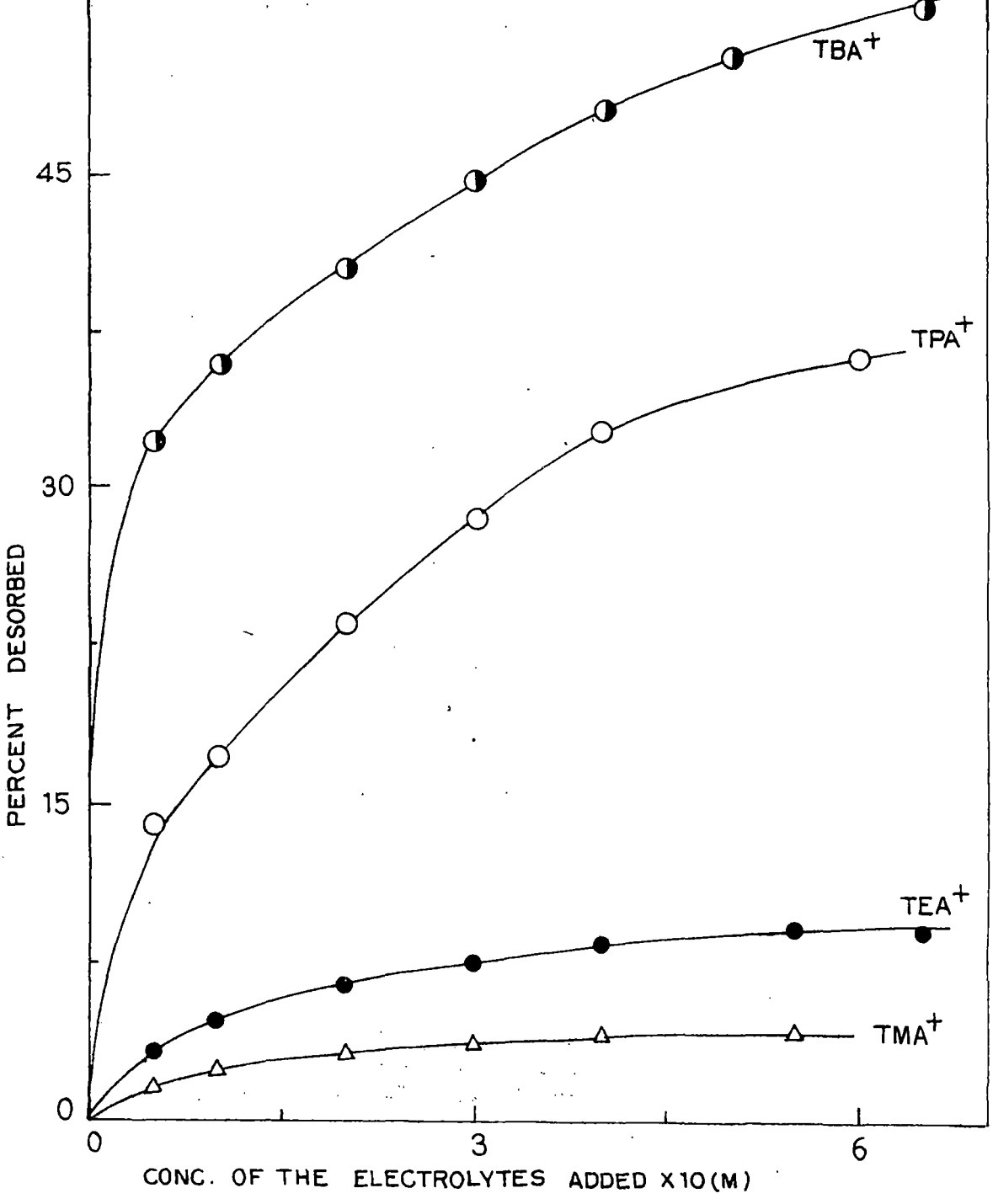

FIG. 45. DESORPTION OF RG FROM Na-LAPONITE-RG BY VARIOUS TETRA ALKYL AMMONIUM HALIDES .

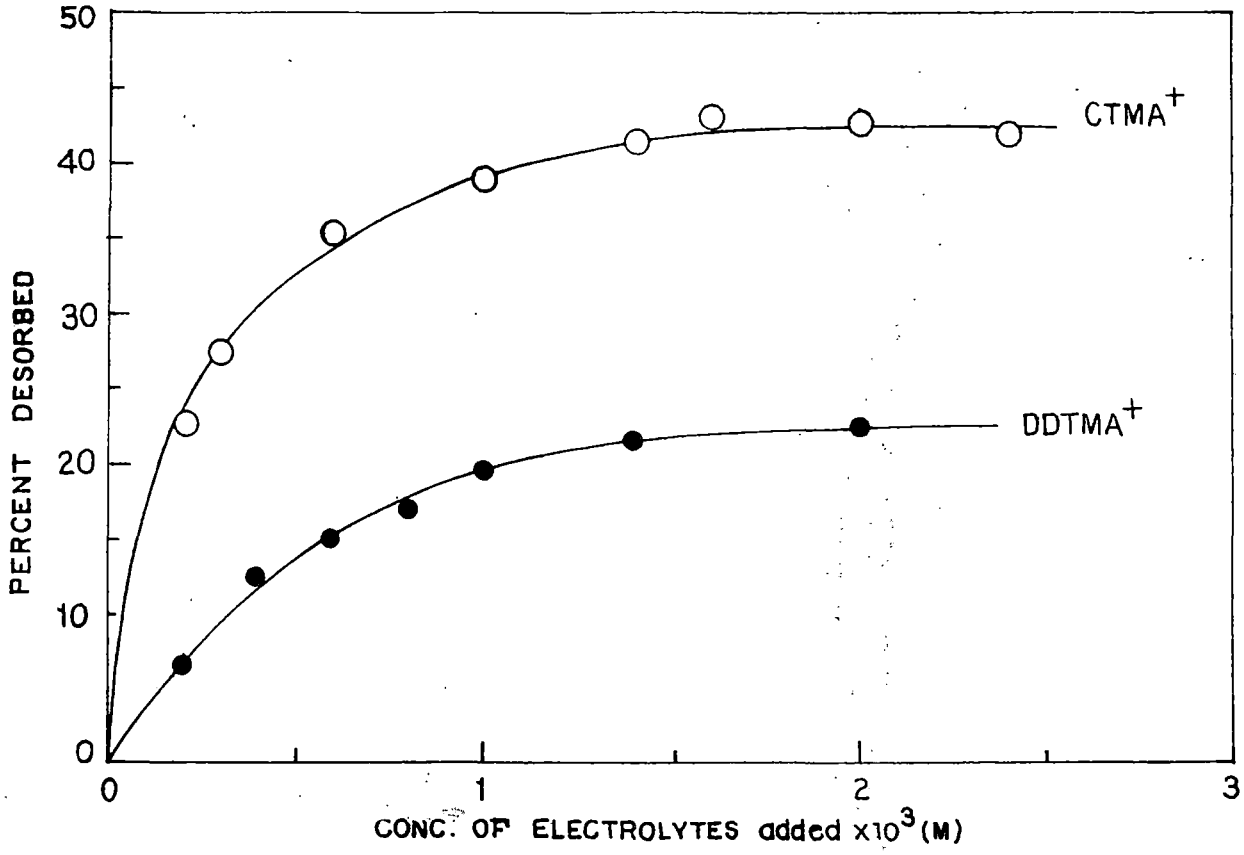

FIG. 46. DESORPTION OF RG FROM Na-LAPONITE-RG BY VARIOUS LONG-CHAIN SURFACE ACTIVE ALKYLTRIMETHYLAMMONIUM HALIDES.

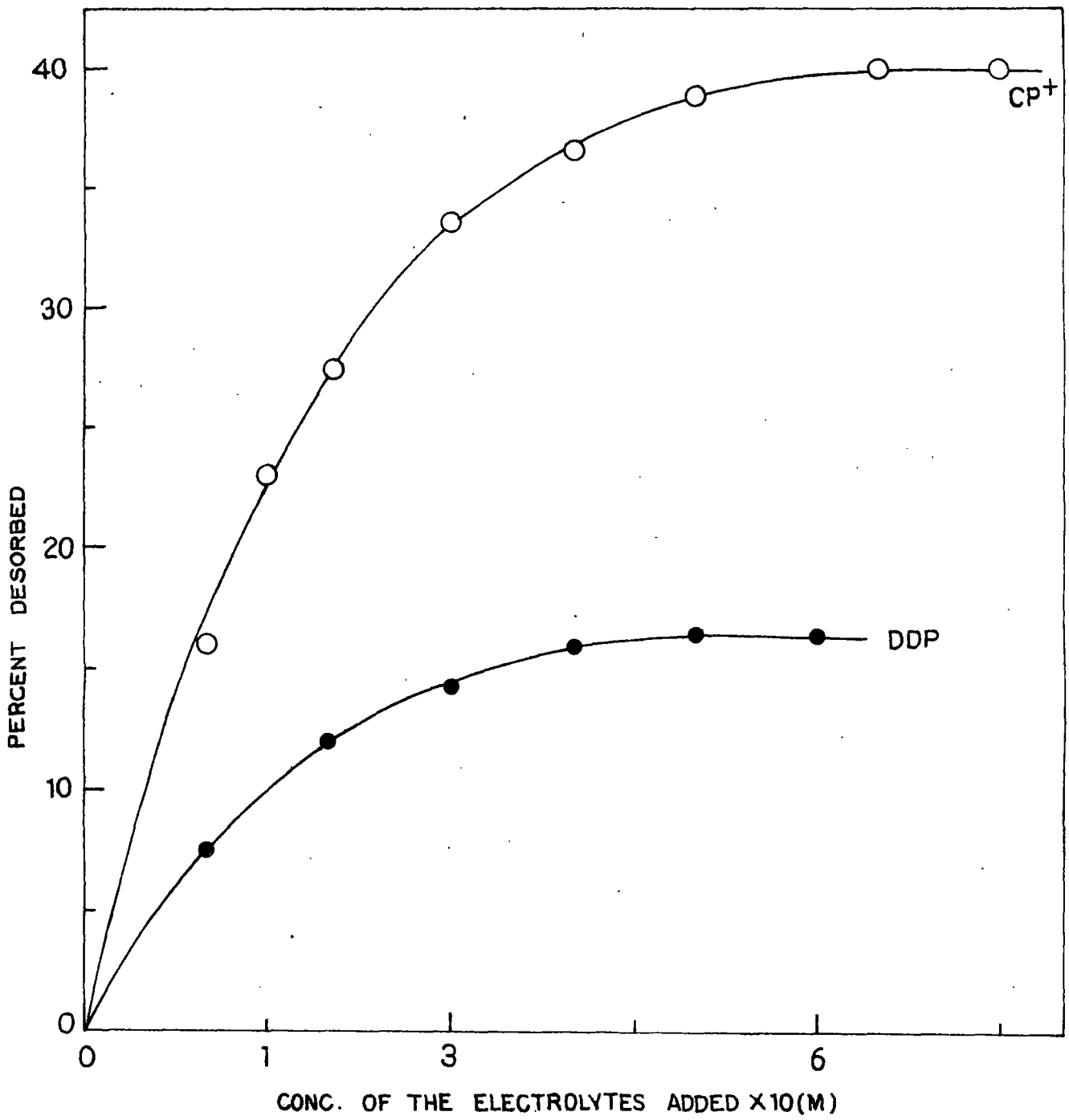

FIG. 47. DESORPTION OF RG FROM Na-LAPONITE-RG BY VARIOUS LONG-CHAIN SURFACE ACTIVE ALKYLPYRIDINIUM HALIDES.

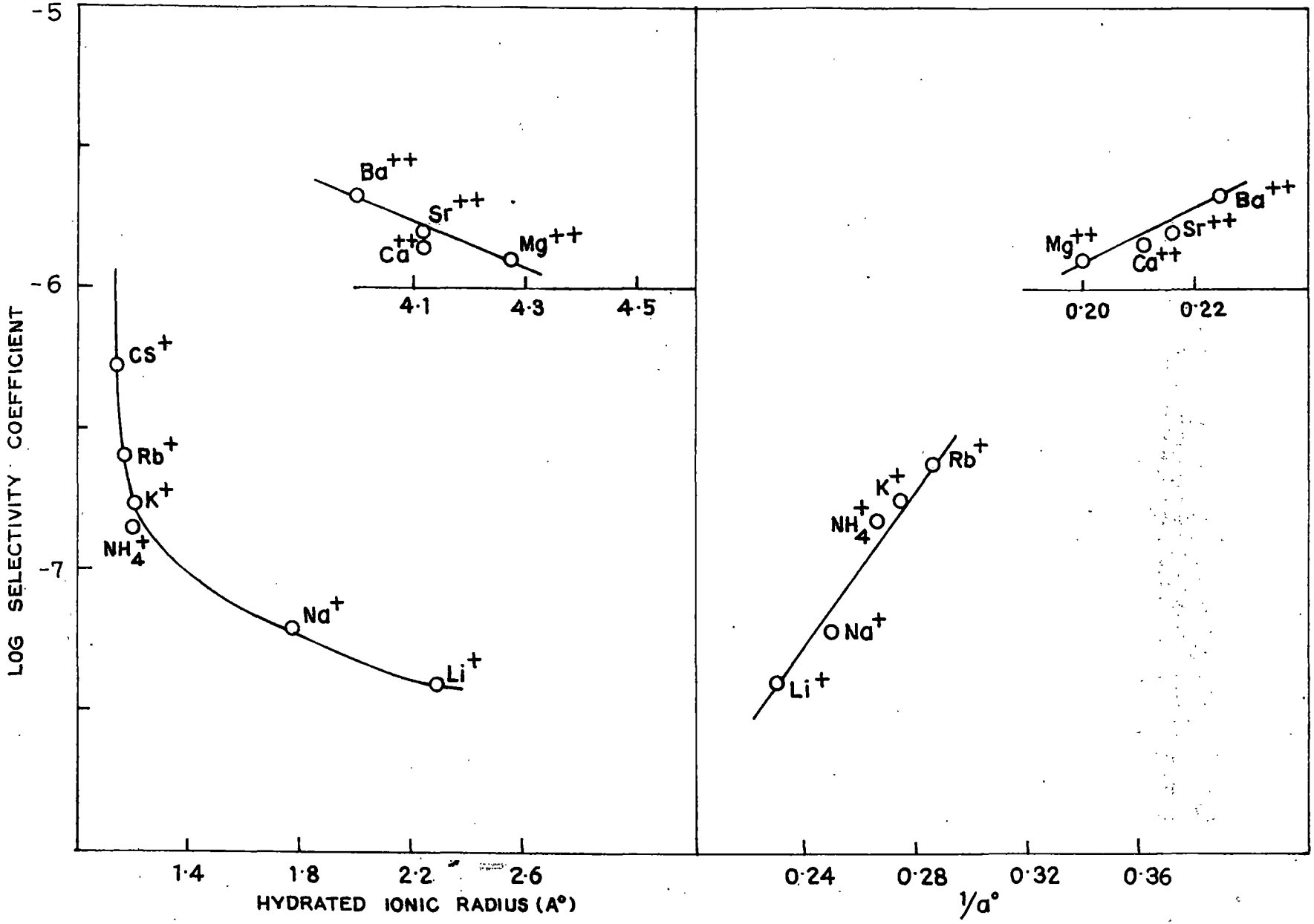

FIG. 48. CORRELATION OF SELECTIVITY COEFFICIENT WITH HYDRATED IONIC RADIUS AND DEBYE-HUCKEL PARAMETER, a°, IN THE DESORPTION OF RG FROM Na - LAPONITE - RG .

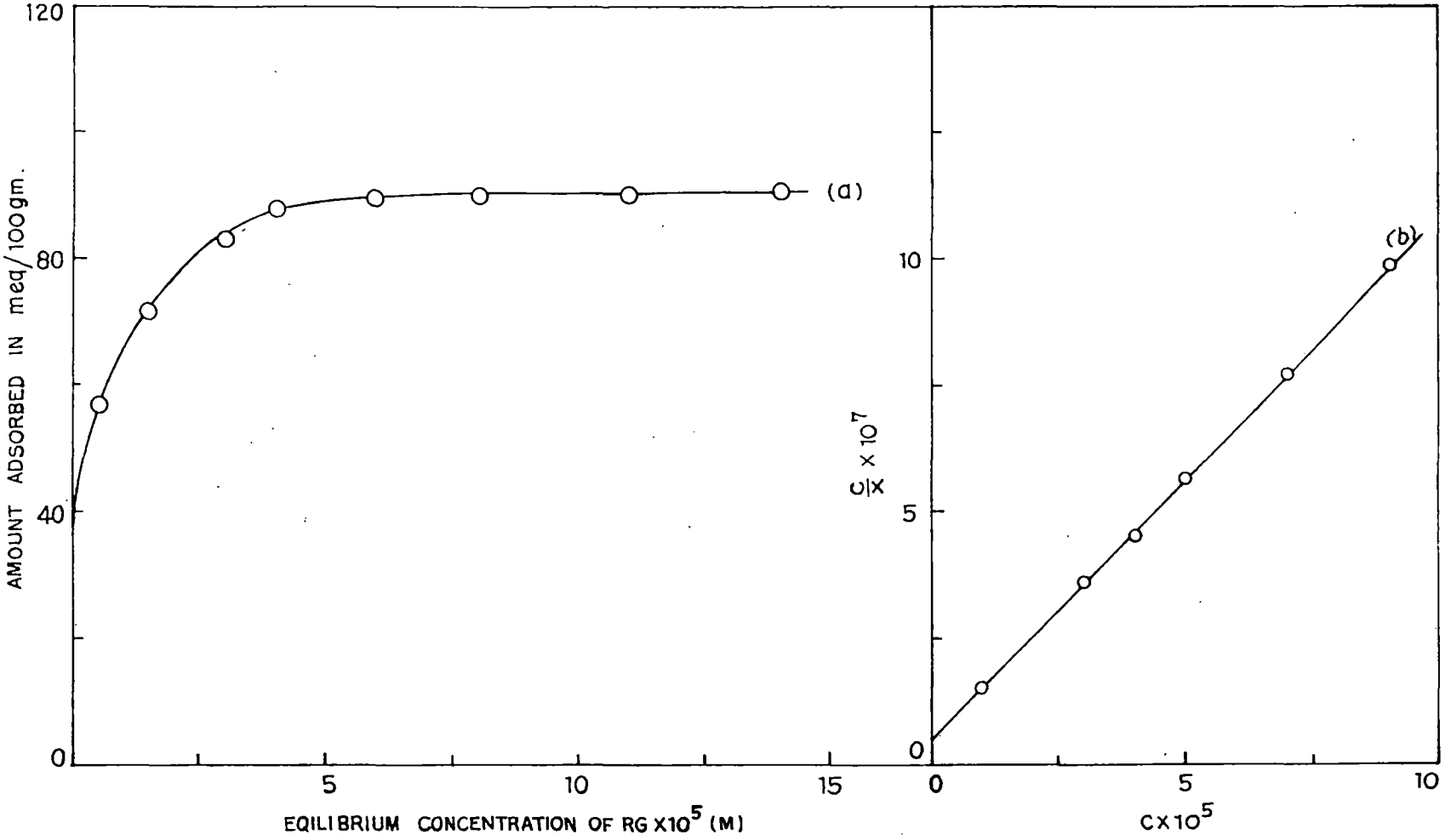

FIG. 49. ADSORPTION ISOTHERMS AT 28°C (a) AND LANGMUIR PLOT (b) OF RB ON Na-LAPONITE .

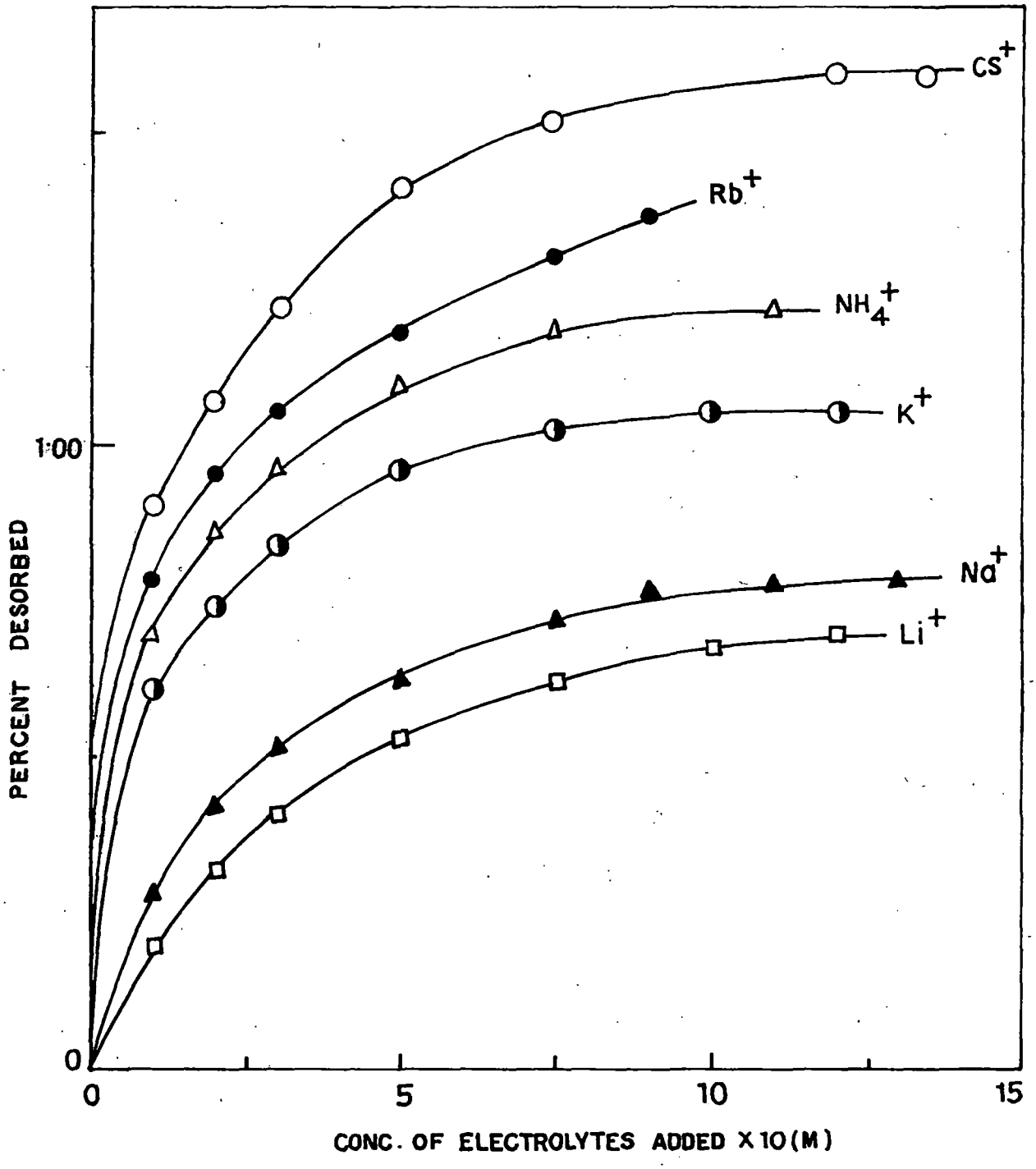

FIG. 50. DESORPTION OF RB FROM Na-LAPONITE-RB BY VARIOUS MONOVALENT IONS.

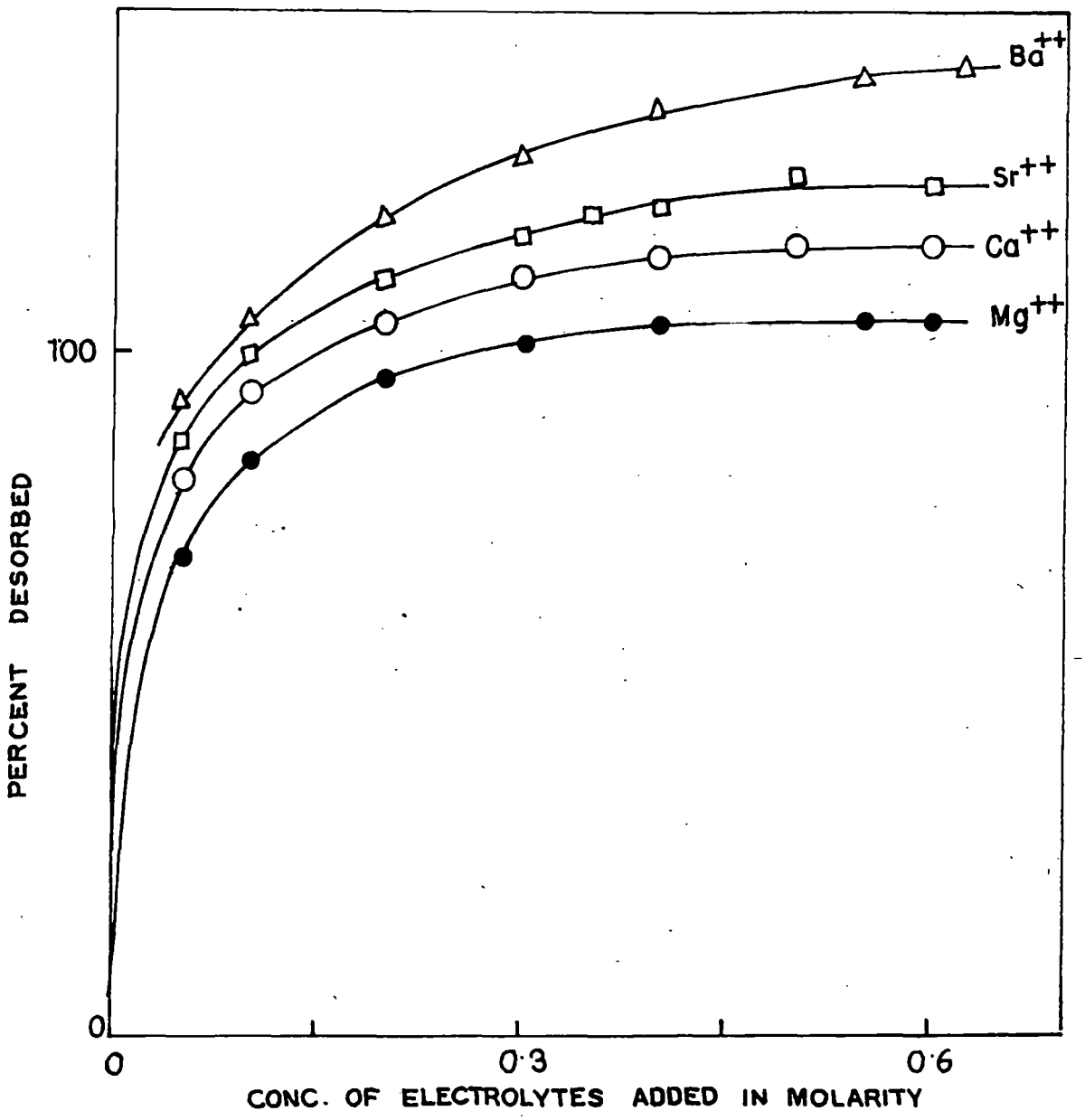

FIG. 51. DESORPTION OF RB FROM Na-LAPONITE-RB BY VARIOUS BIVALENT IONS.

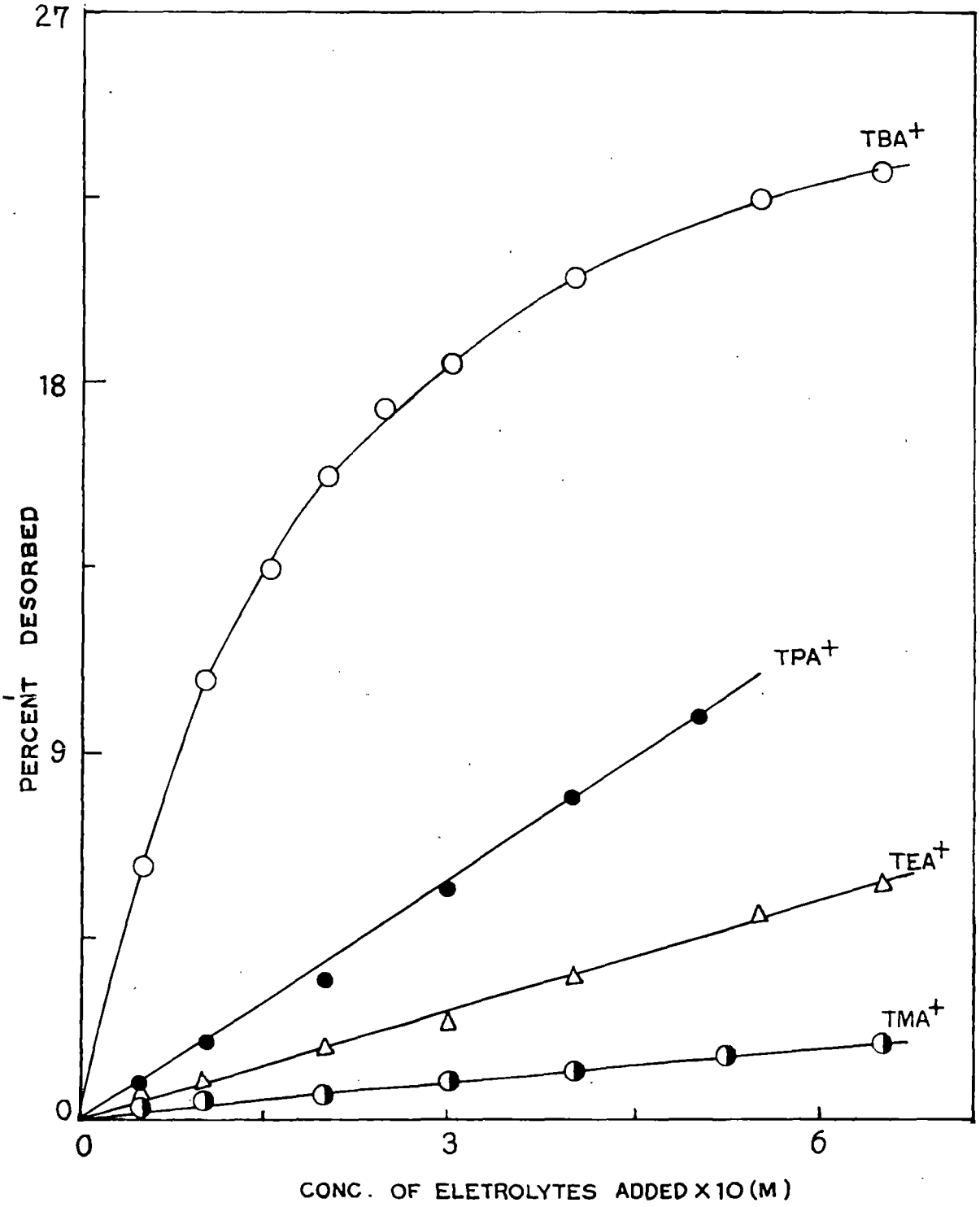

FIG. 52. DESORPTION OF RB FROM Na-LAPONITE-RB BY VARIOUS TETRAALKYLAMMONIUM HALIDES.

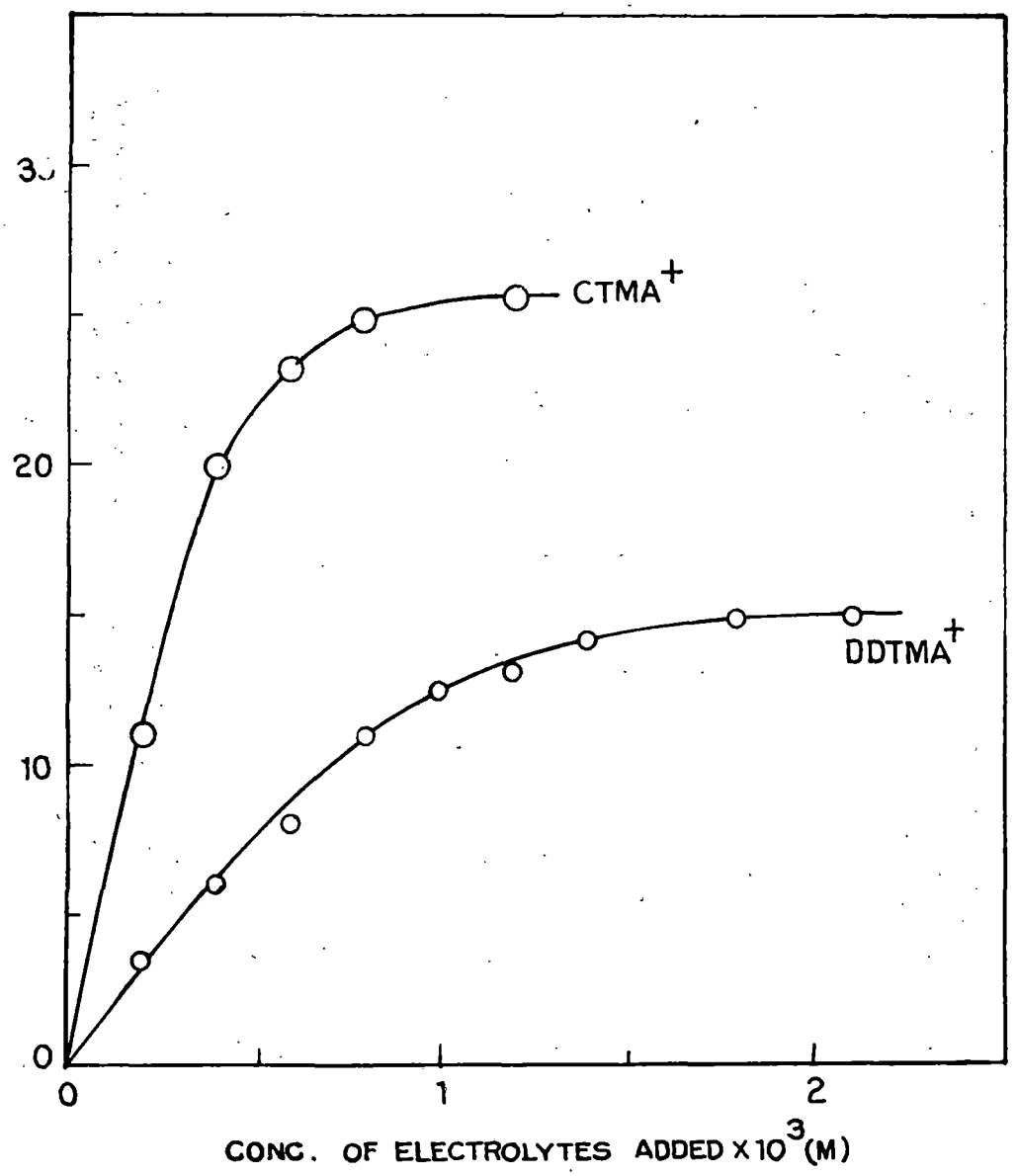

FIG.53. DESORPTION OF RB FROM Na-LAPONITE-RB BY VARIOUS LONG-CHAIN SURFACE ACTIVE ALKYL TRIMETHYL AMMONIUM HALIDES.

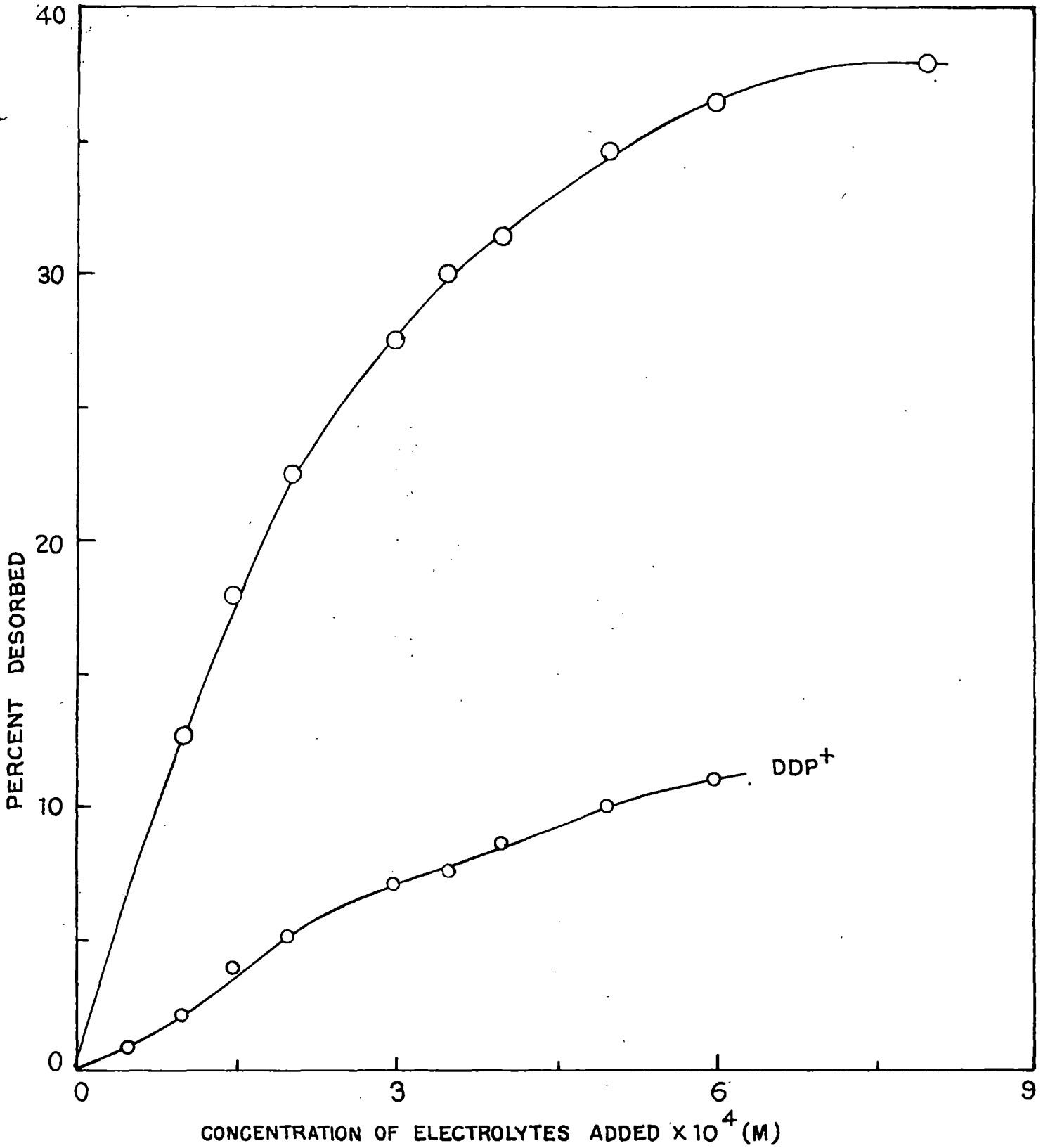

FIG. 54. DESORPTION OF RB FROM Na-LAPONITE-RB BY VARIOUS LONG-CHAIN SURFACE ACTIVE ALKYL PYRIDINIUM HALIDES.

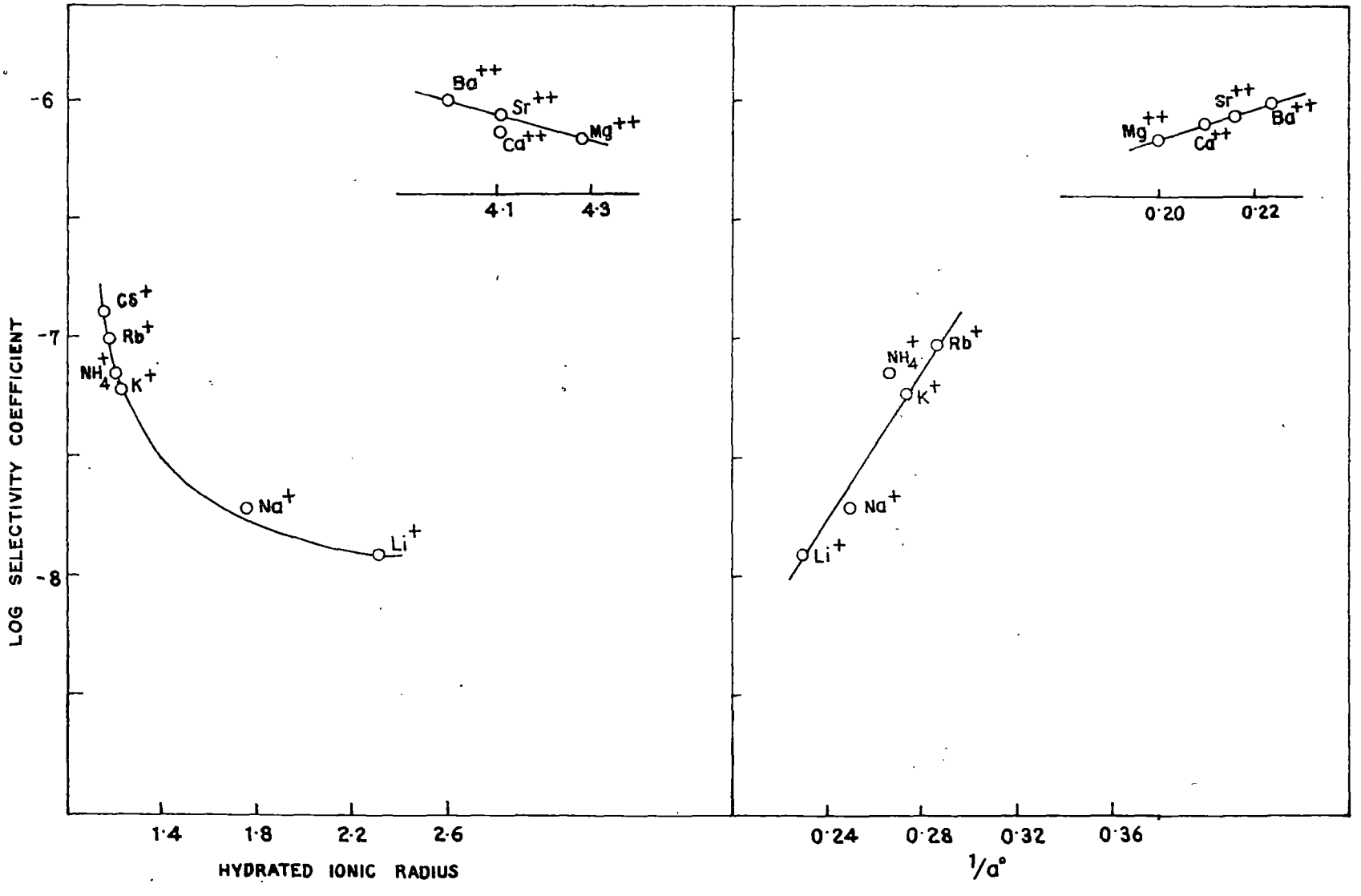

FIG. 55. CORRELATION OF SELECTIVITY COEFFIENT WITH HYDRATED IONIC RADIUS AND DEBYE-HUCKEL PARAMETER, a°, IN THE DESORPTION OF RB FROM Na-LAPONITE-RB.

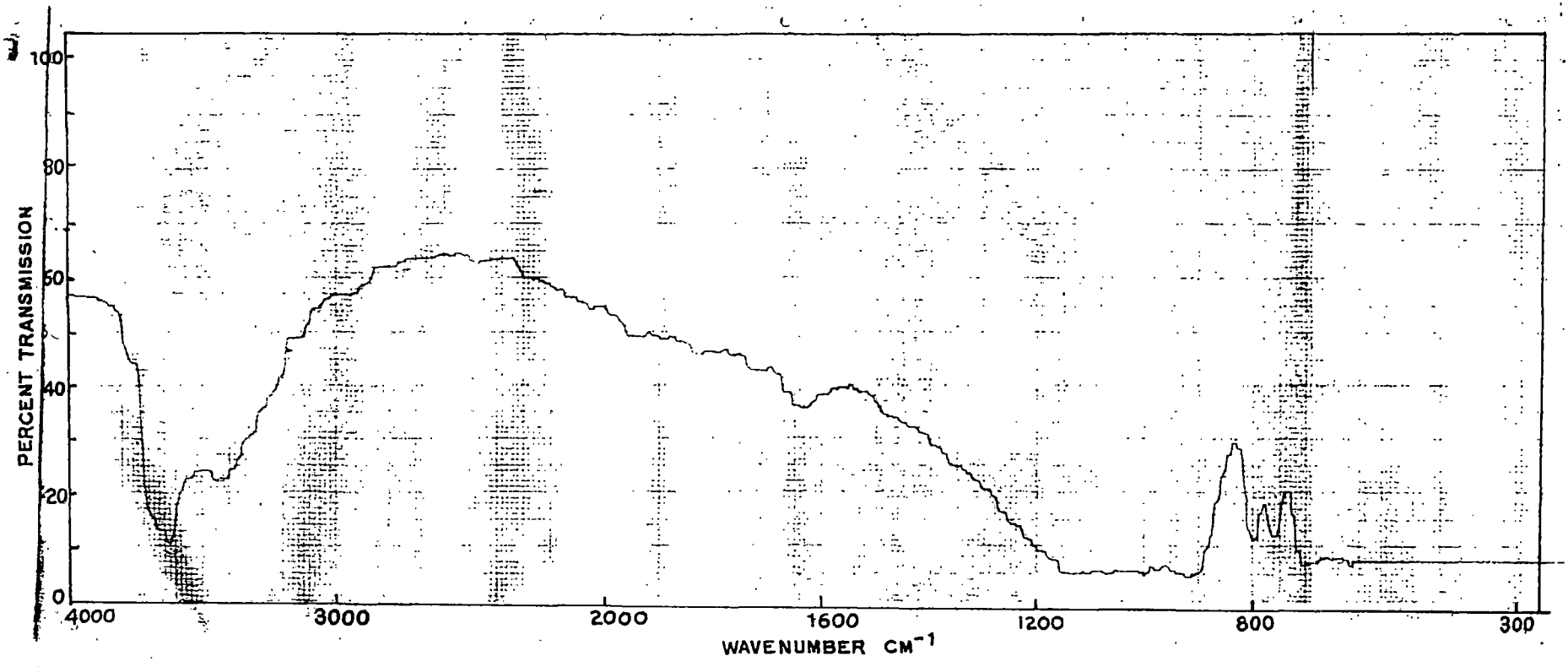

Fig. 56. Infrared Spectrum of Na- Laponite

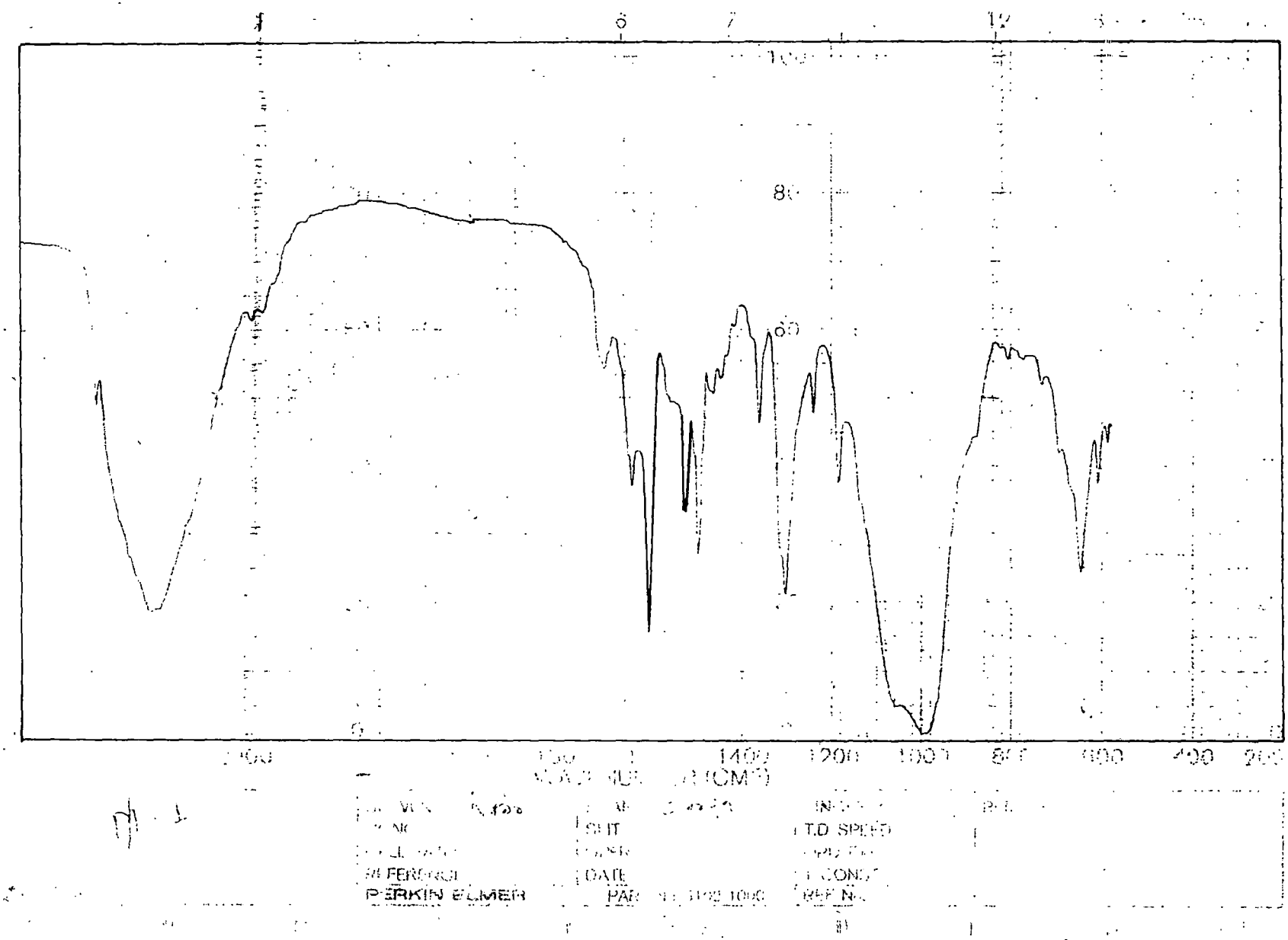

Fig. 57. Infrared spectrum of 100% exchanged Na- Laponite - RG (in KBr pellet).

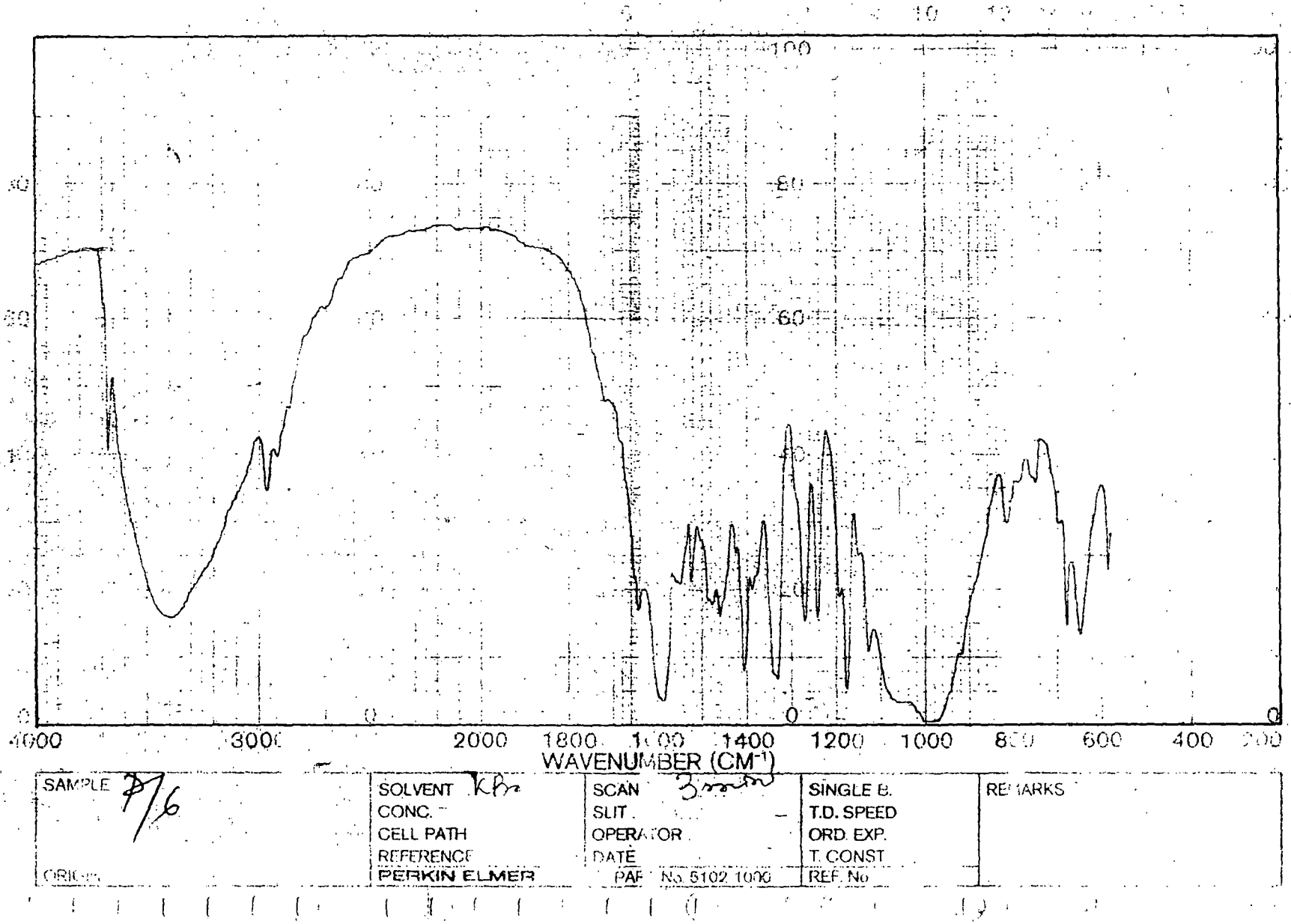

Fig. 58. Infrared spectrum of 100% exchanged Na- Laponite - RB (in KBr pellet)

CHAPTER - VII

Effect of Temperature on the Adsorption of Dyes by Aluminosilicates.

According to thermodynamic principles the adsorption process should be exothermic since it is associated with decrease in entropy and free energy. In fact evolution of heat had been observed by gas adsorption on clean surfaces and on other substrates. Yung Fang and Yu Yao (1) have observed that adsorption of n-propyl, n-butyl, n-amyl amines, tridecyl amine and water in their Vapour states on oxidised and reduced iron surfaces is exothermic.

The adsorption of sphere-like molecules on graphitised carbon black (2), benzene on Cr-Al-K Catalyst (3) is similarly exothermic. The heat of adsorption varies in some cases with the amount of adsorbate, while in others it does not. By plotting the heat of adsorption against the percentage of surface covered Kevorkian et al (4) obtained irregular graphs which they accounted by assuming surface heterogeneity. The adsorption study of neopentane and carbon tetrachloride on carbon black graphitised at 3000^{o}C, shows similar results. The heat of adsorption plotted against amount adsorbed shows a maximum. This has been explained by suggesting that the molecules are adsorbed in a non-localised fashion and that they interact strongly with each other in the adsorbed layer.

Yung Fang and Yu Yao (1) have also observed that the graph of heat of adsorption against the amount of amines adsorbed on reduced and oxidised iron surfaces consists of two plateaus. The first one corresponds to the heat of chemsorption and second one to physical adsorption. But the results of adsorption of Cyclohexane on Cr-Al-K catalyst at 20^{o}, 50^{o} and 150^{o} (5) show that the heats of adsorption are of the order of 10.3 k cals/mol and independent of surface coverage. The differential heats of adsorption of n - C_5H_{11} and n - C_6H_{14} on $BaSO_4$ (6) have been found to be almost constant till the surface is half filled, then they gradually decrease with increase on adsorption because of surface heterogeneity.

In the solution phase, however, endothermic adsorption processes have often been encountered. The adsorption of crystal violet by hydrated ferricoxide (7) and Chromic oxide Sol (8) and that of Congored and fucshine by hydrated thorium oxide Sol (9) are endothermic.

Giles, Eastone, and McKay (10) have observed that certain dyes e.g. magenta and ethyl violet are adsorbed on alumina with absorption of heat, while safranine T and Rhodamine 6B are adsorbed with evolution of heat. No heat change was however, obwerved with methylene blue, rhodamine 3B and rhodamine B. Again with victoria pure blue, negative heat of adsorption has been noticed at low coverage while at high coverage heat has been evolved.

Giles et al (11) found that the values of heat of adsorption of dyes from their aqueous solution on inorganic surfaces ranged between -1.00 and -10.00 Kcal/mole. In the adsorption of some dyes on cellulose acetate the successive heat changes were examined quantitatively by Majury (12). De (13) studied the effect of temperature on the adsorption of methylene blue, malachite green and Crystal violet in aqueous solution of Na-Kaolinite and Na-Bentonite. They found the process to be endothermic for malachite green and crystal violet whereas no appreciable difference was noticed in the case of methylene blue. Narine and Guy (14) recorded a decrease in adsorption of methylene blue by Na-Bentonite from 69.3 ± 3.0 to 64 ± 3.0 to 64 ± 2.0 meq per 100 gm of the clay, when temperature was changed from 3 ^{o}C to 55 ^{o}C . In the study of the effect of temperature of some thiazine dyes with clay minerals by Sunwar (15) it has been noticed that adsorption process of the thiazine dyes on montmorillonite and kaolinite is exothermic in nature but in case of vermiculite the exothermic nature of the curves are altered with change in temperature and concentration. At low concentrations the sorption isotherms at 23 ^{o}C and 40 ^{o}C show exothermicity but at higher concentration these curves exhibit endothermicity.

According to the idea of Bartell, Tudor and Yung Fu (16) though the adsorption process itself is exothermic the solubility

of the adsorbate and its temperature dependence are the significant factors which control the resultant heat of adsorption. Thus, according to them, if the solubility of a substance is inversely related to temperature, the amount adsorbed would increase with rise in temperature, and if the solubility increased with temperature the effect would be the opposite. They observed the adsorption of some low molecular weight aliphatic substances on carbon to be exothermic at low concentration while endothermicity was found at higher concentration. At higher concentrations the effect of temperature on solubility was supposed to be more influenced.

Mundhara et al (17) on the study of adsorption of brilliant cresyl blue and safranine-T on Tin oxide substrats at 30-60^{o}C found the adsorption process to be exothermic at lower concentration but endothermicity at higher concentration of the dyes. They also attributed the endothermic bonding to an increase in the number of available sites with temperature as a consequence of dissociation of the dye aggregates in the substrates. The heat of adsorption values were 23-80 KJ/mole for brilliant cresyl blue and 17-26 KJ/mole for safranine-T. They suggested that concurrence of more than one reaction was responsible for these variable heats of adsorption values.

According to Giles et al (10) the apparent endothermic nature of the adsorption is a result of aggregation of the dye molecules (18) in the solution. They found the adsorption of janus red and lassamine green from their aqueous solution

on inorganic surfaces to be an endothermic reaction. Hajela and Ghosh (7) have also remarked that association of dye molecules in aqueous medium affects the heat of adsorption. According to them, as the disassociated dye molecules are gradually taken up by the adsorbate, more and more of the aggregated dye molecules in solution are dissociated into simpler forms. At each stage the heat of dissociation of the aggregated dye molecules is included in the experimental heat of adsorption. The heat of adsorption is, therefore, controlled by several factors such as solubility, association and actual process of adsorption itself.

From the values of the heat of adsorption, the nature of bonding namely, whether chemical or physical both of the adsorbed species with the substrate surface can be judged (3). Very little data are available in the literature on the heat of adsorption of the dyes by alumino silicate minerals in the form of suspension. In order, therefore, to provide some information on this subject adsorption measurements were carried out at different temperatures with montmorillonite and kaolinite in suspension and RG and RB as adsorbates. The experimental procedure has already been described in Chapter III page 55.

Sorption on Dyes on Na-Montmorillonite and Na-Kaolinite

The temperature dependence of adsorption of RG^+ and RB^+ on Na-montmorillonite and Na-kaolinite is represented graphically by drawing the respective isotherms. The heat of adsorption was calculated using the equation:

$$Q = \frac{RT_1T_2}{T_1-T_2} \times \ln \frac{C_1}{C_2}$$

where C_1 and C_2 are the concentrations of the dye in solution phase at temperature T_1 and T_2 for the same amount of dye adsorbed.

Sorption of RG^+ on Na-montmorillonite:

Fig. 59 represents the adsorption isotherms of RG on Na-montmorillonite at 23°, 38° and 68°C and the inset shows the plot of heat values against the amount of dye adsorbed. The nature of the curves remains unchanged with increase in temperature and the amount adsorbed decreases with increase in temperature indicating the process to be exothermic. All the isotherms are of Langmuir type. Introducing the values of C_1 and C_2 for temperature 23° and 68°C from the graph the heats of adsorption were calculated according to the above mentioned

equation. The results are shown in table 12. It is found that there is variation of the amount of dye adsorbed with the heat of adsorption so it is not a constant quantity. It shows a minimum at a certain value of the dye adsorbed indicating probably to a situation when the monolayer or when the adsorption value approaches the cation exchange capacity of the mineral. From the sorption isotherm it is apparent that the slope gradually decreases with rise in solute concentrations. This is because of the fact that the adsorption first takes place on the higher energy sites of the adsorbent and with the progress in adsorption, the vacant sites become more difficultly accessible. As a consequence the heat of adsorption decreases. The heterogeneity of the montmorillonite surface and the complications in actual systems cause a progressive diminution in the heat of adsorption as the surface coverage increases, long before the monolayer is complete (19). It has been pointed earlier that the experimental heat of adsorption is the net result of several processes such as solubility, association of the dye molecules etc. Where heat may be evolved or adsorbed. In the present study the heat of adsorption is positive. Whereas in the earlier work reported by De (13) this value has been found to be negative. The sorption isotherms have been drawn at equilibrium concentrations that fall mostly within the monomolecular range of the dye. The values of heat of adsorption in this case lie between + 1.25 to + 2.59 K cal per mole and calculated values are shown in Table 12.

Sorption of RB^+ on Na-montmorillonite

The adsorption isotherms of RB on Na-montmorillonite at 23^o, 38^o and 68^o are shown in Fig. 60. The change in temperature does not cause any change in the nature of the curves. It is observed that the amount adsorbed decreases with rise in temperature as in the case of RG sorption. From the plot of heat of adsorption in Kcal/mole vs amount adsorbed in meq/100g a minimum is obtaining at a particular value of the dye adsorbed and this can be explained in similar manner as in the case of sorption of RG considering the equilibrium concentrations of the isotherms to be in the monomolecular range. Also the heat of adsorption lies in the range of + 1.91 to + 4.25 Kcal/mole (Table 12) which is higher than that observed in Na-montmorillonite. RG, suggesting a stronger binding of the former to the clay. The desorption studies of the dyes from their clay mineral complexes with various electrolytes also confirm this conclusion.

Sorption of Dyes on Na-kaolinite

Sorption of RG^+ and RB^+

Isotherm of RG^+ and RB^+ on Na-kaolinite at 26^o, 46^o, 70^o are displayed in Fig. 61 and 62 respectively. All the isotherms are of Langmuir type. The values of C_1 and C_2 for temperatures 26^oC and 70^oC are found out from the graph from which the heat of adsorption was calculated according to the

equation given in page 138 (Table 13). It is found that the heat of adsorption changes with quantity of dye adsorbed but the nature of the sorption remains unchanged at different temperature and the adsorption process in exothermic.

It is interesting to note that in kaolinite the plot of heat of adsorption values against the amount of RG adsorbed does not show a distinct minimum as has been obtained in montmorillonite but increases progressively with adsorption. This is probably due to the adsorption of the dye in the form of aggregated species, which results in the sorption of dye beyond the c.e.c. of the mineral at an early stage when the equilibrium concentration is till quiet low.

The heat of adsorption of RB is greater than that of RG which suggests higher affinity of the former than of the latter to the mineral systems. The desorption studies of the dyes also support this view which have been discussed in the previous chapters.

TABLE - 12

Heat of adsorption when various quantities of dyes are sorbed onto aluminosilicates.

(Sorption of Na-montmorillonite)

Name of the Dye	Amount and dye sorbed in meq/100 gm	Concentration C_1 at temperature $T_1=23^{o}C$	Concentration C_2 at temperature $T_2=68^{o}C$	Heat of adsorption in Kcal/mol
RG	75	0.95×10^{-5} (M)	1.7×10^{-5} (M)	2.59
	80	1.8×10^{-5} (M)	2.85×10^{-5} (M)	2.04
	85	2.9×10^{-5} (M)	4.1×10^{-5} (M)	1.53
	90	4.3×10^{-5} (M)	5.7×10^{-5} (M)	1.25
	95	6×10^{-5} (M)	8.1×10^{-5} (M)	1.33
	97.5	7×10^{-5} (M)	9.6×10^{-5} (M)	1.40
RB	65	1×10^{-5} (M)	2.6×10^{-5} (M)	4.25
	70	1.7×10^{-5} (M)	4×10^{-5} (M)	3.80
	75	3×10^{-5} (M)	5.5×10^{-5} (M)	2.69
	80	4.6×10^{-5} (M)	7.4×10^{-5} (M)	2.11
	85	6.5×10^{-5} (M)	1×10^{-4} (M)	1.91
	87.5	8×10^{-5} (M)	1.4×10^{-4} (M)	2.48

TABLE - 13

Heat of adsorption when various quantities of dyes are sorbed onto aluminosilicates

(sorption on Na-Kaolinite)

Name of the Dye	Amount of dye sorbed in meq/100g	Concentration C_1 temperature $T_1=26^{o}C$	Concentration C_2 at temperature $T_2=70^{o}C$	Heat of adsorption in Kcal/mol
RG	4.5	0.5×10^{-5} (M)	0.7×10^{-5}	1.55
	5	0.9×10^{-5} (M)	1.3×10^{-5}	1.70
	5.5	1.65×10^{-5} (M)	2.5×10^{-5}	1.92
	6	2.78×10^{-5} (M)	4.8×10^{-5}	2.49
	6.25	3.7×10^{-5} (M)	6.6×10^{-5}	2.67
RB	4	0.2×10^{-5}	0.3×10^{-5}	1.87
	4.5	0.8×10^{-5}	1.1×10^{-5}	1.47
	5	1.28×10^{-5}	1.9×10^{-5}	1.82
	5.5	1.95×10^{-5}	3.25×10^{-5}	2.35
	6	3.3×10^{-5}	6×10^{-5}	2.76

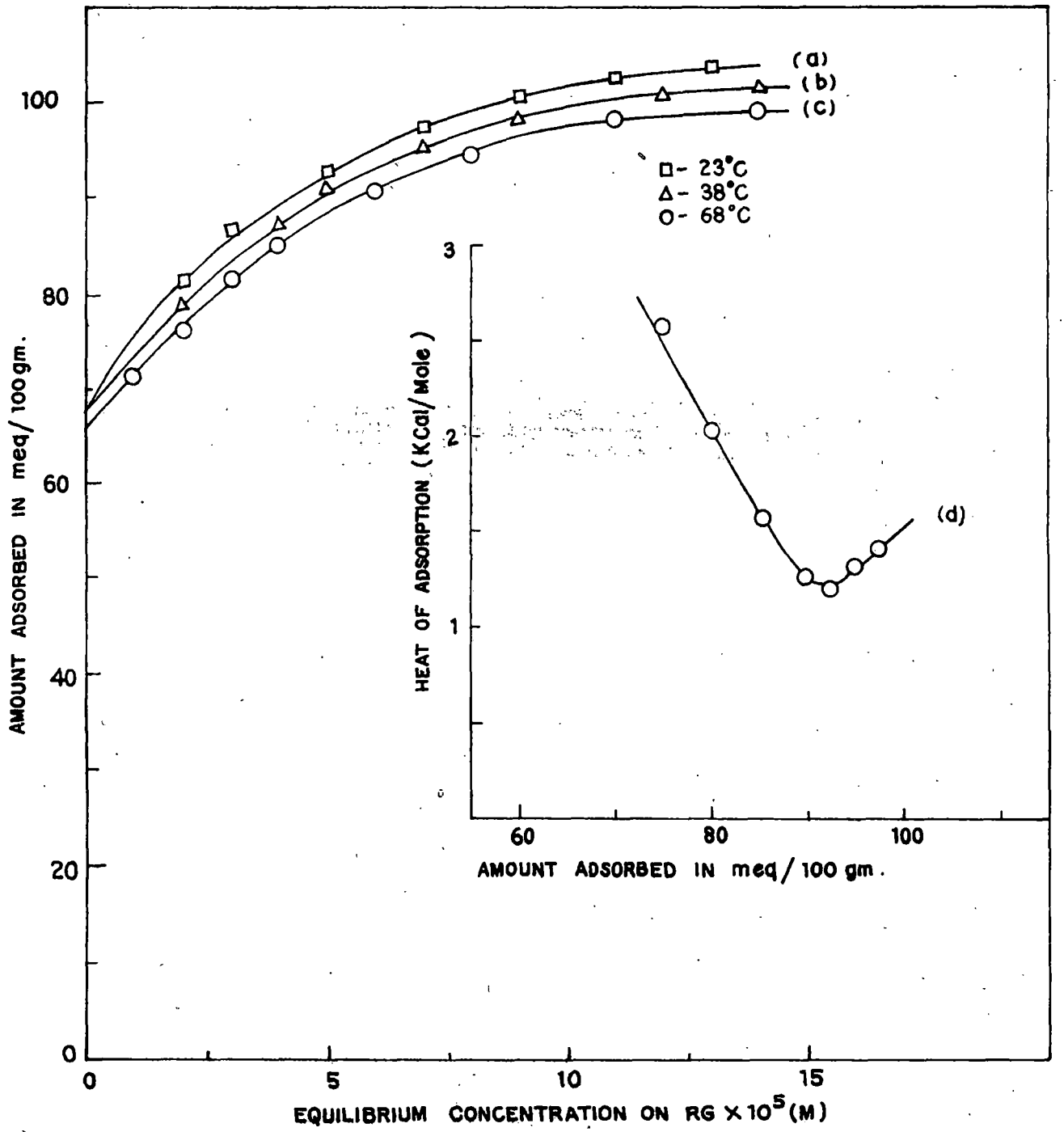

FIG. 59. ADSORPTION ISOTHERMS OF RG ON Na-MONTMORILLONITE AT DIFFERENT TEMPERATURES (a,b,c) AND RELATION OF HEAT OF ADSORPTION WITH THE AMOUNT OF DYE-ADSORBED (d).

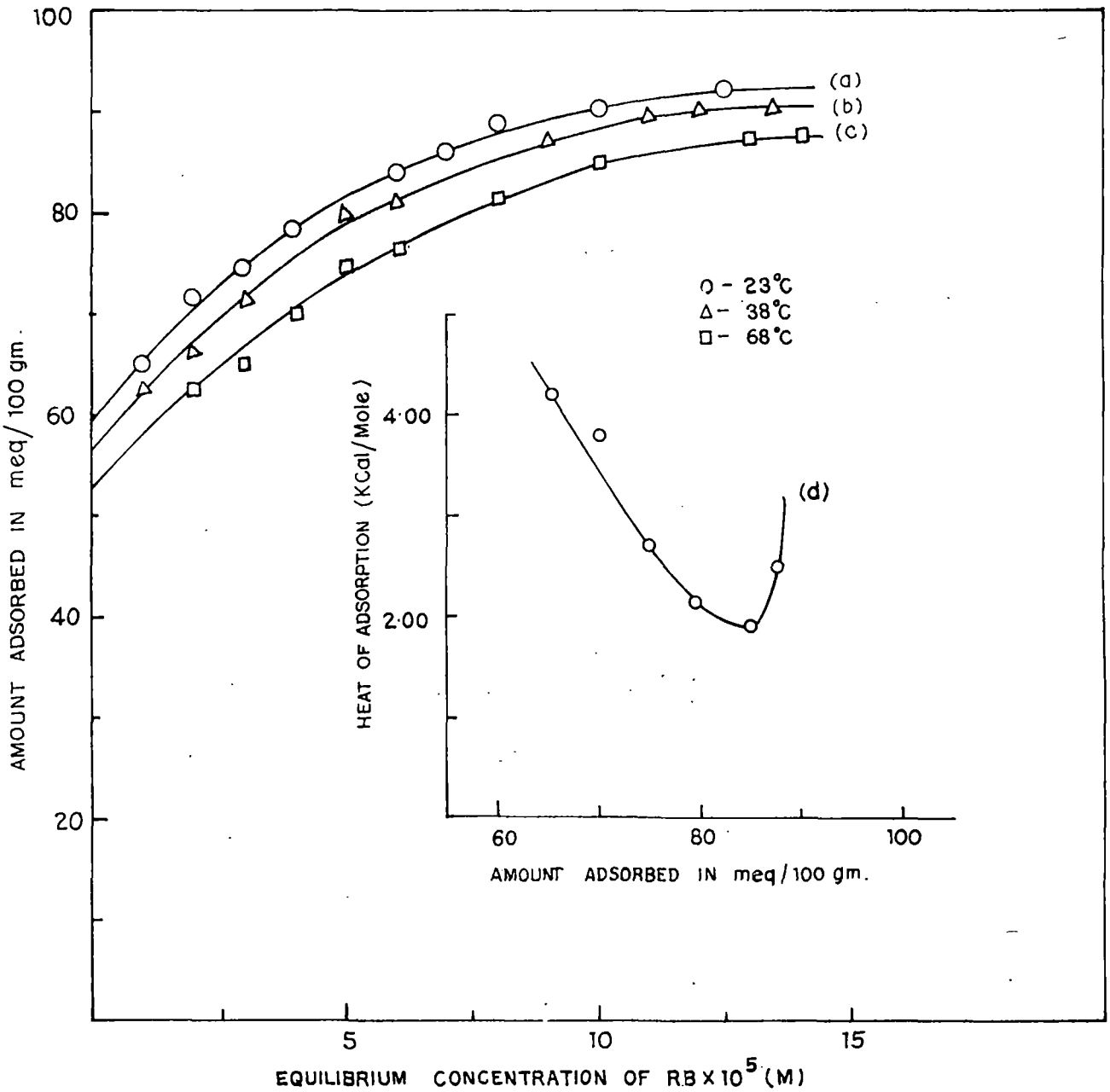

FIG. 60. ADSORPTION ISOTHERMS OF RB ON Na- MONTMORILLONITE AT DIFFERENT TEMPERATURES (a, b, c) AND RELATION OF HEAT OF ADSORPTION WITH THE AMOUNT OF DYE ADSORBED (d).

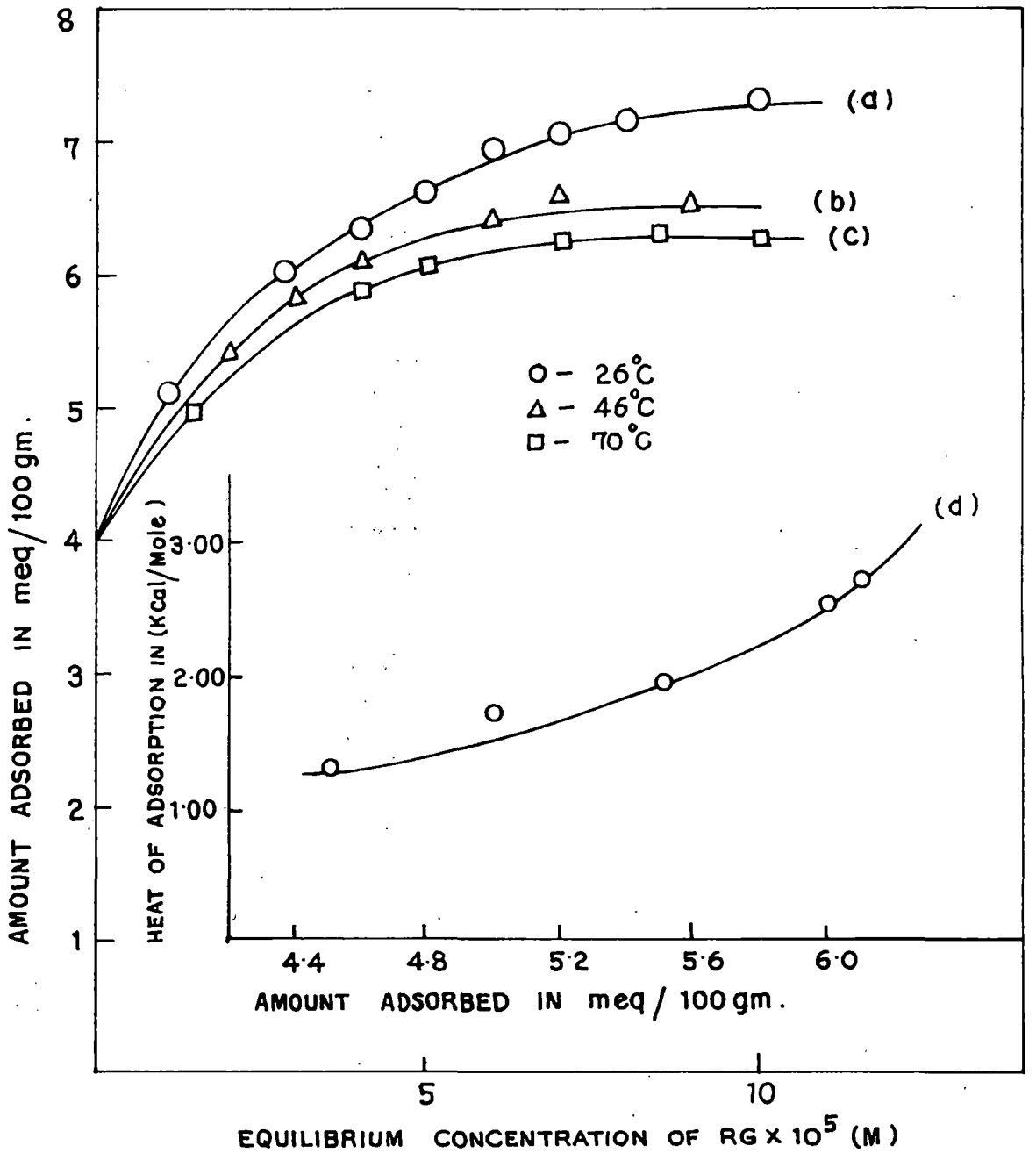

FIG. 61. ADSORPTION ISOTHERMS OF RG ON Na-KAOLINITE AT DIFFERENT TEMPERATURES (a, b, c) AND RELATION OF HEAT OF ADSORPTION WITH THE AMOUNT OF DYE ADSORBED.

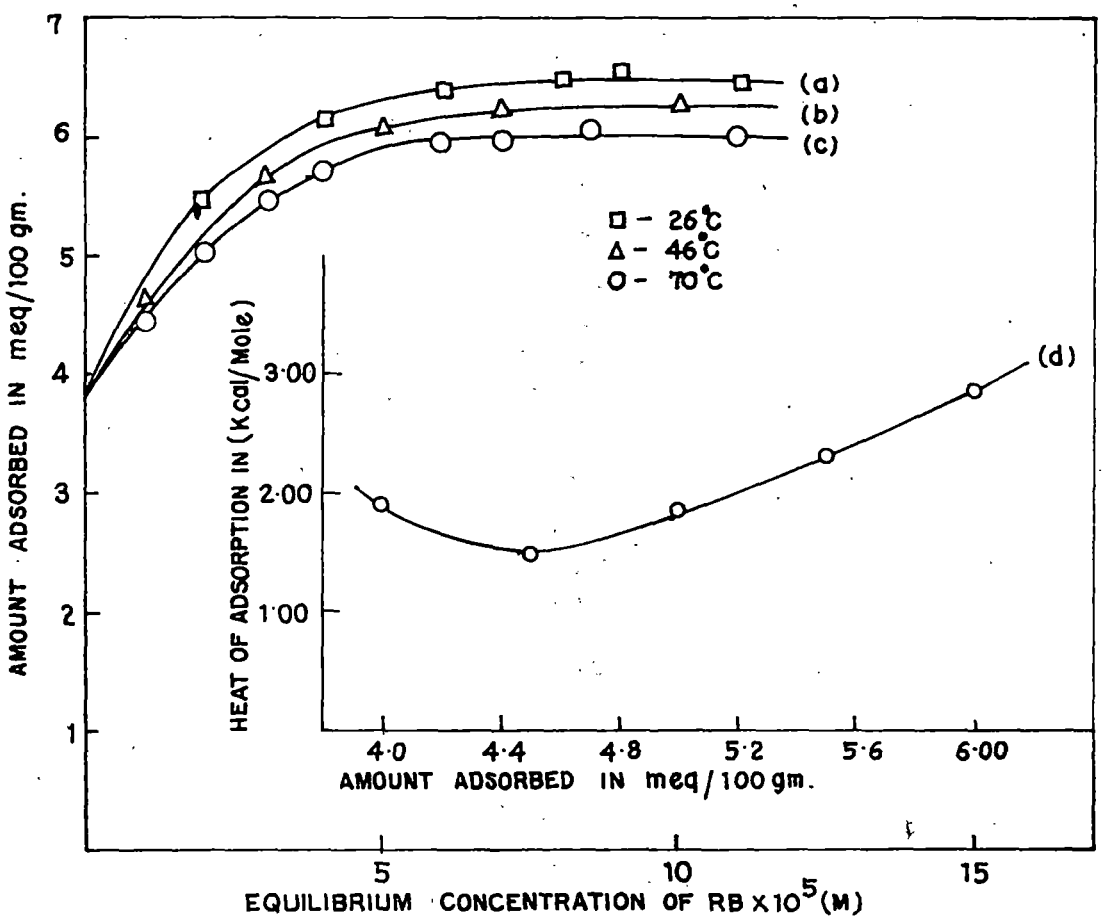

FIG. 62. ADSORPTION ISOTHERMS OF RB ON Na-KAOLINITE AT DIFFERENT TEMPERATURES (a,b,c) AND RELATION OF HEAT OF ADSORPTION WITH THE AMOUNT OF DYE ADSORBED (d).

CHAPTER VIII

Sorption of Brilliant Cresyl Blue on different aluminosilicates.

The sorption of two Xanthene Cationic dyes viz. RG and RB have been studied on the Na-form of different aluminosilicates in previous chapters (IV, V, VI). From such study it reflects that although the sorption of the cationic dyes takes place primarily by ion exchange process (1) but has rather been complicated by other factors such as molecular size, molecular geometry (2), dye-dye interaction (3), besides of course the surface characteristics of the sorbent. Also from the structural point of view (pages 46,47) the oxazine dye BB differs from that of RG and RB. The present study discussed below aims to find the adsorption characteristics of BB. On different aluminosilicates and thus to gain an insight into the effect of molecular size, space and charge of the adsorbate ions on exchange processes.

Sorption of BB^+ on Na-montmorillonite at pH 7:

The adsorption of Brilliant Cresyl Blue on Na-montrmorillonite is shown in Fig. 63(a). The isotherm belongs to the H or high affinity class of Giles et al (4) indicative of strong adsorbate-adsorbent interaction and of species adsorbed flat on the surface. The adsorption data is seen to fit into linear form of the Langmuir

adsorption equation. The plot of c/x vs C where C is the equilibrium concentration of BB and x is the amount adsorbed per 100 gm of the adsorbent yields a linear graph (Fig. 63(b). The value of V_m calculated from the slope of the linear graph [Fig. 63(b)] is equal to .125 m.eq./g. which is more than cation exchange capacity of the mineral viz. 86 meq/100g and the maximum sorption of the dye corresponding to the flat portion of the isotherm (i.e. 121 meq/100g). The excess uptake of the dye may be explained by assuming multilayer formation of the adsorbed dye molecules due to dye-dye interaction and sorption of aggregated cation (3) on the montmorillonite surface. Upto cation exchange capacity, the adsorption is mostly due to ionic and van der Waals forces and beyond it van der Waals forces predominates. The Langmuir bonding constant of the dye to the mineral is 2.17×10^5.

Sorption of BB^+ on Na-Kaolinite:

The sorption isotherm of BB^+ on Na-Kaolinite [Fig. 64(a)] is also of the Langmuir type indicating flat orientation of the adsorbed dyes on to the mineral. Accordingly the plot of C/x vs C is linear [Fig. 64(b)]. From the slope of the line, the value of V_m is found to be 8.1 meq/100g as against the maximum adsorption of the dye 7.8 meq/100g obtained from the isotherm. Both the values are higher than the cation exchange capacity value of Na-kaolinite. This is probably due to sorption of aggregated ions from the solution or dimerisation or stacking of the dye ions over the

ones already present in the adsorbed state. The computed Langmuir constant for the BB^+ on to Na-kaolinite is equal to $1.7 \times 10^5 M^{-1}$.

Sorption of BB^+ on Na-Laponite at pH 8.5

The adsorption isotherm of BB^+ on Na-Laponite is shown in Fig. 65(a). The plot of C/x vs C, where C is the equilibrium concentration of BB^+ and x is the amount adsorbed per 100 gm of adsorbent, produces a good straight line [Fig. 65(b)]. This indicates that the sorption data conform to the Langmuir equation suggesting a monolayer adsorption. Both the value of V_m (120 meq/100g) and the amount of dye exchanged at 7×10^5 (M) equilibrium concentration (117 meq/100 gm) are far in excess of the cation exchange capacity 88 meq/100g of the mineral. The top portion of the isotherm attained a plateau upto the concentration used in this study. This type of characteristics is however not found with the dye in montmorillonite. Since Laponite can swell to an unlimited extent, the dye molecules get sufficient space for an easy entry into the interlamellar region and stack themselves to form a bilayer or multilayer. Also the higher aggregation tendency of the BB^+ in aqueous medium favours the process. The calculated Langmuir bonding constant of the dye to the mineral is $1.51 \times 10^5 M^{-1}$.

It has been found the maximum adsorption study of BB^+ in respect to all the above three minerals is higher than each

of their respective cation exchange capacities of the mineral and also it is higher than that of RG and RB in respect of above mentioned study (pages 59, 91, 112). This type of behaviour of BB compared to that RG or RB is possibly due to the influence of its lesser size and stronger tendency to form aggregates in solution as well as in the adsorbed state. As a consequence when adsorption takes place from their solutions BB is adsorbed with large fraction of the aggregates than RB and RG at any particular concentration thus accounting higher adsorption of BB^+ with respect of those different minerals as studied. Monomer-dimer dissociation constant values of respective dyes are also in conformity with the above values.

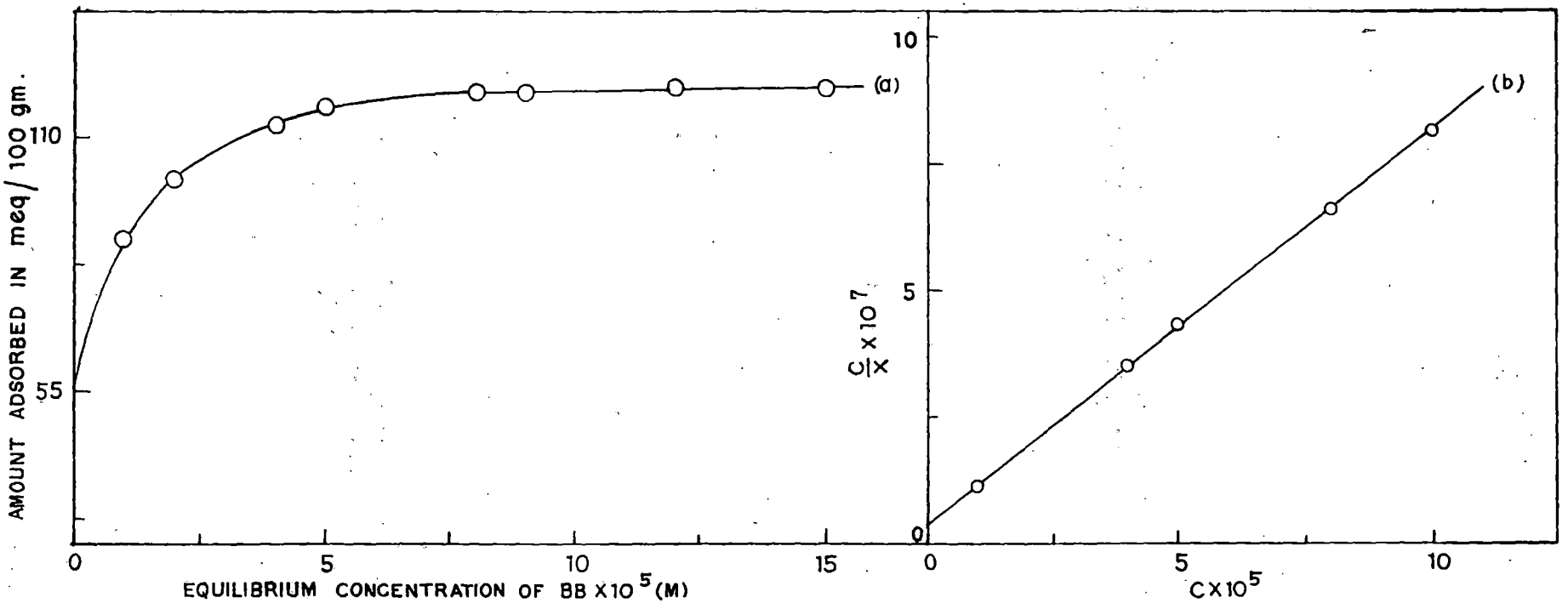

FIG. 63. ADSORPTION ISOTHERM AT 28°C (a) AND LONGMUIR PLOT (b) OF BB ON Na-MONTMORILLONITE .

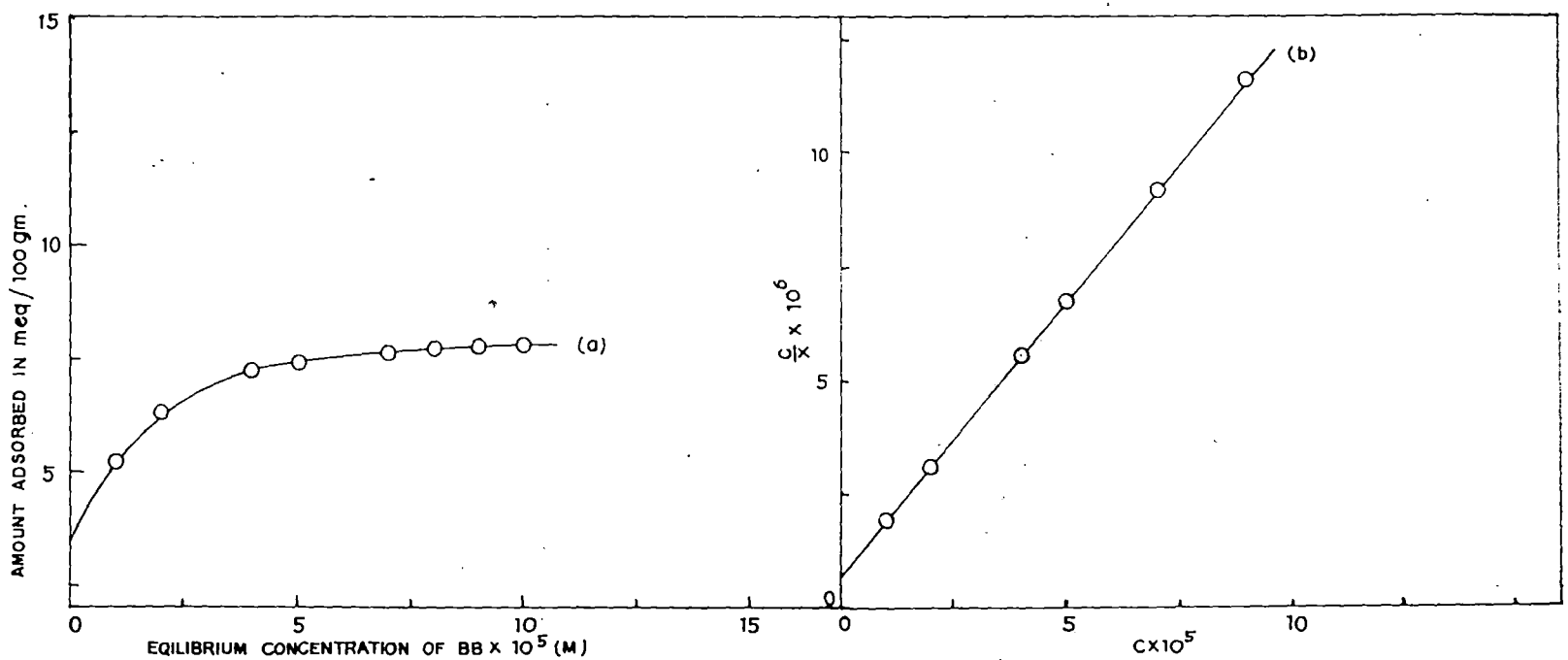

FIG. 64. ADSORPTION ISOTHERM AT 28°C (a) AND LANGMUIR PLOT (b) OF BB ON Na- KAOLINITE .

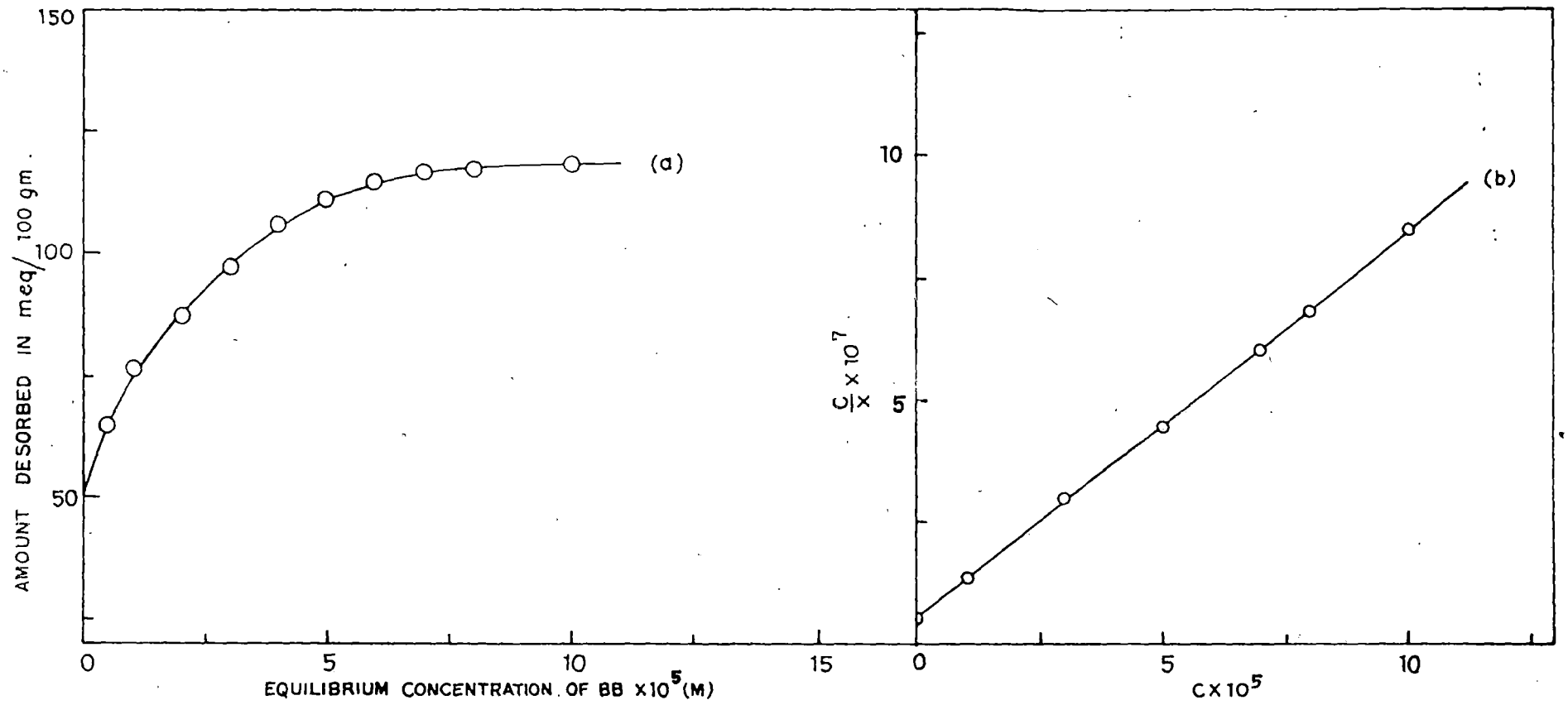

FIG. 65. ADSORPTION ISOTHERM AT 28°C (a) AND LANGMUIR PLOT (b) OF BB ON Na-LAPONITE.

CHAPTER IX

Spectrophotometric study of Dye Aggregation on clay surface

Intermolecular interactions can have a pronounced effect on the absorption spectrum of a molecule. It has been noticed that certain zwitterionic compound produced changes in colour by changing solvent resulting change in λ_{max} value also. This effect is not chemical in origin but results from physical interaction between the solute and the solvent.

Solvent-solute interactions can have various influences on an absorption spectrum. Thus the position and intensity of a band may vary as may the band width and in some cases the appearance or disappearance of vibrational fine structure may be observed.

The interaction of a solvent with a molecule is greatest for polar solvents i.e. those which possess a strong permanent dipole. The interaction is also more pronounced if the solute molecule also possesses a permanent dipole and the solvent molecules then dispose themselves about the solute to minimise the energy of the system. This results a net stabilisation of the ground state of the solute molecule. When the solute absorbs radiation the excited state is less polar than the ground state or has a different charge distribution, the temporarily frozen solvent cage may not be correctly disposed to stabilize the excited state efficiency. Thus we find that the solvent lower the energy of the ground state more than the excited state and relative

to the idealised vapour state spectrum, the solvent produces a hypsochromic shift.

In many coloured molecules however, the ground state is less polar than the excited state, and thus a polar solvent will tend to stabilise the excited state more than the ground state, giving rise to a bathochromic shift.

The adsorption of dyes on solid substrates can be regarded as a special case of solvent-solute interaction and the adsorbed molecules are generally strongly retained in a highly polar environment. Dramatic perturbation due to adsorption is found in the case of organic molecules on silica gel (1,2). This silica gel acts as a super-polar solvent and large shifts of absorption bands can often be observed. Many organic dyes in aqueous solution show an anomalous spectroscopic behaviour and do not appear to obey Beer's law at higher concentrations. Thus the absorbance of the solution does not increase linearly with increasing concentrations but falls below the expected value. This effect can be ascribed to aggregation i.e. the formation of dimers, trimers, higher aggregation of dye molecules. The changes in the appearance of the absorption spectrum due to these aggregates are caused by the same effects as those operating in the solid state.

The structural character and the position of absorption bands depend on the nature of the solvent. Generally, polar solvents tend to shift the position of the bands and diminish the vibrational structure of the bands. Burawoy (3) first employed solvent effects

for the characterization of electronic transition. These ideas have been revived by Kasha (4) and McConnell (5) who have suggested that solvent effects may be of value in distinguishing between $\pi \rightarrow \pi^*$ and $n \rightarrow \pi^*$ transitions. Polar solvents generally (but not always) shift the $n \rightarrow \pi^*$ transition to longer wave length (red shift). The vibrational structure of some $\pi \rightarrow \pi^*$ bands is retained even in polar solvents. While the wave lengths of the $n \rightarrow \pi^*$ bands are generally found to decrease (blue shift) with the increase in polarity of the solvent. The vibrational structure of $n \rightarrow \pi^*$ bands is completely blurred in polar solvents.

It may be generalized that the absorption band of almost all organic molecules normally found in the near ultra-violet and visible region arise from either $n \rightarrow \pi^*$ or $\pi \rightarrow \pi^*$ transition. The $\pi \rightarrow \pi^*$ transition may be very intense (allowed) or weak (forbidden). But the $n \rightarrow \pi^*$ transitions are generally forbidden and consequently of weak intensity.

The wave length and the intensity of absorption bands are both affected when a molecule is in a solvent environment compared with its spectrum in the gas phase. This is due to the unequal perturbation of the ground and the excited states of the molecule which depends on the solvent-solute interaction in the two states. Bayliss (6) has made a quantitative approach to the study of solvent effects on the absorption spectra. Bayliss and McRae (7) have explained solvent effects on absorption spectrum qualitatively in terms of dipole-polarization and hydrogen bonding forces between

the solute and solvent superimposed on one another.

A general polarization red shift which is due to the solvent polarization by the transition dipole and which depends on the solvent refractive index, is observed in the electronic spectra of all organic molecules in solution. When the solute is polar other effects due to dipole-dipole and dipole polarization forces come into operation. Application of the Frank-Condon principle shows that the solvent cage around the solute molecules is strained. This consists of orientation - strain and packing strain of which the former is more important in the case of polar solute and polar solvent. A decrease in the dipole moment of the solute during transition leads to a blue shift of the absorption maxima. On the other hand if the dipole moment increases during transition the absorption maxima will have a red shift.

Clays are known to adsorb basic dyestuffs from their aqueous solutions. Reciprocal Langmuir plots are generally linear indicating a monolayer adsorption of these dyes (8). This adsorbing ability of the clay minerals is attributed to an ion-exchange process. But many clays, particularly of the swelling type viz. bentonite, are found to adsorb dye molecules well in excess of their respective exchange capacities. Various explanations for this behaviour have been proposed amongst which one is based on aggregation of dye molecules. An evidence of such aggregation follows from an examination of the metachromatic shift in the spectrum exhibited by certain dyes (9-11) when sorbed on surfaces of colloidal particles. Coven and Weissbein (12) provided a electron microscopic evidence for the dye association on textile

materials. Bergman and O'Konski (10) studied the metachromasy of methylene blue sorbed on bentonite and concluded that dimerization of the dye takes place on clay surface. However these studies were carried out with a dye which is known to dimerize in solution at high concentration (11) and deviates from Beer-Lambert law. This necessitates further study with dyes differing both in structure and size that would include both those which are structurally hindered to come close enough for aggregation and those which are not. Spectrophotometric study of interactions are likely to reveal some aspects of clay-dye interaction.

The spectra of aqueous solutions of several cationic dyes are dependent on the concentration of the dye (13). In the visible region these spectra are characterised by several maxima, the intensities of which depend on the dye concentration. The adsorption band of the dye at longer wavelength is characteristic of dilute solutions and usually referred to as the α band. Increasing dye concentrations results in the gradual replacement of α-band by a band with a shorter wave length which is assigned as β-band (13-17). Further increase in dye concentration may cause substitution of β-band by another diffused band closer to the blue range of the spectrum. This band is assigned as γ-band. The α-band is attributed to the monomeric form of the dye while the β and γ-bands are attributed to dimeric and higher aggregates of the dye respectively (18). The dye aggregation is caused mainly by the interaction between the electrons of the aromatic rings of the dye cations.

Similar changes in the spectra of the aqueous dye solutions may also be obtained by the addition of salts. This has been interpreted as being due to the 'salting-out' of the dyes (19-22). Addition of polyelectrolytes to a dilute dye solution also causes changes in the spectrum, which are similar to those obtained by increasing the concentration of the dye. In the latter case it is now accepted that cationic dyes are adsorbed by polyelectrolytes and since the concentration of the dye is higher on the polyelectrolyte surface than in the bulk of the solution the adsorbed dye species form dimers and higher aggregates at the adsorption sites. This gives rise to the metachromatic effects in the spectrum. The case, however, seems to be not so simple when clay minerals are involved, which also exhibit metachromatic behaviour when cationic dyes are adsorbed. A short review of the previous work on this line is given in the following paragraphs.

The chromotropic effects in clay minerals were observed by Vedeneva (23) by studying the sorption of malachite green and brilliant green on montmorillonite and kaolinite in 1947. She concluded that the formation of ionic bond between the clay and dye caused a bathochromic shift, while the effect of intensification of the dipole bond was hypsochromic. Schubert and Levine (24) postulated that metachromatic colour was produced as a result of a selective and reversible binding within an anionic cluster of a polymeric dye cation of highest charge available. The effect is that even in dilute dye solutions the concentration of dye cations of high charge is increased in the total micellar and intermicellar space.

Bergmann and O'Konski (10) attributed the spectral shifts of the methylene blue sorbed on Na-bentonite, to dye-dye interaction on the clay surface since these changes were found similar to the spectral shifts accompanying dimerisation and polymerisation of the dye in aqueous solution. According to these authors the dimer is held together by London dispersion forces and hydrophobic bonding. Yariv and Lurie (25) investigated in detail the metachromatic behaviour of methylene blue adsorbed on montmorillonite and showed that the adsorption takes place by a cation-exchange mechanism and the dye can be sorbed either at the edges of the clay platelets or on the oxygen sheets of the silicate layer. The latter-type of sorption leads to metachromasy of the dye with a shift of the absorption band in the visible region to lower wavelegnths. These authors showed, through X-ray diffraction studies, that metachromasy of methylene blue in montmorillonite occurs even when there is only a monolayer of the organic compound that lies parallel to the silicate sheets and concluded that π -interactions between the dye cations and the oxygen plane of the aluminosilicate layer of the montmorillonite lead to metachromasy when clay-dye interactions take place.

Yamagashi and Soma (26) studied the adsorption of several N-alkylated acridine Orange by Na-montmorillonite. In their study they showed that adsorption of cationic dyes which belong to the acridine orange family also results in metachromasy. However, they

considered the clay mineral as a normal polyelectrolyte and believed that the interaction between the negatively charged mineral and the dye cation is a pure electrostatic attraction and that metachromasy resulted from the electronic interaction between neighbouring adsorbed cations.

Recently Cohen and Yariv (27) extended their earlier studies (25) and investigated metachromasy of acridine orange using H-, Mg-, Na-, Al- and Cu-montmorillonite by visible and IR spectroscopy and by X-ray diffraction method. Two types of association between acridine orange and montmorillonite were noted : (i) monolayer of the dye located in the interlayer space, with the aromatic rings parallel to the alumino-silicate layer and (ii) a bilayer in the interlayer space or tilting of the cationic dye relative to the aluminosilicate layer. They concluded that in the association of type (i) metachromasy cannot be attributed to dimerisation of the dye but must be caused by π-interactions between the oxygen of the aluminosilicate and the aromatic ring. Conflicting reports exist in the literature as just metnioned. Present study on the spectroscopic behaviour of RG, RB and BB sorbed by montmorillonite, laponite and kaolinite has been undertaken with a view to throw further light in the subject.

Electronic spectrum of aqueous solutions of RG, RB and BB

Figs. 66,67 and 68 show the electronic spectra of RG, RB and BB in the visible regions at various concentration of the dye in aqueous medium. In aqueous solution these dyes show peaks at 525 nm for RG, 552 nm for RB and 640 nm for BB respectively which are due to $\pi \rightarrow \pi^*$ transition and may be referred to as α-band (17). Shoulders have also been found at the wave lengths 500 nm for RG; 523 nm for RB and 590 nm for BB. These may be referred to as β-band. With the increase in the concentration of the dye the α-band intensity is seen to decrease with a corresponding increase in the β-band intensity. The β-band is characteristic of the dimer and corresponds to an oscillator in the Y-direction (shorter axis in the plane of the molecule). Bergmann and O'Konski (10) believe that the β-band has a transition moment which lies also along the axis of the molecule but is perturbed due to interaction between the transition moments of the monomer units.

Effect of Na-montmorillonite in the absorption spectrum of RG:

It is well documented that the xanthene dyes tend to dimerize at concentration as low as 10^{-4} (M) via interaction. This is usually reflected by the appearance of metachromatic absorption bands (28). The visible spectra of the clay-dye suspension prepared (in 25 ml) are obtained by the method in Chapter III page 54. The spectra and λ max values were recorded

at increasing percentages of the Na-montmorillonite clay in a constant RG dye concentration 1.2×10^{-5} (M) [Fig. 69, table 14 page 165] on this basis, location of the band α can be ascertained in which it is observed to be red shifted upon adsorption on clay. There will be charge transfer complex formation between the dye cation and the electron donating montmorillonite. Similar observation was also reported by Haque et al (29). Protonation of the ring nitrogen may occur that stabilises the excited state and lowers the required energy causing red shift in the adsorption spectrum. The β band shift remains almost constant. The intensity of α band increases gradually indicating the dissociation of dimer into a monomer adsorbed species . Table 14 (page 165) reveals that the whole series can be regarded as a titration of an aqueous solution of RG by the clay. From such analysis the saturation point α can be determined.

At the end point α band makes the major contribution to the maxima at 540 nm. corresponding to dye : clay ratio equal to 55 mM per 100 gm Na-montmorillonite. At lower dye/clay ratio the dye is totally adsorbed by the clay. From the spectral observation (Fig. 69) it appears that the dye adsorbed on Na-montmorillonite suspension upto the clay concentration .001% appears to bear an analogy to those observed for dilute aqueous solution of the dye showing no metachromatic effect. But as more and more dye is adsorbed by the Na-clay the α-band

gradually attains prominence suggesting the penetration of the dye molecule into interlayer spaces. After the saturation point, the nature of the adsorption band tends to be similar as obtained in dilute aqueous solution of dye. Here the α-band indicates hydration statue of the sorbed organic dye molecule. So it appears that the adsorption of the dye cations by the clay affects the absorbance of both α and β bands in the in the spectrum of RG resulting in the change of both bands.

The saturation point has been obtained by a plot of absorption intensity of a fixed dye concentration vs amount of added clay (weight %) [Fig. 50(a)] and λ_{max} value (nm) vs added clay (weight %) [Fig. 50(b)]. It is interesting to note that the Fig. 50(a) shows a minima and Fig. 50(b) shows a maxima. Slight variation of the position of minima and maxima has also been observed from system to system.

From the above study it is clear that the higher the surface coverage, the larger is the red shift in α band.

The fact that the location of α band changes gradually with change of degree of coverage is an indication to a gradual and even distribution upon adsorption. A possible sequence of events is, coverage of isolated plates first and then the adsorption in interlayer spacing. Gradual change in location is an indication for the gradual change in average local polarity; as more dye molecules are adsorbed, the local environment gradually changes to less polar and becomes more hydrophilic.

Indeed, red shifts in RG were observed when water was substituted by a less polar solvent (30). Consequently, the red shift observed even at low coverage may be interpreted as reflecting surface polarity which is not as high as that of water. This observation is in agreement with the known hydrophobicity of the oxygen plane of the clay (31). The decreaee in the absorption intensity is very much similar to the known effect, viz. deviation from Beer-Lambert law upon aggregation.

Effect of Na-laponite in the absorption spectrum of RG:

Experimental procedure is same as mentioned in Chapter III and page 54. From the spectral analysis as recorded in table 15 (page 166) and figure 71 wherein a series of clay dye suspension prepared (in 25 ml) using a fixed concentration. It is apparent that like adsorption of RG on Na-montmorillonite in Na-laponite also red shift is observed in the α-band and its intensities are prominent than that of β-band. Maximum is obtained when the dye : clay ratio is equal to 40 mM dye per 100 gm of Na-laponite. The shifts in maxima and minima have been ascertained from Figs. 72(a) and (b). The position of the α-band can be used as an indicator in explaining the surface polarity. The failure of the dye to exhibit significant spectral change at lower adsorption values may be due to lower charge density vis-a-vis the higher swelling property of the synthetic hectorite.

Effect of Na-Kaolinite in the absorption Spectrum of RG:

For the spectral study (Fig. 73), samples have been prepared in the same way as mentioned in Chapter III and page 54. λ_{max} values are recorded in table 16 (page 167) β band is almost completely suprressed even at low concentration in both the clays whereas intensity of α-band gradually increases. This may be explained by considering the change in the dielectric constant due to addition of the substrates. The solvation shell of the solvent (i.e. water molecules) around the solute molecules (i.e dye ion) forms a microscopic solvent/dye system with an effective dielectric constant so called screening factor on its own (32). Additive that increases the effective dielectric constant will reduce repulsion between similar charged dye ion and facilitate their dimerisation. Increase clay concentration causes increase in the screening factor or the effective dielectric constant of the microscopic dye/ solvent system and hence promote aggregation.

Effect of Na-montmorillonite on the absorption spectrum of RB:

The experimental (Fig. 74) procedure for the above has already been narrated in Chapter III page 54. λ_{max} values are recorded in table 17 (page168). Here also red shift of α-band occurs upon adsorption. Changes in the location of α-band also provides information about RB clay adsorption.

Effect of Na-laponite on the absorption Spectrum of TB:

Same experimental procedure has been followed as mentioned in Chapter III page 54. From Fig. 75 and table 18 (page169) it is observed that λ is red shifted and the change in RG adsorption is not to that extent as in the case of RB adsorption.

Effect of Na-Kaolinite in the absorption Spectrum of RB:

The λ_{max} obtained from spectral study obtained from a total use of 10 ml of clay-dye suspensions containing a fixed amount of dye (Table 19, page170 , Fig. 76) reveals that there is no significant change in its values, when the dye is sorbed by the clays. The spectral pattern is almost the same as that of pure aqueous solution of the dye showing lesser tendency towards adsorption.

Same experimental procedure has been followed in all systems as mentioned in Chapter III page 54 for BB.

Effect of Na-montmorillonite on the absorption Spectrum of Brilliant Cresyl blue:

The adsorption of BB by Na-montmorillonite takes place largely by a cation exchange mechanism. Exchangeable cation is released into the solution when clay is equilibrated with BB as already discussed in previous Chapter III (page 54). The effect of concentration in a constant amount (in 25 ml) of BB (4×10^{-4} (M)) of various clay on the absorption spectrum is

shown in Fig. 77. By comparison of the spectra in Fig. 68 and Fig. 77 it is obvious that the adsorption of BB by Na-montmorillonite results in the combination of two spectroscopic effects. These are (i) metachromasy (ii) partial extinction of the absorption bands.

Metachromasy occurs as soon as BB is adsorbed by Na-montmorillonite even if the adsorption takes place from very dilute solutions of the dye which in the absence of the clay do not show this effect. Significant changes were observed with $\pi \rightarrow \pi^*$ transition band of BB in the visible spectrum when sorbed on Na-clay samples. Effects are similar to those observed for methylene blue and acridine orange (33,34) The λ_{max} values are given in Table 20 (page 171).

On spectral analysis (Fig. 77) it is found that the addition of small amount of Na-montmorillonite to the dye solutions resulted in a deep coloration of the suspension. Visually this effect is independent of the pH of the solution. The whole sequence of addition of varying amount of clays in a fixed dye concentration can be regarded as titration of BB by Na-montmorillonite. At the end point all the BB have been adsorbed by the clay. Band has been blue shifted. λ_{max} value has been recorded in table 20 (page 171). At the end point β band makes the major contribution. Maxima and minima are attained as per Fig. 78(a) and 78(b). With increasing dye concentration the β -band shifts to lower values, reaching a minimum at 556 nm when the clay concentration is .072 which corresponds to an

adsorption of 65 mM per 100 gm clay. At still higher concentration the band shifts again to slightly lower wave length 558 nm at a clay concentration of 0.092 this corresponds to 52 mM per 100 gm clay.

Effect of Na-laponite on the adsorption spectrum of BB:

Here also metachromatic change occurs when BB is adsorbed by Na-laponite. The spectral shifts due to adsorption of dye in a fixed dye concentration with increasing clay concentration are shown in Fig. 79. The λ_{max} values are recorded in Table 21 (page 172). At lower concentration of clay, shift of β band is smaller as compared to Na-montmorillonite BB system. This is attributed to the lower charge density vis-a-vis the higher swelling property of the synthetic hectorite. As a result of high swelling, large amount of water is present in the interlayer space of Na-laponite which permits the hydration status of the adsorbed dye ions to be similar to that existing in dilute aqueous solution of the dye. In addition, the intercalated dye ions in Na-laponite cannot approach the oxygen plane by the silicate layer close enough to induce π - electron interaction. With the increase in clay concentration the β band shifts to 558 nm at 0.08% of the clay concentration which corresponds to the adsorption of 56 nM/100 gm clay as compared to BB in Na-montmorillonite where the value of β band shifts to 556 nm [Fig. 80(a) and 80(b)]. The observation of

metachromasy at high adsorption values of this dye may be ascribed to the decrease in water content and increase of hydrophobic properties of the interlayer space with increasing intercalation of the organic material. This brings forth a situation conducive to π interaction between Laponite oxygen sheet and the dye ions requiring the resulting metachromasy.

Interestingly from the spectral study of BB just mentioned in Na-montmorillonite and Na-laponite it appears that BB has a tendency to form π interaction with the oxygen plane. The gradual changes in the location of band β is to the blue as concentration increases (35). The opposite trend in spectral shift for this dye with other two dyes is an indication for the lack of π interaction in xanthene dyes (36).

Effect of Na-kaolinite on the spectrum of BB:

From the λ_{max} values recorded in table 22 (page 173) and the spectral features (Fig. 81) it is evident that the intensities of both α & β increase with clay concentration where α band remains almost constant but β band is slightly blue shifted. Change in the location of bands provide information about BB clay adsorption.

Table 14

Spectral data of the Sorbed dye RG on Na-montmorillonite

Concentration of dye	Clay concentration weight %	mM of dye added per 100 gm clay	Absorbance	λ_{max} (Sorbed dye nm)	
				β-band	α-band
1.2×10^{-5} (M)	0.00020	697	0.96	500	525
	0.00024	581	0.90	"	525
	0.0010	140	0.80	"	526
	0.0014	100	0.78	"	528
	0.00224	62	0.70	"	532
	0.00252	55	0.72	502	540
	0.0030	46	0.80	502	538
	0.0040	35	0.84	502	537

Table 15

Spectral data of the Sorbed RG on Na-laponite

Concentration of the dye	Clay concentration weight %	nM of dye added per 100 gm clay	Absorbance	λ_{max} (Sorbed dye) nm	
				β-band	α-band
1.8×10^{-5} (M)	0.00124	165	0.80	500	526
	0.0025	81	0.76	"	527
	0.0030	68	0.70	"	528
	0.0035	58	0.60	"	529
	0.0040	51	0.42	"	532
	0.0045	45	0.40	"	530
	0.0050	40	0.86	"	535
	0.0060	34	1.11	"	533
	0.0065	31	1.44	"	533
	0.0070	29	1.46	"	528

Table 16

Spectral data of Sorbed dye RG on Na-kaolinite

Concentration of the dye	Clay concentration weight %	Clay: Dye ratio in mM	Absorbance	λ_{max} (Sorbed dye) nm	
				β-band	α-band
1.8×10^{-6} (M)	0.00014	0.042	0.134	500	527
	0.00028	0.084	0.140	"	527
	0.00056	0.168	0.150	"	528
	0.00070	0.210	0.152	"	528
	0.00098	0.294	0.180	"	529

Table 17

Spectral data of the Sorbed dye RB on Na-montmorillonite

Concentration of the dye	Clay concentration weight %	mM of dye added per 100 gm clay	Absorbance	λ max (Sorbed dye nm) β-band	α-band
1×10^{-5} (M)	0.00024	484	1.44	515	552
	0.00026	426	1.32	"	552
	0.0003	387	1.24	"	553
	0.0005	232	1.10	"	554
	0.0008	145	0.84	"	555
	0.001	116	0.87	520	555
	0.002	58	0.80	525	565
	0.003	38	0.50	525	575
	0.005	23	0.52	525	580

Table 18

Spectral data of the Sorbed dye RB on Na-laponite

Concentration of dye	Clay concentration weight %	mM of dye added per 100 gm clay	Absorbance	λ max (Sorbed dye nm)	
				β-band	α-band
5.4×10^{-6} (M)	0.00024	255	0.60	515	552
	0.00048	128	0.58	"	553
	0.001	61	0.57	"	554
	0.0015	40	0.54	"	555
	0.0018	34	0.64	520	557
	0.002	30	0.72	522	562
	0.004	15	0.76	"	560
	0.006	10	0.78	"	559

Table 19

Spectral data of the Sorbed dye RB on Na-kaolinite

Concentration of dye	Clay concentration weight %	Clay dye ratio	Absorbance	λ max (Sorbed dye) nm	
				β-band	α-band
2×10^{-4} (M)	0.01	0.027	2.40	523	552
	0.02	0.054	2.46	"	"
	0.03	0.081	2.52	"	"
	0.05	0.135	2.53	"	"

Table 20

Spectral data of the Sorbed BB on Na-montmorillonite

Concentration of dye	Clay concentration weight %	mM of dye added per 100 gm clay	Absorbance	λ max (Sorbed dye) nm α-band	β-band
4×10^{-4} (M)	0.01	465	0.92	640	585
	0.03	155	0.90	"	575
	0.05	93	0.78	"	570
	0.07	65	0.54	"	556
	0.09	52	0.58	"	558

Table 21

Spectral data of the sorbed dye BB on Na-laponite

Concentration of dye	Clay concentration weight %	mM of dye added per 100 gm clay	Absorbance	λ max (Sorbed dye) nm	
				β-band	α-band
4×10^{-4} (M)	0.02	227	0.92	640	582
	0.04	113	0.84	"	580
	0.06	75	0.72	"	575
	0.08	56	0.48	"	558
	0.09	50	0.60	"	563

Table 22

Spectral data of the sorbed dye BB on Na-kaolinite

Concentration of dye	Clay concentration Weight %	Clay : dye ratio in mM	Absorbance	λ_{max} (Sorbed dye) α-band	β-band
4.5×10^{-4} (M)	0.01	0.012	0.96	640	580
	0.02	0.024	1.00	"	"
	0.03	0.036	1.14	"	"
	0.05	0.048	1.17	"	581
	0.06	0.072	1.04	"	582

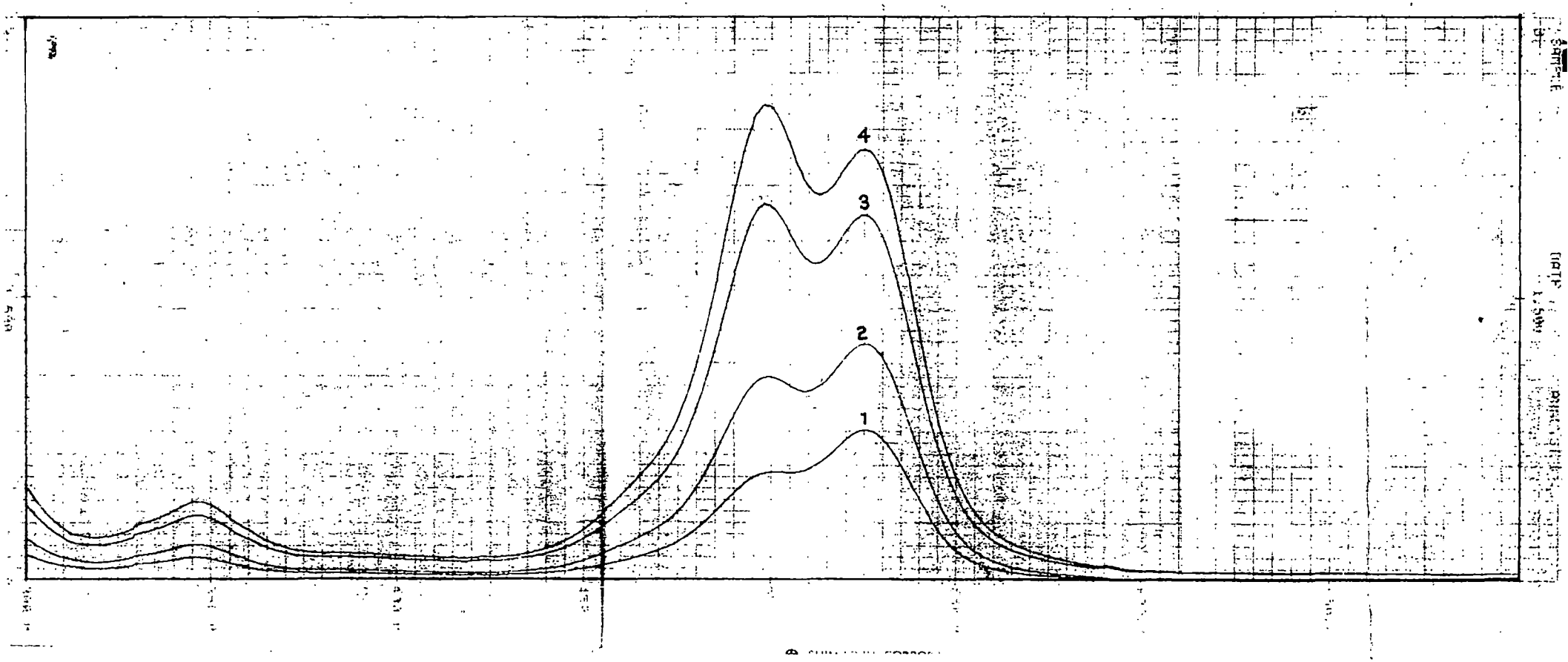

Fig. 66. The electronic spectra of RG at various concentrations (1) 8×10^{-6}(M) (2) $1{\cdot}5 \times 10^{-5}$(M) (3) $2{\cdot}2 \times 10^{-4}$(M) (4) 3×10^{-4}(M) using 1MM path length cell.

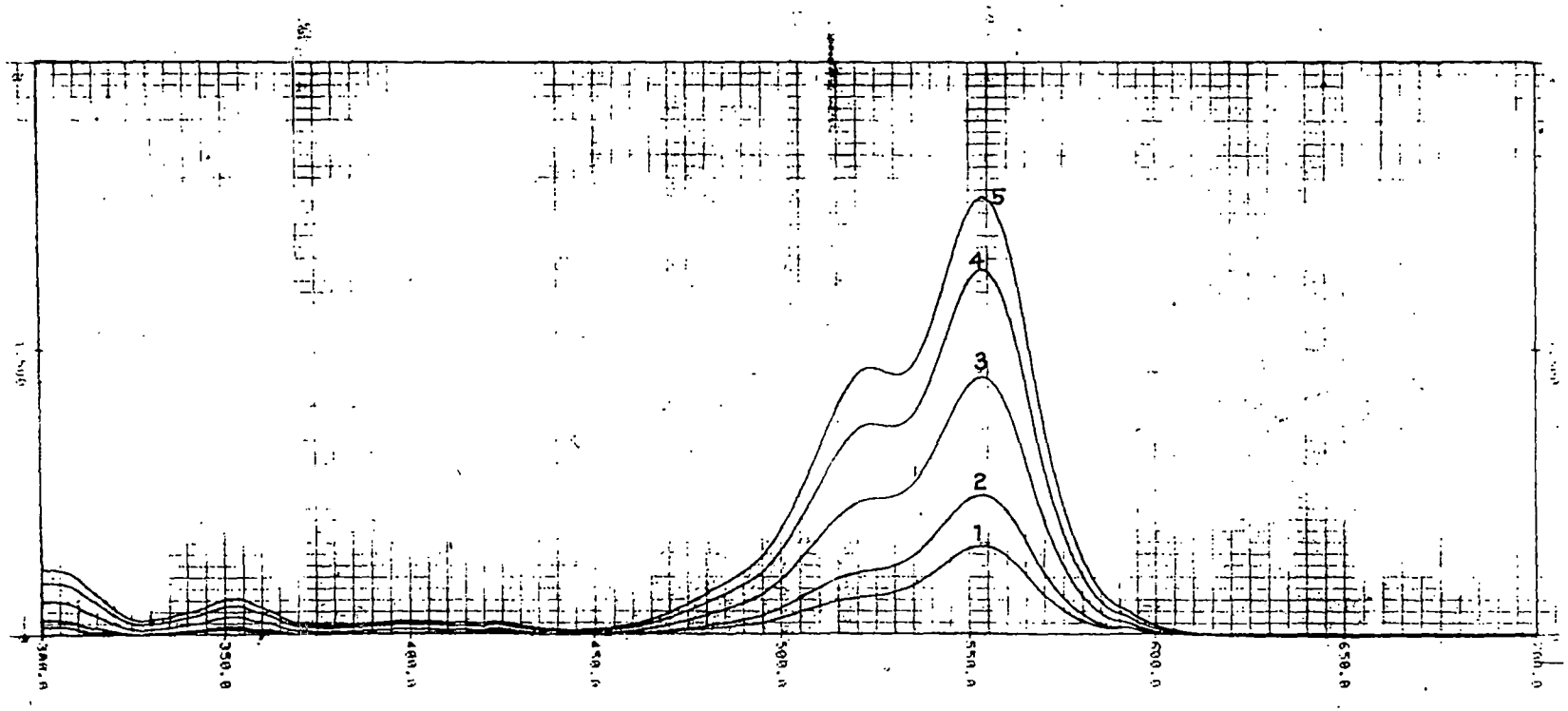

Fig. 67. The Electronic spectra of RB at various concentrations (1) 3×10^{-6}(M) (2) 5×10^{-6}(M) (3) 8×10^{-6}(M) (4) $1{\cdot}4\times10^{-4}$(M) (5) $1{\cdot}8\times10^{-4}$(M) using 1MM Path length cell.

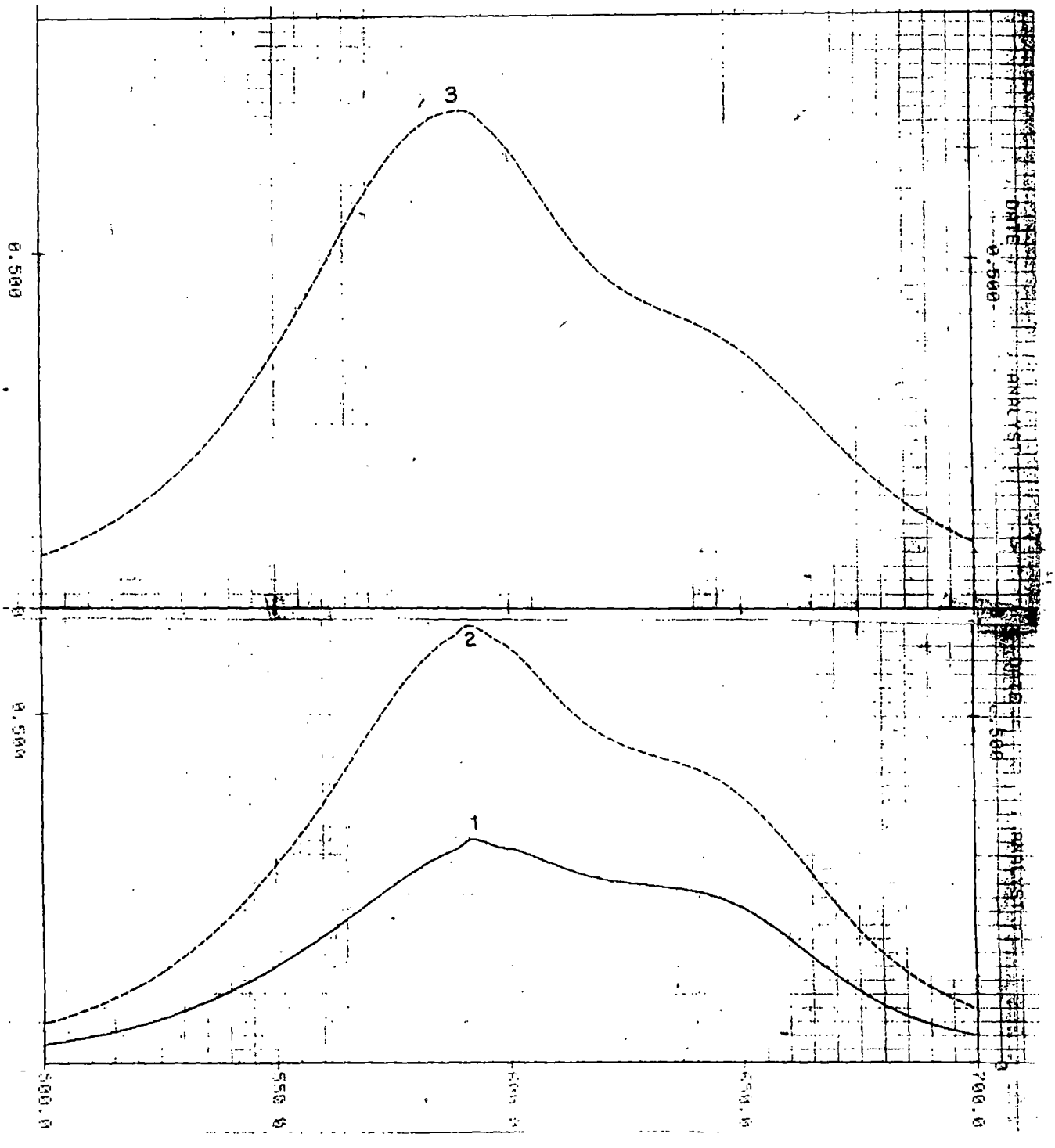

Fig. 68(a). The electronic spectra of BB at various concentrations (1) 8×10^{-5}(M) (2) $1{\cdot}5 \times 10^{-4}$ (M) (3) $1{\cdot}8 \times 10^{-4}$(M) using 1MM path length cell.

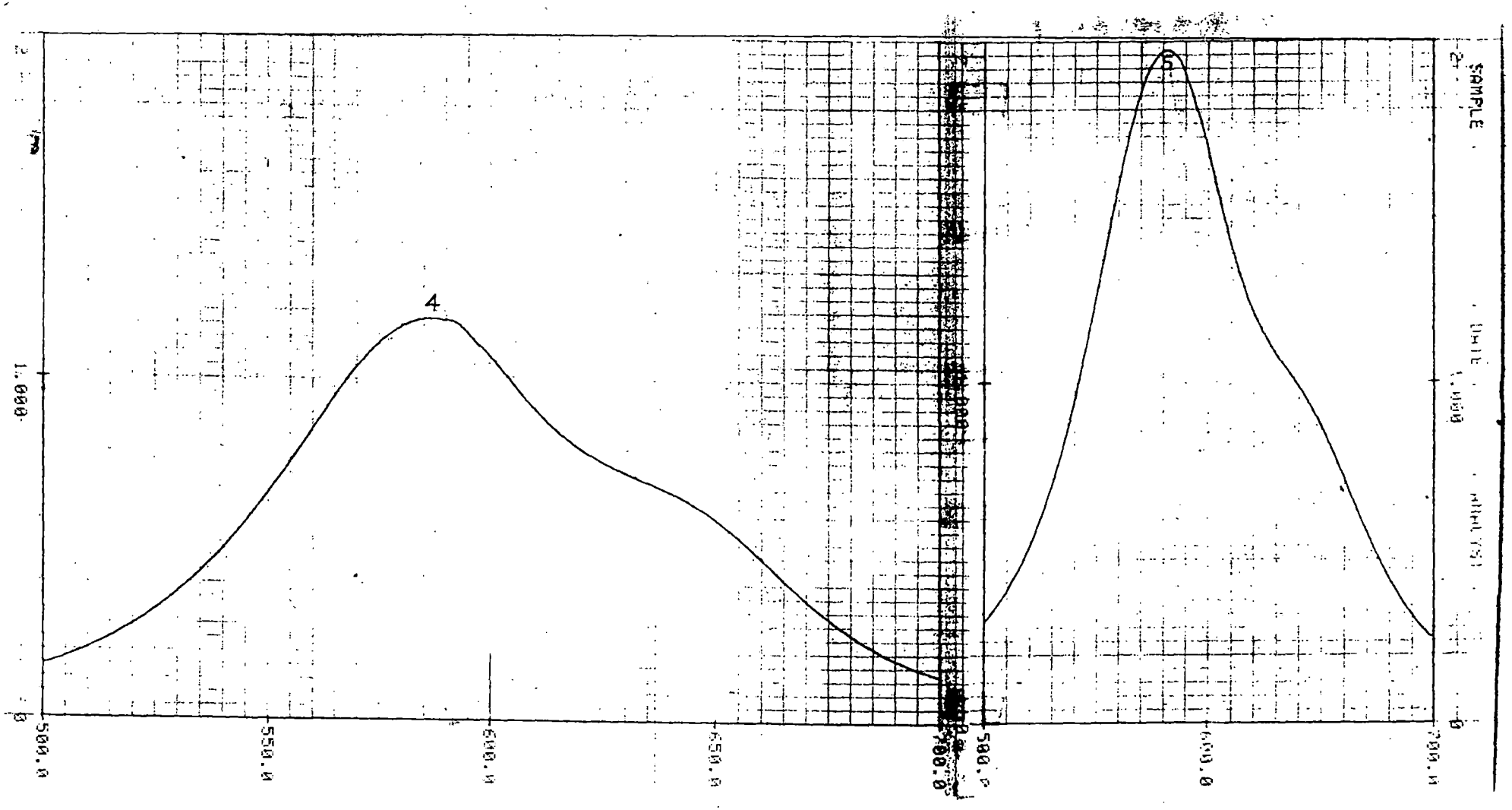

Fig. 68(b). The electronic spectra of BB at various concentrations (4) 2.8×10^{-4}(M) (5) 4×10^{-4}(M) using 1MM path length cell.

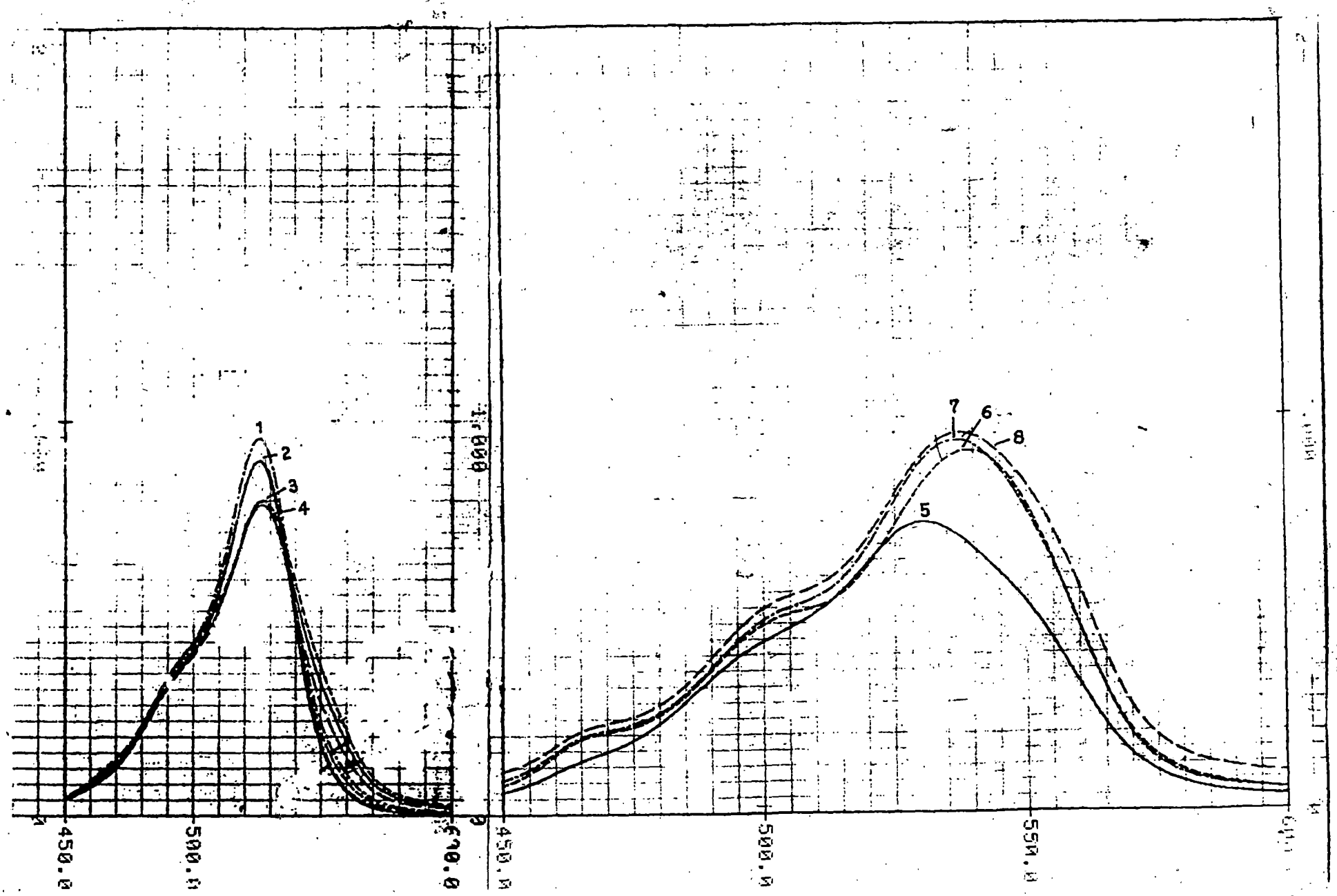

Fig. 69. Effect of Na- Montmorillonite on the absorption spectrum of $1{\cdot}2\times10^{-5}$(M) RG: (1) 0·00020% clay (2) 0·00024% clay (3) 0·0010% clay (4) 0·0014% clay (5) 0·00224% clay (6) 0·00252% clay (7) 0·0030% clay (8) 0·0040% clay.

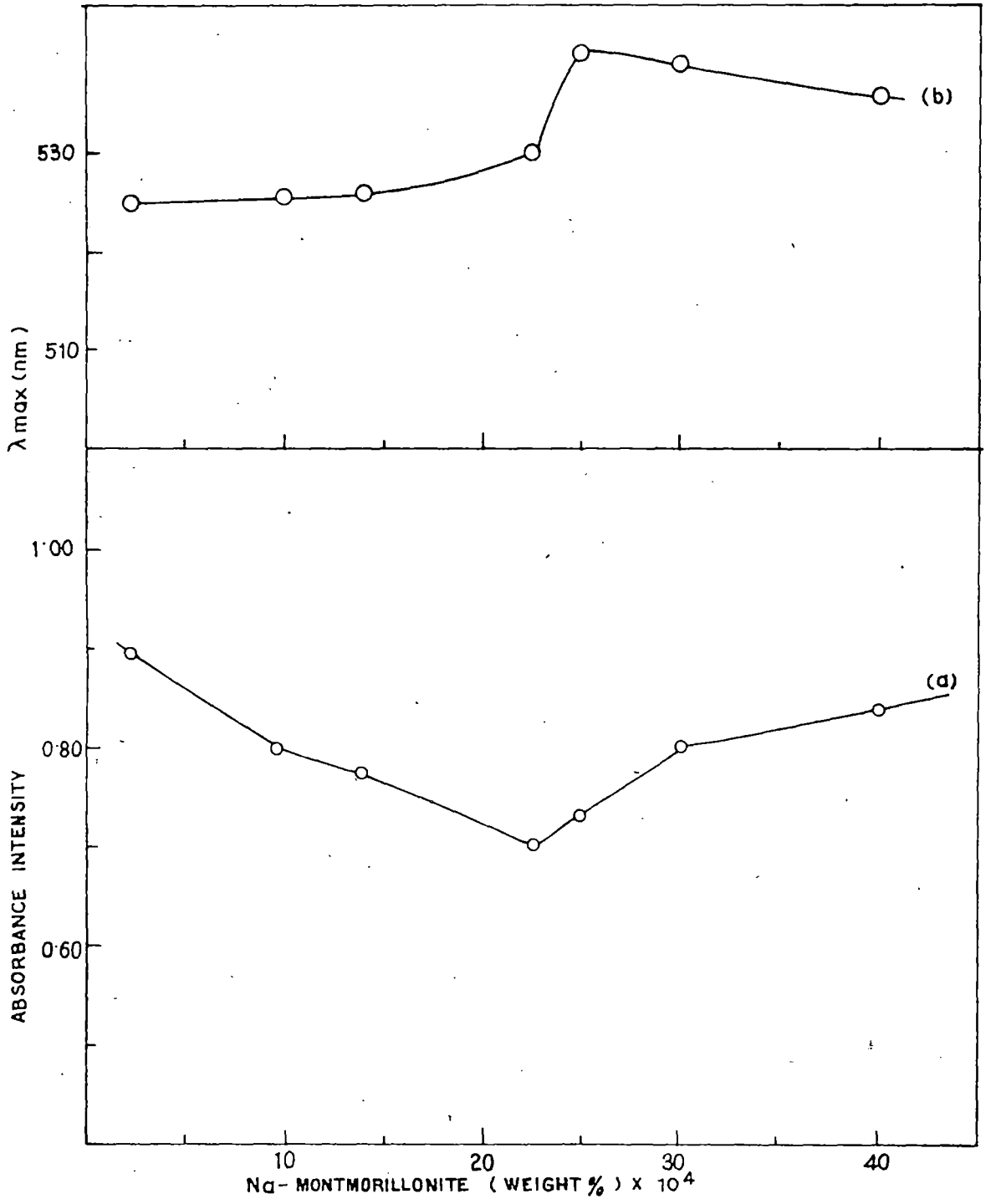

FIG. 70. THE EFFECT OF Na-MONTMORILLONITE ON (a) THE ABSORPTION INTENSITY OF BAND α (b) THE LOCATION OF BAND α AT A FIXED CONCENTRATION OF $1{\cdot}2 \times 10^{-5}$ (M) RG.

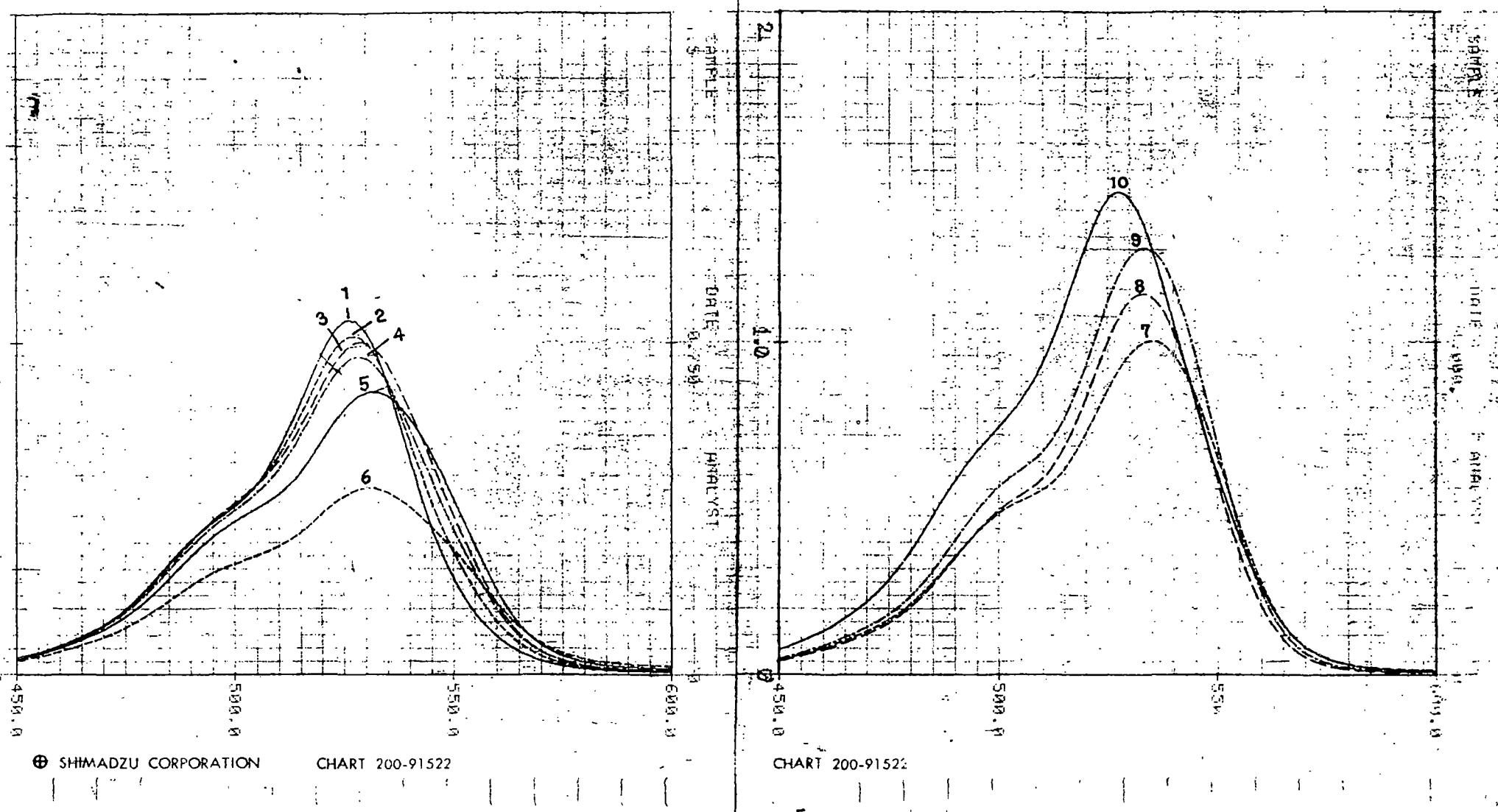

Fig. 71. Effect of Na-Laponite on the absorption spectrum of $1{\cdot}8 \times 10^{-5}$(M) RG : (1) 0·00124 % clay (2) 0·0025% clay (3) 0·0030% clay (4) 0·0035% clay (5) 0·0040% (6) 0·0045% clay (7) 0·0050% clay (8) 0·0060% clay (9) 0·0065% clay (10) 0·0070% clay.

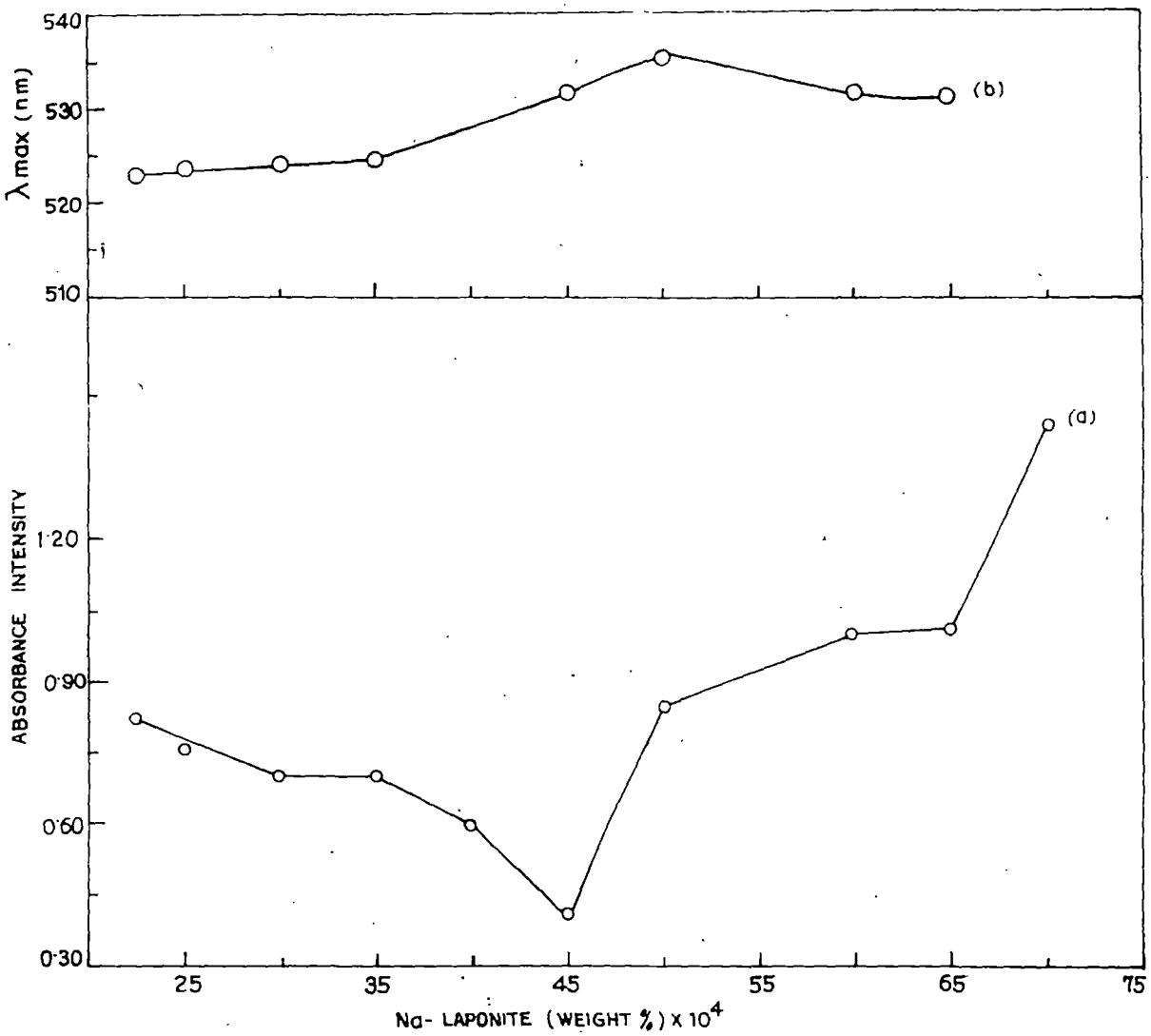

FIG. 72. THE EFFECT OF ADDED Na-LAPONITE ON (a) THE ABSORPTION INTENSITY OF BAND α (b) THE LOCATION OF BAND α AT A FIXED CONCENTRATION OF $1{\cdot}8 \times 10^{-5}$ (M) RG

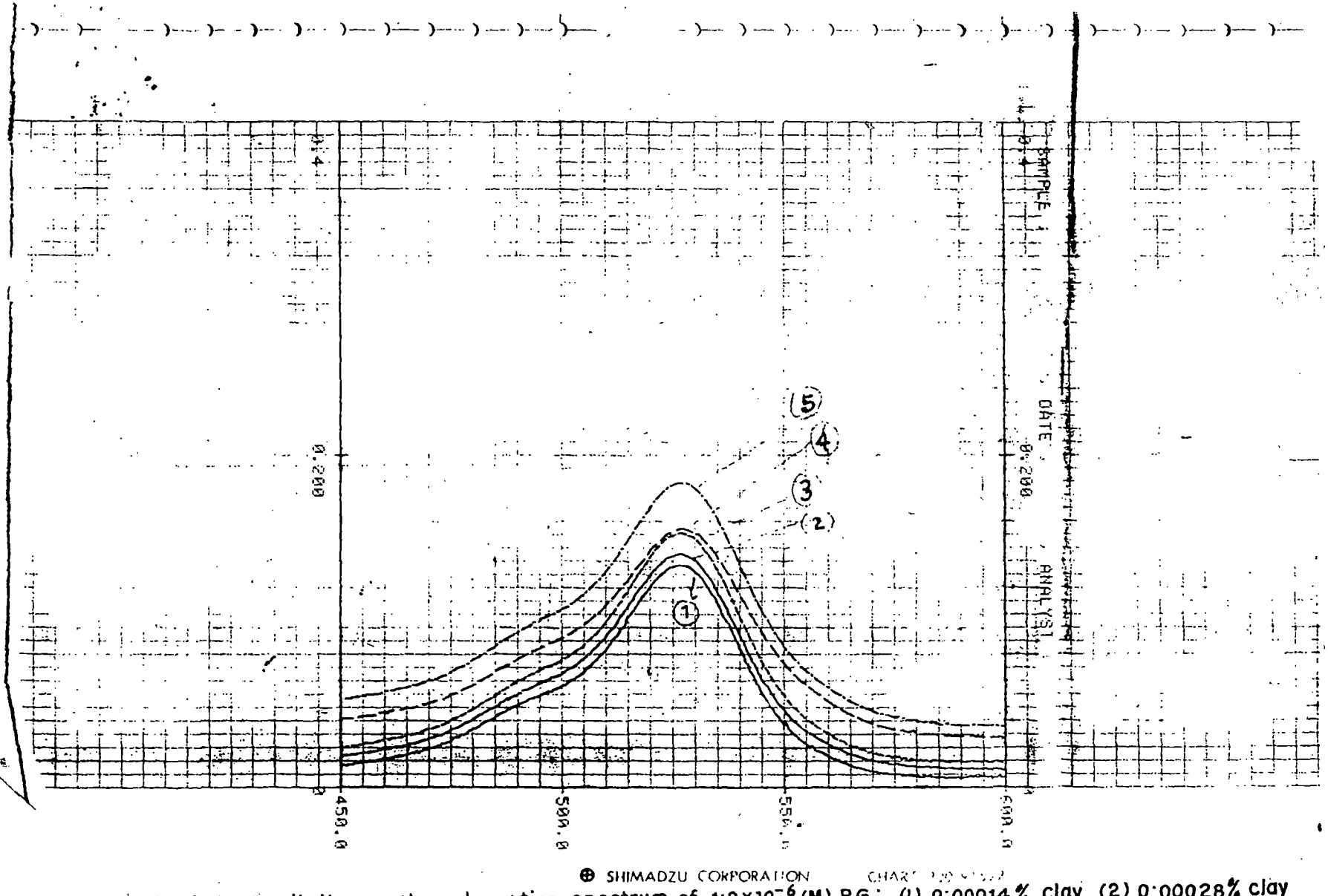

Fig. 73. Effect of Na-Kaolinite on the absorption spectrum of $1{\cdot}8\times10^{-6}$ (M) RG: (1) 0·00014% clay (2) 0·00028% clay (3) 0·00056% clay (4) 0·00070% clay (5) 0·00098 % clay.

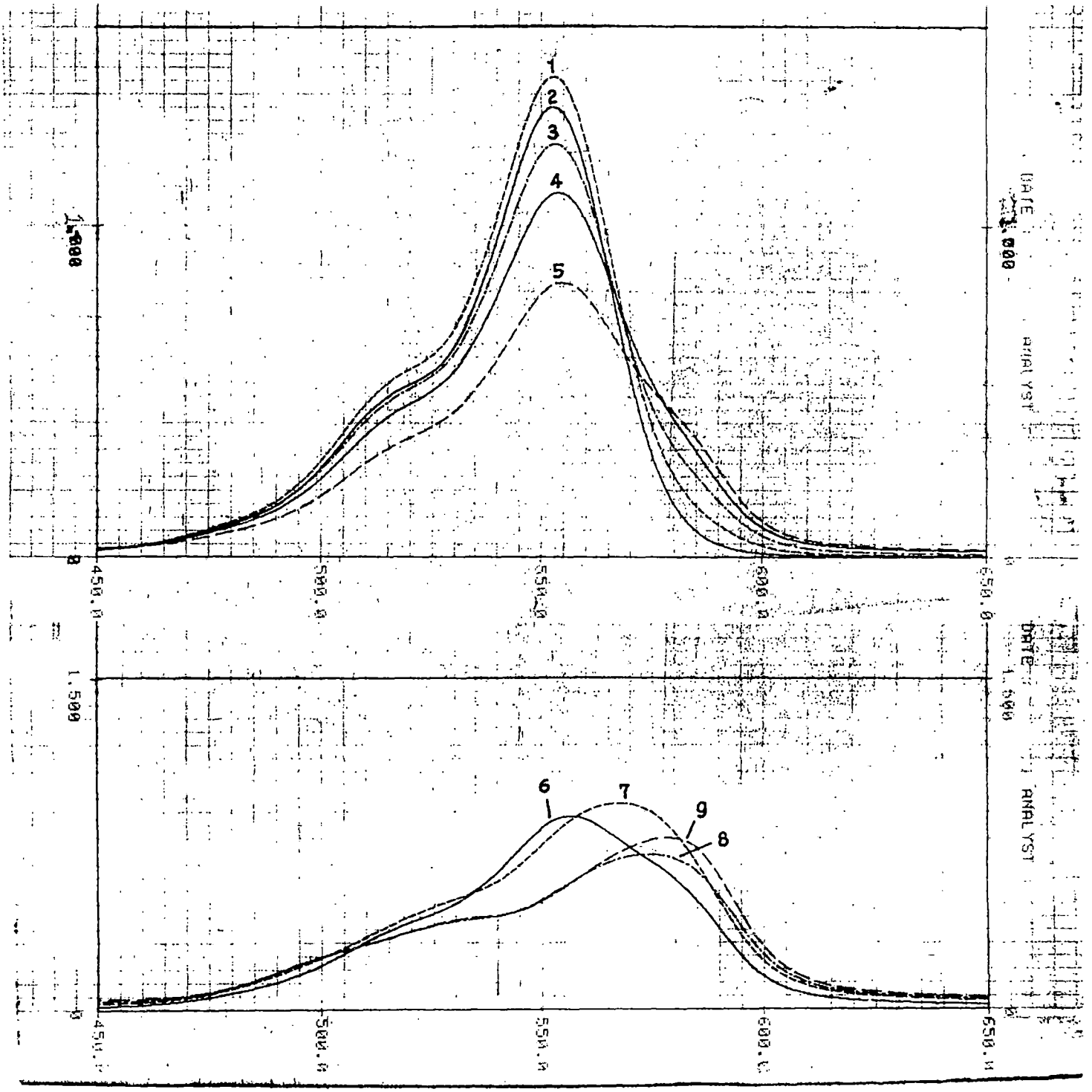

Fig. 74. Effect of Na-Montmorillonite on the absorption spectrum of 1×10^{-5}(M) RB: (1) 0·00024% clay (2) 0·00026% clay (3) 0·0003% clay (4) 0·0005% clay (5) 0·0008% clay (6) 0·001% clay (7) 0·002% clay (8) 0·003% clay (9) 0·005% clay.

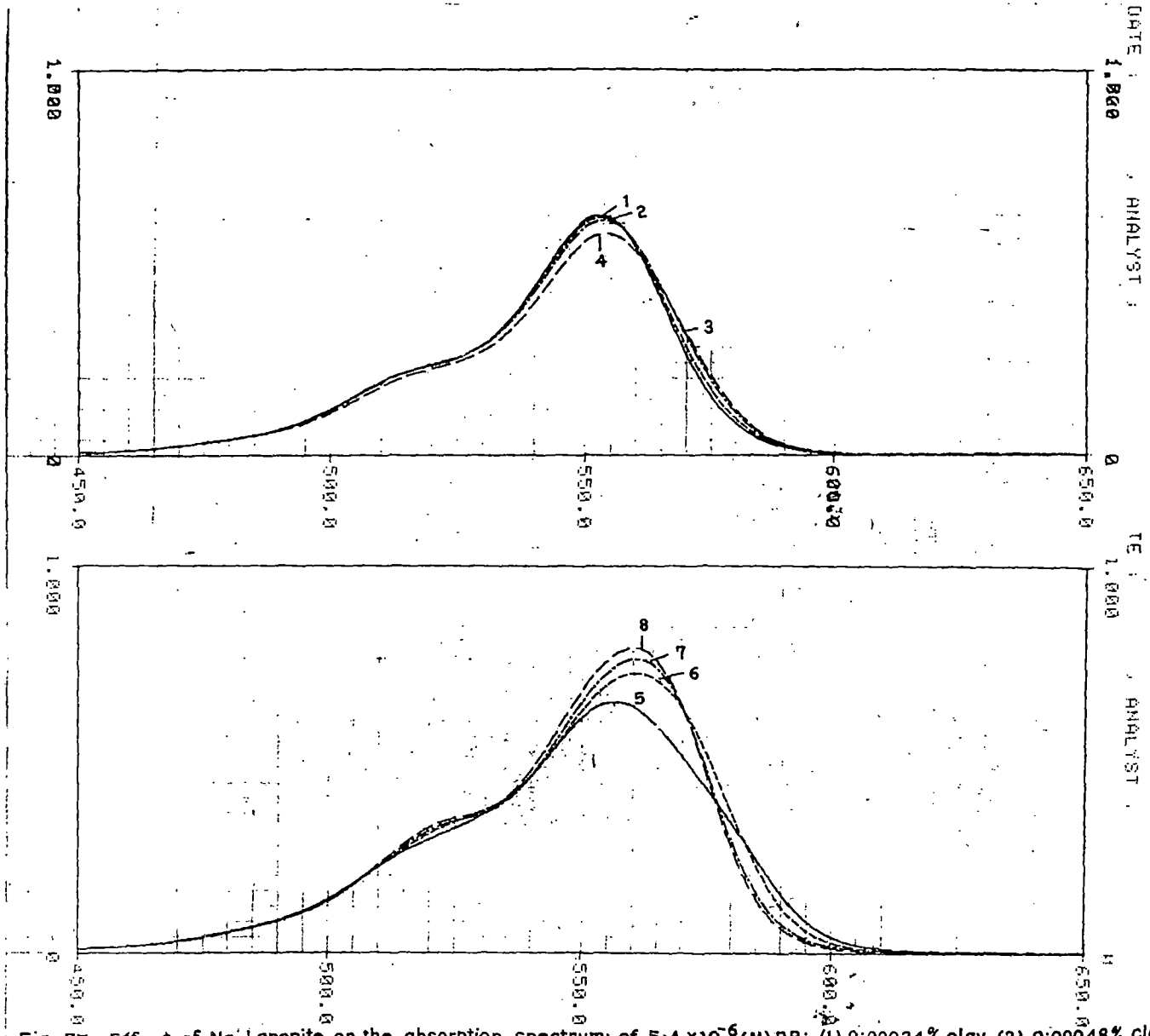

Fig. 75. Effect of Na-Laponite on the absorption spectrum of $5{\cdot}4 \times 10^{-6}$ (M) RB: (1) 0·00024% clay (2) 0·00048% clay (3) 0·001% clay (4) 0·0015% clay (5) 0·0018% clay (6) 0·002% clay (7) 0·004% clay (8) 0·006% clay.

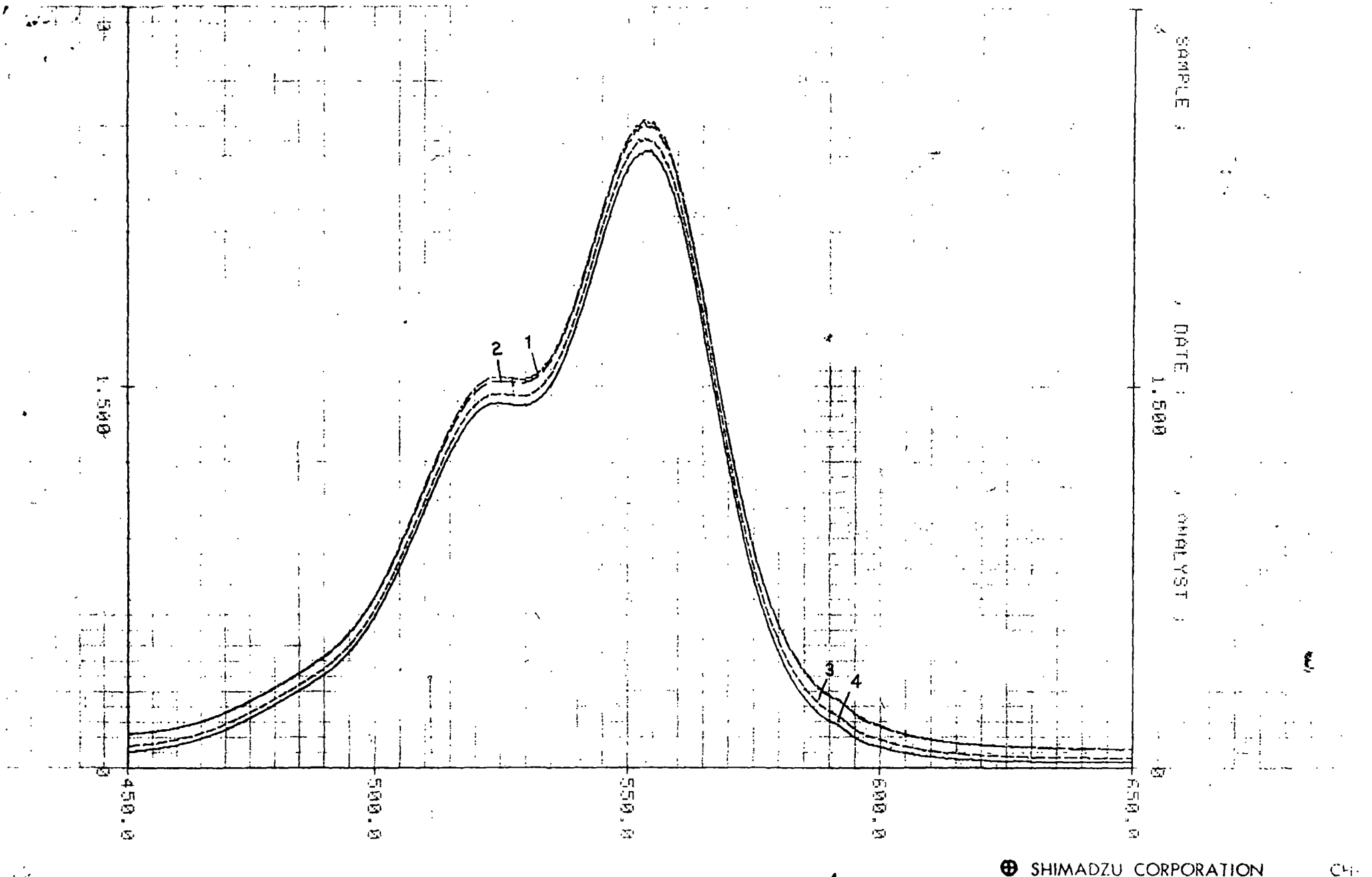

Fig. 76. Effect of Na-Kaolinite on the absorption spectrum of 2×10^{-4}(M) RB: (1) 0·01% clay (2) 0·02% clay (3) 0·03% clay (4) 0·05% clay

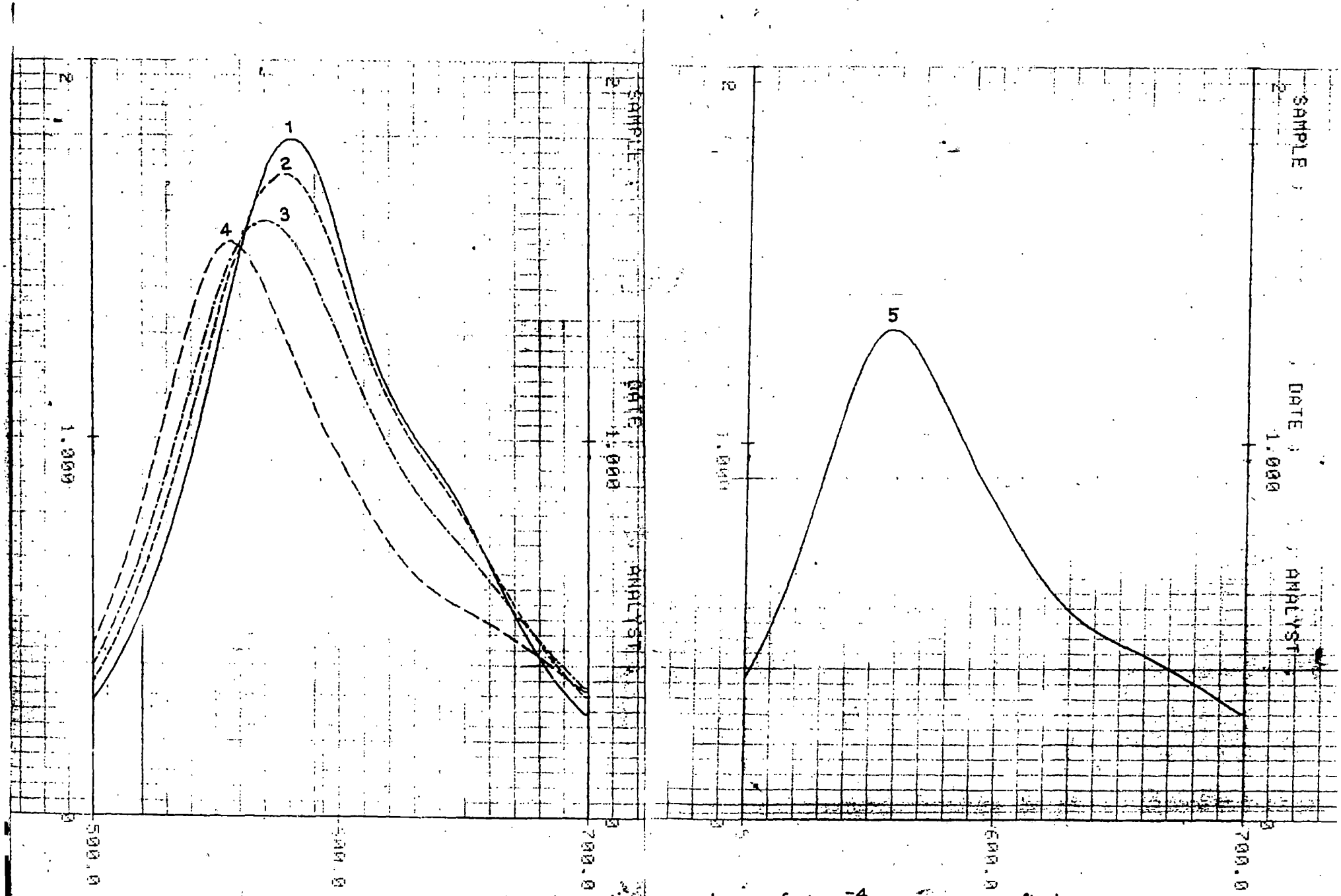

Fig.77. Effect of Na-Montmorillonite on the absorption spectrum of 4×10^{-4}(M) BB: (1) 0·01% clay (2) 0·03% clay (3) 0·05% clay (4) 0·07% clay (5) 0·09% clay.

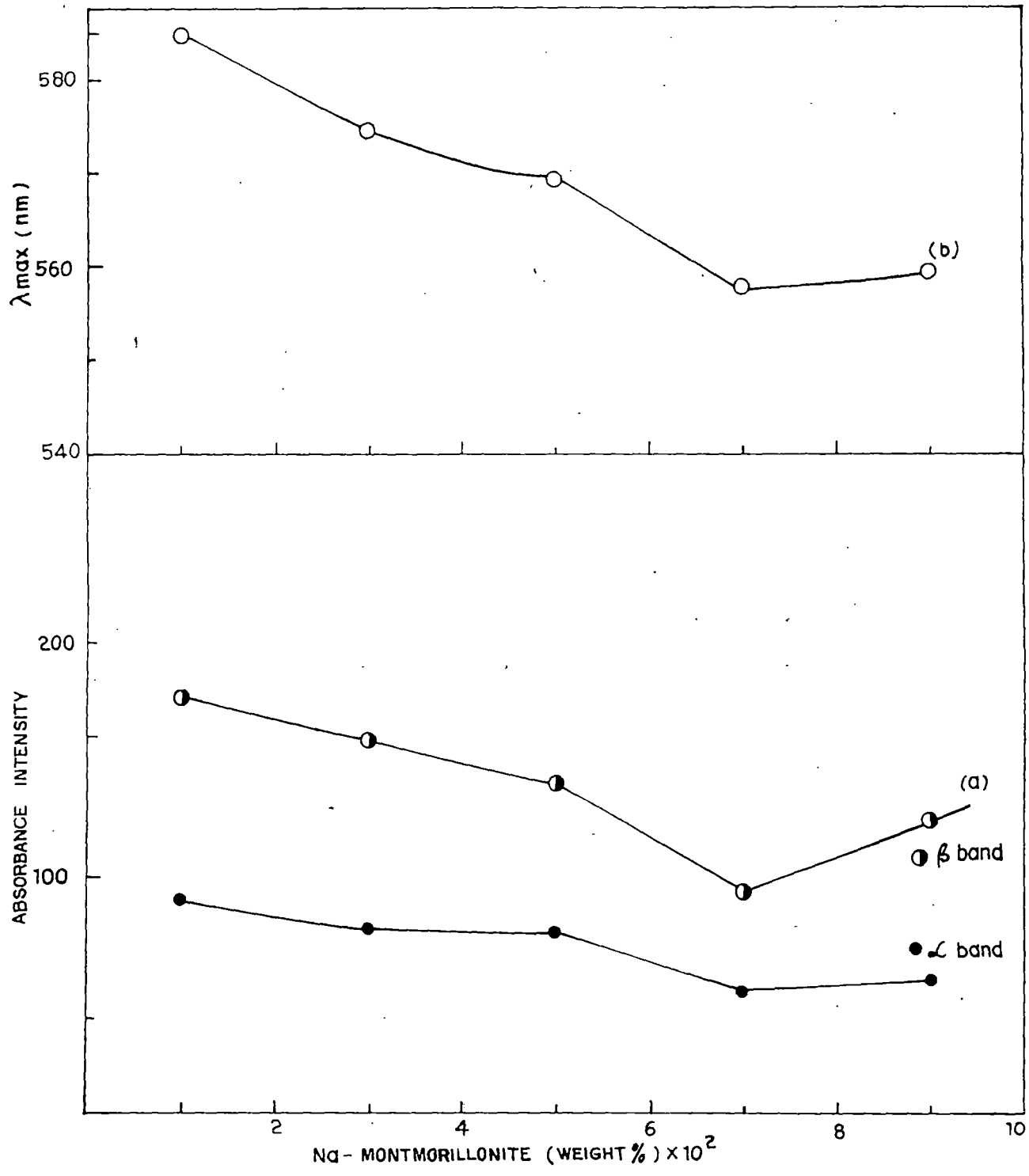

FIG. 78. THE EFFECT OF ADDED Na-MONTMORILLONITE ON (a) THE ABSORPTION INTENSITY OF BAND α AND β AT A FIXED CONCENTRATION OF 4×10^{-4}(M) BB (b) IN LOCATION OF BAND β AT A FIXED CONCENTRATION OF 4×10^{4}(M).

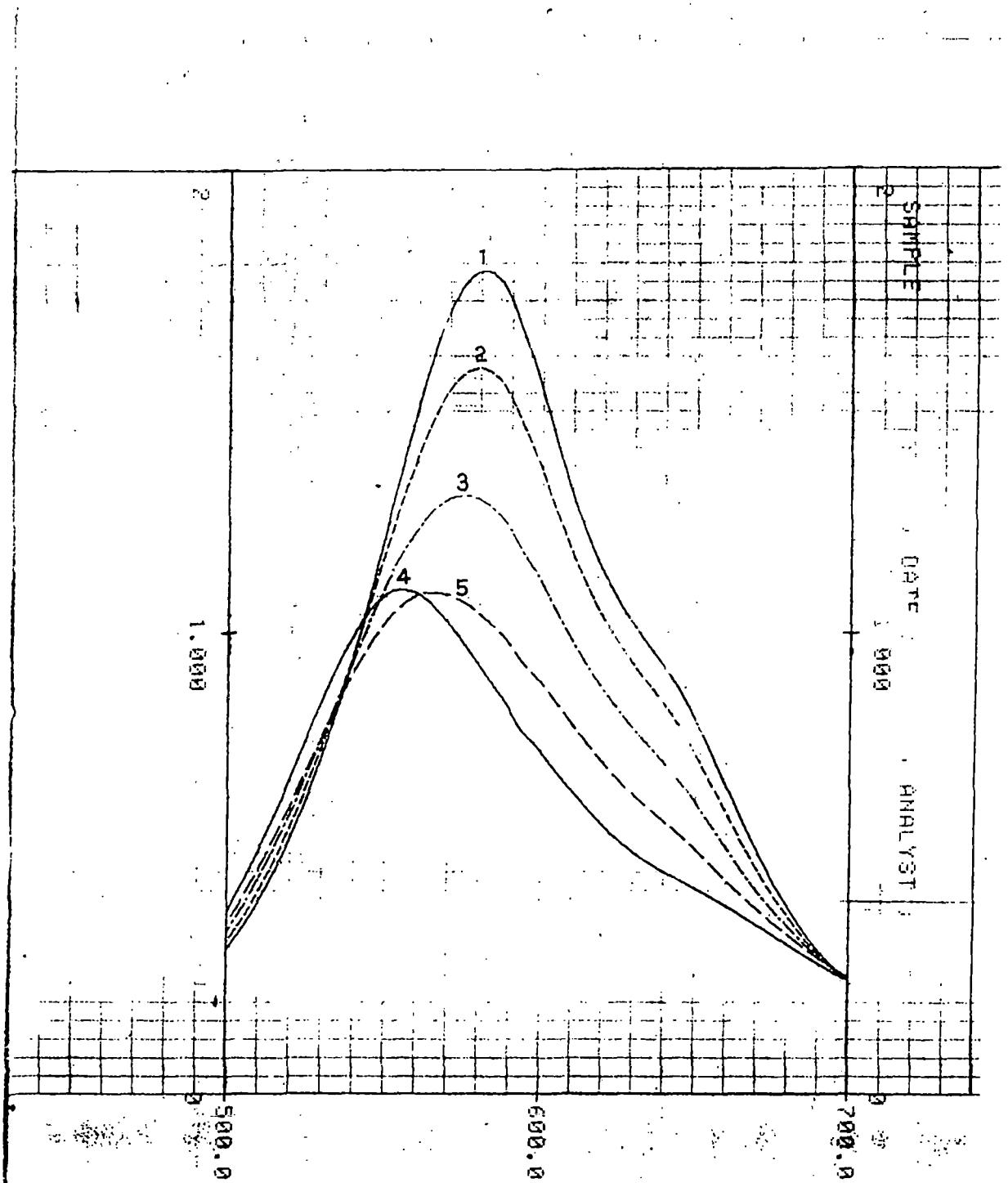

Fig. 79. Effect of Na-Laponite on the absorption spectrum of 4×10^{-4}(M) BB: (1) 0·02% clay (2) 0·04% clay (3) 0·06% clay (4) 0·08% clay (5) 0·09% clay.

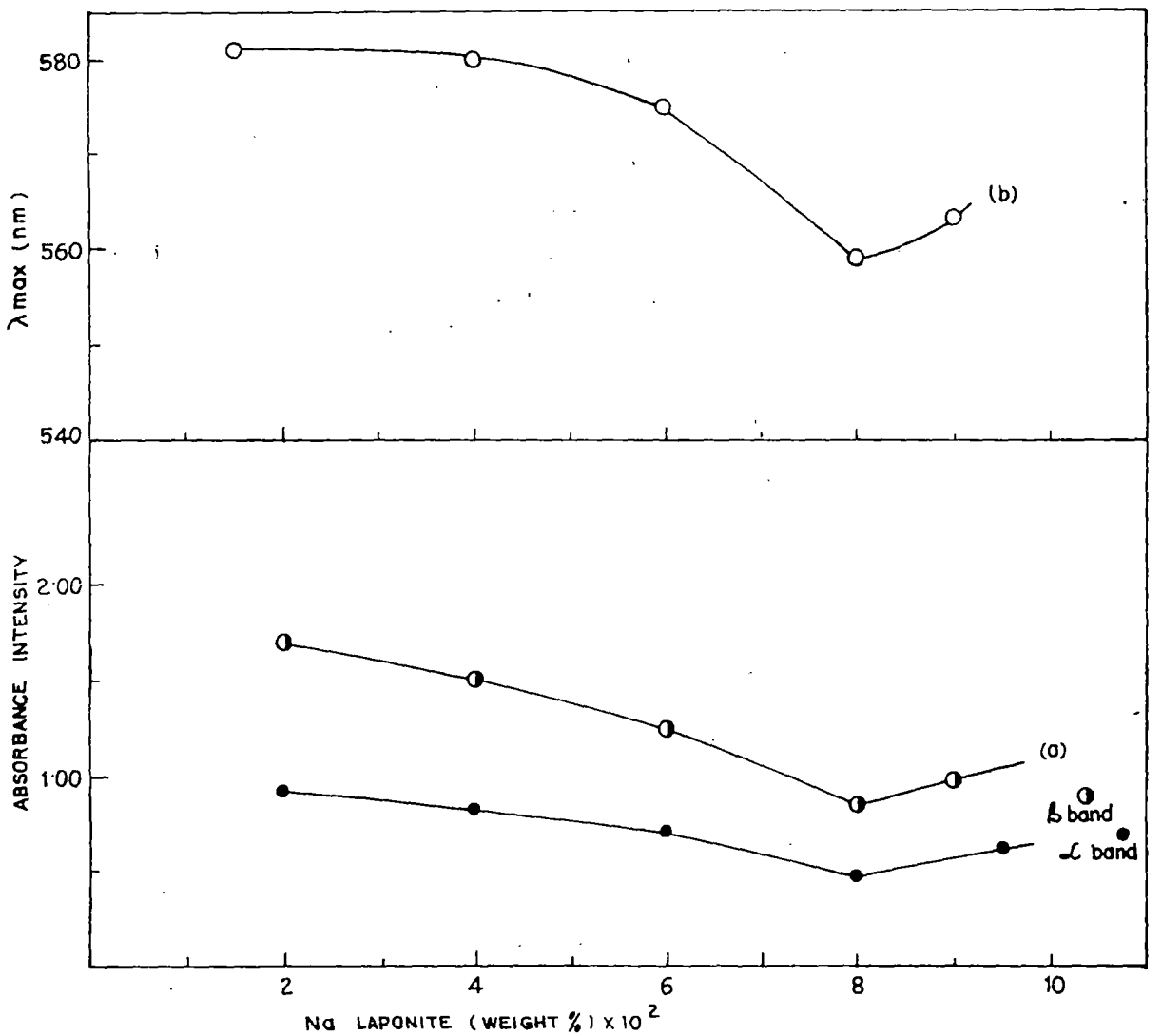

FIG. 80. THE EFFECT OF ADDED Na-LAPONITE ON (a) THE ABSORPTION INTENSITY OF BAND α AND β. (b) THE LOCATION OF BAND β AT A FIXED CONCENTRATION OF 4×10^{-4} (M) BB.

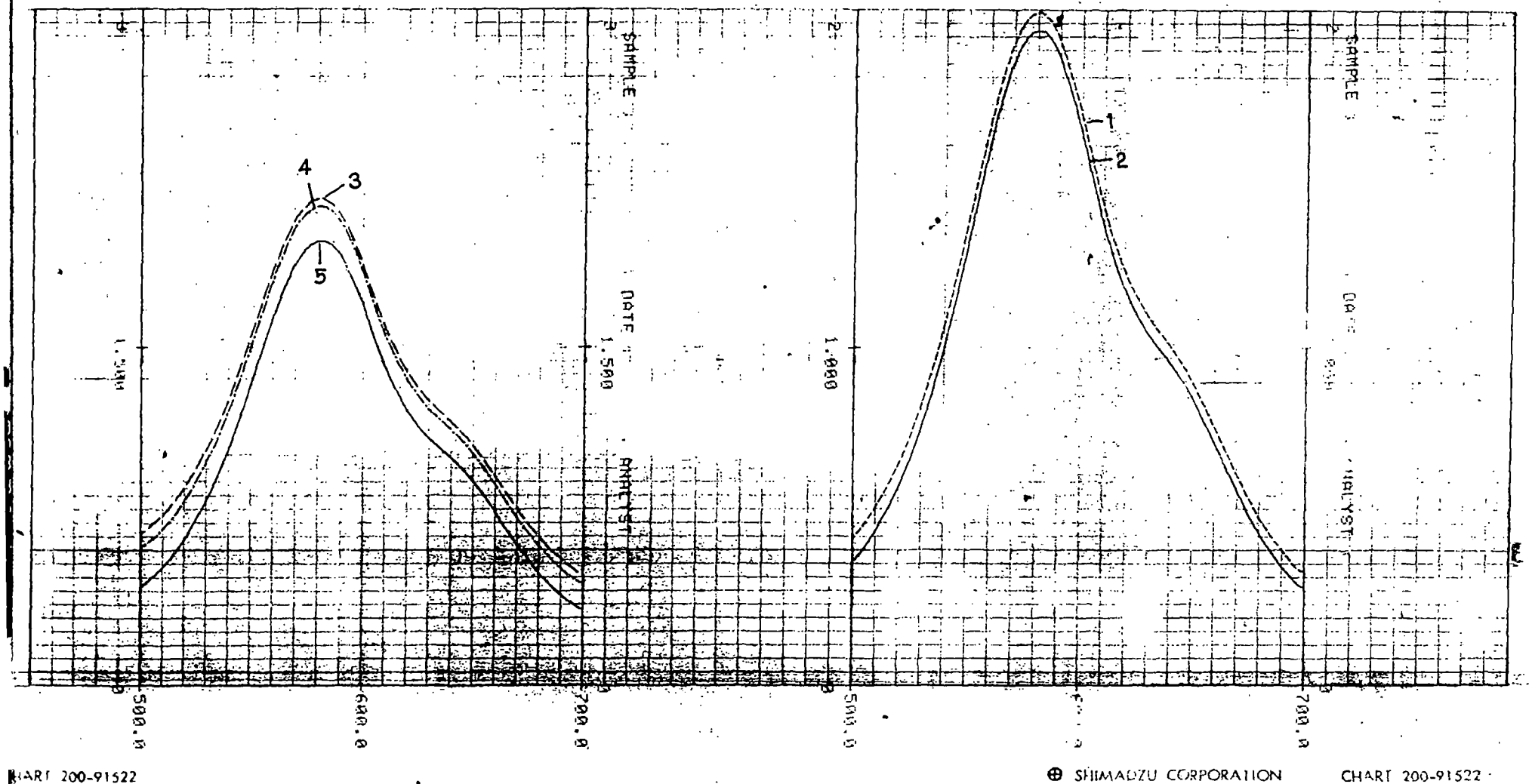

Fig. 81. Effect of Na- Kaolinite on the absorption spectrum of 4.5×10^{-4} (M) BB: (1) 0·01% clay (2) 0·02% clay (3) 0·03% clay (4) 0·05% clay (5) 0·06% clay.

CHAPTER X

SUMMARY AND CONCLUSION

The structures of the clay minerals namely kaolinite, montmorillonite and laponite are briefly discussed. A short review of the earlier studies on the adsorption and desorption of inorganic and organic ions on clay minerals and also other substrates is presented in the introductory Chapter I.

(Pages 1-39)

Chapter II includes the scope and object of the present investigation.

(Pages 40-44)

The methods of analysis and the preparation of materials, experimental details and the preparation of the samples for I.R. spectra, X-ray diffraction analysis are described in Chapter III. Three selected dyes viz. RB, RG, BB belonging in two different categories have been used. All are well established structure recrystallised by usual methods. Their interactions with the above mentioned silicate minerals have been described in order to find out their adsorption and desorption behaviour vis-a-vis the structural characteristics of both the adsorbent and the adsorbate.

(Pages 45-56)

The adsorption isotherms of Rhodamine 6G and Rhodamine B on Na-montmorillonite are of the H-type, indicative of strong sorbate-sorbent interactions, with the species being adsorbed flat on the surface. The adsorption data of both the dyes on Na-montmorillonite are found to fit in well with the Langmuir equation. The Langmuir bonding constant of RB^+ is higher than RG^+ suggesting a stronger binding of the former dye with the Na-montmorillonite. The maximum sorption of both the dyes exceeds the C.E.C. of the clay, RG^+ being adsorbed more than RB^+. The higher uptake of RG^+ by Na-montmorillonite is due to its greater dimerisation or aggregation tendency than RB^+ in aqueous solution. When adsorption takes place from solutions the former is sorbed with a larger fraction of the aggregates than that of the latter at any particular concentration. Ionic and van der Waals forces are most likely operated during adsorption upto cation exchange capacity and beyond it only van der Waals forces predominates.

The efficiency of the inorganic ions in desorbing the dye molecules from the Na-montmorillonite matrix generally increases with the crystallographic radius of the ions and follows the lyotropic series with few exceptions. The orders of selectivity for the monovalent and bivalent inorganic ions are :

$Cs > Rb > NH_4 \geq K > Li > Na$ and $Ba > Sr > Ca > Mg$

The plots of log (selectivity coefficient) against hydrated ionic radius and the reciprocal of the Debye Huckel parameter, a^o yield straight lines in the case of alkaline earth metal cations while for the alkali metal ions the latter plot is only linear. The cause of non linearity in case of alkali metal ions has been attributed to the unequal fixation tendencies of the ions vis-a-vis interlayer collapse of the clay structure. However, the plot of log (selectivity coefficient) vs $\frac{1}{a^o}$ is based on the simple ion-exchange model of Pauley, and the above observations suggest that electrostatic attraction between the counterions and the fixed ionic groups is the significant factor in the process of displacement of the dye ions from the clay matrix by the inorganic ions. These plots may be used to correlate and predict the relative affinities of the ions for the mineral in terms of their a^o values and hydrated ionic radii.

The exchangeability of organic ions from the respective Na-montmorillonite dye complexes is much higher than that by the inorganic ions and also increases with increasing size of the ions. This is due to increased contribution of the van der Waals forces to the adsorption energy and to changes in the hydration status of the ions in the clay interlayer. The desorption curves of both the dyes with quaternary ammonium

ions on Na-montmorillonite complexes are almost S-shaped which indicates co-operative sorption with solute molecules tending to be adsorbed or packed in rows or clusters. Giles et al, through theoretical treatment have shown recently that S-curve occurs when the activation energy for the desorption of the solute is concentration dependent, and/or is markedly reduced by large negative contributions of the solvent or a second solute. It is apparent from the selectivity data that monovalent long-chain surfactant ions like CP^+ or $CTMA^+$ are more preferred by clay matrix than those of other organic ions studied. Again CP^+ desorbs a large amount of dye than $CTMA^+$ owing to the lower cmc (critical micelle concentration) of the former. From higher values of selectivity coefficients of the monovalent long chain surface active ions it may therefore be concluded that shape and size of these ions and the degree of van der Waals contact between the organic ions and the clay surface are significant factors to be considered during desorption process. Besides, the solubility of the organic cations decreases as the size increases and there is obviously less tendency of the larger ions, once adsorbed, to get desorbed back into the solution. The percentage of desorption of RG^+ from this clay by various electrolytes and their respective distribution and selectivity coefficients are higher than those of RB^+. So the order of the affinity of the dyes for the mineral surface which is in the reverse order of their desorption is $RB^+ > RG^+$, which

is also reflected in the Langmuir constant value.

(Pages 57-88)

The adsorption isotherms of RG^+ and RB^+ onto Na-kaolinite are of the high affinity class. Both RG^+ and RB^+ are adsorbed upto a maximum, well in excess of the c.e.c. of the clay mineral. This is due to the sorption of aggregated dye-ions and/or the unionised dye molecules by the mineral. The desorption isotherms of the two dyes for Na-kaolinite complexes differ in two aspects for those two other complexes of the clays studied here viz. the percentage of desorption of the dyes from their Na-kaolinite complexes by monovalent and bivalent inorganic ions is the highest while it is the lowest for the larger organic ions. The extent of desorption however, increases with the size of the ions in both the cases. This behaviour towards inorganic ions is due to the fact that the binding strength to this clay mineral is weak as compared to the other minerals, since the exchange sites in Na-kaolinite are located only on the external surface of the crystal.

The desorption isotherm of both the dyes from their aqueous Na-kaolinite complexes are S-shaped for some of the surfactant ions like CP^+, $CTMA^+$, DDP^+. Similar explanation can be given as in case montmorillonite system. Plot of log (selectivity coefficient) vs hydrated ionic radius and $1/a^o$ for monovalent and bivalent inorganic ions are similar to

systems already studied. As in other adsorbent systems used in earlier studies, the affinity of the dye ionsfor Na-kaolinite surface have the order $RB^+ > RG^+$.

(Pages 89-109)

The adsorption isotherms of RG^+ and RB^+ on Na-laponite, a synthetic hectorite also belongs to the H-class of isotherm and the exchange data obey Langmuir equation. The amount of exchange here for RG^+ are in excess of c.e.c. of the mineral RG^+ being adsorbed more than RB^+. Sorption of dyes in aggregates as well as bilayer formation tendency of the dye ions in the interlamellar space, due to unlimited swelling of Laponite having lower charge density may account for this observation. A higher fraction of aggregated RG ions is sorbed onto the mineral surface due to higher dimerisation tendency of this dye. As a result of which, the extent of adsorption of RG^+ is greater than RB^+. Like the other two minerals the desorption isotherm in Na-laponite system is similar in nature. The extent of desorption here by inorganic ions is much lower than that observed in montmorillonite system. This can be explained in the light of wider spacing between the exchange spots in the Laponite minerals, as a result of which small sized inorganic desorbing ions are unable to approach these sites as effectively as in montmorillonite to displace the adsorbed dye ions.

The relationship of hydrated ionic radii and $1/a^{o}$ with log (selectivity coefficient) is the same as that in montmorillonite and kaolinite. The obedience of the exchange data to Pauley's model demonstrates that coulombic interaction between the counter ions and the fixed ionic groups is the important factor in this type of exchange reactions.

The desorption of both the dyes by various organic ions increases with size of the ions which is usually found in expanding type of clay mineral and is ascribed to the increased contribution of van der Waals forces to the adsorption energy and also to the changes in the hydration status of the ions in the clay interlayer. Here also the affinity of these dyes to laponite surface is $RB^{+} > RG^{+}$. This is also reflected in the higher Langmuir bonding constant of RB.

(Pages 110-132)

On varying at three different temperatures it may be concluded from the respective adsorption isotherm that the adsorption process of both the selected xanthene dyes on to Na-montmorillonite and Na-kaolinite is exothermic with heats of adsorption lying between 1 and 5 Kcal/mole and that the nature of the isotherm is unaffected by temperature variations. The experimental heat of adsorption may be regarded due to the net result of several processes such as solubility of the dyes, association of the dye molecules etc. where heat may be evolved or adsorbed.

It has been found that the heat of adsorption is not a constant quantity but changes with the amount of dye adsorbed, showing a minimum at a certain value of the dye adsorbed. The minimum point probably may occur to a situation when the monolayer is just complete or when the adsorption value approaches the c.e.c. of the mineral. In case of kaolinite the plot of heat of adsorption does not show a distinct minimum, but tends to increase regularly with adsorption. The result may be explained on the basis of adsorption of aggregated species by the clay minerals.

The heats of adsorption of RB > RG in the two minerals studied suggesting a stronger binding of the former dye to the mineral surfaces.

(Pages 133-143)

From the structure of the dye molecules it is clear that BB molecule can enter into an exchange type of sorption through $-\overset{+}{O}-$ group or through $\rightarrow\overset{+}{N}$ - group and RB, RG through $\rightarrow\overset{+}{N}$ - group, which become positive charge centres by resonance and can arrange themselves flat or in end-on or dye-on position. The resonance structure of the dye ion indicate three positive charge centers on BB and three on RB and RG. The structural consideration assigns to the dyes predominantly flat orientation on to clay surface. However other possibilities are not entirely excluded.

The probability of distribution among the different orientations is conditioned by various factors such as the basicity of Nitrogen group, the number of resonating structures, the molecular geometry of the dye cation, the nature of exchange sites etc. It is however to be noted that the flat position is possibly attended with minimum potential energy. The excess uptake of the dyes may be explained largely by assuming the sorption of aggregated dye cations onto montmorillonite surface and partially by the intercalation of the unionized dye molecules by the interlamellar space. Since the dye molecules are not staggered and can approach each other close enough, the adsorption of the dyes on montmorillonite probably imparts greater mobility to bring them in optimum proximity and proper orientation for micellation.

In the case of kaolinite BB^+ is adsorbed well in excess of c.e.c. as compared to RB and RG. The adsorption isotherm of BB^+ onto Na-kaolinite as onto other minerals studied are of high affinity class. The excess uptake may be due to sorption of aggregated dye ions and/or the unionised dye molecule by the mineral.

The adsorption isotherm of BB^+ on Na-laponite are of Langmuir type and the amount of the dye exchange are far in excess of the c.e.c. of the mineral compared to that of RB and RG. This higher adsorption of BB^+ is possibly due to its lesser size compared to RB^+ or RG^+ and stronger tendency of BB

molecules to form aggregates in solution as well as in the adsorbed state. The influence of the size of the dye is also significant during adsorption to the mineral.

From the values of the bonding constants obtained from intercepts of the Langmuir plots, it is noticed that the values of the constants for each mineral increase in the order RB> RG> BB.

Since Langmuir constants increased proportionately to the heat of adsorption, the higher value of the constant indicates greater heat of adsorption and also binding of the dyes to the higher energy sites of the adsorbent in the above order of the dyes.

Desorption studies on the sorbed xanthene dyes with various inorganic and organic cations also supports the view that dyes are attached to the minerals with increasing bond strength in the order RB > RG.

(Pages 144-147)

The adsorption spectra of the selected cationic dye by different aluminosilicates have been studied by visible spectroscopy. Adsorption of dyes takes place by the mechanism of cation exchange. The adsorbed cationic dye is located in the interlayer space. A study of the effect of varying concentration of different clay in a constant volume of specific dye on the location and intensity of bands proved to be useful in determining the adsorption capacity of the clay. Adsorbent

survaces imparts mobility to the sorbed dye molecules and hence bring them in optimum proximity and proper orientation for dimerization or a higher degree of aggregation. Steric hindrance is assumed to be responsible for the lesser tendency towards aggregation. However, adsorption on clay surface can modify this effect. The change in spectral shift in RG, RB and BB in all systems studied here indicates their respective behaviour towards aggregation.

(Pages 148-173)

From the above summary discussion it may be concluded that various attempts has been made to present a comprehensive picture on different aspects of exchange equilibrium and the interaction of the selected dyes with clay minerals. It is observed that the adsorption of dye ions, although taking place through ion exchange, is associated with a number of factors such as molecular sizes, molecular geometry, dye-dye interaction and the surface characteristic of sorbents.

Abilities for desorption by various inorganic and organic ions from clay-dye complexes according to the order of preference are being summarised in table 21 (page 186). The sequences of desorbing ions have been justified in terms of size, shape, charge and steric hindrance of the adsorbates and the desorbing ions as well as the charge density and swelling properties of the aluminosilicates. The architectural dissimilarities of the aluminosilicates, specificities of certain

ions, hydrophobicity, hydration energy of the ions, give rise to occasional differences in the exchange behaviour of the clay minerals as discussed earlier.

Attempts have been made throughout the present investigation to explain the data in the light of various theories and models.

Table 23

The order of preference of the various ions for the aluminosilicate surface against RG and RB ions.

Na-montmorillonite-RG complex	Na-montmorillonite-RB complex
a) $Na^+ \angle Li^+ \geqslant K^+ \angle NH_4^+ \angle Rb^+ \angle Cs^+$	a) $Li^+ \leqslant Na^+ \angle K^+ \angle NH_4^+ \angle Rb^+ \angle Cs^+$
b) $Mg^{2+} \angle Ca^{2+} \angle Sr^{2+} \angle Ba^{2+}$	b) $Mg^{2+} \angle Ca^{2+} \angle Sr^{2+} \angle Ba^{2+}$
c) $TMA^+ \angle TEA^+ \angle TPA^+ \angle TBA^+$	c) $TMA^+ \angle TEA^+ \angle TPA^+ \angle TBA^+$
d) $DDTMA^+ \angle DDP^+ \angle CTMA^+ \angle CP^+$	d) $DDTMA^+ \angle DDP^+ \angle CTMA^+ \angle CP^+$
Na-kaolinite-RG complex	**Na-kaolinite-RB complex**
a) $Li^+ \angle Na^+ \angle K^+ \leqslant NH_4^+ \angle Rb^+ \angle Cs^+$	a) $Li^+ \angle Na^+ \angle K^+ \angle NH_4^+ \angle Rb^+ \angle Cs^+$
b) $Mg^{2+} \angle Ca^{2+} \angle Sr^{2+} \angle Ba^{2+}$	b) $Mg^{2+} \angle Ca^{2+} \angle Sr^{2+} \angle Ba^{2+}$
c) $TMA^+ \angle TPA^+ \angle TEA^+ \angle TBA^+$	c) $TMA^+ \angle TPA^+ \angle TEA^+ \angle TBA^+$
d) $DTMA^+ \angle DDTMA^+ \angle CTMA^+ \angle CP^+$	d) $DTMA^+ \angle DDTMA^+ \angle CTMA^+ \angle CP^+$
Na-Laponite-RG complex	**Na-Laponite-RB complex**
a) $Li^+ \angle Na^+ \angle K^+ \leqslant NH_4^+ \angle Rb^+ \angle Cs^+$	a) $Li^+ \angle Na^+ \angle K^+ \angle NH_4^+ \angle Rb^+ \angle Cs^+$
b) $Mg^{2+} \angle Ca^{2+} \angle Sr^{2+} \angle Ba^{2+}$	b) $Mg^{2+} \angle Ca^{2+} \angle Sr^{2+} \angle Ba^{2+}$
c) $TMA^+ \angle TEA^+ \angle TPA^+ \angle TBA^+$	c) $TMA^+ \angle TEA^+ \angle TPA^+ \angle TBA^+$
d) $DDTMA^+ \angle DDP^+ \angle CTMA^+ \angle CP^+$	d) $DDTMA^+ \angle DDP^+ \angle CTMA^+ \angle CP^+$

R E F E R E N C E S

CHAPTER -I (Section 'A')

1. Grim, R.E. : 'Clay Mineralogy' Mc Graw Hill Book Co. Inc., 1953

2. Robinson, G.W. : 'Soils, their drigin, constitution and classification, 2nd edition, p. 16', Thomabs Murby and Co. London, 1936

3. Marshal, C.E. : Zeit fur krist (A) 90, 8, 1935

4. Troug, E, Taylor, J.R., Pearssour, R.W., Weeks, M.E. and Simphson, R.W. : 'Soil Sci. Soc.' Amer. Proc. I, 101, 1936

5. Pauling, L. : Proc. Natl. Acad. Sci. U.S., 16, 578-584, 1930

6. Bragg, W.L. : Atomic Structure of Minerals, Cornell Univ. Press, Ithaca, 1937

7. Gruner, J.W. : Z. Krist., 83, 75-88, 1932

8. Brindley, G.W. and Robinson, K. : Mineralogy Mag., 27, 242, 1946

9. Hofmann, U., Endoll, K. and Wilm, D. : Z. Krist., 86, 340, 1933

10. Marshall, C.E. : Ibid, 91, 433, 1935

11. Hendricks, S.B. and Jefferson, M. : Am. Miner., 24, 729, 1939

12. Mauguin, C.H. : Bull. Soc. Franc. Min., 51, 285, 1928

13. Jackson, W.W. and West, J. : Z. Krist., 85, 160, 1933

14. Mc Murchy, R.C. : Ibid, 88, 420, 1934

15. Barshad, I. : Am. Miner., 34, 675, 1949

16. Walker, G.F. : Nature, 163, 726, 1949

17. Grim, R.E., Bradley, W.F. and Brown, G. : The Mica Clay Minerals, Chap. V. pp. 138-172, Mineralogical Society of Great Britain Monograph, 1951

18. Mac Ewan, D.M.C. : J. Soil Sci., 1, 90, 1949

19. Kelley, W.P. : Cation Exchange in Soils, Reinhold, New York, 1948

20. Marshall, C.E. and Krinbill, C.A. : J. Phys. Chem., 46, 1077, 1942

21. Page, J.B. and Baver, L.D. : Proc. Soil Sci. Soc. Am., 4, 150, 1939

22. Bar, A.L.S. and Tenderloo, H.J.E. : Koll. Beih., 14, 97, 1936

23. Hendricks, H.B. and Alexander, L.T. : Proc. Soil Sci. Soc. Am., 5, 95, 1940

24. Schachtschabel, P. : Koll. Beih., 51, 199, 1940

25. Mukherjee, S.K. : Indian Soc. Soil Sci. Bull., 6, 67, 1951

26. Marshall, C.E. : 'The Colloid Chemistry of Silicate Minerals', Academic Press, Inc., N.Y., 1949

27. Grim, R.E. : 'Clay Mineralogy', McGraw-Hill Book Co., Inc., N.Y., 1953

28. Smith, C.R. : J. Am. Chem. Soc., 56, 1561, 1934

29. Gieseking, J.E. : Advances in Agron., 1, 598, 1949

30. Gieseking, J.E. and Ensminger, L.E. : Soil Sci., 51, 125, 1941

31. Chakravarti, S.K. : J. Indian Soc. Soil Sci., 5, 90, 1957

32. Renold, A. : Kolloid Beih., 43, 1, 1936

33. Jenny, H. and Elgabaly, M.M. : J. Phys. Chem., 47, 399, 1943

34. Basu, A.N. and Mukherjee, S.K. : J. Indian Soc. Soil Sci., 14, 95, 1966

35. Idem : Ibid, 13, 251, 1965

36. Martin, I and Glaeser, R. : Bull. Groupe Franc. Aygiles, 12, 88, 160

37. Chakravarti, S.K. and Laitinen, H.A. : N.S.F. Report (U.S.A.), 1962

38. Das Kanungo, J.L., Chakravarti, S.K. and Mukherjee, S.K. : J. Indian Chem. Soc., 44, 339, 1967

39. Idem : Ibid, 45, 685, 1968

40. Das Kanungo, J.L. and Chakravarti, S.K. : Kolloid Z. U.Z. Polymere, 251, 154, 1973

41. Sarkar, G.N. and Das Kanungo, J.L. : J. Indian Soc. Soil Sci., 31, 118, 1983

42. Thielman V.J. and MacAtee, J.L. Jr. : J. Chromatography, 105, 115, 1975

43. Knudson, M.L. Jr. and McAtee, J.L. Jr. : Clays and Clay Miner., 21, 19, 1973

44. Barrer, R.M. and Townsend, R.P. : J. Chem. Soc., Faraday Trans., 1, 72, 2650, 1976

45. Hendricks, S.B. : J. Phys. Chem., 45, 65, 1941

46. Gieseking, J.E. : Soil Sci., 47, 1, 1939

47. Greenland, D.J. : Soils and Fertilizers, 28, 415, 1965

48. Mortland, M.M. : Advan. Agron., 22, 75, 1970

49. Theng, B.K.G. : 'The Chemistry of Clay-Organic Reactions', Adam Hilger Ltd., 1974

50. Jordan, J.W. : J. Phys. and Colloid Chem., 53, 294, 1949

51. Cowan, C.T. and White, D. : Trans. Farad. Soc., 54, 691, 1958

52. Diamond, S. and Kinter, E.B. : Clays and Clay Miner., 10, 163, 1963

53. Weiss, A. : Ibid, 10, 191, 1963

54. Theng, B.K.G., Greenland, D.J. and Quirk, J.P. : Clay Miner., 7, 1, 1967

55. Walker, F.F. : Ibid, 7, 129, 1967

56. Vansant, E.F. and Uytterheoven, J.B. : Clays and Clay Miner., 20, 47, 1972

57. Maes, A., Marynen, P. and Gcremers, A. : Ibid, 25, 309, 1977

58. Barrer, R.M. and Brummer, K. : Trans. Faraday Soc., 59, 959, 1963

59. Mare, R. : Z. Physik, Chem., 73, 685, 1910

60. Ramchandran, W.B., Kacker, K.P. and Patwardhan, N.P. : The American Mineralogists, 47, 165, 1962

61. Brooks, C.S. : Kolloid Zeitschrift Fur Polymere Band 199, Heft I Seite 31, 1964

62. Plesch, P.H. and Robertson, R.H.S. : Nature, 161, 1020, 1948

63. Bergman, K. and O'Konski, C.T. : J. Phys. Chem., 67, 2169, 1963

64. Ewing, W.W. and Liu, F.W.J. : J. Colloid Sci., 8, 204, 1953

65. Clauss, A., Rohem, H.P. and Hofmann, U. : Z. Anorg. Chem., 290, 35, 1957

66. Loss, L.M. and Tompkins, C.K. : Canad. J. Chem., 37, 315, 1959

67. Langville, R.C., Braid, P.E. and Kenrick, F.B. : Can. J. Research, 23B, 31, 1945

68. Hans A. Bensi : Anal. Chem., 32, 11, 1960

69. Giles, C.H. and Nakhwa, S.N. : J. Appl. Chem. (London), 12, 266, 1962

70. Kipling, J.J. and Wilson, R.B. : J. Appl. Chem., 10, 109, 1960

71. Hofmann, U, Kottenhahn, H and Morcos, H. : Angew. Chem. Intern. Ed. Engl. 5(2), 242, 1966

72. Orr, C. : Special Rept. No. 1 Project, 143-168, 1950. Jorgians Inst. of Technology, State Engineering Expt. Station, Atlanta

73. Orr, C. : Special Rept. No. 2 Project, Ibid.

74. Darau, R. : Z. Physik, 37, 419, 1926

75. van der Grinter, K. : J. Chim. Phys., 23, 209, 1926

76. Bancellin, F. : Ibid, 22, 513, 1925

77. Bancroff, W.D. and Barnett, C.E. : Colloid Symposium Monograph, 6, 73, 1928

78. Subrahmanya, K.S., Rao, M.R.A. and Doss, KS.G. : Proc. Indian Acad. Sci., 34A, 324, 1951

79. Doss, KS.G. and Singh, A. : J. Sci. Ind. Research (India), 12B, 79, 1953

80. Margaret, M, Allingham, Cullen, J.W., Giles, G.H., Jain, S.K. and Woods, J.S. : J. Appl. Chem., 8, 108, 1958

81. Weissbein and Goven : Textile Res. J., 30, 58, 62, 1960

82. Lenhar, S. and Smith, J.E. : Ind. Eng. Chem., 27, 20, 1935

83. Lenhar, S. and Smith, J.E. : J. Am. Chem. Soc., 57(1), 495, 504, 1935

84. Vickerstaff, T. and Lenin, D.R. : Nature, 157, 373, 1946

85. Mukherjee, P. and Ghosh, A.K. : J. Amer. Chem. Soc., 92, 6403-6407, 1970

86. Idem : Ibid., 92, 6419-6425, 1970

87. Ghosh, A.K. and Mukherjee, P. : Ibid, 92, 6408-6412, 1970

88. Hertz, A.H., Danner, R.P. and Janusouis, G.A. : Advances Chem. Ser. 79. Am. Chem. Soc., Washington D.C., 173-210, 1968

89. Hertz, A.H. : Adv. Colloid Interface Sci., 8, 237-250, 1977

90. Kongonovoskii, A.M. : Kolloidn Zh. 28(1), 1966

91. Pham Thi Hang and Brindley, G.W. : Clays and Clay Minerals, 18, 203-213, 1970

92. Faruki, F.A., Okuda, S. and Williamson, W.O. : Clay Minerals, 7, 19-31, 1967

93. Bodenbeimer, W. and Heller, L. : Israel J. Chem., 6, 307-314, 1968

94. West, W., Carrol, B.H. and Whitcomb, D.H. : J. Phys. Chem., 56, 1054, 1952

95. De, D.K., Das Kanungo J.L. and Chakravarti, S.K. : Indian J. Chem., 11, 802-805, 1973

96. Idem : Ibid, 12, 165-166, 1974

97. Idem : Ibid, 12, 1187-1189, 1974

98. De, D.K., Das Kanungo, J.L. and Chakravarti, S.K. : J. Indian Chem. Soc., LVI, 608-611, 1979

99. Idem : Ibid, L. 507-510, 1973

100. Idem : J. Indian Soc. Soil Sci., 27(1), 85-87, 1979

101. Idem : Ibid, 21(2), 137-141, 1973

102. Idem : Ibid, 21(3), 251-255, 1973

103. Idem : Ibid, 26(2), 225-227, 1978

104. Idem : Ibid, 30(3), 369-373, 1982

105. Narine, D.R. and Guy, R.D. : Clays and Clay Minerals, 29(3), 205-212, 1981

106. Yamagashi, A. : J. Phys. Chem., 85, 3090-3092, 1981

107. Solomon, D.H. and Ross, M.J. : J. Appl. Polym. Sci., 9, 1261, 1965

108. Ramesh, K. Mishra, Mundhara, G.L., Tiwari, J.S. and Moitra, S. : J. Indian Chem. Soc., LXI, 44-49, 1984

109. Reed, G.H. and Rogers, L.B. : Anal. Chem., 37(7), 861, 1965

CHAPTER - I (Section 'B')

1. Mukherjee, S.K. : Prof. J.N. Mukherjee's 60th Birthday Commemoration, 127, 1953

2. Bolt, G.H. : Neth. J. Agr. Sci., 15, 81, 1967

3. Helfferich, F. : Ion Exchange, McGraw Hill Book Co., Inc., New York, 1962

4. Babcock, K.L. : Hilgardia, 34, 417, 1963

5. Weigner, G. : G. Zum-Basen austausch in der Ackekerde, J. Land 60, 111, 1922

6. Weigner, G. and Jenny, H. : Kolloid Z., 43, 268, 1927

7. Marshall, C.E. and Gupta, R.S. : J. Soc. Chem. Ind. 52, 433T, 1933

8. Shaw, D.J. : 'Introduction to Colloid and Surface Chemistry, Butterworths, London, 1970

9. Vageler, P. : Der Kationen und. Miner. haushalt des Mineralbod ens, Springer, Berlin, 1932

10. Vageler, P. and Woltersdorf, J. : Z. Pflanzenernahr, Dung. U. Boderk, A15, 329, 1930

11. Weber, J.B., Ward, T.M. and Weed, S.B. : Soil Sci. Soc. Am. Proc. 32, 197, 1968

12. Kerr, H.W. : J. Am. Soc. Agron., 20, 309, 1928

13. Gapon, E.N. : J. Gen. Chem., USSR, 3, 144, 1933

14. Burns, I.G. and Hayes, M.H.B. : Residue Reviews, 52, 117, 1974

15. Kunin, R. : 'Ion Exchange Resins' - John Wiley and Sons, Inc. New York, U.S.A., 1958

16. Jenny, H. : J. Phys. Chem., 40, 501, 1936

17. Davis, L.E. : J. Colloid. Sci., 5, 71, 1950

18. Davis, L.E. and Ribli, J.M. : Ibid, 5, 81, 1950

19. Krishnamoorthy, C. and Overstreet, R. : Soil. Sci., 69, 41, 1950

20. Gansen, R. : Centl. Miner. Geol. Palacut., 728, 1913

21. Bauman, W.C. : J. Am. Soc. 69, 2830, 1947

22. Gregor, H.P. : Ibid, 69, 1293, 1948

23. Boyd, G.E., Adamson, A.W. and Schubert, J. : J. Am. Chem. Soc., 69, 2818, 1947

24. Vanselow, A.P. : Soil Sci., 33, 95, 1932

25. Weigner, G. : Trans. 3rd Int. Cong. Soil Sci., 3, 5, 1935

26. Bolt, G.N., Summer, M.E. and Kamphorst, A. : Soil Sci. Soc. Am. Proc., 27, 294, 1963

27. Schouwenburg J. Ch. Van and Schufflen, A.C. : Neth J. Agri. Sci., 11, 13, 1963

28. Mukherjee, J.N. : Trans. Farad Soc., 16, 103, 1920-21

29. Mukherjee, J.N. and Mitra, R.P. : J. Colloid. Sci. 1, 141, 1946

30. Mitra, R.P. and Bagchi, S.N. : J. Ind. Soc. Soil Sci., 6, 1951

31. Ganguli, A.K. and Mukherjee, S.K. : J. Phys. Coll. Chem. 56, 1952

32. Chakravarti, S.K. : J. Indian Soc. Soil. Sci., 2, 127, 1954

33. Gaines, G.L. and Thomas, H.C. : J. Chem. Phys. 21, 714, 1953

34. Idem : Ibid, 23, 2322, 1955

35. Heald, W.R., Frere M.H. and Wit, C.T.de : Soil Sci. Soc. Am. Proc., 28, 622, 1964

36. Shavinberg I, and Kemper, W.D. : Soil Sci. Soc. Am. Proc., 30, 707, 1966

37. Idem : Soil Sci., 103, 4, 1967

38. Duncen, J.F. : Australian J. Chem. 8, 1, 1955

39. Ekedahl, E, Hogfeldt, E. and Sillen, L. : Acta, Chem. Scand., 4, 556, 1950

40. Kagawa I and Kasashi, R. : J. Chem. Soc., Japan, 54, 242, 1951

41. Fuoss, R.J. : Gen. Phys. 32, 453, 1949

42. Katchaesky, A. : J. Polymer. Sci., 16, 221, 1955

43. Pauley, J.L. : J. Am. Chem. Soc., 76, 1422, 1954

CHAPTER - I (Section 'C')

1. Burns, F.G. and Haylys, M.H.B. : Residence Reviews 52, 117, 1974

2. Bailev, G.W. and White, J.L. : Residue Reviews, 32, 29, 1970

3. Hendricks, S.B. : J. Phys. Chem., 45, 65, 1941

4. Helfferich, F. : Ion Exchange, McGraw Hill Book Co., Inc., New York, 1962

5. Basu, A.N. and Mukherjee, S.K. : J. Indian Soc. Soil Sci., 14, 95, 1966

6. Gregor, H.P. : J. Am. Soc., 69, 1293, 1948

7. Banin, A. : Isr. J. Chem., 6, 27, 1968

8. Carlson, R.M. and Overstreet, R. : Soil Sci., 103, 213, 1967

9. Clark, J.S. and Turner, R.C. : Soil Sci. Soc. Am. Proc., 29, 271, 1966

10. Foscoles, A.E. : Soil Sci. Soc. Am. Proc., 32, 350, 1968

11. Foscoles, A.E. and Barshad, I. : Ibid, 33, 242, 1969

12. Gast, R.G., Van Bladel, R. and Deshpande, K.B. : Ibid, 33, 661. 1969

13. Juo, A.S.R. and Barber, S.A. : Soil Sci., 109, 143, 1970

14. Kddah, M.T. : Soil Sci., 106, 67, 1968

15. Kunishi, M.M. and Heald, W.R. : Soil Sci. Soc. Am. Proc., 32, 201, 1968

16. Lin, C. and Coleman, N.T. : Ibid, 24, 44, 1960

17. Sawhney, B.L. : Ibid, 28, 183, 1964

18. Idem : Ibid, 29, 25, 1965

19. Snyder, G.H., Mclean E.O. and Franklin, R.E. : Soil Sci., Soc. Am. Proc., 33, 392, 1969

20. Uehara, G. and Mortlan, M.M. : Ibid, 24, 26, 1960

21. Franklin, R.E. and Snyder, G.H. : Ibid, 29, 508, 1965

22. Gast, R.E. : Ibid, 33, 37, 1969

23. Idem : Ibid, 36, 14, 1972

24. Landelout, H., Van Bladel, R. and Robeyns, J. : Soil Sci., 111, 211, 1971

25. Yaalon, D.H. and Koyumdjisky, H. : Isr. J. Chem., 6, 189, 1968

26. Cremers, A.E. and Thomas, H.C. : Ibid, 6, 949, 1968

27. Das Kanungo, J.L. and Chakravarti, S.K. : Kolloid Z. and Z. Polym., 248, 953, 1971

28. Uskova, E.T., Vasil'ev, N.G. and Uskov, I.A. : Colloid J. USSR, 30, 118, 1968

29. Tramers, M.A. and Thomas, H.C. : J. Phys. Chem., 64, 29, 1960

30. du Plessie, M.C.F. and Kroontje, W. : Soil Sci. Soc. Am. Proc., 31, 176, 1967

31. Yaalon, D.H. and Koymudjisky, H. : Soil Sci., 105, 403, 1968

32. Gilbert, M. and Laudelout, H. : Ibid, 100, 157, 1965

33. Deist, J. and Talisbudeen, O. Ibid, 104, 119, 1967

34. Mitra, R.P. and Kapoor, B.S. : Ibid, 108, 11, 1969

35. Baron, P. and Shainberg, I. : Ibid, 109, 241, 1970

36. Riley, D. and Arnold, P.W. : Soil Sci. Soc. Am. Proc., 24, 165, 1960

37. Basu, A.N. and Mukherjee, S.K. : J. Indian Soc. Soil Sci., 13, 251, 1965

38. Hodgson, J.F. : Soil Sci. Soc. Am. Proc., 24, 165, 1960

39. Kown, B.T. and Ewing, B.B. : Soil Sci., 108, 231, 1969

40. Dolcater, D.L., Lotse, E.G., Syers, J.K. and Jackson, M.L. : Soil Sci. Soc. Am. Proc., 32, 795, 1968

41. Gilbert, M. : Soil Sci., 109, 23, 1970

42. Goldsmith, W.A. and Middlebrooks, E.J. : J. Am. Water Works Ass., 58, 1052, 1966

43. Juo, A.S.R. and Barber, S.A. : Soil Sci. Soc. Am. Proc., 33, 360, 1969

44. Mclean, E.O., Arscott, T.G. and Volk, V.V. : Ibid, 24, 453, 1960

45. Rhoades, J.D. : Ibid, 31, 361, 1967

46. Van Bladel, R. and Laudelout, H. : Soil Sci., 104, 134, 1967

47. Mclean, G.W. and Pratt, P.F. and Page, A.L. : Soil Sci. Soc. Am. Proc., 30, 804, 1966

48. Paliwal, K.V. and Maliwal, G.L. : Proc. Indian Nat. Sci. Acad., Part A, 37, 114, 1971

49. Peterson, F.F., Rhoades, J, Acra, M. and Coleman, N.T. : Soil Sci. Soc. Am. Proc., 29, 327, 1965

50. Wild, A. and Keay, J. : J. Soil Sci., 15, 135, 1964

51. Tiller, K.G. and Hodgson, J.F. : Clays and Clay Minerals, 9, 393, 1962

52. Gille, G.L. and Graham, E.R. : Soil Sci. Soc. Am. Proc., 35, 414, 1971

53. Bolt, G.H. : Soil Sci., 79, 267, 1955

54. Coulter, B.S. : J. Soil Sci., 20, 72, 1969

55. Levy, R. and Hillel, D. : Soil Sci., 106, 393, 1968

56. Slabaugh, W.H. and St. Clair, A.D. : J. Colloid Interface Sci., 29, 586, 1969

57. Knibbe, W.G.J. and Thomas, G.W. : Soil Sci. Soc. Am. Proc., 36, 568, 1972

58. Bonner, O.D. : J. Phys. Chem., 58, 318, 1954

59. Idem : Ibid, 59, 719, 1953

60. Bonner, O.D. and Smith, L.L. : Ibid, 61, 326, 1957

61. Salmon, J.E. and Hale, D.K. : 'Ion Exchange, A Laboratory Manual', Academic Press, Inc., N.Y., 1959

62. Ref. No. 45, Chapter I, Section 'A'

63. Ref. No. 54, Chapter I, Section 'A'

64. Mortland, M.M. and Barake, N. : Trans. 8th International Congr. Soil Sci., Vol. 3, 433, 1964

65. Ref. No. 58, Chapter I, Section 'A'

66. McBride, M.B. and Mortland, M.M. : Clay Miner., 10, 357, 1975

67. Vansant, E.F. and Peeters, G. : Clays and Clay Miner., 26, 279, 1978

68. Ref. No. 47, Chapter I, Section 'A'

69. Ref. No. 56, Chapter I, Section 'A'

70. Ref. No. 57, Chapter I, Section 'A'

71. Serratosa, J.M. : Clays and Clay Miner., 14, 385, 1966

72. Clark, J.S. and Turner, R.C. : Soil Sci. Soc. Am. Proc., 29, 3, 1965

73. McAtee, J.L., Jr. : Clays and Clay Miner., 9, 444, 1962

74. Ref. No. 96, Chapter I, Section 'A'

75. Ref. No. 99, Chapter I, Section 'A'

76. Ref. No. 100, Chapter I, Section 'A'

77. Ref. No. 104, Chapter I, Section 'A'

CHAPTER - III

1. Ruzicka, E. and Kotouck, M. : J. Anal. Chem., 180, 429-433, 1961

2. Bromfield, S.M. : Aust. J. Soil Res., 3, 31, 1965

3. Ref. No. 10 Chapter I, Section 'A'

4. Pham Thi Hang and Brindley, G.W. : Clays and Clay Miner., 18, 203-212, 1970

5. McAtee, J.L. and Hackmann, J.R. : The Am. Mineralogists, 49, 1569, 1964

6. Cohen, R. and Yariv, S. : J. Chem. Soc. Farad. Trans., 80, 1705-1715, 1984

7.

CHAPTER - IV

1. Barrer, R.M. and Perry, G.S. : J. Chem. Soc., 842, 1961

2. Chakravarti, S.K. : Science and Culture 22., 170(1956)

3. Chakravarti, S.K. : J. Ind. Soc. Soil. Sci., 7(1), 27, 1959

4. Giles, C.H., Mac Ewan, T.H. Nakhwa, S.N. and Smith, D. : J. Chem. Soc., 3973, 1960

5. Ref. No. 63 Chapter I, Section 'A'

6. De, D.K., Das Kanungo, J.L. and Chakravarti, S.K. : J. Indian Soc. Soil Sci., 27, 85, 1979

7. McBride, M.B. and Mortland, M.M. : Clays and Clay Miner., 21, 323, 1973

8. Greenland, D.J. : Soils and Fertilizers, 28, 415, 1965

9. Judith E.Slewyn and Jeffrey I Steinfeld : Jr. of Phys. Chem. Vol. 76, 5, 1972

10. Green Kally R : Trans Faraday Soc. 51, 412, 1955

11. Cohen R. and Yariv S. : J. Chem. Soc. Faraday Trans 1, 80, 1705-1715, 1984

12. Brooks, C.S. : Kolloid Zeit schrift Fur Polymers Band 199, Heft I Seite 31, (1964)

13. Gieseking, J.E. and Jenny, H. : Soil Sci., 42, 273, 1936

14. Das Kanungo, J.L. and Chakravarti, S.K. : Kolloid Z. and Z. Polym., 248, 953, 1971

15. Hendricks, S.S. : J. Phys. Chem., 45, 65, 1941

16. Fendler, J.H. and F. Fendler, E.J. : 'Catalysis in Micellar and Macromolecular Systems', Academic Press, N.Y., 1975, p. 20

17. Greenland, D.J., Laby, R.H. and Quirk, J.P. : Trans. Faraday Soc., 58, 829, 1962

18. Sarkar, G.N. and Das Kanungo, J.L. : J. Indian Chem. Soc., Vol. LX, 940, 1983

19. De, D.K., Das Kanungo, J.L. and Chakravarti, S.K. : J. Indian Soc. Soil Sci., 26, 225, 1979

20. Giles, C.H. Smith, D. and Huitson, A. : J. Colloid Interface Sci., 47, 755, 1974

21. Greenland, D.J., Laby, R.H. and Quirk, J.P. : Trans. Faraday Soc., 61, 2013, 1965

22. Greenland, D.J. and Quirk, J.P. : Clays and Clay Miner., 9, 484, 1962

23. Landolt-Bornstein's Tabellen : Ergan Zungsband, IIIC, 2059, 1936

24. Stokes, R.H. and Robinson, R.A. : J. Am. Chem. Soc., 70, 1870, 1948

25. Pauley, J.L. : J. Am. Chem. Soc., 76, 1422, 1954

26. Stanford, G. : Soil Sci. Soc. Am. Proc., 12, 167, 1948

27. Barshard, I. : Am. Miner., 35, 225, 1950

28. Wear, J.I. and White, J.I. : Soil Sci., 71, 1, 1951

29. Shainberg, I. and Kemper, W.D. : Soil Sci. Soc. Am. Proc., 30, 707, 1966

30. Kittrick, J.A. : Soil Sci. Soc. Am. Proc., 30, 801, 1966

31. Gregg, S.J. : 'The surface chemistry of solids', Chapman and Hall, London, 1961, p. 50.

CHAPTER - V

1. Ref. No. 5, Chapter I, Section 'A'

2. Ref. No. 7, Chapter I, Section 'A'

3. Brindley, G.W. and K. Robinson : The structure of Kaolinite, Mineralog. Mag., 27, 242-253(1946)

4. Brindley, G.W. : The Kaolin Minerals, "X-ray Identification and structure of the clay Minerals", Chap II pp 32-75 Mineralogical Society of Great Britain, Monograph (1951)

5. Gruner, J.W. : Zeit, Krist. 83, 75, 394, 1932

6. Grim, R.E., Allaway, W.H. and Cuthbert : J. Am. Ceram. Soc., 30, 137-142, 1947

7. Mortensen, J.L. : Proc. 9th National Clay Conference, 530-545, Pergamon Press, N.Y., 1962

8. Ref. No. 97, Chapter I, Section 'A'

9. Van Olphen H. and Fripiat, J.J. : 'Data Hand Book for Clay Minerals and other Non-metallic Minerals', Pergamon Press, 1979, pp 3941

CHAPTER - VI

1. Ref. No. 67, Chapter I, Section 'C'

2. Ref. No. 27, Chapter I, Section 'A'

3. Van Olphen, H. : 'An introduction to Clay Colloid Chemistry', John Wiley, N.Y., 1977

4. Fripiat, J.J. : Summary Review, O.E.C.D. Project, 1969

5. Newmann, B.S. and Sansom, K.G. : Isr. J. Chem., 8, 315, 1970

6. Idem : J. Soc. Cosmetic Chem., 21, 237, 1970

7. Perkins, R., Brace, R. and Mtijevio E. : J. Colloid and Interface Sci., 48, 417, 1974.

8. Ref. No. 11, Chapter IV

9. Bhattacharjya, D.P. : Exchange behaviour of a Bipyridinium Herbicide, Diquat, in clay Minerals and other Model Adsorbents', Ph.D. Thesis, University of North Bengal, 1984, pp. 104-105

10. Sunwar, C.B. : Interaction of some thiazine Dyes with clay Minerals", Ph.D. Thesis, University of North Bengal,, 1985, pp. 116-117

11. Van Olphen H. and Fripiant, J.J. : 'Data Hand Book for Clay Minerals and other Non-metallic Minerals', Pergamon Press, 1979, p. 3941

12. Greenland, D.J. : Soils and Fertilisers, 28, 415, 1965

13. Kittrick, J.A. : Soil Sci. Soc. Am. Proc., 30, 801, 1966

14. Ref. No. 29, Chapter IV

CHAPTER - VII

1. Yung Fang and Yu Yao : J. Phys. Chem., 67, 2055, 1963

2. Avgul, N.N., Kiselev, A.V. and Lygina, I.A. : Trans. Faraday Soc., 59 (489), Part 9, 2113, 1963

3. Rubistein, A.M., Slovetskaya, K.I. and Bruova, T.R. : Dokl. Akad. Nauk, SSSR, 151(3), 580, 1963 CA 59, 13376a (1963)

4. Kevorkian, V. and Steiner, R.C. : J. Phys. Chem. 67, 545 (1963)

5. Rbunstein, A.M., Slovetskaya, K.I., Klyachko, I.A. and Bruova, R. : Dokl. Akad. Nauk, SSSR, 151(2), 343 (1963), CA 59, 1337h (1963)

6. Avgul, N.N., Berezin, G.I. Kiselev A.V. and Lygina, I.A. : Izv. Akad. Nauk, SSSR, otd. Khim Nauk (1960) 1948, CA 57, 89f (1962)

7. Hajela, R.B. and Ghosh, S. : J. Ind. Chem. Soc., 41(1), 1964

8. Idem : Kolloid Z., 181, 149, 1962

9. Prasad, R. and De, A.K. : Ibid, 183, 153, 1962

10. Giles, C.H., Easton, I.A. : J. Chem. Soc., 858, 4495, 1964

11. Giles, C.H., Greczek, J.J. and Nakhwa, S.N. : J. Chem. Soc., pp. 93-95, Jan. 1961

12. Marjury, T.G. : J. Soc. of Dyers and Colourists, 70, 442, 1954

13. De, D.K. : 'Studies on sorption and desorption of dyes on aluminosilicates', Thesis submitted to the University of Kalyani, India, 1968

14. Ref. No. 105, Chapter I, Section 'A'

15. Ref. No. 9 Chapter VI

16. Bartell, F.E., Tudor, L. Thomas and Yung Fu : J. Phys. and Colloid Chem., 1456, 1951

17. Mishra, R.K., Mundhara, G.L., Tiwari, J.S. and Moitra, S. : J. Indian Chem. Soc., LXI, 44-49, 1984

18. O'Connor, D.J. and Buchanan, A.S. : Trans. Faraday Soc., 52 397, 1956

19. Malik, W.U., Srivasta S.K. and Gupta, D. : Clay Miner., 9, 369, 1972

CHAPTER - VIII

1. Brooks, C.S. : Z. Kolloid, 199, 31 (1964)
2. Ramchandran, W.S., Kacker, K.P. and Patwardhan, N.P. : Amm. Mineral., 47, 165 (1962)
3. Ref. No. 63, Chapter I, Section 'A'

CHAPTER - IX

1. Robin, M. and Trueblood K.N. : J. Am. Chem. Soc. 79, 5138, 1957
2. Leermakers, P.A., Thomas, H.T., Weis, L.D. and James, F.C. : J. Am. Chem. Soc., 88, 5075, 1966
3. Burawoy, A. : Ber., 63, 3155, 1963; J. Chem. Soc., 1177, 1939
4. Kasha, M. : Discussions Faraday Soc., 9, 14, 1950
5. McConnell, H. : J. Chem. Phys., 20, 700, 1952
6. Bayliss, N.S. : J. Chem. Phys., 18, 292, 1950
7. Bayliss, N.S. and McRae, E.G. : J. Phys. Chem. 58, 1002, 1006, 1954
8. De, D.K., Chakravarti, S.K. and Mukherjee, S.K. : J. Indian Chem. Soc. 44, 744, 1967
9. Michaelis, L. and Grannick, S. : J. Am. Chem. Soc. 66, 199, 1945
10. Ref. No. 63, Chapter I, Section 'A'
11. Morton, R.A. : Ann. Rep. Chem. Soc. 38, 21, 1941
12. Coven, G and Weissbein, L. : Textile Res. J. 30, 30, 1960

13. Vitagliano, V. : 'Interaction between Cationic Dyes and Polyelectrolytes in Chemical and Biological Applications of Relaxation Spectrometry' ed. E. Wyn-Jones (D. Riedel), Dordrecht, 1975, pp. 437-466

14. Rabinowitch, E and Epstein, L.F. : J. Am. Chem. Soc. 63, 69, 1941

15. Zanker, V. : Z. Phys. Chem., 199, 225, 1952

16. Lamm, M.E. and Neville, D.M., Jr. : J. Phys. Chem., 69, 3872, 1965

17. Michaelis, P. : J. Phys. Colloid Chem., 54, 1-17, 1950.

18. Paddav, J.F. : J. Phys. Chem., 71, 3488, 1967

19. Schwarz, G., Kmose, S. and Balthasar, W. : Eur. J. Biochem., 12, 454, 1970

20. Schwarz, G. and Balthasar, W. : Ibid, 12, 461, 1970

21. Haugen, G.R. and Hardwich, E.R. : J. Phys. Chem., 67, 725, 1963

22. Barone, G., Costantino, L. and Vitagliano, V. : Ric. Sci. Parte 2, Sex. A., 34, 87, 1964

23. Vedeneva, J. : J. Phys. Chem. U.S.S.R., 21, 881, 1947

24. Schubert, M. and Levine, A. : J. Am. Chem. Soc., 77, 4197, 1955

25. Yariv, S. and Lurie, D. Isr. J. Chem., 9, 537-552, 1971

26. Yamagashi, A. and Soma, M. : J. Phys. Chem., 85, 3090, 1981

27. Cohen, R. and Yariv, S. : J. Chem. Soc. Faraday Trans., 80, 1705-1715, 1984

28. Selwyn, J.E. and Steinfeld, J.L. : J. Phys. Chem. 76, 762, 1972

29. Haque, R., Lilly, B. and Cashow, W.R. : J. Colloid Interface Sci., 33, 185, 1970

30. Chu G and Xingkang, Z : Acta. Opt. Sinica 3, 64 (1983)

31. Yariv, S. and Cross, H. : Geochemistry of Colloid Systems, Springer, Berlin, 1970

32. Herz, A.H. : Photographic Sci. and Engineering, 18, 323, 1974

33. Yariv, S. and Lurie, D. : Israel J. Chem. 9, 537, 553, 1971

34. Cohen, R and Yariv, S. : J. Chem. Soc. Faraday Trans. I, 80, 1705-1715, 1984

35. Idem : Ibid

36. Arheloa, F.L., Gonzalez, I.L., Oseda, P.R. and Arheloa, I.L. : J. Chem. Soc. Faraday Trans II, 78, 989 (1982)

WEST BENGAL